Natural Resources Canada
Ressources naturelles Canada

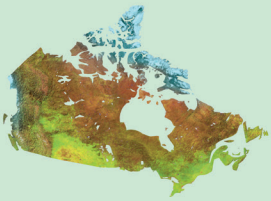

# Geological Survey of Canada
# Bulletin 613

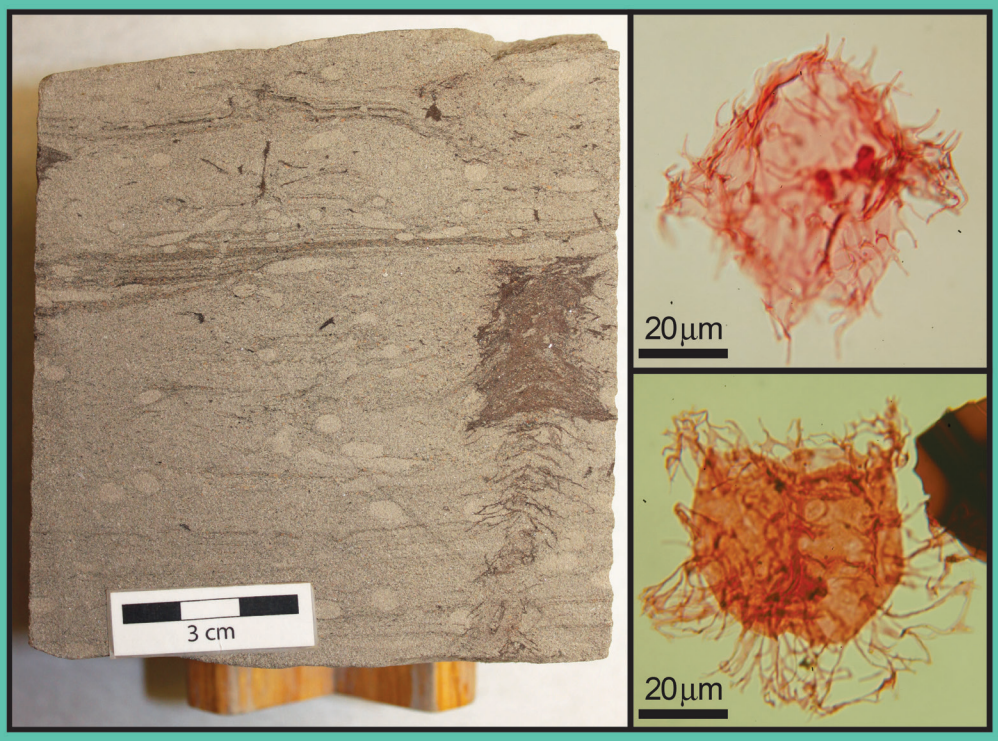


# Lithological, sedimentological, ichnological, and palynological analysis of 37 conventional core intervals from 15 wells, offshore Labrador (Newfoundland and Labrador) and southeast Baffin Island (Nunavut)

L.T. Dafoe and G.L. Williams

2020

Canada


Geological Survey of Canada
Bulletin 613

# Lithological, sedimentological, ichnological, and palynological analysis of 37 conventional core intervals from 15 wells, offshore Labrador (Newfoundland and Labrador) and southeast Baffin Island (Nunavut)

L.T. Dafoe and G.L. Williams

**2020**

ISSN 2560-7219
ISBN 978-0-660-32753-2
Catalogue No. M42-613E-PDF
https://doi.org/10.4095/315362

A copy of this publication is also available for reference in depository libraries across Canada through access to the Depository Services Program's Web site at http://dsp-psd.pwgsc.gc.ca.

This publication is available for free download through GEOSCAN (https://geoscan.nrcan.gc.ca).

**Recommended citation**

Dafoe, L.T. and Williams, G.L., 2020. Lithological, sedimentological, ichnological, and palynological analysis of 37 conventional core intervals from 15 wells, offshore Labrador (Newfoundland and Labrador) and southeast Baffin Island (Nunavut); Geological Survey of Canada, Bulletin 613, 146 p. https://doi.org/10.4095/315362

**Cover illustration**

The Snorri J-90 well, offshore Labrador, represented by samples from conventional core 1 from 2496.04–2504.54 m depth in the well. The image on the left shows a section of the core interval comprising a fine-grained sandstone with planar laminations and thin mudstone laminae. Infaunal activity has reworked the sediment and produced Macaronichnus (macaroni-shaped) trace fossils, as well as Spirophyton (muddy, tree-like structure), and small muddy Helminthopsis ichnofossils. The images on the right show palynomorphs extracted from the same core at 2501.85 m depth: Apectodinium quinquelatum (top right) and Areoligera gippingensis (bottom right). These fossils confirm a late Thanetian to early Ypresian age, and combined with the sedimentology and trace fossils, a delta-front paleoenvironment was confirmed for this interval in the well.

***Critical review***
***R. Fensome***
***N. Bingham-Koslowski***

***Authors***

***L.T. Dafoe (lynn.dafoe@canada.ca)***
***G.L. Williams(graham.williams@canada.ca)***
***Geological Survey of Canada***
***1 Challenger Drive***
***Dartmouth, Nova Scotia***
***B2Y 4A2***

# CONTENTS

**APPENDICES**



**FIGURES**

**TABLE**



**PLATES**

# Lithological, sedimentological, ichnological, and palynological analysis of 37 conventional core intervals from 15 wells, offshore Labrador (Newfoundland and Labrador) and southeast Baffin Island (Nunavut)


## *Abstract*

*The Labrador Sea began forming during rifting between Greenland and North America in the Early Cretaceous, resulting in grabens and half grabens infilled with syn-rift sediments. These strata were later draped during a sag-basin phase in the Late Cretaceous. Seafloor spreading was initiated in the Maastrichtian, but was regionally taking place by the Paleocene, and the Labrador margin was subsequently overlain by a thick Cenozoic sedimentary wedge. To refine the understanding of this stratigraphic succession, conventional core intervals from exploration wells were analyzed to reassess the biostratigraphy and depositional paleoenvironments. Findings are based on lithological, sedimentological, ichnological, and palynological studies of 37 core intervals from 15 wells along the Labrador margin and southeast Baffin Shelf. Five cores consist of gneissic to granitic Precambrian basement rocks and three are from the Early Cretaceous Alexis Formation basalts, for which general descriptions are provided. The 14 cores from the Bjarni Formation are Barremian to Albian–Cenomanian and represent mostly marginal marine settings. Eight cores from the Upper Cretaceous Markland Formation are early Campanian to Maastrichtian and represent shoreline (Freydis Member), shelf, and slope settings. Three cored intervals from unnamed Paleocene basalt flows from the northern part of Saglek Basin are also evaluated. The youngest four core intervals are from the Gudrid and Cartwright formations of Selandian to earliest Ypresian age and represent tidal channel, deltaic, and shoreface settings. Overall results form the basis for future work, delineating the nature and age of stratigraphic horizons and packages along the Labrador margin.*

## *Résumé*

*La formation de la mer du Labrador s'est amorcée par le rifting entre le Groenland et l'Amérique du Nord au Crétacé précoce et les grabens et demi-grabens alors formés ont été comblés par des sédiments syn-rift. Cette accumulation sédimentaire a par la suite été recouverte par une succession moulante au cours d'une phase de formation de bassins d'affaissement au Crétacé tardif. L'expansion océanique a commencé au Maastrichtien, mais s'est étendue à l'échelle régionale au Paléocène, et la marge du Labrador a ensuite été recouverte par un important prisme sédimentaire au Cénozoïque. Afin d'approfondir notre compréhension de cette succession stratigraphique, nous avons analysé des intervalles de carottes classiques extraites de puits d'exploration pour réévaluer la biostratigraphie et les paléoenvironnements sédimentaires. Nos conclusions sont fondées sur des études lithologiques, sédimentologiques, ichnologiques et palynologiques de 37 intervalles de carottes provenant de 15 puits situés le long de la marge du Labrador et de la plate-forme continentale sud-est de Baffin. Cinq carottes sont constituées de roches gneissiques et granitiques de socle du Précambrien et trois proviennent des basaltes du Crétacé précoce de la Formation d'Alexis, pour lesquelles nous fournissons des descriptions générales. Les 14 carottes de la Formation de Bjarni datent quant à elles du Barrémien à l'Albien-Cénomanien et rendent compte surtout de milieux marginomarins. Les âges de huit carottes de la Formation du Markland du Crétacé supérieur s'échelonnent du Campanien précoce au Maastrichtien, et celles-ci sont représentatives de milieux de littoral (Membre de Freydis), de plate-forme continentale et de talus continental. Nous évaluons également trois intervalles de carottes extraites de basaltes non dénommés du Paléocène provenant de la partie nord du bassin de Saglek. Les quatre intervalles de carottes les plus récents proviennent des formations de Gudrid et de Cartwright et fournissent des âges s'échelonnant du Sélandien à l'Yprésien précoce et rendent compte de milieux de chenaux de marée, de delta et d'avant-plage. Nos résultats globaux constituent la base des futurs travaux de détermination de la nature et de l'âge des ensembles et des horizons stratigraphiques le long de la marge du Labrador.*

## SUMMARY

Rifting between Greenland and North America in the Early Cretaceous initiated the formation of the Labrador Sea. During this time, grabens and half grabens formed and the Bjarni Formation accumulated as nonmarine and marginal marine deposits during rifting; Alexis Formation basalt flows also accumulated during the early rifting stage. Extension in the Late Cretaceous focused offshore of the present-day shelf resulting in sag-basin formation further inboard where exploration wells record a blanket of marine Markland Formation mudstone with local Freydis Member sandstone units. During the end of Markland Formation deposition, seafloor spreading began in the Maastrichtian and was taking place regionally by chron C27n in the early Paleocene. Following this, the Cartwright Formation marine shale and coeval Gudrid Formation shoreline sandstone were deposited in the mid-Paleocene to early Eocene. These were succeeded by the transgressive Kenamu Formation marine mudstone and then the Mokami Formation shelfal mudstone and relatively coeval Saglek Formation shoreline sandstone units that built up the present-day shelf.

This stratigraphic succession has been studied from a variety of perspectives, including lithostratigraphy, biostratigraphy, and seismic stratigraphy; however, many questions still remain about the timing of events and depositional history. In this study, conventional cores collected from exploration wells were analyzed to further refine the understanding of the depositional paleoenvironments and age of key stratigraphic intervals. The approach herein differs from previous studies of these rocks in that paleoenvironmental analyses from both core observations and palynological analyses were combined to provide a more robust interpretation. In addition, not only were lithology and sedimentary structures within the cores used, but also the ichnological assemblages that can provide key information about the depositional setting and paleoenvironmental conditions. Palynology assessment also provides a means of studying both the first and last occurrences of dinoflagellate cysts and miospores (pollen and spores) since the rocks are in situ, unlike cuttings samples, thus providing more accurate age determinations. In addition to providing age constraints, palynomorph assemblages provide information about paleoenvironments through nonmarine (lacking dinocysts) and marine settings whereby they suggest a relative proximity to the shoreline.

In this study of the cores, key intervals of crystalline basement were investigated, as well as Alexis Formation basalt units and unnamed Paleocene basalt units, the latter of which are restricted to the northern part of the Saglek Basin. Sedimentary intervals



## SOMMAIRE

Le rifting entre le Groenland et l'Amérique du Nord au Crétacé précoce a entraîné la formation de la mer du Labrador. Au cours de cette période, des grabens et des demi-grabens se sont formés et la Formation de Bjarni s'est accumulée dans des milieux marginomarins et non marins au cours du rifting; des coulées de basalte de la Formation d'Alexis se sont également déposées au début de la phase de rifting. La déformation par extension au Crétacé tardif a été concentrée au large de la plate-forme continentale actuelle, ce qui a entraîné la formation de bassins d'affaissement plus près de la côte où des puits d'exploration ont recoupé une nappe de mudstones marins appartenant à la Formation de Markland et des unités locales de grès du Membre de Freydis. Vers la fin du dépôt de la Formation de Markland, l'expansion océanique a commencé au Maastrichtien et s'est étendue à l'échelle régionale lors du Chron C27N, au début du Paléocène. Par la suite, les shales marins de la Formation de Cartwright et les grès littoraux du même âge de la Formation de Gudrid se sont déposés du Paléocène moyen à l'Éocène précoce. À ces dépôts ont succédé les mudstones marins transgressifs de la Formation de Kenamu, puis les mudstones de plate-forme continentale de la Formation de Mokami, ainsi que les grès littoraux à peu près du même âge de la Formation de Saglek, le tout formant la plate-forme continentale que l'on connaît aujourd'hui.

Cette succession stratigraphique a été étudiée sous différents angles et a notamment fait l'objet d'analyses lithostratigraphiques, biostratigraphiques et sismostratigraphiques; cependant plusieurs questions demeurent quant à la chronologie des événements et à l'histoire sédimentaire. Dans la présente étude, nous analysons des carottes classiques tirées de puits d'exploration afin d'approfondir notre compréhension des paléoenvironnements sédimentaires et de l'âge des principaux intervalles stratigraphiques. Notre approche diffère des études antérieures sur ces mêmes roches puisque nous combinons des analyses paléoenvironnementales réalisées à partir d'observations de carottes et des analyses palynologiques afin de proposer une interprétation plus solide. De plus, nous utilisons non seulement la lithologie et les structures sédimentaires des carottes, mais aussi les assemblages ichnologiques qui peuvent fournir des renseignements clés sur le milieu sédimentaire et les conditions paléoenvironnementales. L'évaluation palynologique nous a également permis d'étudier les premières et dernières occurrences de kystes de dinoflagellés et de miospores (pollen et spores) puisque les roches sont en place, contrairement aux échantillons de déblais de forage, nous permettant ainsi de déterminer l'âge avec une plus grande précision. En plus d'établir des limites en matière d'âge, les assemblages de palynomorphes fournissent des renseignements sur les paléoenvironnements par l'intermédiaire de milieux non marins (absence de dinokystes) et marins, ce qui suggère une proximité relative avec la ligne de rivage.

Dans le cadre de l'analyse des carottes, nous avons également examiné des intervalles clés du socle cristallin, de même que des basaltes de la Formation d'Alexis et des basaltes non dénommés du Paléocène, ces derniers étant limités à la partie nord du bassin de Saglek. Nous nous sommes concentrés sur les intervalles

were the focus, but the analysis of gneissic and granitic basement rock, five intervals in total, provided information about local sediment sources, especially within the Bjarni Formation that was deposited during early rifting, when local basement highs would have been important sediment sources. The basalt units are also informative when understanding processes of emplacement, including subaerial or subaqueous conditions, and they sometimes preserve biostratigraphic age markers, and can also be local sediment sources. Whereas the three studied core intervals of the Alexis Formation basalt units appear to reflect subaerial flows, the unnamed Paleocene basalt units, also sampled in three core intervals, include both flows and subaqueous hyaloclastic lava delta accumulations.

Most of the sedimentary cores are from the Bjarni Formation: 14 core intervals from ten wells. The age of some palynology samples were well constrained, but others were less so, as the number of palynological events in the Early Cretaceous is limited. The strata were found to be as old as Barremian–Aptian to as young as middle Albian–Cenomanian, although most intervals are from the Albian since many of the cores sampled upper portions of the Bjarni Formation within the wells. Lithologically, the Bjarni Formation is diverse and includes sandstone, shale and/or mudstone, conglomerate, and even an interval of volcanic rock. Paleoenvironmental interpretations indicate overwhelmingly shallow-marine conditions, mostly deltaic (river-influenced, river-dominated, and wave-influenced), as well as restricted marine bay settings. Only one Barremian–Aptian core is fluvial in origin. Detailed paleoenvironments are primarily derived from core observations as dinocysts are commonly absent from the samples; however, in some instances, dinocysts help to confirm a marginal marine setting that is not apparent from the sedimentology or ichnology.

The Markland Formation is intersected by eight core intervals with some sampling the Freydis Member sandstone units. These cores range from early Campanian at the oldest to Maastrichtian. The Markland Formation itself is comprised of shale and sandy mudstone, whereas the Freydis Member is heterolithic sandstone and mudstone and/or shale or bioturbated sandstone. Paleoenvironments are marine, with the Freydis Member sandstone reflecting distributary channels and deltaic deposition (river-influenced), shoreface, and inner shelf conditions. Conditions were comparatively more distal during Markland Formation deposition with

sédimentaires, mais l'analyse des roches gneissiques et granitiques du socle, appartenant à cinq intervalles au total, nous a permis d'obtenir plus d'information sur les sources locales de sédiments. C'est particulièrement le cas pour la Formation de Bjarni dont les sédiments se sont accumulés au début du rifting, alors que des hauteurs locales du socle constituaient d'importantes sources de sédiments. Les unités de basalte s'avèrent également instructives lorsque vient le temps de mieux comprendre les processus de mise en place, y compris dans des conditions subaériennes ou subaquatiques, et elles préservent parfois des marqueurs biostratigraphiques de l'âge, en plus de constituer à l'occasion des sources locales de sédiments. Les trois intervalles de carottes des unités de basalte de la Formation d'Alexis étudiés semblent indiquer qu'il s'agit de coulées subaériennes tandis que les unités de basalte non dénommées du Paléocène, également échantillonnées dans trois intervalles de carottes, comprennent des coulées ainsi que des accumulations deltaïques de lave hyaloclastique de milieu subaquatique.

La plupart des carottes sédimentaires proviennent de la Formation de Bjarni : 14 intervalles de carottes provenant de 10 puits. Alors que l'âge de certains échantillons palynologiques était bien circonscrit, ce n'était pas le cas pour d'autres échantillons étant donné le nombre limité d'événements palynologiques au Crétacé précoce. Nous avons établi que l'âge des strates, des plus anciennes aux plus récentes, se situe entre le Barrémien-Aptien et l'Albien moyen-Cénomanien. La plupart des intervalles sont toutefois associés à l'Albien puisque plusieurs des carottes prélevées dans les puits proviennent des parties supérieures de la Formation de Bjarni. Sur le plan lithologique, la Formation de Bjarni est diversifiée et comprend des grès, des shales et/ou des mudstones, des conglomérats et même un intervalle de roches volcaniques. Les interprétations paléoenvironnementales indiquent la prédominance de conditions de milieu marin peu profond, principalement de milieu deltaïque (sous influence fluviale, sous influence fluviale prédominante et sous influence des vagues), ainsi que des conditions de baie marine à circulation restreinte. Une seule carotte du Barrémien-Aptien est d'origine fluviale. La détermination des paléoenvironnements dans le détail provient principalement d'observations de carottes puisque les dinokystes sont généralement absents des échantillons. Cependant, dans certains cas, des dinokystes permettent de confirmer l'existence d'un milieu marginomarin, ce qui ne pourrait être établi à partir des analyses sédimentologiques ou ichnologiques.

Huit intervalles de carottes recoupent la Formation de Markland, dont certains ont permis d'échantillonner les unités de grès du Membre de Freydis. L'âge de ces carottes s'étend, des plus anciennes aux plus récentes, du Campanien précoce au Maastrichtien. La Formation de Markland est composée de shales et de mudstones gréseux, tandis que le Membre de Freydis est constitué de grès hétérolithiques, de mudstones et/ou de shales ou de grès bioturbés. Les paléoenvironnements sont de type marin, où les grès du Membre de Freydis rendent compte d'un dépôt dans des chenaux distributaires et des deltas (sous influence fluviale), ainsi que dans des milieux d'avant-plage et de plate-forme continentale interne. En comparaison, les conditions étaient davantage distales lors du dépôt en milieu marin ouvert de la Formation de

open-ocean, slope-equivalent water depths, and distal inner shelf to distal outer shelf settings. The palynomorph assemblages show general agreement with core observations, but in some instances suggest proximity to a nearby deltaic source of terrestrial detritus, and in others suggest a more distal setting due to rich dinocyst assemblages.

Stratigraphically lying above the Markland Formation, four core intervals from the Gudrid Formation sandstone and correlative Cartwright Formation sandy mudstone were found to be Selandian at the oldest and basal Ypresian at the youngest. The Gudrid Formation intervals reflect a variety of settings including tidal channels, shoreface and/or delta front, and storm-dominated proximal and distal delta front. The relatively proximal sample of the Cartwright Formation is indicative of a wave-influenced prodelta setting. Depositional settings interpreted from palynomorphs correlate with core observations.

Overall, the analyses of conventional cores generally provide more well constrained biostratigraphic ages from the in situ samples as compared to results from cuttings. Independent paleoenvironmental assessments using the sedimentology and ichnology, in addition to palynological analyses provide a robust interpretation of the setting. Especially in marginal marine settings, the two approaches complement one another as dinocysts can be suppressed in brackish conditions resulting in a nonmarine interpretation; however, in other instances, the presence of dinocysts can help to constrain a marine paleoenvironment that can sometimes be inconclusive from core observations. These integrated core analyses provide small windows into the age and depositional settings of major lithostratigraphic units of the Hopedale and Saglek basins that can be further utilized to understand the stratigraphic succession when extrapolated within and between wells.

Markland à des profondeurs d'eau équivalentes à celles du talus continental, dans des milieux allant de la partie distale de la plate-forme continentale interne à la partie distale de la plate-forme continentale externe. Les assemblages de palynomorphes concordent généralement avec les observations tirées des carottes, mais suggèrent dans certains cas la proximité d'une source deltaïque de débris terrestres et, dans d'autres cas, un milieu plus distal d'après la richesse des assemblages de dinokystes.

Quatre intervalles de carottes extraites des grès de la Formation de Gudrid et des mudstones gréseux corrélatifs de la Formation de Cartwright, qui surmontent stratigraphiquement la Formation de Markland, dateraient, des plus anciens aux plus récents, du Sélandien à l'Yprésien basal. Les intervalles de la Formation de Gudrid témoignent d'une variété de milieux, notamment de chenaux de marée, d'avant-plage et/ou de front deltaïque, ainsi que des milieux proximaux et distaux d'un front deltaïque sous influence prédominante des tempêtes. L'échantillon relativement proximal de la Formation de Cartwright témoigne d'un milieu prodeltaïque sous influence des vagues. Les milieux sédimentaires interprétés à partir des palynomorphes concordent bien avec les observations tirées des carottes.

Dans l'ensemble, les analyses des carottes classiques provenant d'échantillons en place fournissent généralement des âges biostratigraphiques mieux encadrés que ceux livrés par les déblais de forage. Les évaluations paléoenvironnementales indépendantes fondées sur des analyses sédimentologiques et ichnologiques, en plus des analyses palynologiques, offrent une solide interprétation du milieu sédimentaire. C'est particulièrement le cas pour ce qui est des milieux marginomarins où les deux approches se complètent puisque l'existence de conditions saumâtres peut empêcher la présence de dinokystes, ce qui mène à une détermination de milieu non marin. Cependant, dans d'autres cas, les dinokystes peuvent indiquer l'existence d'un paléoenvironnement marin, ce que les carottes ne pourraient permettre de confirmer de façon concluante. Les analyses de carottes intégrées ne fournissent que d'étroites fenêtres quant à l'âge et aux milieux sédimentaires des principales unités lithostratigraphiques des bassins de Hopedale et de Saglek, mais contribuent à une meilleure compréhension de la succession stratigraphique lorsque des extrapolations sont réalisées entre les puits.

## INTRODUCTION

The Labrador Sea (Fig. 1) developed through rifting as Greenland separated from North America, beginning in the Early Cretaceous (Roest and Srivastava, 1989). During this time, on the Labrador margin, rifting was initially focused under what is today the shelf and slope. In the Late Cretaceous, however, active extension migrated farther offshore (Dickie et al., 2011) with mantle serpentinization taking place in the Late Cretaceous (Keen et al., 2018a). Seafloor spreading began as early as the Maastrichtian (chron C31) along the central Labrador margin (Keen et al., 2018a), but was regionally taking place in the Paleocene (chron C27n; Oakey and Chalmers, 2012; Keen et al., 2018b). Extension then ceased in the late Eocene by chron C13 (Oakey and Chalmers, 2012).

The Hopedale and Saglek basins of offshore Labrador (Fig. 1) lie along the southern and northern parts of the margin, respectively, and are separated by the Okak Arch, a prominent east-trending basement high (Balkwill, 1987). To the south, the Hopedale Basin extends to the Cartwright Arch. Northward, the Saglek Basin terminates at the Lady Franklin Arch (Balkwill, 1987) and near a zone of regional transform, strike-slip faulting, the Ungava Fault Zone, that developed during a change in seafloor-spreading direction that took place between chrons C24n and C25n

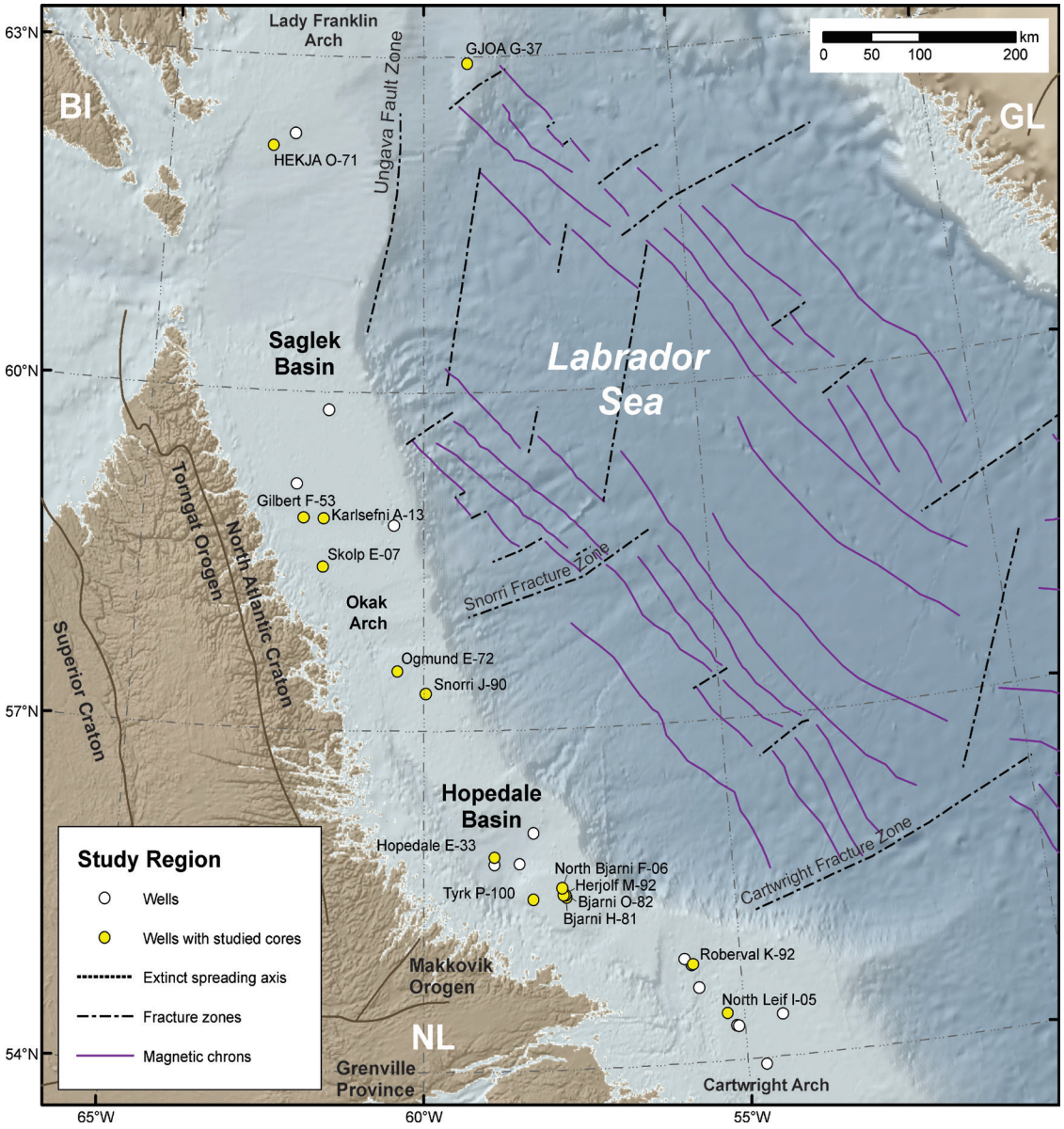


**Figure 1.** Regional map of the Labrador margin and southeast Baffin Island margin. Industry wells in yellow and labelled are those with conventional core samples that were analyzed in this study. Onshore cratonic boundaries are from St-Onge et al. (2009). The extinct spreading axis, oceanic fracture zones, and magnetic chrons (starting with C31 as the oldest) are from Oakey and Chalmers (2012). BI = Baffin Island, NL = Newfoundland and Labrador, GL = Greenland.

(Thanetian; Oakey and Chalmers, 2012). The rift history of the Labrador Sea is recorded in 29 exploration wells in the Hopedale and Saglek basins. These wells were drilled during petroleum exploration activities in the region during the 1970s to 1980s.

Umpleby (1979) was first to establish a formal lithostratigraphic terminology for units underlying the Labrador Shelf; he defined four formations and constituent members based on the observations from nine wells. McWhae et al. (1980) revised Umpleby's lithostratigraphy of the Labrador margin to propose a total of eight formations, that are still recognized: Alexis, Bjarni, Markland, Cartwright, Gudrid, Kenamu, Mokami, and Saglek (Fig. 2). In a more regional study of the Eastern Canadian margin, McWhae (1980) linked these formations to the presence of five regional unconformities, two in the Cretaceous and three in the Cenozoic. Using this earlier work and integrating it with seismic mapping, the Labrador Sea Atlas project (Bell, 1989) compiled regional maps of lithostratigraphic intervals, structure, and paleogeography. Balkwill and McMillan (1990) further commented on the lithostratigraphy and nature of the units, and their distribution along the margin.

Various biostratigraphic studies have been conducted on the wells of the Labrador Shelf including palynological, foraminiferal, and lesser nannofossil studies (e.g. Robertson Research (North America) Ltd., 1974; Robertson Research Canada Ltd., 1979, 1980; Williams, 1975, 2007a, b, c, d, e, 2017; Bujak Davies Group, 1989a, b, c, d, e, f, g, h; Ainsworth et al., 2014, 2016; Fensome, 2015; Nøhr-Hansen et al., 2016). These have formed a key age framework for

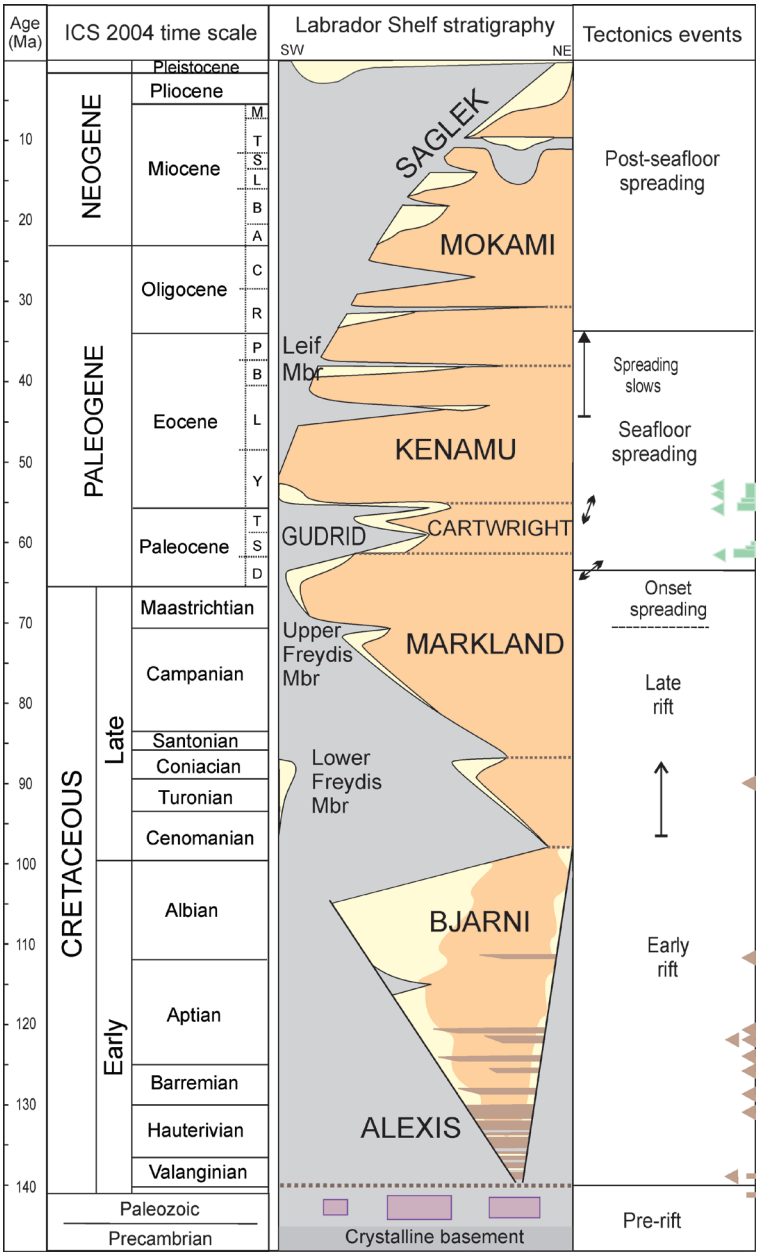


**Figure 2.** Labrador margin tectonostratigraphic column (*modified from* Dickie et al., 2011 and based on McWhae et al., 1980). Formation names are in capital letters and members (Mbr) are shown in sentence caps. In the tectonics column, Alexis Formation basalt in wells (triangles) and onshore dykes (lines) is shown in brown, as well as Paleocene–Eocene volcanic rocks in wells (triangles) and flood basalt units (lines) in green. The orientation of fractures is also shown in the tectonics column. In the Paleogene and Neogene, ages are denoted by their first letter within the corresponding Epoch.

the lithostratigraphy. Other studies have further refined the understanding of the subsurface geology through integration of the lithostratigraphy with seismic stratigraphy of the Labrador margin (Jauer et al., 2009, 2014; Wielens and Williams, 2009; Dickie et al., 2011). Dickie et al. (2011) used a modern (post-1990s) seismic data set to build an updated tectonostratigraphic chart that incorporated consistent biostratigraphically derived ages from key wells (Fig. 2).

Whereas previous work conducted along the Labrador margin has provided a solid framework for understanding the stratigraphy, questions remain about the nature of stratigraphic surfaces, depositional history, and the timing of events, some of which can be answered by studying the rock units. Much of the well geology is sampled only by cuttings; however, several conventional cores were recovered mostly from the exploration targets — the Bjarni and Gudrid formation sandstone units. These rocks have been analyzed previously by numerous geologists to understand the lithology, porosity and permeability, organic content, paleoenvironment of deposition, and petrology. The purpose of this study is to reassess these conventional core materials in light of biostratigraphic age and sedimentary environment using a combination of techniques. Thirty-seven core intervals were studied from 15 wells. Focus was on the sedimentary intervals for which the sedimentology and ichnology are described and interpreted from a paleoenvironmental perspective. This part of the study compares and shows good correlation between these observations and depositional paleoenvironments suggested by the palynomorphs, in addition to reassessing the age. Furthermore, results are compared with previous interpretations that were based on analyses of cuttings and included examination of lithology, foraminifera, and palynomorphs. New results are presented which, when combined with more regional correlations and mapping efforts, will help to shed light on the development of the margin through time.

## METHODS

Industry wells within the Hopedale and Saglek basins of offshore Labrador and the southeastern Baffin Island margin were drilled between 1971 and 1983. Conventional cores were taken in several of the wells, with samples from offshore Labrador curated at the Canada–Newfoundland and Labrador Offshore Petroleum Board (C–NLOPB). Cores from offshore southeastern Baffin Island margin are curated by the Canada–Nova Scotia Offshore Petroleum Board (C–NSOPB) on behalf of the National Energy Board (NEB). A total of 37 core intervals were analyzed from 15 wells. Cores were selected with a focus on Mesozoic and Cenozoic sedimentary rocks with some key intervals assessed from Precambrian basement, Alexis Formation basalt units, and unnamed Paleocene basalt units. The lithostratigraphic assignments of Moir (1987a, b, 1989) were utilized. The cores were photographed and logged for lithology, sedimentary structures, ichnology, and paleontology. Some core intervals are discussed in terms of a larger interval within the well, based on cuttings descriptions from Canstrat (www.canstrat.com).

The lithology of the rocks, in combination with sedimentary structures and trace fossils, were assessed to provide one line of evidence for paleoenvironmental interpretation. Sedimentary structures can be informative about the energy of the system and depositional conditions, such as current and wave activity. Trace fossils are also sensitive to environmental conditions. This study followed the ichnofacies model in Pemberton et al. (2001), whereby organism behaviours are shown to reflect the changing depositional conditions from the beach to shelf; however, in Figure 3 (*see* below), their model is shown relative to the paleoenvironmental terminology used in this study and with the addition of the *Nereites* Ichnofacies representing slope and deeper water settings. Along the Labrador margin, shelf and slope settings were not established prior to deposition of the Kenamu Formation in the Eocene (Dickie et al., 2011). Accordingly, for this study the term 'shelf' or 'shelfal' is used to indicate settings with equivalent water depths of about 200 m or less, and 'slope' is used to indicate water depths greater than about 200 m. Normal marine trace-fossil assemblages reflecting ichnofacies can be modified where they reflect environmentally stressful conditions in which the diversity, abundance, ethology, and size of trace fossils are affected (MacEachern et al., 2010), reflecting brackish or anoxic conditions, for example. In these instances, the rock unit is described as possessing a 'stressed expression' of a particular ichnofacies.

From 28 of the core intervals, 95 samples, at approximately 1–2 m intervals, were taken for palynological processing and analyses (where useful, previously collected slides from the same core intervals were also analyzed). Samples were processed for palynomorphs by Global Geolabs Ltd. in Medicine Hat, Alberta or the Geological Survey of Canada in Calgary, Alberta. The samples were first crushed, then treated with hydrochloric and hydrofluoric acids to remove carbonate and silicate minerals, respectively, with thorough washing after both treatments. Another treatment of hot, concentrated hydrochloric acid was undertaken, followed by centrifuging to remove the hydrochloric acid. Further concentration of the remaining fraction involved centrifuging in heavy liquid zinc bromide. Following this stage, a fraction of each sample was saved and used to make a kerogen slide. The remaining residue was then oxidized with Schulze solution. Then the samples were placed in a 10% solution of ammonium hydroxide for about 5 minutes. On completion of this phase, Safranin red was added to stain the material and a second slide was prepared for counts to determine variations in abundances of taxa (unsieved slide). Further processing involved sieving the samples through a 30 μm screen, a technique that is invaluable for concentrating dinoflagellate cysts (dinocysts) and larger miospores. Slides were then prepared from both the +30 μm and -30 μm fractions. Residues were smeared on a cover slip, which was inverted and placed on a slide using the mounting medium, clear casting resin. A set of the palynology slides used for this study are curated at the Geological Survey of Canada (Atlantic), Dartmouth, Nova Scotia and a second set of slides is curated at the Canada–Newfoundland and Labrador Offshore Petroleum Board (C-NLOPB) in St. John's, Newfoundland. Photographs of specimens were taken

using a Zeiss photomicroscope, generally with a 50x objective lens. Select palynomorph specimens are illustrated in the accompanying plates and the associated slides are curated in the National Collection of Type Invertebrate and Plant Fossils, Geological Survey of Canada, 601 Booth Street, Ottawa, Ontario (at the time of writing, this material is on long-term loan to the Geological Survey of Canada (Atlantic), Bedford Institute of Oceanography, Dartmouth, Nova Scotia).

In a well, one of the major advantages of biostratigraphic data from the analysis of conventional cores is that the palynomorph specimens in each sample are known to be in place, that is, they are not derived from caved material, as is the case with cuttings. Conventional cores should also be free of contamination, which is a problem with both sidewall cores and cuttings samples, although the latter can give reliable data on last or youngest occurrences. The standard practice in assessing palynomorphs to determine ages for intervals in a well or surface section is to plot last or youngest occurrences. A major advantage of analyzing conventional core samples is that first or oldest occurrences can also be used as there are no concerns about cavings.

In this study, the age of each palynology sample has been described separately based on the assemblage present: these results are then combined in each core summary and compared with previous biostratigraphic studies. Paleoenvironments are also reported for each palynology sample and then rationalized with the interpretation from core observations in the summary section. Palynomorphs are extremely useful for determining paleoenvironments because they include nonmarine and marine organisms. The nonmarine forms are the spores and pollen, which are herein collectively termed miospores, but these can also be transported into marine settings. Marine palynomorphs are primarily dinocysts, although acritarchs (organic walled microfossils of unknown origin) can also be informative; however, dinocysts tend to denote distance from shore rather than water depth, so they can give misleading results. Regardless, four categories of settings can still be differentiated based on key marker species: coastal and/or marginal marine, inner neritic, outer neritic, and open ocean (Fig. 3; Nøhr-Hansen et al., 2016), bearing in mind that these categories indicate relative rather than precise water depths. Figure 3 also shows the generalized correlations between paleoenvironmental terminology derived from core observations and that from palynomorphs. The timescale of Gradstein et al. (2012) is used in discussions in this publication.

# RESULTS

Results for the conventional cores are described below according to the alphabetic position of the well name, as follows: Bjarni H-81, Bjarni O-82, Gilbert F-53, Gjoa G-37, Hekja O-71, Herjolf M-92, Hopedale E-33, Karlsefni A-13, North Bjarni F-06, North Leif I-05, Ogmund E-72, Roberval K-92, Skolp E-07, Snorri J-90, and Tyrk P-100. For each core interval, core observations are described and interpreted, each palynology sample is described and interpreted, and then the interpretations are combined in the summary section and compared with previous studies. A summary of the results is presented in Table 1.

## Bjarni H-81

Bjarni H-81 was drilled in the Hopedale Basin offshore Labrador (Fig. 1) in 1973–1974, to 2515.2 m depth. The exploration target was the sedimentary interval overlying a horst-type structure (Corgnet and McWhae, 1973). Three core intervals were recovered within Mesozoic rocks near the base of the well, one from the Bjarni Formation and the lower two from the Alexis Formation basalt units.

### *Core 1: fine- to medium-grained sandstone (2157.1–2164.11 m)*

#### *Core description and interpretation*

Core 1 of the Bjarni H-81 well had poor recovery from within the Bjarni Formation, with only 2.44 m of section, which includes a basal unit of rubbly medium-grained sandstone and about 50 cm of missing core (Fig. 4, 5a). The basal rubbly sandstone is poorly sorted and buff with small pebbles (less than 2 cm in diameter) of quartzite and probable orthoclase feldspar. Possible tabular crossbedding is observed in this unit and it is capped by a thin pyrite-bearing shale. The uppermost section of the core contains poorly sorted, fine- to medium-grained sandstone with sharp bedding contacts. Thin mudstone laminae are common (Fig. 5b, d, e) and sedimentary structures include planar laminations (Fig. 5e), microfaults (Fig. 5b, d), and massive bedding (Fig. 5c). Organic detritus is also noted in addition to scattered pebbles. Trace fossils in the upper part of the core include rare to moderate abundances of *Helminthopsis* (Fig. 5b, e) and rare *Phycosiphon* and *Chondrites*, with bioturbation comprising less than 10% of the core.

Massive bedding and microfaults suggest high sedimentation rates, and organic detritus indicates proximity to a terrestrial environment. Furthermore, pebbles imply high current strength, whereas shale interlaminations indicate alternating depositional regimes and possible hyperpycnal flows (MacEachern et al., 2005). The trace-fossil assemblage comprises marine deposit-feeding and grazing traces in low abundance and diversity, consistent with a shallow brackish-marine setting and highly stressed expression of the *Cruziana* Ichnofacies. High sedimentation rates and a heterolithic lithology are consistent with a deltaic setting. The lack of vertical trace fossils suggests high concentrations of suspended sediment and enhanced water turbidity, inhibiting suspension-feeding activities of infaunal organisms. Overall, the core appears to reflect a river-influenced deltaic setting in which brackish conditions preclude faunal colonization and sedimentation rates are relatively high.

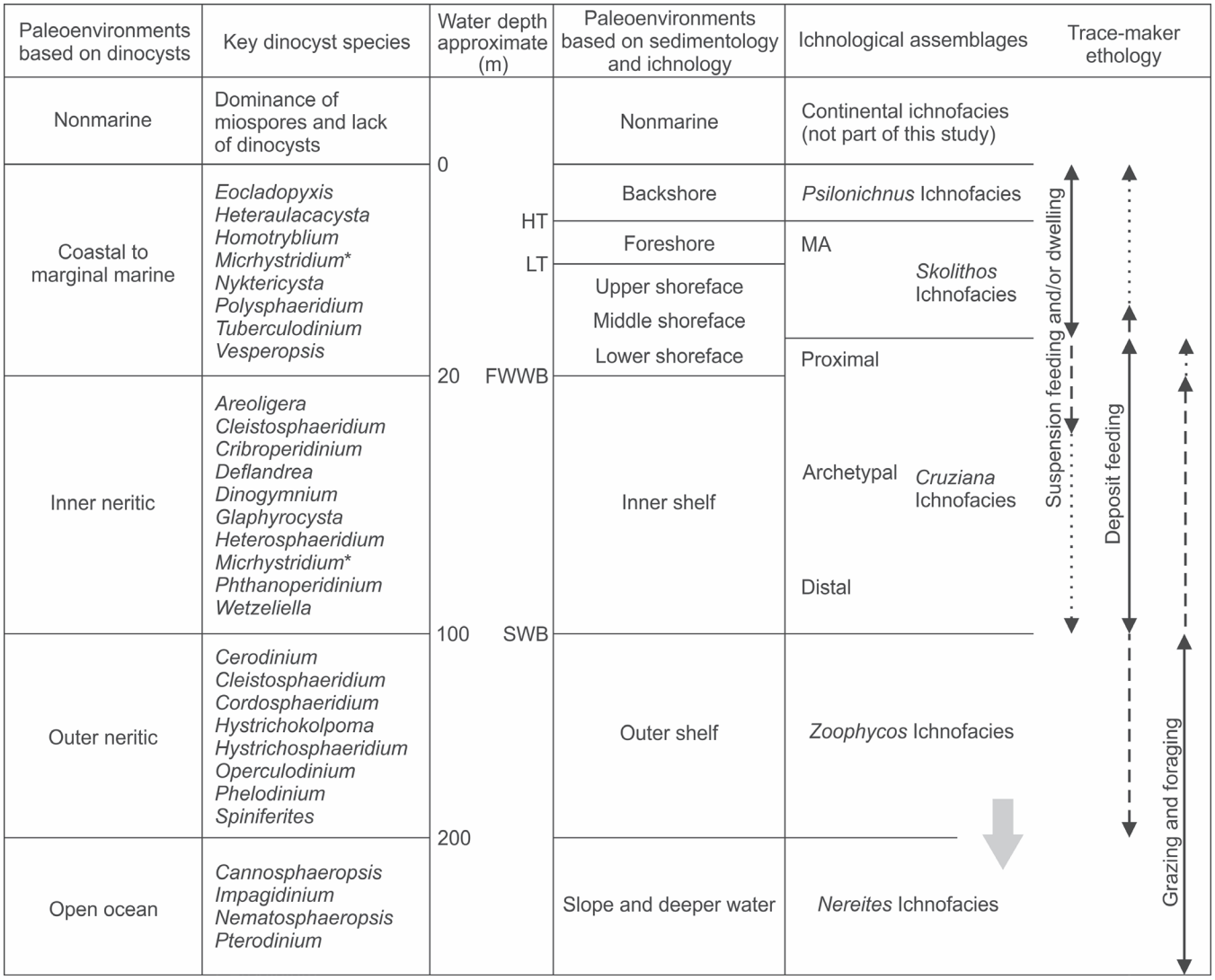


**Figure 3.** Paleoenvironmental comparison chart. The two leftmost columns show the paleoenvironments based on dinocysts and related key species from Nøhr-Hansen et al. (2016; * indicates acritarch taxa). The water depth is approximate and the high tide (HT), low tide (LT), fair-weather wave base (FWWB), and storm wave base (SWB) are also shown. Paleoenvironments based on sedimentology and ichnology from core observations and the related ichnological assemblages and trace-maker ethologies are *modified from* Pemberton et al. (2001) and shown to the right of the figure with the addition of the *Nereites* Ichnofacies. The *Macaronichnus* Assemblage (MA) can colonize the foreshore and the *Zoophycos* Ichnofacies can also be found beyond the shelf (as indicated by the grey arrow). In general, the ichnofacies are not necessarily restricted to the normal marine settings shown, but can also be found in other settings that might have similar environmental conditions such as deltas and restricted embayments.

## *Palynology*

The palynomorphs from two samples in core 1 were analyzed. The lower sample at 2159.1 m contains the miospores *Abiespollenites*, *Alnipollenites*, *Caryapollenites*, *Lycopodiumsporites*, and *Verrucosisporites*. This is a mixed assemblage, including some taxa — such as *Alnipollenites* and *Caryapollenites* — known only from the Cenozoic. Presumably *Alnipollenites* and *Caryapollenites* are contaminants from the drilling mud (Fig. 4), since this sample must be the same age or older than the sample at 2157.0 m. Overall, the dominance of miospores, the presence of one acritarch, and the absence of dinocysts leads to the conclusion that the paleoenvironment was terrestrial, with possible fluvial influence.

In the higher sample at 2157.0 m, miospores are the dominant palynomorphs. By far the most abundant of these are the bisaccates (conifer pollen), including *Abiespollenites*, *Parvisaccites*, *Piceapollenites*, and *Pinuspollenites*. There are three dinocysts specimens present, a peridiniacean, and two assignable to *Microdinium*, as well as a single acritarch, included here in the genus *Baltisphaeridium*. The age of the sample is unclear, but no younger than Barremian–Aptian because of the presence of the miospores *Cerebropollenites*

**Table 1.** Summary table of the 37 core intervals and their lithostratigraphic assignment, lithology, age, and paleoenvironmental interpretations from this study.

| Well | Core no. | Formation | Lithology | Age (this study or otherwise indicated) | Paleoenvironment | | |
|---|---|---|---|---|---|---|---|
| | | | | | From core observations | From palynological observations | Integrated interpretation |
| Gjoa G-37 | 1 | Unnamed basalt | Basalt and amygdaloidal basalt | 59.5 ± 1.0 Ma and 59.2 ± 1.8 Ma (Williamson and Villeneuve, 2002) | Subaerial basalt flow, possibly weathered | | |
| Hekja O-71 | 2 | Unnamed basalt | Volcaniclastic | Selandian | Subaerially weathered volcaniclastic accumulation | Marine | Shallow marine to possibly intermittently subaerially exposed lava delta |
| Hekja O-71 | 3 | Unnamed basalt | Basalt | 48.7 ± 1.3 Ma (Williamson and Villeneuve, 2002) | Hyaloclastic lava delta | | |
| | | | | | | | |
| Hekja O-71 | 1 | Gudrid | Coarse-grained sandstone | Latest Thanetian | Tidal channel | Nonmarine and marginal marine to inner neritic | Tidal channel with significant terrestrial influx |
| Karlsefni A-13 | 1 | Cartwright | Sandy mudstone | Selandian to Thanetian | Wave-influenced prodelta | Coastal or marginal marine to inner neritic | Wave-influenced prodelta |
| Ogmund E-72 | 1 | Gudrid (revised from Markland assignment) | Homogeneous sandstone | Basal Ypresian | Moderate to possibly high-energy setting | Coastal | Shoreface or delta front |
| Snorri J-90 | 1 | Gudrid | Bioturbated sandstone | Late Thanetian–earliest Ypresian | Storm-dominated proximal and distal delta front | Inner neritic | Storm-dominated proximal and distal delta front |
| | | | | | | | |
| Gilbert F-53 | 1 | Markland (Freydis Member) | Heterolithic sandstone and mudstone | Late Campanian | River-influenced distributary channels and distal delta front, as well as lagoonal | Inner to outer neritic | River-influenced distributary channels and distal delta front, as well as lagoonal |
| Gilbert F-53 | 2 | Markland (Freydis Member) | Heterolithic sandstones and shale | Late Campanian | River-influenced distributary channels and delta front | Inner neritic | River-influenced distributary channels and delta front |
| Roberval K-92 | 1 | Markland | Dark grey shale | Early Campanian most likely | Slope-equivalent water depth | Open ocean, deeper water | Open ocean, slope-equivalent water depth with distal terrestrial influx |
| Skolp E-07 | 1, 2 | Markland (and Freydis Member) | Medium grey shale | Maastrichtian | Proximal inner shelf to distal outer shelf or restricted marine bay | Inner neritic to neritic | Proximal inner shelf to distal outer shelf |
| Skolp E-07 | 3 | Markland | Medium grey shale and bioturbated sandy mudstone | Early Maastrichtian | Distal inner shelf to distal outer shelf | Inner neritic, marginal marine, deltaic | Distal inner shelf to distal outer shelf with deltaic influence |
| Skolp E-07 | 4 | Markland (Freydis Member) | Fine-grained, bioturbated sandstone | Indeterminate | Shoreface to inner shelf | Nonmarine | Shoreface to inner shelf |
| Skolp E-07 | 5 | Markland | Dark grey, sandy mudstone | Late Campanian | Proximal outer shelf | Neritic with deltaic influence | Proximal outer shelf with deltaic influence |
| | | | | | | | |
| Bjarni H-81 | 1 | Bjarni | Fine- to medium-grained sandstone | Barremian–Aptian | River-influenced delta | Nonmarine to deltaic | River-influenced delta with significant terrestrial influx |
| Bjarni O-82 | 1 | Bjarni | Interbedded volcanic rocks | Middle Albian–Cenomanian | Shallow aquatic volcanic rocks | Nonmarine | Shallow nearshore setting |
| Bjarni O-82 | 2 | Bjarni | Heterolithic sandstone and shale | Middle to late Albian | Delta front (possibly river-influenced) | Shallow to marginal marine | Delta front, possibly river-influenced |

**Table 1** (cont.)

| Well | Core no. | Formation | Lithology | Age (this study or otherwise indicated) | Paleoenvironment | | |
|---|---|---|---|---|---|---|---|
| | | | | | From core observations | From palynological observations | Integrated interpretation |
| Herjolf M-92 | 1 | Bjarni | Coarse-grained sandstone and thin shale | Albian | River-influenced delta front and distributary channels | Coastal to marginal marine | River-influenced delta front and distributary channels |
| Herjolf M-92 | 2 | Bjarni | Brown-grey shale | Barremian–Aptian | Restricted marine bay | Nonmarine to marginal marine | Restricted marine bay, highly brackish |
| Hopedale E-33 | 1 | Bjarni | Dark grey shale | Early Aptian to early Albian or older | Restricted marine bay and bayhead delta | Nonmarine | Restricted marine bay and bayhead delta, highly brackish |
| North Bjarni F-06 | 1 | Bjarni | Massive, pebbly sandstone | Early Albian or older | Fluvial, alluvial or deltaic | Marginal marine | Deltaic, possibly river-influenced |
| North Leif I-05 | 1 | Bjarni | Heterolithic sandstone, siltstone, and shale | Middle–late Albian | River-dominated distal delta front | Nonmarine | River-dominated distal delta front, highly brackish |
| North Leif I-05 | 2 | Bjarni | Dark grey shale | Middle–late Albian | River-dominated prodelta | Nonmarine | River-dominated prodelta, highly brackish |
| Ogmund E-72 | 2 | Bjarni | Heterolithic sandstone and mudstone | Early and middle–late Albian | Wave-influenced distal delta front | Nonmarine to marginal marine | Wave-influenced distal delta front |
| Ogmund E-72 | 3 | Bjarni | Matrix-supported conglomerate | Aptian | Alluvial | Marginal marine | High-energy shoreface or delta front |
| Roberval K-92 | 2 | Bjarni | Heterolithic sandstone and siltstone | Early Albian or older | River-influenced delta front | Nonmarine to marginal marine | River-influenced delta front |
| Skolp E-07 | 6 | Bjarni | Sandstone and conglomerate | Aptian | Fluvial and channel abandonment | Nonmarine | Fluvial and channel abandonment |
| Tyrk P-100 | 1 | Bjarni (revised from Gudrid Formation assignment) | Medium grey shale | Middle to late Albian to late Albian | Distal outer shelf or restricted marine bay | Nonmarine | Restricted marine bay or lagoon |
| | | | | | | | |
| Bjarni H-81 | 2 | Alexis | Green-black basalt | 122 ± 6 Ma (~Aptian; Corgnet and McWhae, 1973) | Subaerial basalt flow | | |
| Bjarni H-81 | 3 | Alexis | Red-brown to olive green basalt | 139 ± 7 Ma (~Valanginian; Corgnet and McWhae, 1973) | Subaerial basalt flow, possibly weathered | | |
| Herjolf M-92 | 3 | Alexis | Green-brown basalt | 121 ± 5 Ma (Umpleby, 1979) | Basalt flows | | |
| | | | | | | | |
| Gilbert F-53 | 3 | Basement | Gneiss | 3742 ± 12 Ma (Wasteneys et al., 1996) | | | |
| Herjolf M-92 | 4 | Basement | Granodiorite | 1801.4 ± 5 Ma (Wasteneys et al., 1996) | | | |
| Karlsefni A-13 | 2 | Basement | Gneiss | 2680 Ma (Wasteneys et al., 1996) | | | |
| Skolp E-07 | 7 | Basement | Gneiss | 3213 +21/-3.6 Ma (Wasteneys et al., 1996) | | | |
| Tyrk P-100 | 2 | Basement | Granite | 1864.4 ± 3.1 Ma and 1839.1 ± 4.7 Ma (Wasteneys et al., 1996) | | | |

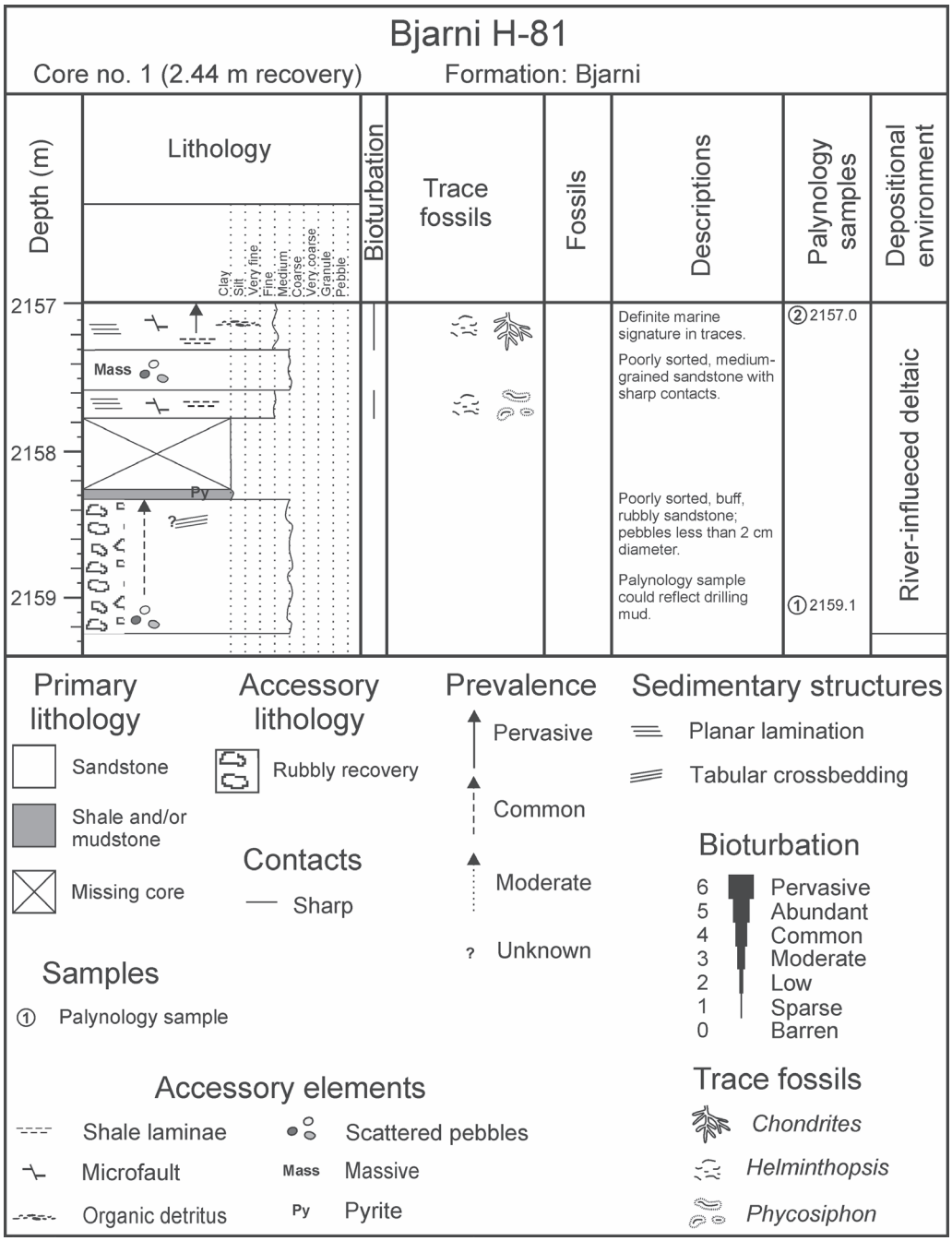


**Figure 4.** Log of core 1, Bjarni H-81. The lower section of the core is rubbly and a portion of the middle of the core is missing.

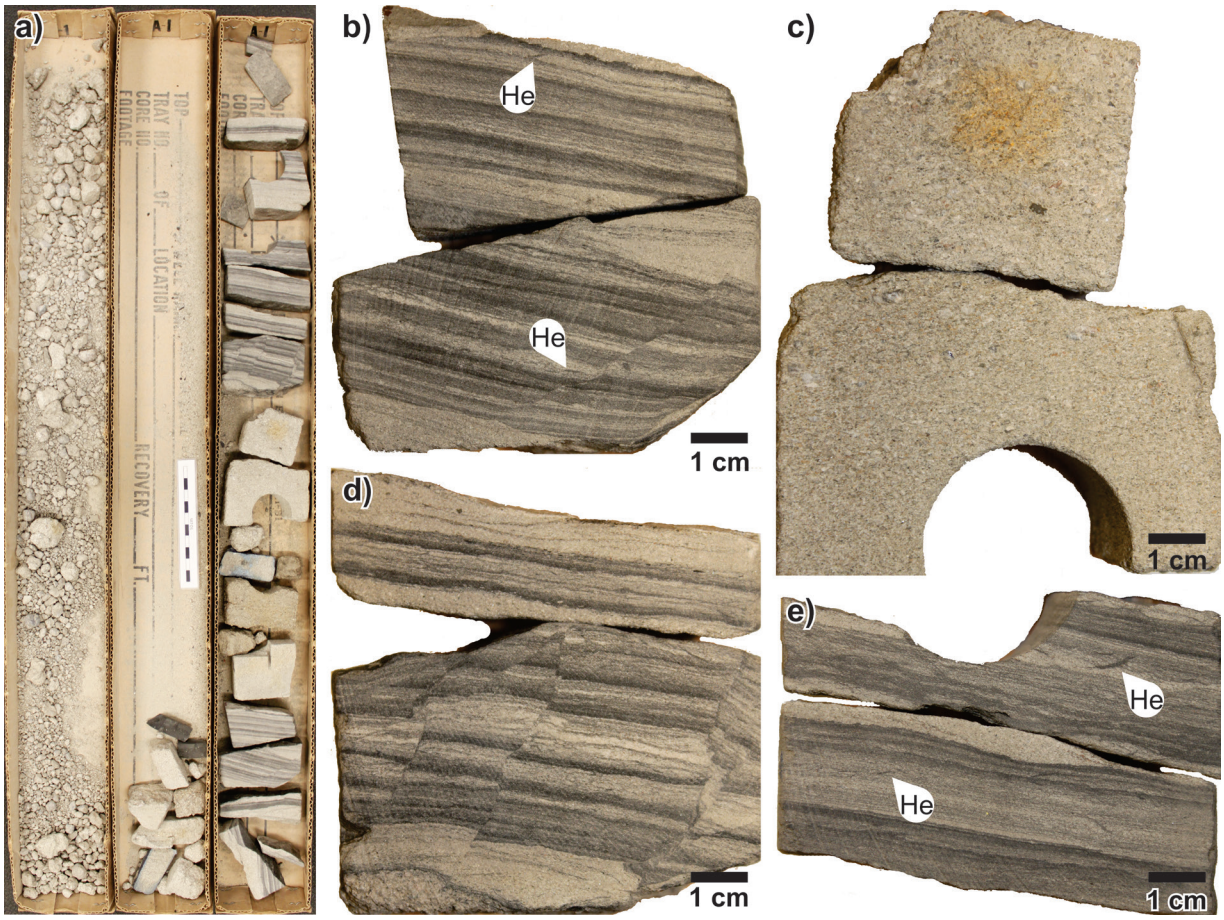


**Figure 5.** Photographs of core 1, Bjarni H-81. **a)** Core box sleeves containing the core materials with a significant portion of box 2 missing core (scale bar = 10 cm). NRCan photo 2019-291. **b)** Finely laminated, fine-grained sandstone and mudstone and/or siltstone layers with microfaulting and rare *Helminthopsis* (He) traces. NRCan photo 2019-292. **c)** Massive, medium-grained sandstone with rare granules. NRCan photo 2019-293. **d)** Finely laminated sandstone and mudstone with microfaulting suggesting high sedimentation rates. NRCan photo 2019-294. **e)** Laminated sandstone and siltstone and/or mudstone with prominent, large *Helminthopsis* traces (He). NRCan photo 2019-295. All photographs by L.T. Dafoe.

*macroverrucatus* and *Parvisaccites amplus*. This accords with the findings of Nøhr-Hansen et al. (2016), who placed the last occurrences of these taxa within the Aptian. Although the assemblage is not especially diverse or abundant, the dominance of the bisaccates with only three dinocysts and one acritarch suggests a very shallow, nearshore or deltaic paleoenvironment. A large amount of vitrinite, which is consistent with a marked influx of terrestrial material, tends to support a deltaic interpretation.

### *Summary*

From cuttings, this interval of the Bjarni Formation was dated as (?)Barremian–Aptian by Williams (1979a), consistent with this study's findings of Barremian–Aptian. Previous interpretations from cuttings suggest a nonmarine braided fluvial to possible alluvial fan (Miller and D'Eon, 1987) or supralittoral (Robertson Research (North America) Ltd., 1974) setting. From the present core interpretation, a river-influenced, deltaic setting generally agrees with a terrestrial influence, but places it in a shallow-marine setting. The palynological analysis of a nonmarine to possibly deltaic setting agrees with results from current core observations, but brackish conditions likely hampered dinocyst abundances.

## *Core 2: green-black basalt (2271.4–2275.36 m)*

### *Core description and interpretation*

The second core of Bjarni H-81 comprises basalt, some amygdaloidal, that is green to black with some rubbly sections (Fig. 6). Circular to irregularly shaped vesicles are filled

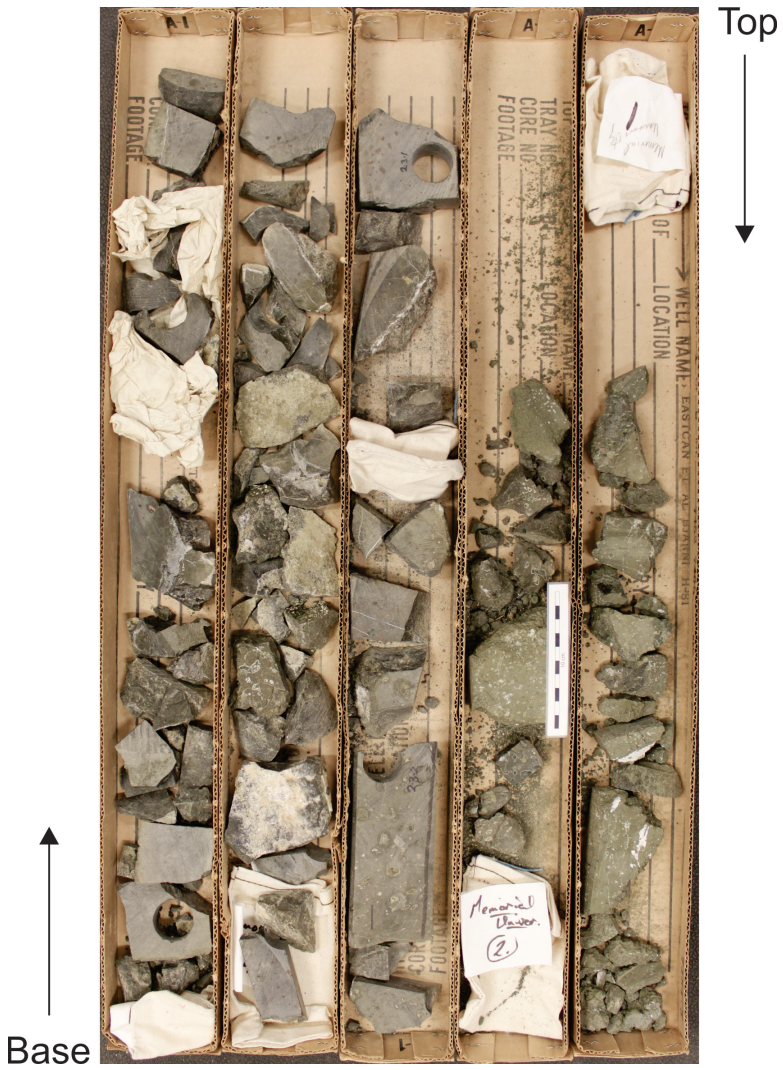


**Figure 6.** Photograph of core 2, Bjarni H-81. Scale bar = 10 cm. NRCan photo 2019-296. Photograph by L.T. Dafoe.

with white to pink or red zeolite minerals (Fig. 7). Amygdales tend to increase in prevalence upward; some amygdales are rimmed and infilled with a distinctly different, dark-coloured mineral. Fractures (Fig. 7e) are present near the base of the core in the intervals of solid basalt.

These rocks represent the Alexis Formation. The increase in vesicles toward the top of the core suggests increased gas content and may reflect a location in the uppermost part of a subaerial basalt flow. This portion of the core also appears to be more weathered than the base of the core. Potassium-argon dating for a sample of the core placed it at 122 ± 6 Ma (approximately Aptian; Corgnet and McWhae, 1973).

## *Core 3: red-brown to olive green basalt (2511.28–2515.24 m)*

### *Core description and interpretation*

Similar to core 2, the lowermost core 3 in Bjarni H-81 is represented by red-brown to olive green basalt (Fig. 8). Overall the core is in fair condition with some rubbly sections. Fractures are rare, and the basalt is primarily amygdaloidal. The size of the filled vesicles increases toward the top of the core, and white to pink zeolite minerals form the amygdale infills (Fig. 8c).

Core 3 also represents basalt of the Alexis Formation. The subaerial lava flows possessed a high gas content, resulting in the vesicular to amygdaloidal texture of the rock. The rubbly

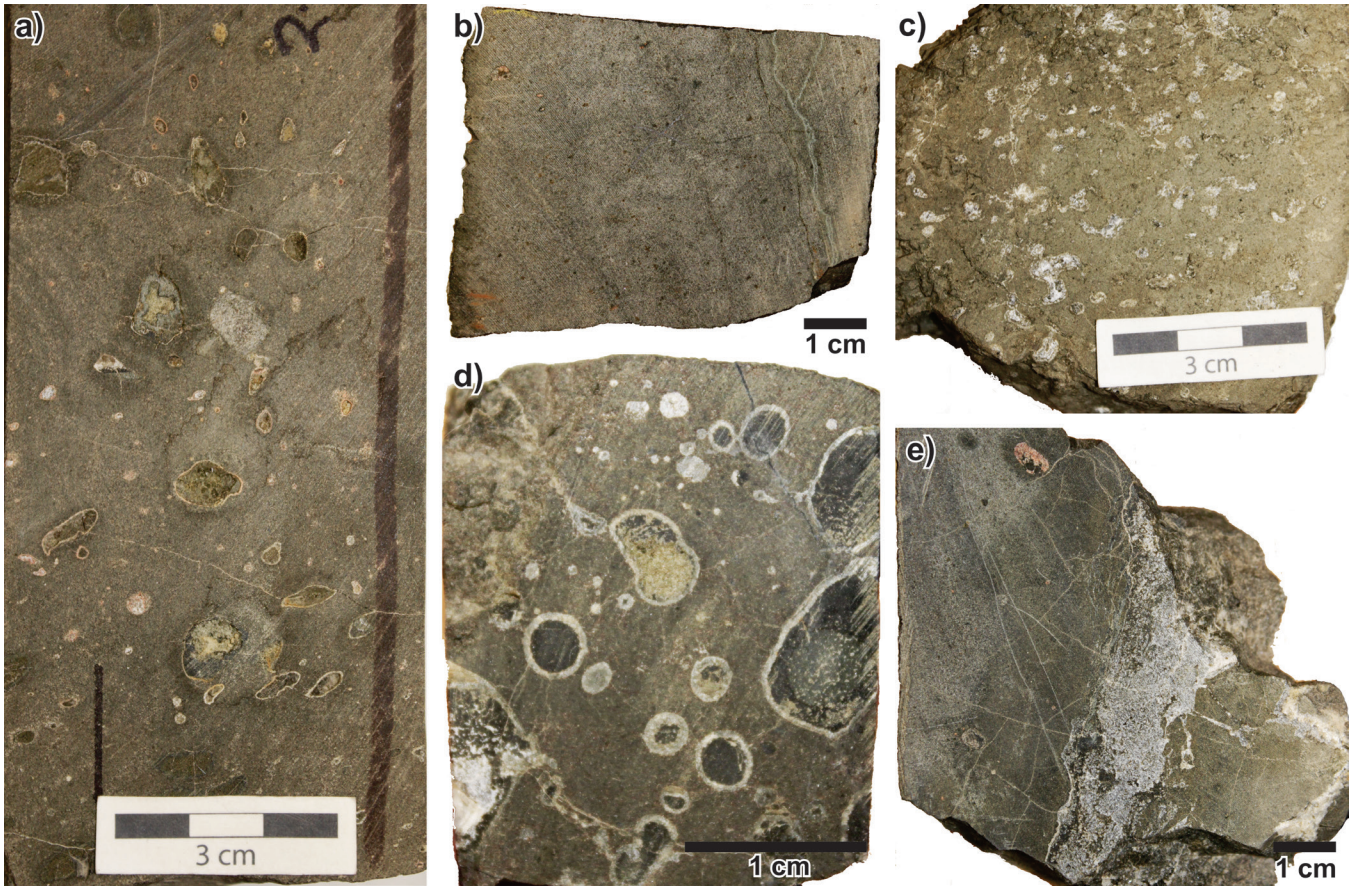


**Figure 7.** Photographs of core 2, Bjarni H-81. **a)** Amygdaloidal green-brown basalt with zeolite mineral infills or partial infills. NRCan photo 2019-297. **b)** Grey-brown, fine-grained basalt. NRCan photo 2019-298. **c)** Weathered green-brown, amygdaloidal basalt. NRCan photo 2019-299. **d)** Well preserved circular vesicles with zeolite mineral rims and secondary infills with a darker (unknown) mineral infill. NRCan photo 2019-300. **e)** Large fracture in fresh basalt with minor infilled vesicles. NRCan photo 2019-301. All photographs by L.T. Dafoe.

nature and reddish coloration may indicate some subaerial exposure and weathering of the basalt. Potassium-argon dating from a sample of this basalt gave an age of 139 ± 7 Ma (approximately Valanginian; Corgnet and McWhae, 1973). Cores 2 and 3 are separated by over 300 m of basalt and numerous flows, but the lava flows do not likely represent 17 Ma of accumulation. It is known that potassium-argon age dating from whole-rock analyses does not necessarily provide results that are as accurate as the more modern Ar-Ar techniques (Lee, 2014), so these ages are somewhat suspect.

## Bjarni O-82

Bjarni O-82 was drilled in the Hopedale Basin, offshore Labrador, in 1979 and reached a total depth of 2650 m (Fig. 1). The exploration target was the potentially gas-bearing Bjarni structure (Total Eastcan Exploration Ltd., 1979a). Two core intervals were recovered within Mesozoic rocks near the top of the Bjarni Formation.

### *Core 1: interbedded volcanic rocks (2291.0–2293.0 m)*

#### *Core description and interpretation*

Core 1 of the Bjarni Formation consists of interbedded bands of white to buff, tuffaceous material and dark grey to black basalt. The basalt is very fine grained and glassy in places with small mineral fragments present at some intervals (Fig. 9, 10). The basaltic bands are generally thin (1–2 cm), but may be locally thicker, are sharp-topped (Fig. 10b, c, d), and are incorporated into the underlying, white to buff tuffaceous layers (Fig. 10d). Locally, fragments of tuffaceous material appear to be intermixed with the basalt. The tuffaceous material is more thickly banded (1–3 cm on average; Fig. 10b, c, d, e) than the basalt, but the layers are distorted, apparently lensoidal in places, likely reflecting the overlying emplacement of basaltic bands. The tuffaceous layers are softer, contain small mineral fragments, and appear to be locally banded (Fig. 10e). At its upper end, the core is more rubbly, light pinkish grey, and may reflect a weathered horizon (Fig. 10a).


**Figure 8.** Photographs of core 3, Bjarni H-81. **a)** Core box sleeves with red-brown to olive green basalt, showing the rubbly and weathered nature of the core (scale bar = 10 cm). NRCan photo 2019-302. **b)** Close-up of fine-grained, fractured basalt. NRCan photo 2019-303. **c)** Weathered amygdaloidal basalt with white to pink zeolite mineral infills. NRCan photo 2019-304. All photographs by L.T. Dafoe.

The presence of volcanic rocks at this interval is unexpected and inconsistent with other wells in the general vicinity that do not contain volcanic rocks above the Early Cretaceous Bjarni Formation. Based on the cuttings analysis by Canstrat, the cored interval falls within a sandstone- and shale-dominated succession. Due to the well preserved alternation of beds and presence of tuff and glassy (quickly quenched) basalt, this interval may reflect emplacement of air-fall tuffs within a shallow aquatic setting (D. Piper, pers. comm., 2014).

## *Thin-section analysis*

Two thin sections from 2292.40 m and 2293.05 m were studied for overall mineralogy and texture (Fig. 11). In these, minerals such as plagioclase, microcline, quartz, and possibly sanidine were noted. Overall, the sections show a layered texture alternating with dark fine-grained units and lighter coloured, coarse-grained units. Analysis of thin sections confirmed the presence of pumice and ash, and thus of volcanic or volcaniclastic material.

## *Palynology*

Two samples from core 1 were analyzed for palynomorphs. The lower from 2292.46 m is devoid of dinocysts and contains only the coniferous pollen *Pinuspollenites* and *Piceapollenites*. These pollen cannot be used for precise age control. They also provide limited information on paleoenvironments, since they can be transported by wind over vast distances, even into the mid-oceanic realm.

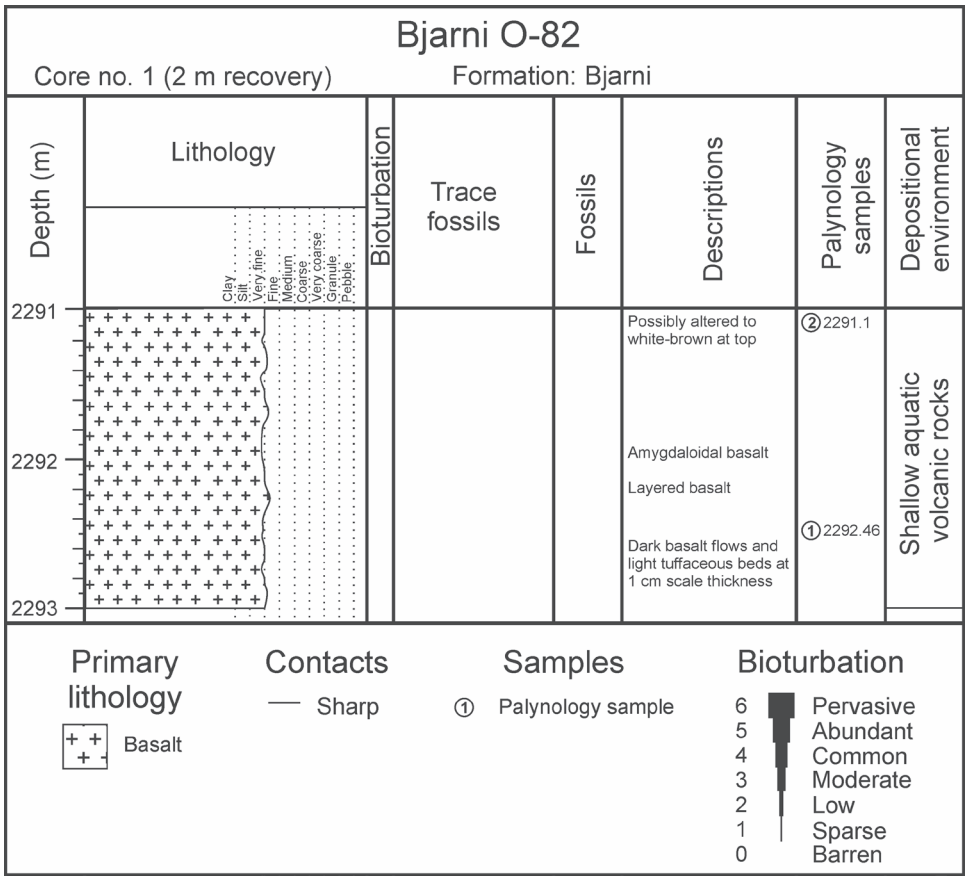


**Figure 9.** Log of core 1 Bjarni O-82, comprising interbedded tuffaceous and basalt layers.

The upper sample from 2291.1 m also contains only pollen, with taxa including *Alnipollenites verus*, *Betulaepollenites*, *Caryapollenites*, *Gothanipollis* sp., *Momipites tenuipolus*, *Momipites ventifluminus*, *Ostryoipollenites* sp., *Pterocaryapollenites*, and *Retitricolpites vulgaris*. All of these except for the last one are predominantly Cenozoic taxa. Frederiksen and Christopher (1978) stated that *Momipites tenuipolus* is restricted to the Paleocene. Nichols (2003) considered *Momipites ventifluminus* to be later Paleocene. According to Singh (1971), *Retitricolpites vulgaris* has a stratigraphic range of middle Albian to Cenomanian. The overall evidence suggests that the age of the sample is Paleocene, with *Reticolpites vulgaris* being reworked. The absence of dinocysts in both samples indicates a nonmarine paleoenvironment.

## *Summary*

Core 1 of the Bjarni Formation lies just above the interval identified as Turonian–Coniacian by Williams (2007d) and Bujak Davies Group (1989b) and below their Campanian picks. Also based on cuttings, Robertson Research Canada Ltd. (1980) dated the interval sampled by core 1 as Early Cretaceous. The interpretation from the core suggests a vastly different age of Paleocene; however, considering that Williams (2007d) did not find Paleocene rocks in the well until 2155 m (over 100 m above core 1), core 1 is unlikely Cenozoic and drilling mud contamination may have occurred within the softer tuffs. Accordingly, the sample may instead reflect the range of *Retitricolpites vulgaris* of middle Albian to Cenomanian age (and still within the Bjarni Formation). The unusual lithology may alternatively suggest that palynomorph contamination has taken place, but cannot be confirmed. Previous interpretations of the paleoenvironment within cuttings suggested a marginal marine to inner shelf (Miller and D'Eon, 1987) or an outer neritic to open ocean setting (Williams, 2007d). The lithology suggests that the unit may reflect air-fall tuffs in a shallow aquatic setting and a nonmarine origin is suggested by palynological analyses in the present study; however, the core is situated between the underlying shallow-marine Bjarni Formation rocks of core 2 (*see* below) and overlying deeper marine rocks of the Markland Formation, indicating that a nonmarine setting is unlikely. Accumulation of the alternating volcaniclastic layers would appear to be more consistent with a quiet water, possibly nearshore setting. In general, volcanic rocks near the top of the Bjarni Formation is an unusual occurrence.

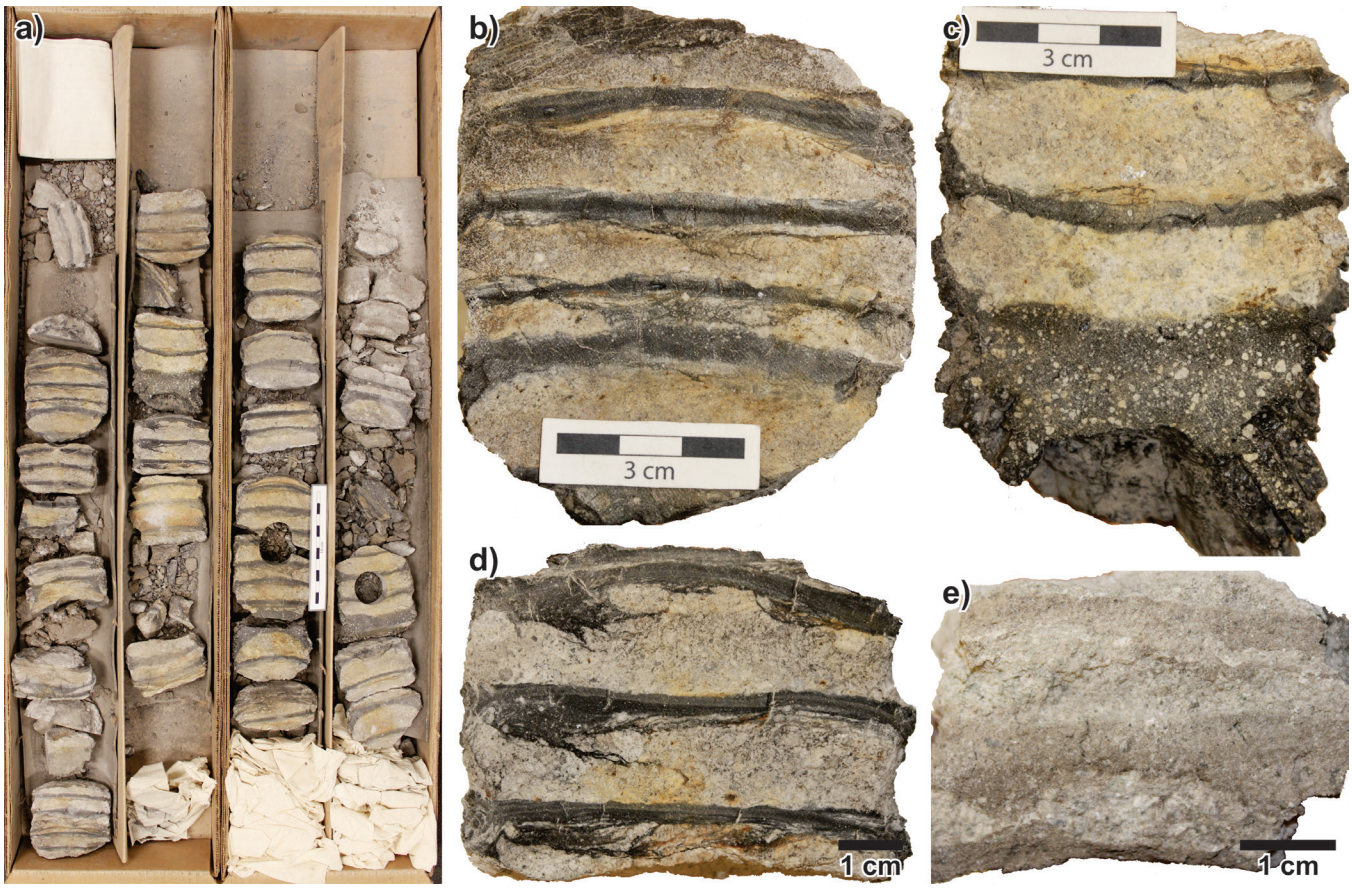


**Figure 10.** Photographs of core 1, Bjarni O-82. **a)** Total remaining core (scale bar = 10 cm). NRCan photo 2019-305. **b)** Interbedded basalt and white to buff tuffaceous material. NRCan photo 2019-306. **c)** A thick glassy unit with mineral fragments. NRCan photo 2019-307. **d)** Intermixing of layered basalt units (rapidly quenched) with tuffaceous material. NRCan photo 2019-308. **e)** A thick tuff bed with mineral fragments present. NRCan photo 2019-309. All photographs by L.T. Dafoe.

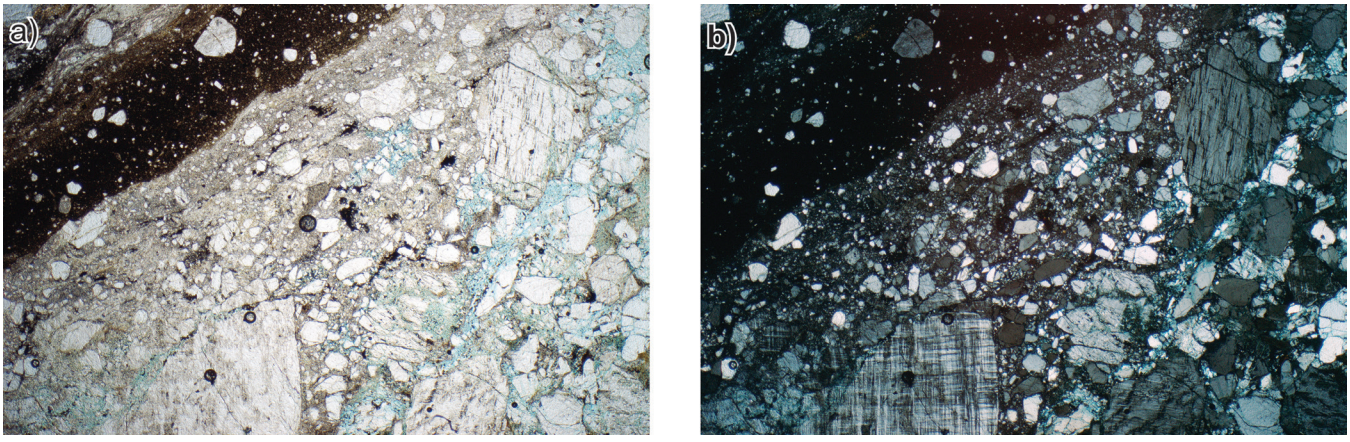


**Figure 11.** Thin-section photographs of core 1, Bjarni O-82 from 2292.4 m **a)** in plain light and **b)** polarized light at 2.5x magnification. A dark, fine-grained layer, seen in the upper left, alternates with a coarser quartz and feldspar-rich layer, seen in the lower right. NRCan photo 2019-310, 2019-311, respectively. Both photographs by L.T. Dafoe.

## *Core 2: heterolithic sandstone and shale (2293–2304 m)*

### *Core description and interpretation*

Although recovery of the Bjarni Formation within core 2 (0.3 m) from Bjarni O-82 was poor, the overall condition of the core is good (Fig. 12, 13). The succession shows a coarsening-upward trend, from a shale-dominated unit toward the base to a sandstone-dominated unit at the top (Fig. 13a). Scattered granules and pebbles occur throughout and may be related to the volcaniclastic material seen in core 1 that directly overlies this core (with some missing core likely separating the two cored intervals). Overall, the core is finely laminated, with some thicker, perhaps convoluted beds containing coarser grained clastic material (Fig. 13). Loading is seen at the base of coarser grained units, although compaction may also have had a role in the distortion of the beds.

This core interval yields limited sedimentological information. Heterolithic mudstone and sandstone units indicate changing sediment supply and/or current energy. Some thicker mudstone laminae may reflect hyperpycnal or hypopycnal conditions typical of deltaic settings. Coarse-grained clasts indicate reworking or high-energy conditions. Accordingly, the presence of coarse-grained material intermixed with heterolithic sandstone and shale may suggest a delta-front setting. Bioturbation is absent, which may indicate a highly brackish (environmentally stressful) marine setting or changes in water chemistry related to the onset of volcanism as suggested by the overlying core 1 interval.

### *Palynology*

A single sample from 2293.3 m in core 2 yielded a few dinocysts, as well as miospores and one specimen of *Tasmanites*, a prasinophyte alga. Dinocyst taxa include *Spiniferites ramosus* and several unidentified forms possibly assignable to the genera *Palaeocystodinium* and *Xenascus*. The presence of the miospores *Cicatricosisporites augustus*, *Parvisaccites radiatus*, and *Rugubivesiculites reductus* are indicative of a middle to late Albian age. Pedersen and Nøhr-Hansen (2014) placed the first or oldest occurrence of the genus *Rugubivesiculites* within the Albian. Nøhr-Hansen et al. (2016) considered the last or youngest occurrence of *Parvisaccites radiatus* to be around the top of the Aptian; however, oldest occurrences are usually more reliable. Although the recovery of palynomorphs is sparse, the dominance of miospores suggests a nearshore setting. The few dinocysts indicate a probable shallow to marginal marine paleoenvironment.

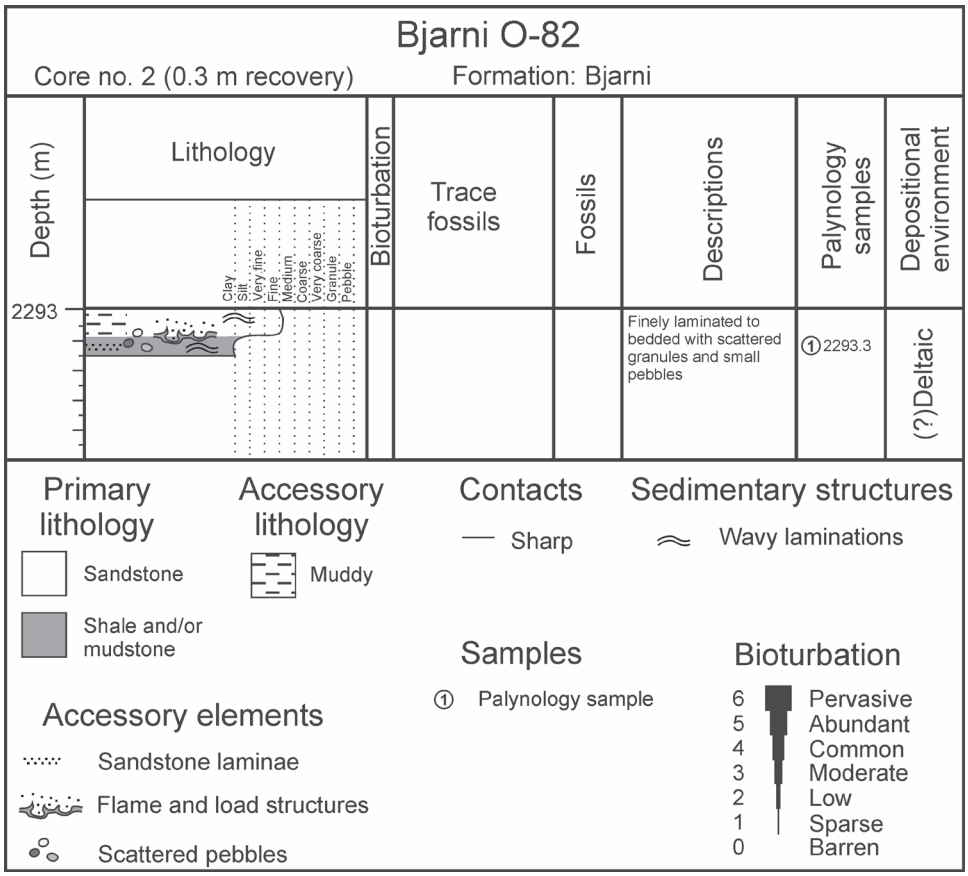


**Figure 12.** Log of core 2 from Bjarni O-82.

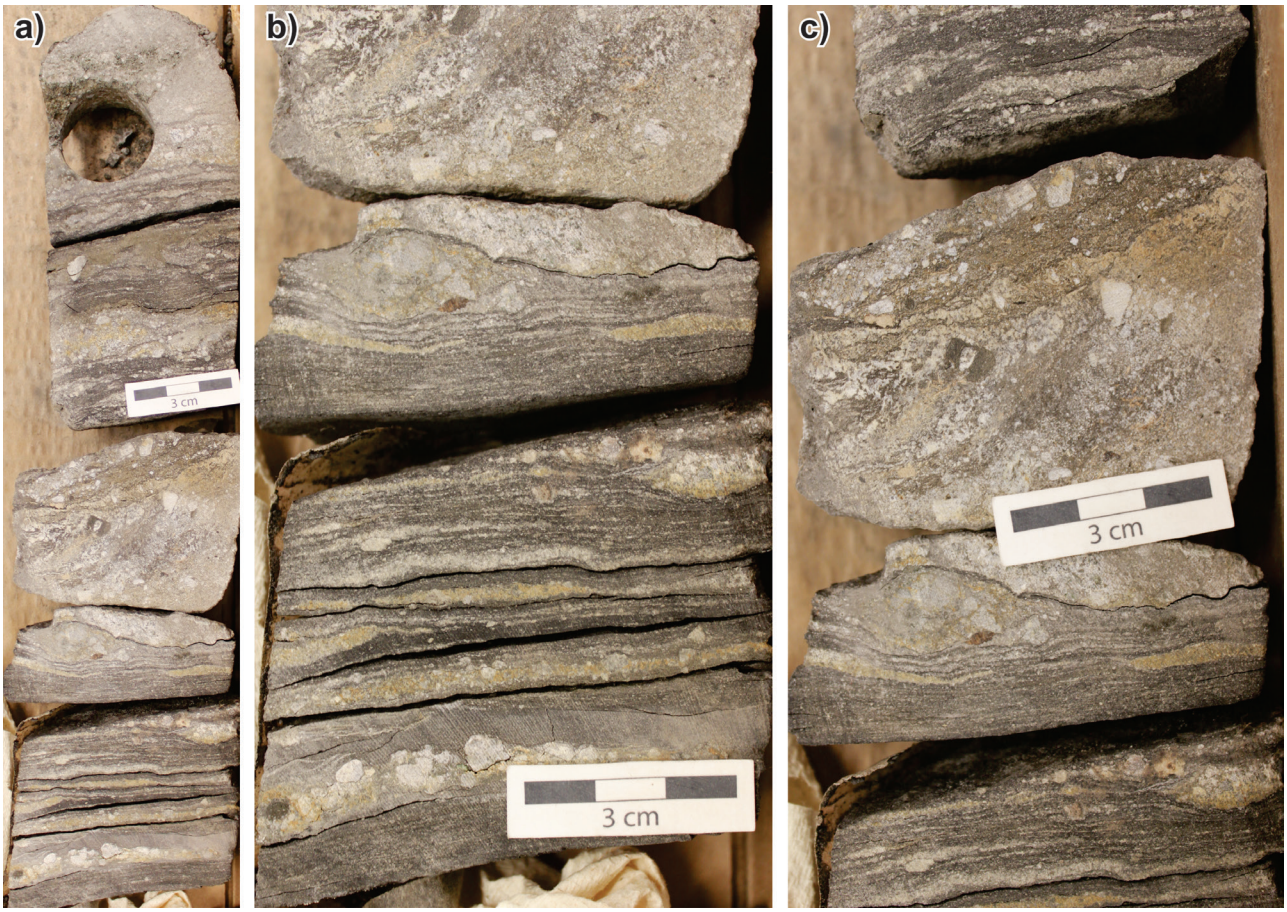


**Figure 13.** Photographs of core 2, Bjarni O-82. **a)** Core box. NRCan photo 2019-312. **b)** Close-up of finely laminated shale and thin sandstone. NRCan photo 2019-313. **c)** Thicker, deformed, sandstone bed with sub-angular clasts. NRCan photo 2019-314. All photographs by L.T. Dafoe.

*Summary*

Williams (2007d) interpreted the interval sampled by core 2 as Turonian–Coniacian based on analysis of cuttings samples within the Bjarni Formation; however, samples from the core suggest a middle to late Albian age, consistent with the broad Early Cretaceous assignments of Robertson Research Canada Ltd. (1980). In order to rationalize the well constrained age from conventional core with those from cuttings, it is likely that the underlying (?)Cenomanian and Turonian–Coniacian intervals of Williams (2007d) reflect cavings from either a horizon above the cored interval or from reworked palynomorphs within Upper Cretaceous rocks above it. The presence of a few dinocysts, indicating marginal marine conditions, confirms the delta-front interpretation from core observations. Previous interpretations of the paleoenvironment from cuttings are the same as for core 1 (both shallow and distal marine), and results of the current study are broadly consistent with that of Miller and D'Eon (1987). More specifically, comparison to the other Bjarni Formation cores from nearby wells (e.g. Herjolf M-92, *see* below) suggests a similar river-influenced deltaic setting is plausible. Ample fluvial influx could account for highly brackish conditions, resulting in a paucity of infaunal reworking and a limited dinocyst assemblage.

## Gilbert F-53

Gilbert F-53 was drilled in the southern Saglek Basin, offshore Labrador, in 1979–1980 (Fig. 1). The objective was to test the potential of the lower Paleozoic and/or Upper Cretaceous intervals in a structural closure (Total Eastcan Exploration Ltd., 1979b); total depth was 3608 m. Two core intervals were recovered from the Upper Cretaceous Freydis Member of the Markland Formation.

### *Core 1: heterolithic sandstone and mudstone (3251–3258 m)*

*Core description and interpretation*

Core 1 within the Freydis Member of the Gilbert F-53 well (Fig. 14) can be subdivided into three facies: predominately massive sandstone, shale, and heterolithic sandstone and mudstone (Fig. 15). The base of the well is characterized by the dark grey to black shale to mudstone, which is locally fissile and/or friable and contains rare organic detritus and slickensides (Fig. 16a). No bioturbation was recorded from this facies.

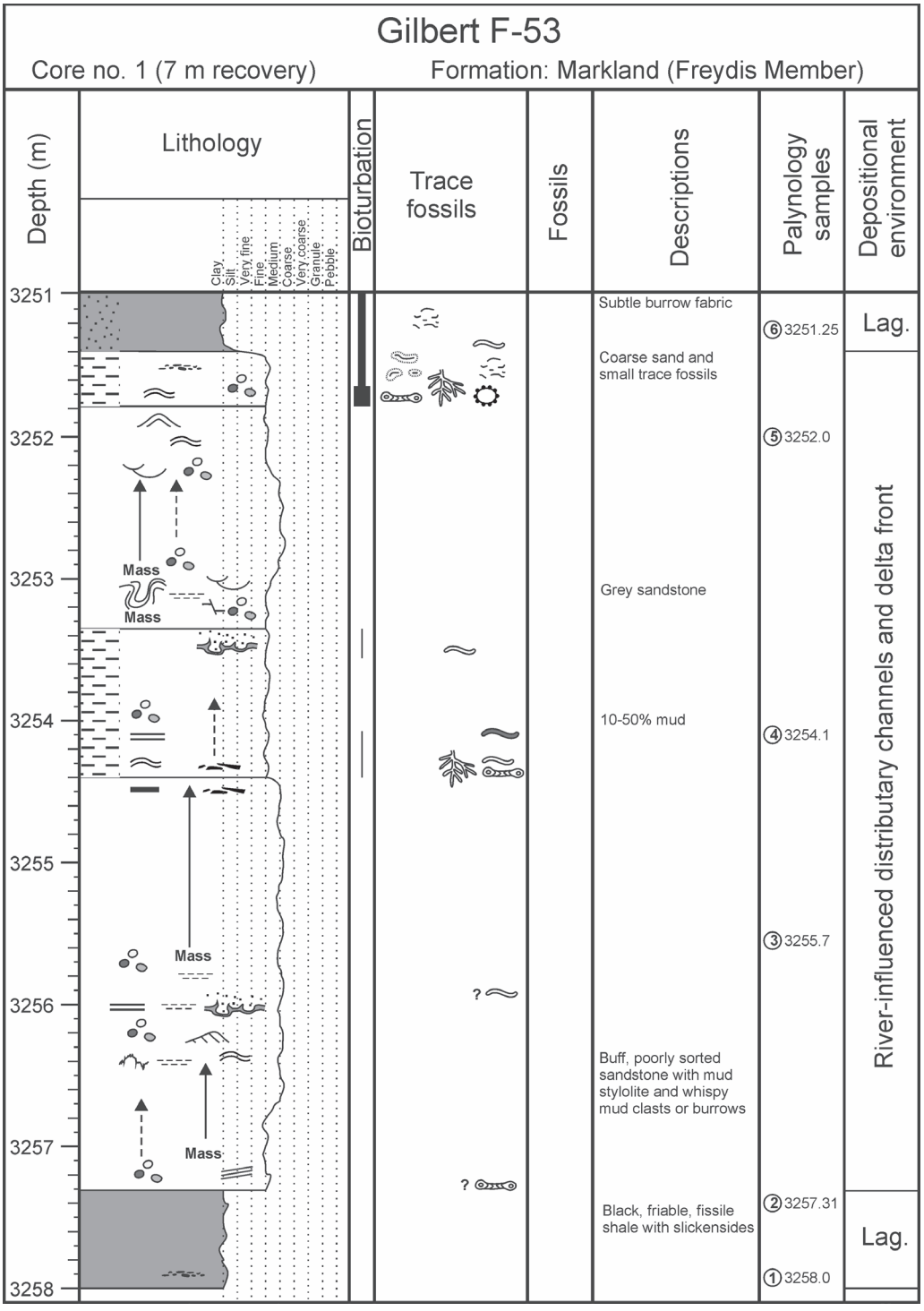


**Figure 14.** Log of core 1 from Gilbert F-53 comprising sandstone and shale facies. Lag. = lagoonal.

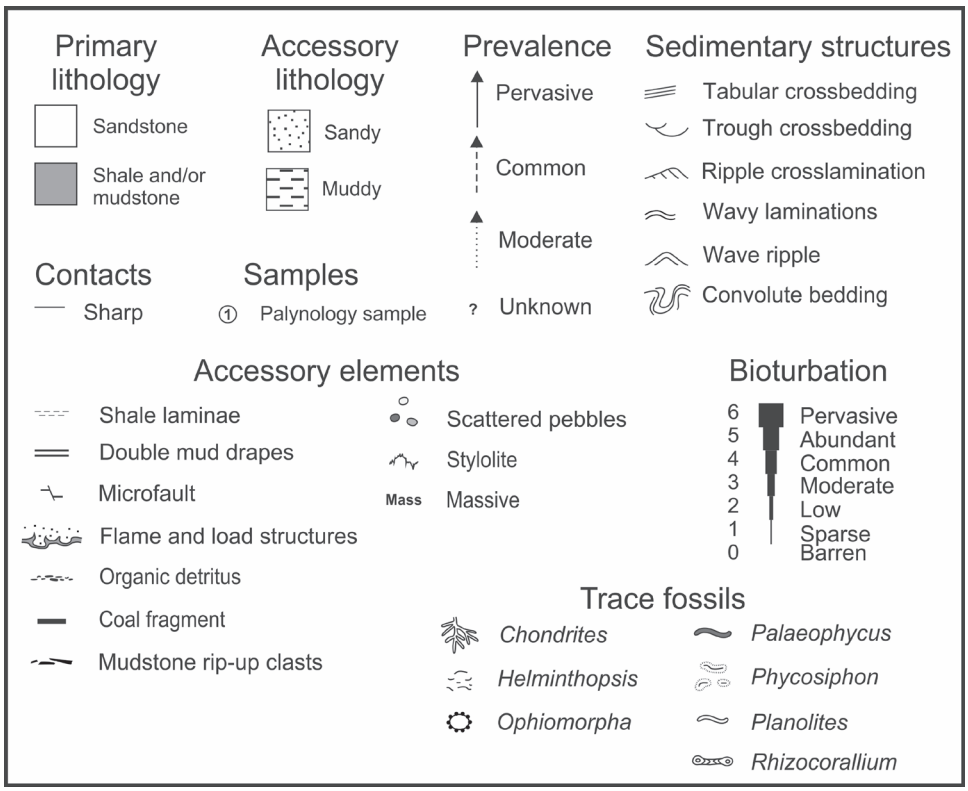


**Figure 14.** (cont.)


**Figure 15.** Photographs of core 1, Gilbert F-53. Scale bar = 10 cm. NRCan photo 2019-315, 2019-316. Both photographs by L.T. Dafoe.

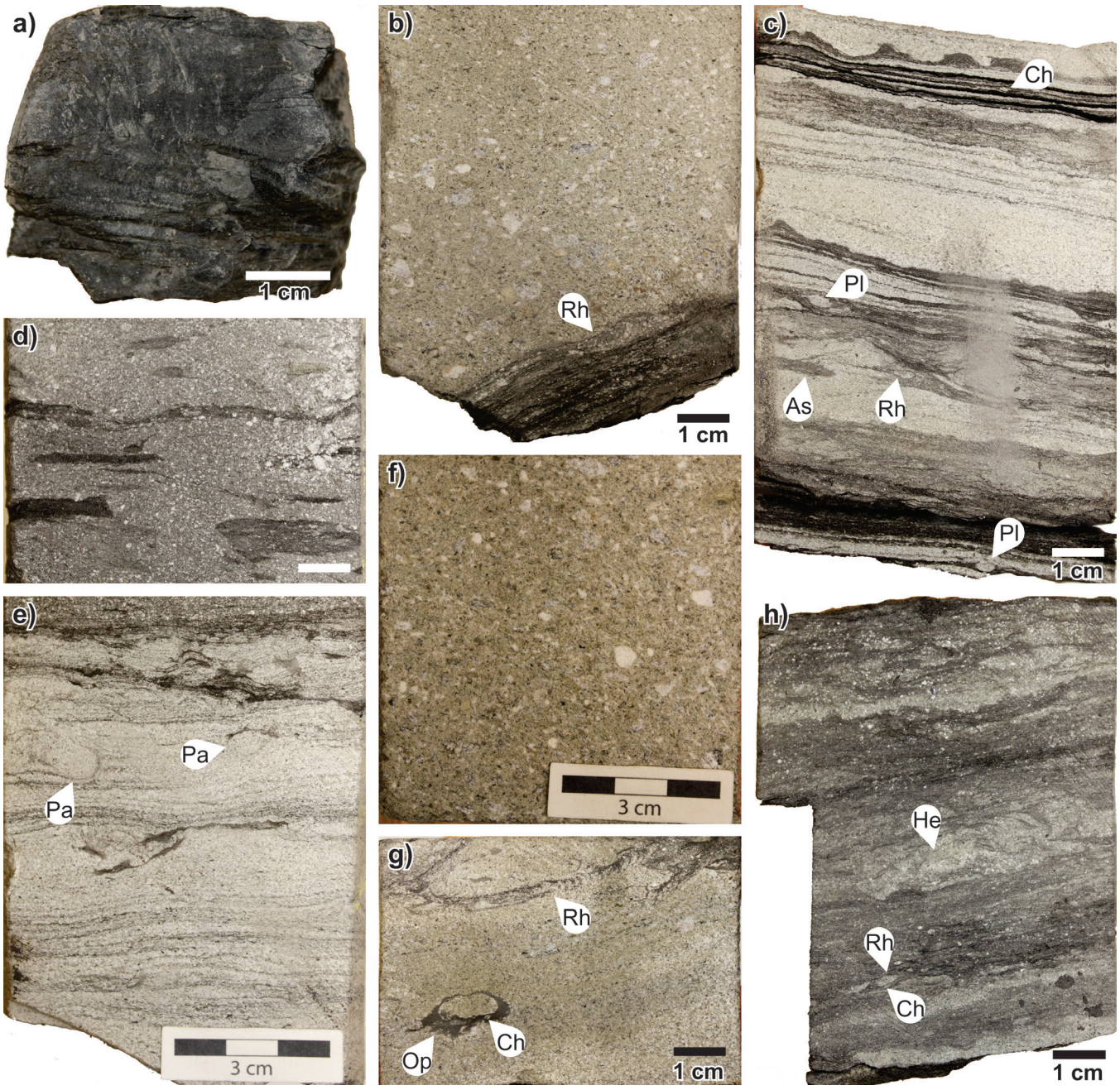


**Figure 16.** Photographs of core 1, Gilbert F-53. **a)** Shale and/or mudstone facies at the base of the core. NRCan photo 2019-317. **b)** Crossbedded to massive sandstone with granules and small pebbles lying atop the facies seen in Figure 16, with *Rhizocorallium* (Rh) at the interface. NRCan photo 2019-318. **c)** Heterolithic sandstone and mudstone unit with planar parallel laminations, load casts, and flame structures near the top of the core and bioturbation including *Asterosoma* (As), *Chondrites* (Ch), *Planolites* (Pl), and *Rhizocorallium* (Rh). NRCan photo 2019-319. **d)** Mudstone rip-up clasts of the heterolithic facies. NRCan photo 2019-320. **e)** Wavy-laminated fine-grained sandstone with thin carbonaceous mudstone interrupted by bioturbation including *Palaeophycus* (Pa). NRCan photo 2019-321. **f)** Granule-bearing, medium-grained sandstone. NRCan photo 2019-322. **g)** Fine-grained sandstone with clear *Ophiomorpha* (Op) reburrowed by *Chondrites* (Ch) and below *Rhizocorallium* (Rh). NRCan photo 2019-323. **h)** Uppermost mudstone-dominated facies with *Helminthopsis* (He), *Chondrites* (Ch), and *Rhizocorallium* (Rh). NRCan photo 2019-324. All photographs by L.T. Dafoe.

The sandstone, which is buff and well to poorly sorted with varying degrees of incorporated granules or small pebbles (Fig. 16f), consists of more common coarsening-upward and less common fining-upward beds of fine- to medium-grained sandstone. Overall, this facies is generally characterized by massive bedding with lesser amounts of crossbedding (Fig. 16b), current-ripple crosslamination, wavy laminations, wave ripples, and trough crossbedding. Carbonaceous mudstone laminae are rare and sometimes associated with stylolites, soft-sediment deformation, microfaulting, mudstone rip-up clasts, and convoluted bedding. Bioturbation is very rare, but there is some evidence of *Rhizocorallium* (Fig. 16b) at the boundary with the underlying shale facies, as well as possible *Planolites*.

The heterolithic facies (Fig. 16c, d, e, h) is characterized by fine-grained sandstone and mudstone with 10–80% mud content. This facies is dominated by planar to wavy lamination (Fig. 16e) and contains mudstone rip-up clasts (Fig. 16d), less common granules and/or coarse sand and rare organic detritus (Fig. 16h). This unit is more prominently bioturbated with 5–80% bioturbation indicated by the presence of *Planolites*, *Chondrites*, *Helminthopsis*, *Phycosiphon*, and lesser *Rhizocorallium*, *Palaeophycus*, and rare *Ophiomorpha* (Fig. 16g). Overall, the trace fossils are generally diminutive relative to typical occurrences.

The shale facies contains little sedimentological information to interpret a depositional environment aside from a quiet-water setting with terrestrial influx. The dark coloration may indicate anoxic conditions, which would explain the lack of bioturbation. Massive bedding and deformation structures within the sandstone facies suggest high sedimentation rates, whereas unidirectional and bidirectional currents are indicated by the crossbedding and current and wave ripples. The presence of *Rhizocorallium* indicates a marine setting, but the overall lack of trace fossils suggests an environmentally stressful depositional setting, possibly a distributary channel. The heterolithic facies suggests lower flow-regime conditions and deposition of possible hyperpycnal carbonaceous mudstone and finer grained sediment. The trace-fossil suites are consistent with a stressed archetypal *Cruziana* Ichnofacies in that they are dominated by deposit-feeding and grazing traces, but with low overall abundance. The deposits are interpreted as indicating a distal delta-front setting with mudstone rip-up clasts suggesting movement of channels on the delta plain. The overall deltaic setting is river-influenced based on the lack of vertical traces of inferred suspension-feeding animals, which is consistent with high sedimentation rates and water turbidity. The above evidence suggests that the shale facies represents a lagoonal, highly brackish setting adjacent to the delta.

## Palynology

Six samples from core 1 were analyzed for palynomorphs. The lowermost at 3258 m contains several dinocysts, including *Achomosphaera ramulifera*, *Hystrichosphaeridium quadratum*, *Hystrichosphaeridium tubiferum*, *Laciniadinium williamsii*, *Odontochitina costata*, and *Trichodinium castanea*. Also present are some miospores, including bisaccates, and *Palambages*, which Manum and Cookson (1964) considered to represent colonies of green algae. Nøhr-Hansen et al. (2016) considered the last or youngest occurrence of *Trichodinium castanea* to be in the latest Campanian. Another consistent marker with its last or youngest occurrence at the Campanian–Maastrichtian boundary is *Odontochitina costata*, according to Nøhr-Hansen et al. (2016). Thus, the sample is Campanian or older. The presence of several dinocysts indicates a neritic environment.

Dinocysts dominate the palynomorph assemblages in the overlying sample at 3257.31 m, constituting about two-thirds of the total. Taxa include *Heterosphaeridium bellii*, *Hystrichokolpoma* sp., *Hystrichosphaeridium quadratum*, and *Odontochitina costata*. Radmacher et al. (2014) gave a range for *Heterosphaeridium bellii* of late Campanian to Maastrichtian, whereas Nøhr-Hansen et al. (2016) considered the last or youngest occurrence of the species to be in the late Campanian. *Heterosphaeridium bellii* bears a remarkable resemblance to *Cleistosphaeridium diversispinosum*, and may be a taxonomic junior synonym of that species; however, both are retained based on uncertainty as to whether *Heterosphaeridium bellii* has an offset sulcal notch and the apparently disparate stratigraphic ranges of the two species, with *Cleistosphaeridium diversispinosum* not being recorded from pre-Cenozoic rocks. Based on the presence of *Heterosphaeridium bellii*, the age of this sample is provisionally considered to be late Campanian. The paleoenvironment is interpreted as outer neritic, based on the dominance of dinocysts and few miospores other than *Pinuspollenites*.

From the sample at 3255.7 m, only one specimen of *Pinuspollenites* and one specimen of the acritarch *Micrhystridium stellatum* were recorded. Consequently, the age or paleoenvironment cannot be determined at this time.

Dinocysts are common, but miospores are absent in the sample from 3254.1 m. *Spinidinium echinoideum* is particularly common. Other taxa include *Circulodinium distinctum*, *Cleistosphaeridium*? sp., *Eatonicysta* sp., *Exochosphaeridium arnace*, *Fibrocysta vectensis*, *Heterosphaeridium difficile*, *Hystrichodinium pulchrum*, *Hystrichosphaeridium quadratum, Hystrichosphaeridium tubiferum, Hystrichosphaeridium sp., Leberidocysta chlamydata*, *Odontochitina costata*, *Palaeoperidinium pyrophorum*, *Phelodinium kozlowskii, Subtilisphaera* sp., *Trichodinium castanea*, and *Trithyrodinium suspectum*. In a study of dinocyst assemblages from the Northwest Territories (sensu stricto), McIntyre (1975) plotted the stratigraphic range of *Phelodinium kozlowskii* as late Campanian to early Maastrichtian. As noted previously, the dinocysts *Odontochitina costata* and *Trichodinium castanea* do not range above the late Campanian, so the sample must be Campanian or older. The palynological assemblage indicates a neritic setting, with high concentrations of *Spinidinium echinoideum*, suggesting, specifically, inner neritic (Harland, 1973).

The age of a sample from 3252 m, could not be determined since it contains only the coniferous pollen *Pinuspollenites*. The genus is found throughout the Mesozoic and Cenozoic and is identical to pollen produced today by pine trees. This pollen type can be found in all environments from terrestrial to open ocean, but the absence of dinocysts suggests that it is close to shore or even nonmarine.

The uppermost sample from 3251.25 m contains several dinocyst taxa, including *Elytrocysta* sp., *Florentinia mantellii*, *Gonyaulacysta* sp., *Heterosphaeridium* "*elegantulum*", *Hystrichosphaeridium tubiferum*, *Isabelidinium cooksoniae*, *Microdinium* sp. A sensu Ioannides, 1986, *Odontochitina diducta*, *Palaeoperidinium pyrophorum*, *Palaeotetradinium silicorum*, and *Spinidinium echinoideum*. According to Nøhr-Hansen et al. (2016), *Isabelidinium cooksoniae* has its last or youngest occurrence in the Maastrichtian. *Odontochitina diducta* was described by Pearce (2010) from the upper Santonian to Campanian rocks of southeastern England, and Williams et al. (2004) placed the first or oldest occurrence of *Palaeotetradinium silicorum* within the late early Campanian. Thus, it seems reasonable to assume that the sample is Campanian. The dominance of dinocysts (84% of the palynomorph assemblage) and the few miospores indicate that the paleoenvironment was neritic. Furthermore, the high percentage of *Spinidinium echinoideum* supports an inner neritic setting.

### *Summary*

This core interval of the Freydis Member falls in between interpreted cuttings samples of both Williams (2007e) and Bujak Davies Group (1989c), who consistently interpreted the age as late Campanian below core 1 and earliest Maastrichtian above. The present study indicates a continued late Campanian age in agreement with previous results, based on the presence of *Heterosphaeridium bellii, Odontochitina diducta*, and *Palaeotetradinium silicorum*. This interval was previously interpreted as inner to outer neritic (Williams, 2007e) and inner shelf to marginal marine (estuarine distributary mouth bar and/or delta front; Miller and D'Eon, 1987). The setting from palynological analyses of five of the samples seems to be inner to outer neritic, which is consistent with the findings of Williams (2007e). This interpretation reflects a more distal setting compared to the sedimentological and ichnological data from the core, which denotes a shallower, river-influenced delta front to lagoonal setting; however, indications of an inner-shelf setting in some of the palynology samples agrees more closely with the core observations. Dinocysts are more abundant in the mudstone, suggesting a decrease in fluvial influence and more normal marine salinity. The wealth of dinocysts in the samples may be related to only weak brackish conditions, whereas turbidity and sedimentation rates may have played a more prominent role in limiting infaunal colonization.

## *Core 2: heterolithic sandstone and shale (3403–3412 m)*

### *Core description and interpretation*

The Freydis Member sandstone of core 2 (Fig. 17) from the Gilbert F-53 well can be divided into two facies: a primarily massive-bedded sandstone and a sandstone with convoluted bedding (Fig. 18). The massive sandstone is generally coarsening upward from fine- to medium-grained and is light grey to buff (Fig. 19a, b, c, d). White quartzite granules are present locally throughout the facies. The sandstone contains local mudstone laminae (Fig. 19c, d), organic detritus (Fig. 19c), planar parallel laminations, rare high-angle crossbedding (Fig. 19c), pyrite nodules, and green grains (possibly glaucony or forms of the mineral more commonly known as glauconite). Trace fossils are very rare and include *Asterosoma*, *Rhizocorallium*, *Planolites*, and *Palaeophycus* (Fig. 19a, d).

The convolute-bedded sandstone is fine grained with granules throughout and is light to medium grey (Fig. 19e, f). Colour variation highlights the deformed nature of the facies. Angular, dark grey mudstone rip-up clasts are also seen throughout the facies, and there are rare planar laminations and carbonaceous mudstone laminae also present. No trace fossils were noted.

The massive bedded sandstone facies is similar to core 1 of this well and suggests deposition under high sedimentation rates; the presence of carbonaceous mudstone and associated organic detritus suggests proximity to a fluvial source. A few scattered, deposit-feeding trace fossils (some of strictly marine origin) imply a shallow-marine setting. This facies was likely deposited in a deltaic distributary channel environment or proximal delta front. The convolute-bedded sandstone contains rip-up clasts that suggest possible reworking of muddier delta-plain deposits. The convoluted bedding indicates slumping and destabilization of channel banks likely associated with channel migration. Overall, the trace-fossil assemblage is very low in diversity and abundance and is especially lacking in vertical structures of inferred suspension feeders common to a normal marine, shoreface environment. Thus, this core is interpreted to represent deltaic distributary channels and delta-front deposits in a river-influenced delta-front setting where high suspended load and water turbidity interfere with the filter-feeding capabilities of suspension feeders.

### *Palynology*

Four samples from core 2 were analyzed for palynomorphs. The assemblage from the sample at 3410.9 m includes the dinocysts *Cauca parva*, *Muderongia* sp., *Spinidinium echinoideum*, and *Spiniferites ramosus*; the pollen *Triporopollenites*; and a microforaminifera. According to McIntyre (1974), *Cauca parva* has its last or

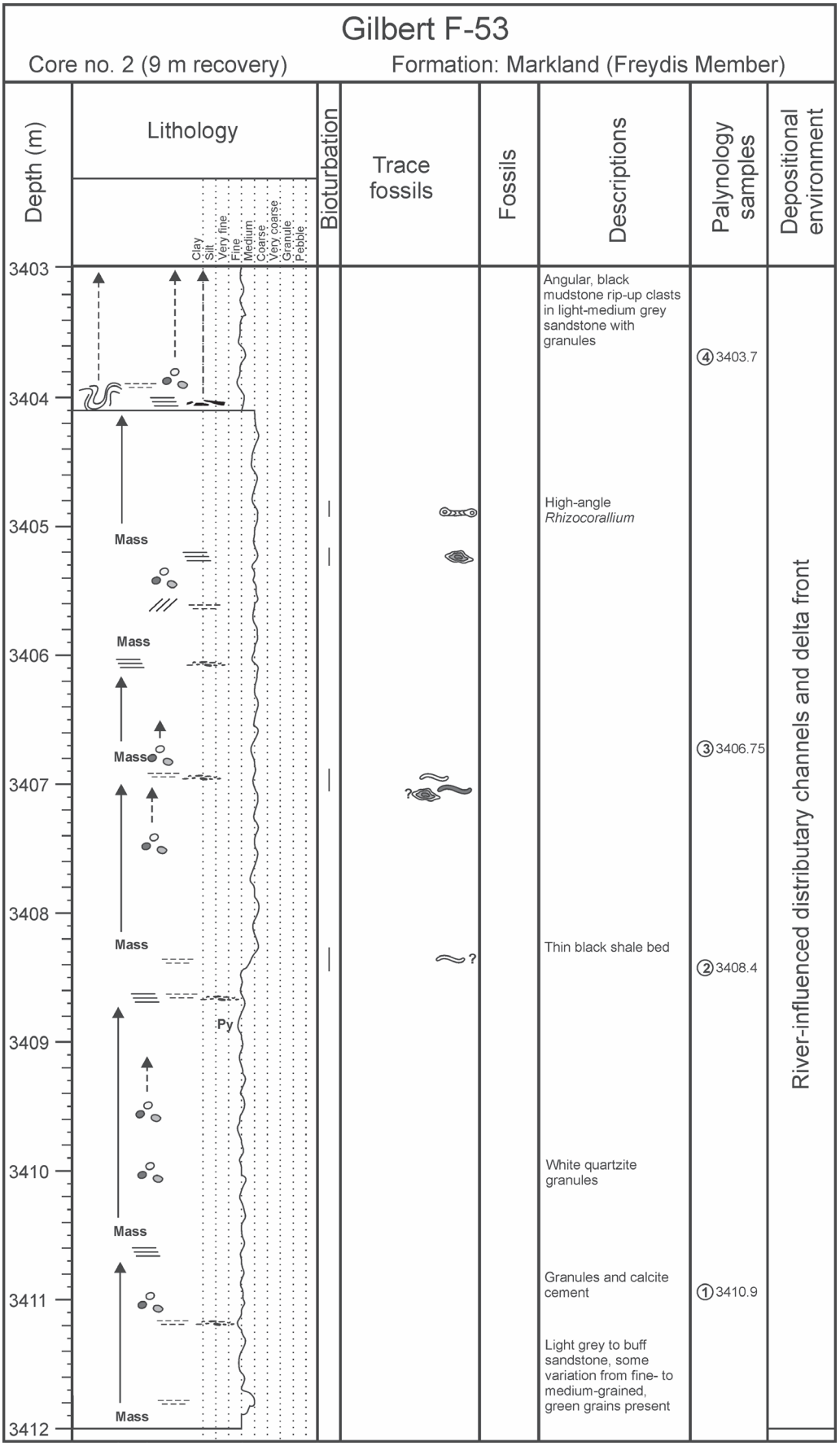


**Figure 17.** Log of core 2 from Gilbert F-53 showing predominance of fine- to medium-grained sandstone.

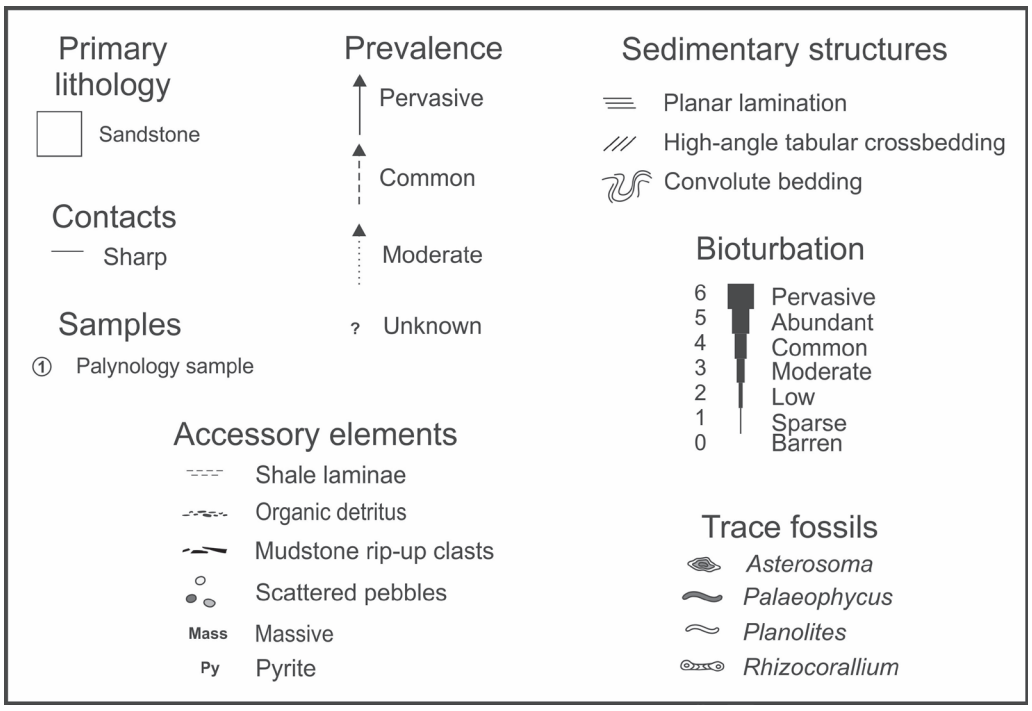


**Figure 17.** (cont.)

youngest occurrence in the Santonian in the Horton River section of the Northwest Territories. Williams et al. (2004) placed the first or oldest occurrence of *Spinidinium echinoideum* in the Santonian. Thus, the age of this sample appears to be Santonian, which is older than the age determined from the samples described below. One explanation is that the single specimen of *Cauca parva* is reworked as presumably is the single *Muderongia* sp. From the presence of *Spiniferites ramosus* and *Spinidinium echinoideum*, the paleoenvironment was marine, probably inner neritic.

Palynomorphs recovered from the sample at 3408.40 m are all dinocysts and include *Alterbidinium minor*, *Heterosphaeridium bellii*, *Hystrichosphaeridium quadratum*, *Microdinium* sp., *Spiniferites ramosus,* and *Spongodinium*? sp. The presence of *Heterosphaeridium bellii* indicates that the sample is late Campanian. A neritic paleoenvironmental setting is interpreted in this study, based on the dominance of the dinocysts and the low number of miospores. The high number of peridinioid specimens suggests an inner neritic setting, although the gonyaulacoids may indicate a setting farther from shore.

The sample at 3406.75 m also contains a mixed assemblage, including the miospores *Laevigatisporites* and *Pinuspollenites*, the dinocysts *Alterbidinium* and *Microdinium*, and the acritarchs *Baltisphaeridium* and *Veryhachium europaeum*. Unfortunately, none of the taxa provide a definitive age. The authors interpret the assemblage as denoting an inner neritic paleoenvironment, but the evidence is weak.

Vitrinite is the only organic matter present in the sample from 3403.7 m, indicating that the paleoenvironment was nonmarine to coastal.

## *Summary*

Findings of this study indicate that this core interval is late Campanian, with the possible exception of the bottommost sample at 3410.9 m, and support the findings of previous studies by Bujak Davies Group (1989c) and Williams (2007e), who reported a late Campanian age from cuttings of the Freydis Member. The sparse dinocyst assemblage in the bottommost sample does not provide convincing evidence of a Santonian age. The paleoenvironmental setting was previously interpreted as inner shelf (Williams, 2007e) or inner shelf to marginal marine (delta front, distributary mouth bar; Miller and D'Eon, 1987), which is somewhat consistent with the interpretations presented above. The present palynological results of a generally inner neritic setting also agree well with the interpretation from the core of deltaic distributary channels in a river-influenced delta-front setting. Interestingly, dinocysts are relatively common, considering the general lack of trace fossils, possibly indicative of high sedimentation rates and unstable substrate for infaunal colonization.


**Figure 18.** Photographs of core 2, Gilbert F-53. Scale bar = 10 cm. NRCan photos 2019-325, 2019-326, 2019-327, 2019-328. All photographs by L.T. Dafoe

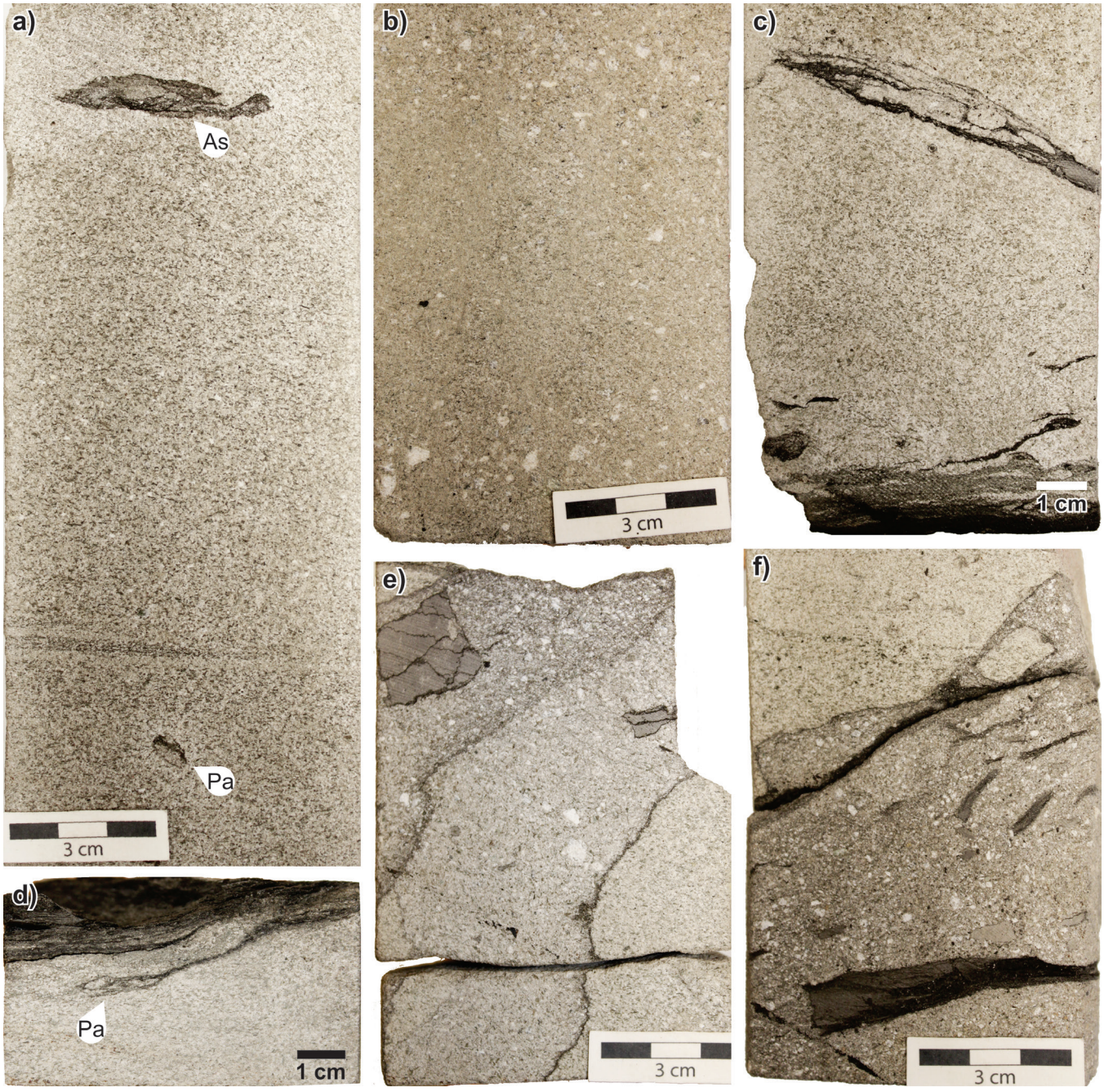


**Figure 19.** Photographs of core 2, Gilbert F-53. **a)** *Asterosoma* (As) in massive bedded sandstone with some evidence of planar parallel lamination above a *Palaeophycus* (Pa) trace fossil. NRCan photo 2019-329. **b)** Massive sandstone with granules and small pebbles. NRCan photo 2019-330. **c)** Sandstone with organic detritus (plant stems). NRCan photo 2019-331. **d)** *Palaeophycus* (Pa) below the base of a carbonaceous mudstone. NRCan photo 2019-332. **e)**, **f)** Convoluted bedding with large mudstone rip-up clasts. NRCan photo 2019-333, 2019-334. All photographs by L.T. Dafoe.

### *Core 3: gneiss (3605–3606.2 m)*

#### *Core description and interpretation*

Core 3 in the Gilbert F-53 well is characterized by variously banded and fractured gneiss (Fig. 20). Rodrigue (1980) described this core as granodiorite to quartz diorite with a foliated to cataclastic texture. The rock, which is amphibolite and amphibolite-facies gneiss (Harris, 1980), was also described by Wasteneys et al. (1996) as amphibolite gneiss with an age of 3742 ± 12 Ma based on U-Pb isotopic age dating. These authors further indicated an association of this gneiss with the onshore Nain Province (or North Atlantic Craton; Fig. 1).

## Gjoa G-37

Gjoa G-37 was drilled in the Davis Strait, within the northern part of the Saglek Basin in 1979 (Fig. 1). The well penetrated more deeply than planned due to the presence of volcanic rocks (Esso Exploration Ltd., 1979), with total depth recorded at 3998 m. A single core was taken within the upper part of an unnamed interbedded basalt and shale interval.

### *Core 1: basalt flows (2912.0–2920.5 m)*

#### *Core description and interpretation*

In Gjoa G-37, the single core taken from between 2912.0 m and 2920.5 m is 8.5 m long and about 8 cm in diameter (Fig. 21). The core is entirely igneous and is characterized by fine-grained, dark-grey to brown-grey basalt to amygdaloidal basalt. Overall, the core consists of more massive basalt at the base (unit 1; Fig. 22a), becoming more amygdaloidal in the centre (unit 2; Fig. 22b, c, d, e) and with large infilled vesicles predominating toward the top of the core (Fig. 22f). The more massive basalt contains small, black phenocrysts, and amygdales are circular to ovate and infilled with zeolite minerals (Fig. 22a, b). This unit transitions upward to the slightly more rubbly, brown-grey amygdaloidal basalt (Fig. 22c) of unit 2. Brecciated basalt clasts (Fig. 22d) are present within this uppermost interval above 2918.7 m. Zeolite minerals infill vesicles, and the spaces between brecciated clasts generally become larger and more irregular in shape near the top of the core (Fig. 22f). From about 2916.5–2914.5 m, the core has an overall concretionary appearance (Fig. 22e).

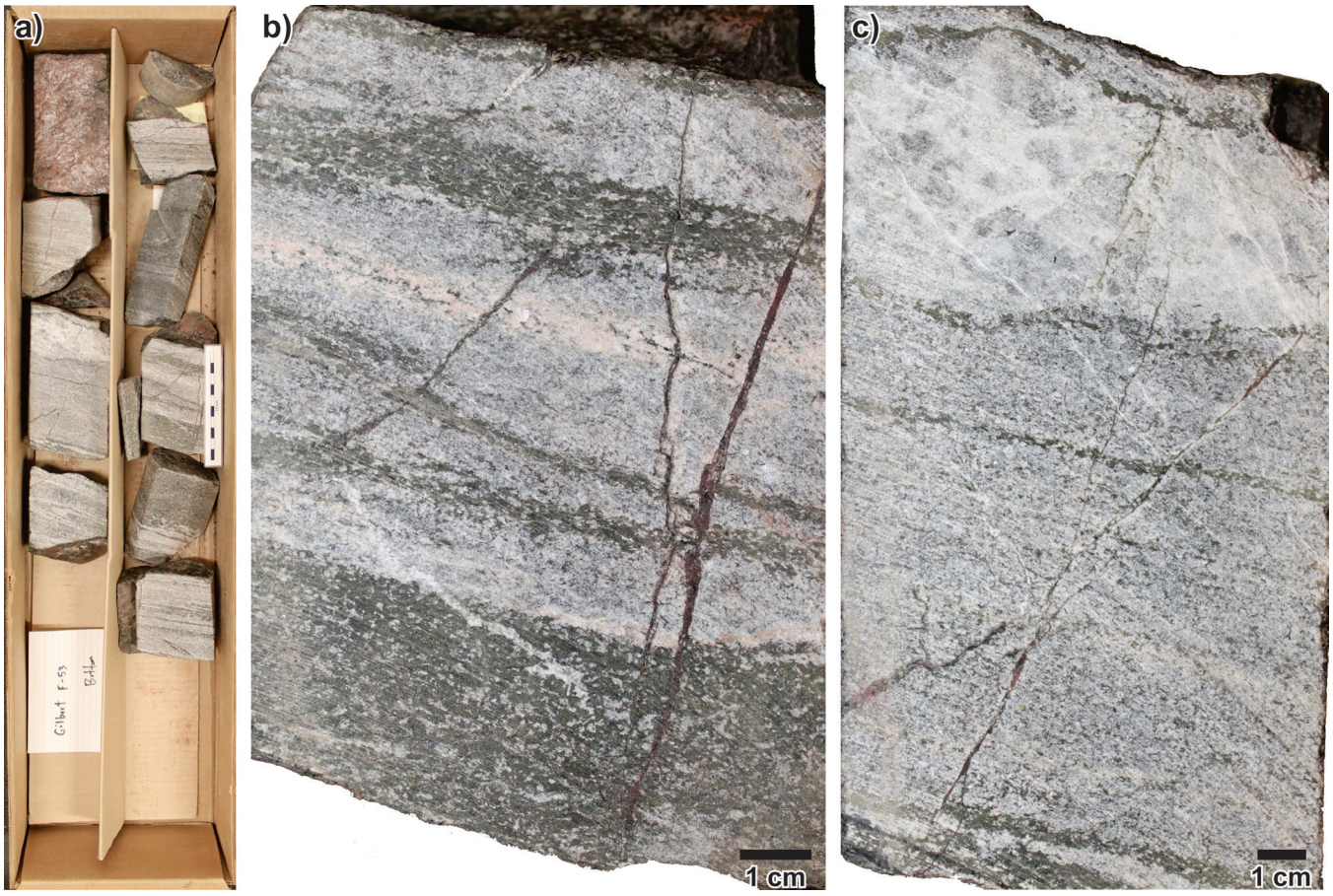


**Figure 20.** Photographs of core 3, Gilbert F-53. **a)** Core-box photo of the entire core interval. NRCan photo 2019-335. **b)** Close-up showing the banded texture of the fine-grained gneiss. NRCan photo 2019-336. **c)** A quartz-rich band in foliated gneiss. NRCan photo 2019-337. All photographs by L.T. Dafoe.


**Figure 21.** Photographs of core 1, Gjoa G-37 showing the entire cored interval. Scale bar = 10 cm. NRCan photos 2019-338, 2019-339, 2019-340. All photographs by L.T. Dafoe.

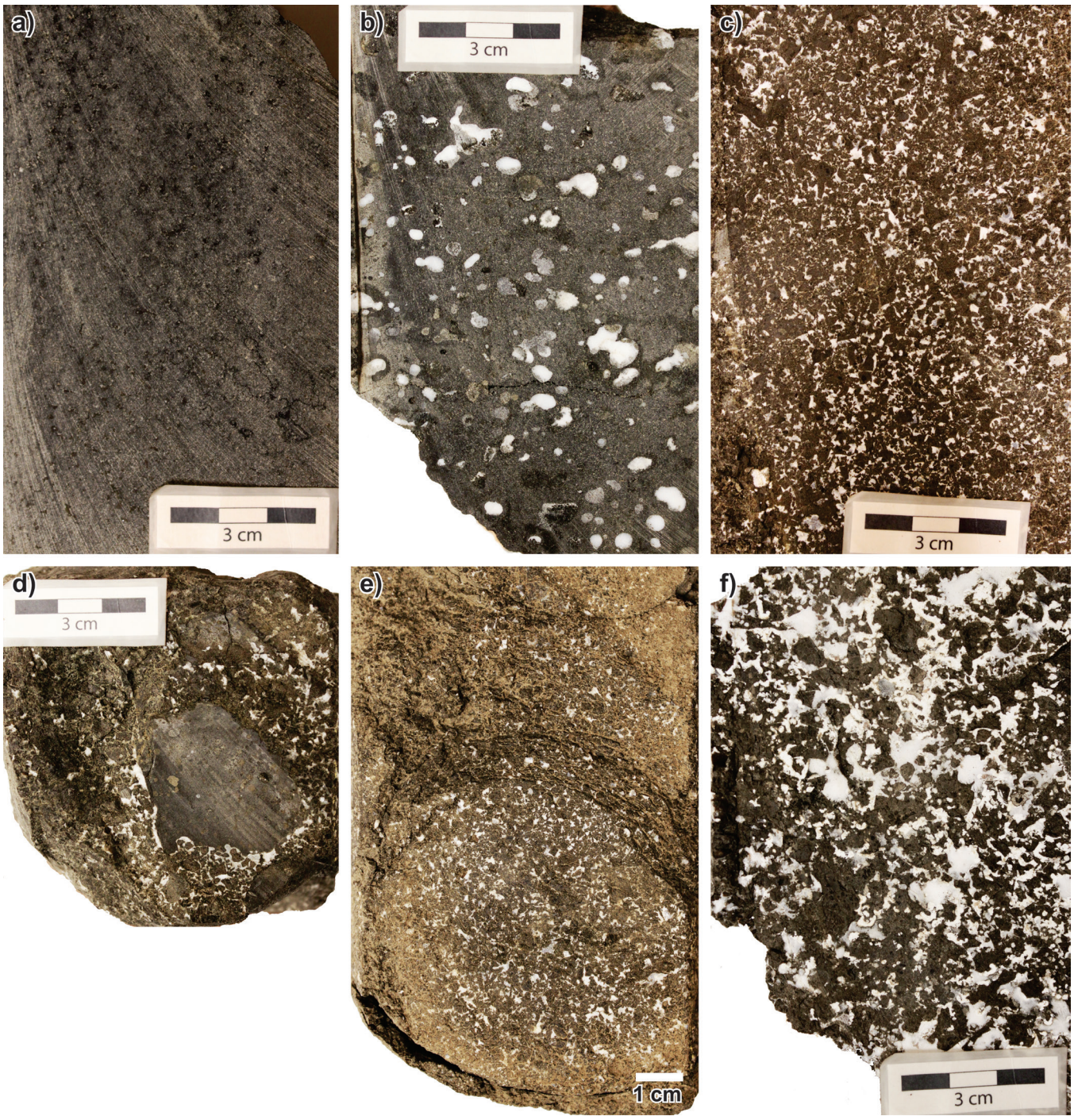


**Figure 22.** Photographs of core 1, Gjoa G-37. **a)** Solid basalt interval. NRCan photo 2019-341. **b)** Amygdaloidal basalt with large, filled vesicles. NRCan photo 2019-342. **c)** Amygdaloidal basalt with smaller vesicles. NRCan photo 2019-343. **d)** Amygdaloidal basalt with brecciated basalt clasts. NRCan photo 2019-344. **e)** Concretion-like appearance to the basalt. NRCan photo 2019-345. **f)** Highly amygdaloidal basalt near the top of the core. NRCan photo 2019-346. All photographs by L.T. Dafoe.

Gjoa G-37 core 1 is interpreted as subaerial basalt flows. The lowermost unit, unit 1, reflects the interior of a flow that is less frothy and gas prone compared to the flow top. The uppermost unit, unit 2, appears to reflect the upper portion of the flow, where abundant gas is trapped in the lava to create vesicles that were later infilled by zeolite minerals. The locally rubbly nature and change in coloration of unit 2 may reflect enhanced subaerial exposure, whereas brecciated clasts suggest incorporation of earlier flows perhaps through weathering processes or inclusion in hot lava flows. This interpretation is consistent with that of Williamson and Villeneuve (2002). Equivalent cuttings samples were dated as Late Paleocene (Selandian) by Williams (2007c). This age corresponds well with the Ar-Ar age of 59.5 ± 1.0 to 59.2 ± 1.8 Ma (Williamson and Villeneuve, 2002).

## Hekja O-71

Hekja O-71 was drilled in Davis Strait, within the northern part of the Saglek Basin, in 1979–1980 (Fig. 1). The objective was to test a structure near the Ungava Fault Zone (Aquitaine Company of Canada Ltd., 1980), reaching a total depth of 4566 m. Three cores were recovered: the uppermost core is from a thin sandy succession about 300 m above the basalt interval in the Gudrid Formation; the middle core is from near the top of the unnamed basalt unit; and the bottommost is from within the basalt near the base of the well.

### *Core 1: coarse-grained sandstone (3250.1–3257.10 m)*

#### *Core description and interpretation*

Core 1 (Fig. 23) comprises primarily coarse-grained sandstone forming two facies of the Gudrid Formation. Contacts at facies boundaries can only be described as sharp since the core material has undergone extensive sampling and there is likely significant missing core (Fig. 24). One facies comprises fine- to very coarse-grained sandstone, with moderately sorted medium- to coarse-grained sandstone being dominant (Fig. 25). This buff-beige sandstone is noncalcareous and quartz-rich with rare dark chert grains. The unit includes intervals that are massive (Fig. 25f) and others with low-angle crossbedding (Fig. 25c), trough crossbedding (Fig. 25a), and lesser planar and possible wavy laminations. Granules and small pebbles are common (Fig. 25a, b, c, f) and organic material is rare. Compositionally, pyrite, rose quartz, and mafic minerals can be seen defining crossbeds. More commonly, rusty red grains are scattered throughout the core with rare turquoise-green grains also observed locally; both are unknown minerals. Dark grey, mudstone rip-up clasts were noted at one horizon (Fig. 25b). The second facies comprises similar buff-beige, fine-grained sandstone; it is noncalcareous and well sorted (Fig. 25). This facies occurs in thin intervals that are dominated by herringbone cross-stratification, where bedsets dip in opposing directions, as well as tabular crossbedding (Fig. 25d, e). No bioturbation or fossil material was noted from this core interval; however, the facies contains abundant anomalous green and red grains as described above.

Based on the sedimentological characteristics, deposition of the sandstone units, especially those with massive bedding, was relatively rapid. Current activity is indicated by tabular and trough crossbedded intervals. Coarser grained horizons may indicate erosive channel bases, and mudstone rip-up clasts suggest nearby low-energy settings, possibly floodplains. The lack of wave-formed structures suggests a nonmarine fluvial setting; however, the interval of herringbone cross-stratification suggests tidal influence under alternating current directions. Based on rapid sedimentation, strong current activity and tidal influence, the most likely depositional setting is a tidal channel. The red and green grains resemble the volcaniclastic rocks seen in core 2 (*see* below) and are likely the product of weathering of similar material.

#### *Palynology*

Seven samples were analyzed from core 1. The lowermost sample, from 3258.5 m, was collected previously (in 1980) and corresponds to the base of core. The inconsistency in the depth relative to that shown in Figure 23 is due to missing core intervals from sampling, which now results in a reduced overall measured core length. This sample, was, however, relatively productive and contains several specimens of bisaccate (coniferous) pollen such as *Abiespollenites*, *Piceapollenites*, and *Pinuspollenites* and one trilete spore, a specimen of *Cicatricosisporites*. Dinocysts include *Apectodinium homomorphum*, *Apectodinium parvum*, *Areoligera gippingensis*, *Glaphyrocysta divaricata*, *Hafniasphaera*, *Operculodinium centrocarpum*, *Palaeocystodinium golzowense*, and *Spiniferites ramosus*. Harland (1979) considered *Apectodinium parvum* to occur only in the latest Thanetian, indicating that the sample is latest Paleocene. The postulated paleoenvironment is inner neritic or marginal marine. Degraded herbaceous material is abundant in the sample, supporting the current interpretation of a nearshore setting. One surprise is the presence of *Nyktericysta*, a dinocyst that is known only from the Barremian–Aptian and which is obviously reworked.

The sample at 3257.1 m contains only two palynomorphs, one of the pollen genus *Pinuspollenites* and one of the dinocyst species *Thalassiphora pelagica*. Also present are numerous small vitrinite fragments and some woody material. Terrestrial organic material dominates. The overlying sample at 3255.4 m has several pollen grains, including a questionable specimen of *Wodehouseia stanleyi* that was recorded from the Maastrichtian by Srivastava (1966); however, the presence of *Caryapollenites* indicates a Cenozoic age. The sample at 3254.3 m has a nondescript assemblage, primarily angiosperm pollen; however, there are several specimens of *Taxodiaceaepollenites* that Sweet (2015) considered indicative of the Paleocene. The sample from 3252.7 m

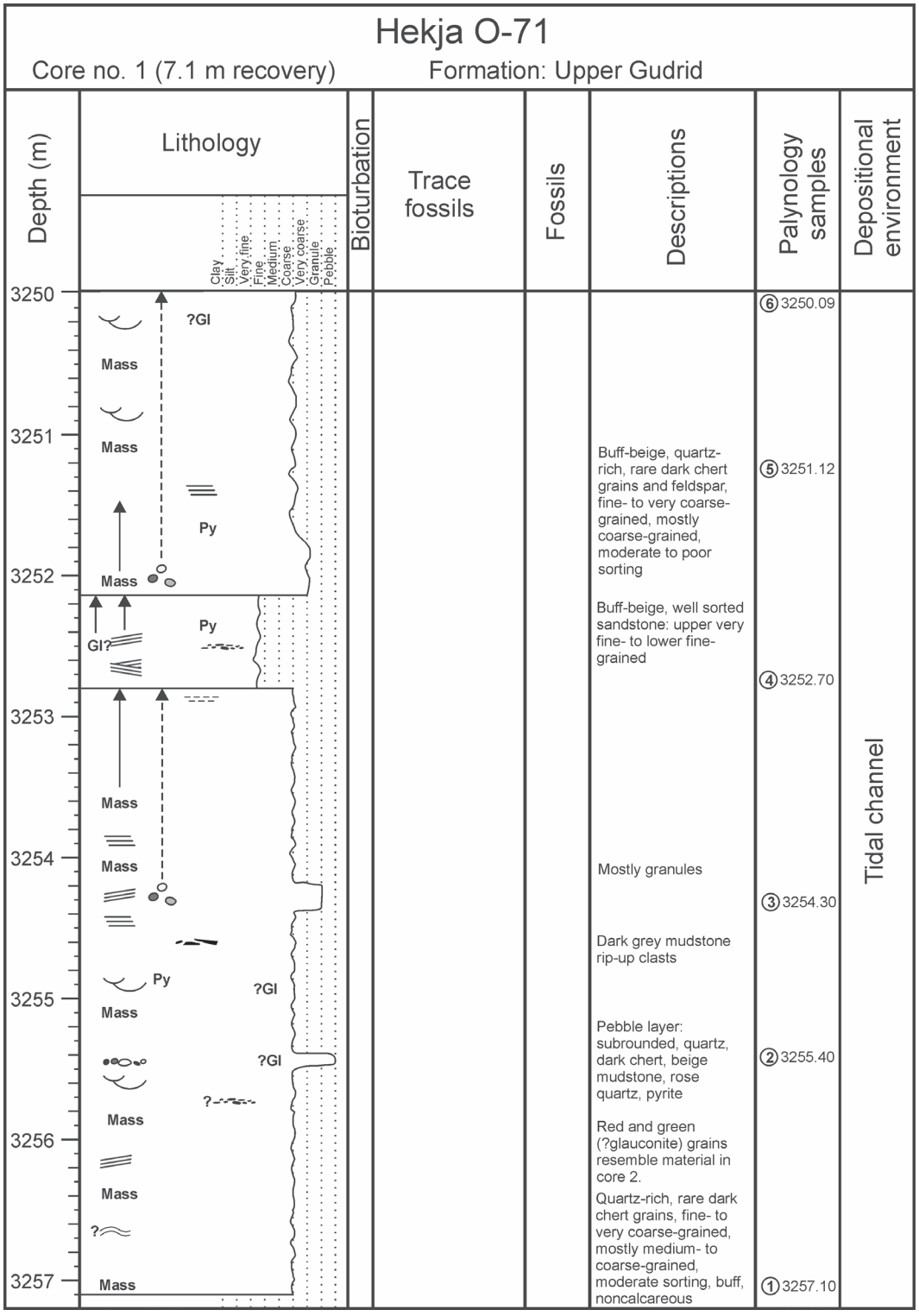


**Figure 23.** Log of core 1 from Hekja O-71. The core is composed of sandstone primarily ranging from fine- to coarse-grained.

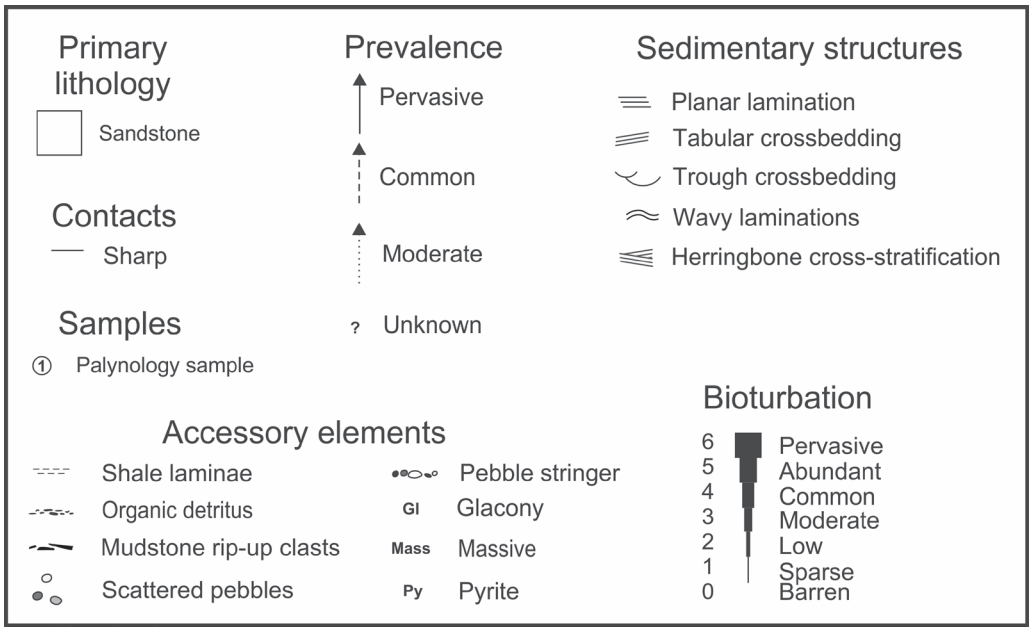


**Figure 23.** (cont.)


**Figure 24.** Photographs of core 1, Hekja O-71, showing the heavily sampled nature of the sandstone. NRCan photos 2019-347, 2019-348. Both photographs by L.T. Dafoe.

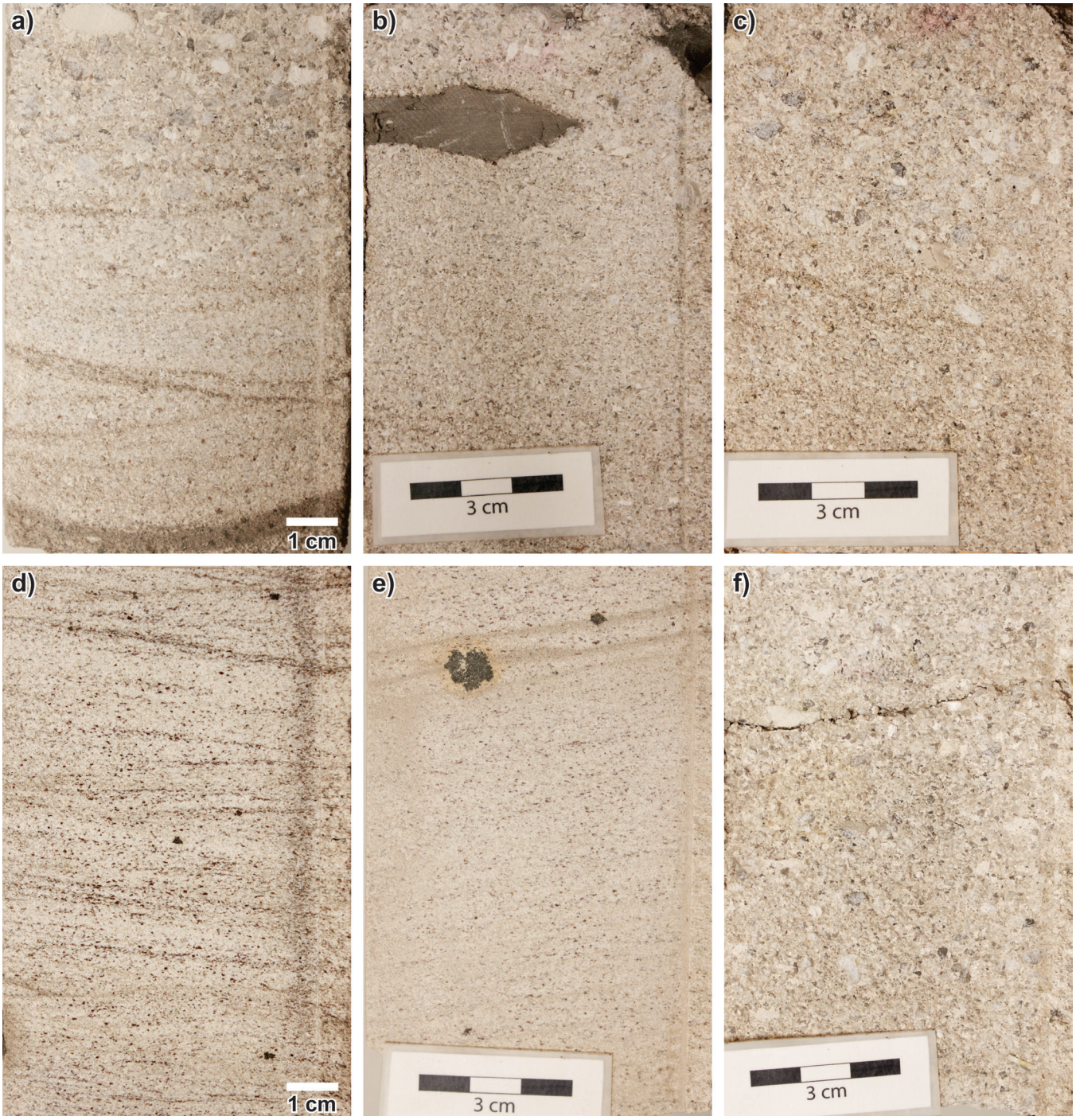


**Figure 25.** Photographs of core 1, Hekja O-71. **a)** Trough crossbedding with gradation from sandstone to pebbly sandstone. NRCan photo 2019-349. **b)** A prominent dark grey mudstone rip-up clast. NRCan photo 2019-350. **c)** Tabular crossbedding and an overlying pebbly sandstone. NRCan photo 2019-351. **d)** The finer grained unit with herringbone cross-stratification and abundant rusty-red grains and scattered pyrite. NRCan photo 2019-352. **e)** Framboidal pyrite in tabular crossbedding within the fine-grained sandstone, also containing abundant rusty-red grains. NRCan photo 2019-353. **f)** Massive pebble- and granule-bearing sandstone. NRCan photo 2019-354. All photographs by L.T. Dafoe.

contains three miospores, but no dinocysts. Amorphous kerogen is common and there is some carbonized material. *Alnipollenites*, *Taxodiaceaepollenites*, and *Betulaepollenites* all occur in the overlying sample at 3251.12 m. According to Sweet (2015) *Betulaepollenites* is indicative of a Cenozoic age. Confirmation of the age of core 1 is the presence of *Caryapollenites wodehouseia* in the sample at 3250.09 m. Nichols (2003) considered this species to be restricted to the later Paleocene. Although the present study recorded a single dinocyst, it could be reworked, leading to the conclusion that the paleoenvironment was presumably nonmarine.

### *Summary*

From the present analysis of the sample at 3258.5 m, the age of this unit of the Gudrid Formation is latest Thanetian. This agrees with the age determination of Nøhr-Hansen et al. (2016), but is slightly at odds with Williams (2007a), who designated it early Eocene. The depositional setting suggested by Williams (2007a) was inner neritic, whereas Miller and D'Eon (1987) interpreted a marginal marine (fluvial, estuarine, swamp, and/or marsh) setting, both somewhat consistent with this study. The palynology indicates a marginal marine to inner neritic paleoenvironment, which agrees well with the tidal channel setting from core observations. The dominance of organic material in several palynology samples further confirms a nearshore setting dominated by terrestrial influx.

## *Core 2: volcaniclastic rocks (3555.0–3556.0 m)*

### *Core description and interpretation*

In the Hekja O-71 well, core 2 lies just above the top of a succession of unnamed basalt flows sampled by the underlying core 3 (*see* below). This 1 m long core, from 3555.0 m to 3556.0 m, is rubbly, and above it, no core was recovered in the interval from 3556.0 m to 3560.0 m (Fig. 26). The core is variably coloured (Fig. 27a), including intermixed beige, light-green, and rusty-red variations. Despite the rubbly nature of the core, some intervals are apparently well indurated (Fig. 27b), whereas others include soft powdery 'clasts' (Fig. 27c, e). The core interval appears to be brecciated throughout (Fig. 27f), with evidence of angular or irregular clasts. Subsequent diagenesis may play a factor in the overall varying coloration of the breccia due to a red mineralization that coats green and beige clasts (Fig. 27b, e). The core materials contain one large calcite-filled fracture near the top of the core (Fig. 27c), as well as minor ones throughout. Some clasts appear to be amygdaloidal in nature (Fig. 27f).

The lithology of this core is difficult to define based only on macroscopic observations; however, the softness of some clasts and the variable colour suggest a pedogenic interpretation. The location at the top of the basalt unit may indicate significant weathering and alteration of

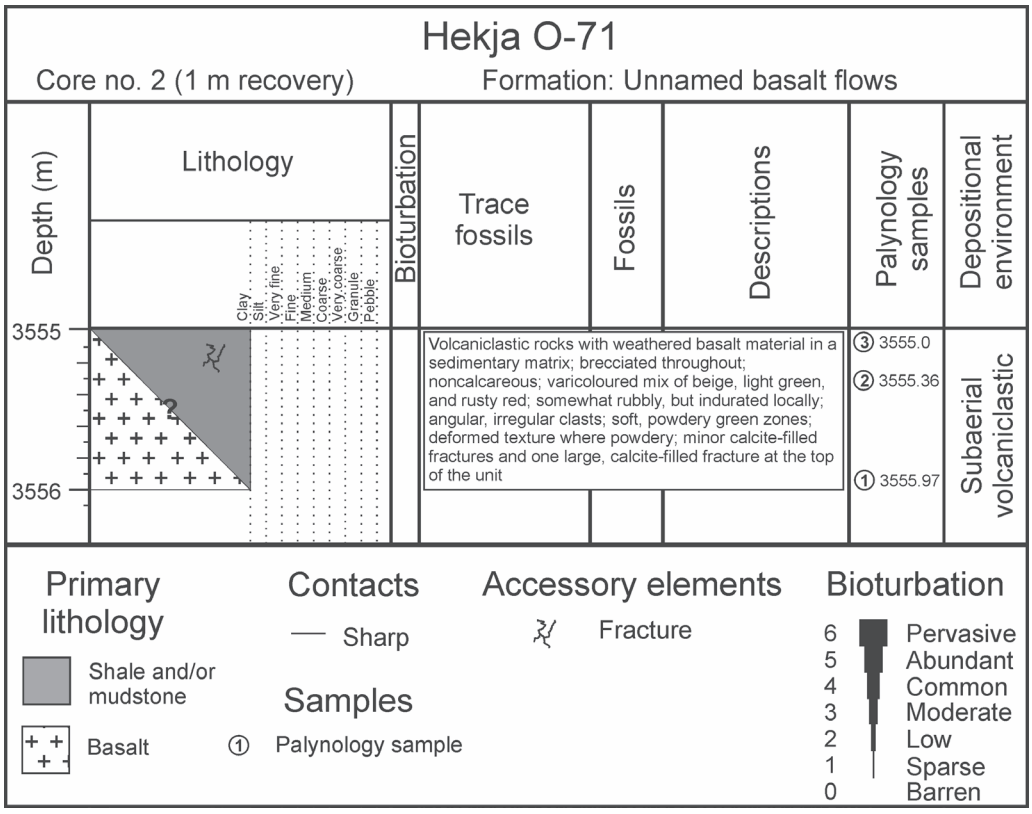


**Figure 26.** Log of core 2 from Hekja O-71. Note that the lithology is uncertain and likely represents volcaniclastic material.

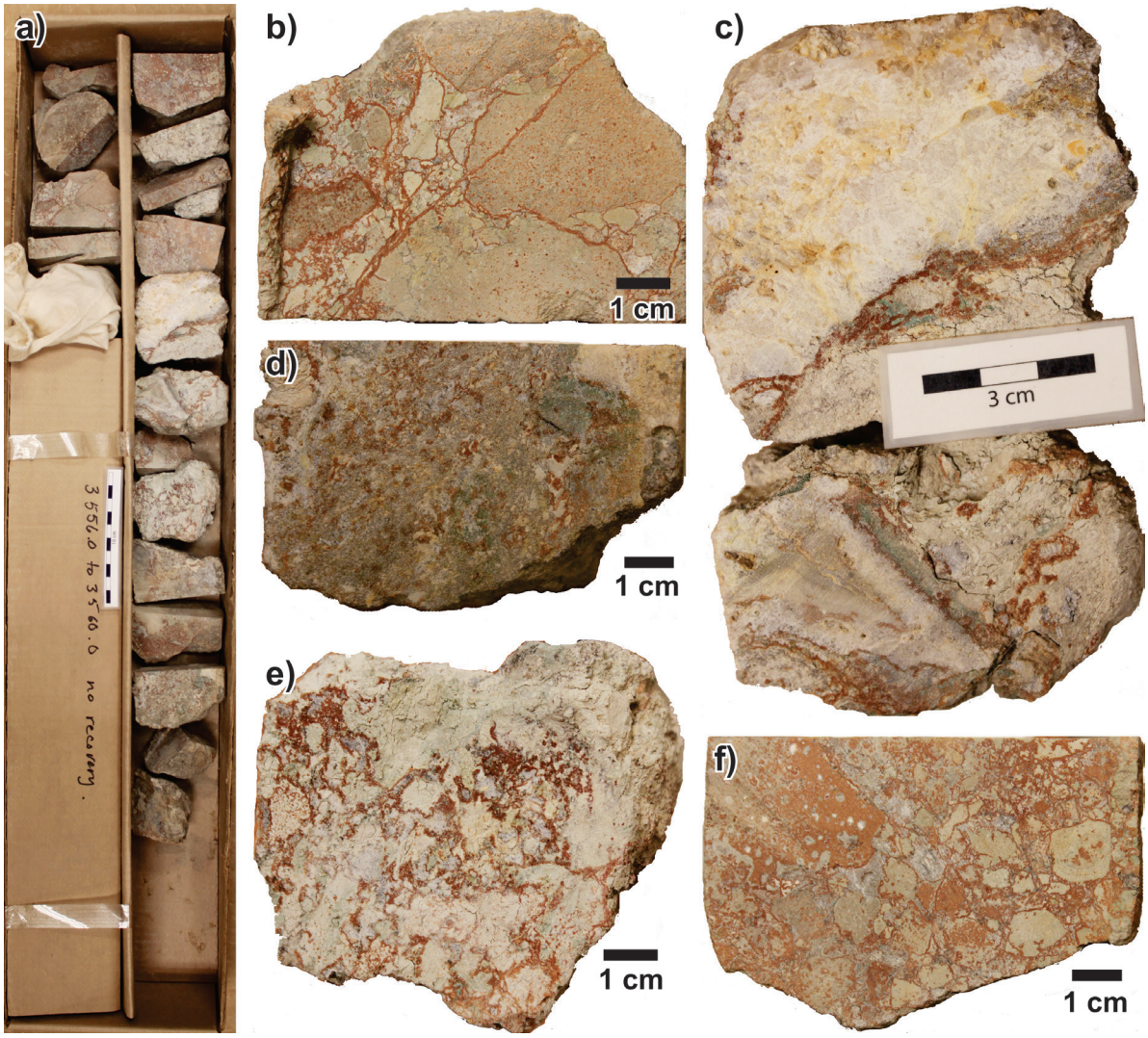


**Figure 27.** Photographs of core 2, Hekja O-71. **a)** Core box showing the entire core 2 (scale bar = 10 cm). NRCan photo 2019-355. **b)** Brecciated fragments rimmed by a rust-red material. NRCan photo 2019-356. **c)** A large calcite vein above poorly indurated, powdery, beige material. NRCan photo 2019-357. **d)** Red, green, and beige material, well indurated. NRCan photo 2019-358. **e)** Soft beige material, rimmed with rusty red mineralization. NRCan photo 2019-359. **f)** Possible amygdaloidal clast (upper left) with other beige to light brown fragments. NRCan photo 2019-360. All photographs by L.T. Dafoe.

volcanic flows or volcaniclastic sedimentation. The reddish rims around clasts may represent some form of weathering or oxidation, further suggesting a subaerial nature.

## *Thin-section analysis*

Two thin sections were prepared from samples of core 2 (Fig. 28). The sample at 3555.0 m commonly contains fractures lined by calcite, quartz, and/or chalcedony, and possible siderite. The silt-sized quartz matrix is likely chalcedony (it includes well developed six-sided crystals). Fragments of basalt with opaque minerals are present, but less common. The sample at 3555.36 m consists of clasts of weathered basalt within a silty or siliceous matrix. The basalt clasts contain opaque minerals, possibly magnetite, and possibly altered olivine crystals. Veins of calcite and possibly siderite are present, as well as rare six-sided quartz grains and/or crystals. Overall, this material likely represents volcaniclastic rocks, including weathered basalt clasts that have become incorporated into rhyolitic or siliceous material.

## *Palynology*

Three samples from core 2 were processed and analyzed. The lowermost one at 3555.97 m contains diatoms, which are usually destroyed by hydrofluoric acid. Also present is one specimen of the conifer *Pinuspollenites* and a questionable specimen of the dinocyst *Palaeocystodinium bulliforme*. If the latter identification is accepted, the age would be Selandian (Nøhr-Hansen et al., 2016). Two samples from 3555.36 m and

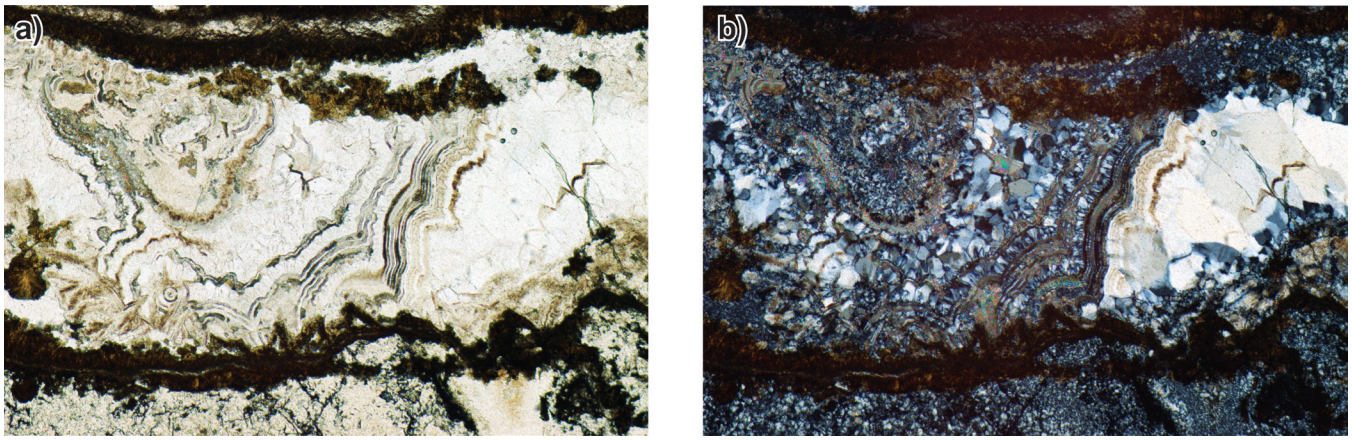


**Figure 28.** Thin section photographs of core 2, Hekja O-71 from 3555.0 m in **a)** plain light and **b)** polarized light (right) at 5x magnification. A thick vein of quartz and/or chalcedony and calcite within an overall fine siliceous (chalcedony) matrix. Brown material may indicate the presence of siderite. NRCan photo 2019-361, 2019-362, respectively. Both photographs by L.T. Dafoe.

3555.00 m, respectively, contained diatoms, but no palynomorphs. The presence of a dinocyst indicates a marine setting, but diatoms can be found in a wide variety of settings.

### *Summary*

Based on cuttings, Williams (2007c) dated this interval as Thanetian. The present observations indicate a possible Selandian age. Previous interpretations by Miller and D'Eon (1987) suggested a marginal marine subaerial to subaqueous setting and Williams (2007a) found the interval to represent inner neritic conditions. Keen et al. (2012) interpreted the basalt units in this well (i.e. those sampled by the underlying core 3) to reflect a lava delta formed as part of a typical magma-rich (volcanic) margin. The core itself appears to reflect weathered basalt within a siliceous or rhyolitic matrix, indicating a likely shallow-marine to possibly intermittently subaerially exposed setting at the top of the lava delta.

## *Core 3: basalt (4351.6–4355.31 m)*

### *Core description and interpretation*

The lowermost core 3 of the Hekja O-71 well primarily comprises brecciated basalt intervals and fewer, well indurated solid basalt intervals (Fig. 29). The basalt is dark grey to black and locally brown-green (Fig. 30). Brecciated basalt fragments are larger and more common upward and are typically irregular in shape and fine grained (Fig. 31). Some larger brecciated clasts have green-brown rims up to 2.5 mm thick, which is in contrast to the dark grey central portions of the clasts (Fig. 31b, e). There is some evidence of amygdales within clasts, but the pink and white zeolite minerals also infill voids between brecciated clasts. Calcite-filled fractures are also present.

These basalt flows comprise the lava delta seen in seismic data that is intersected by the well (cf. Keen et al., 2012). A lack of vesicles confirms that a submarine origin is most likely. Rimming of the brecciated clasts likely reflects quenching of the basalt when it came into contact with water and so also suggests a submarine origin (Ayres et al., 1991; Brewer et al., 1998). The breccia therefore would be consistent with hyaloclastic formation (cf. Brewer et al., 1998), likely in shallow oceanic water as the lava delta was developing. Core 3 is a representative sample of the basaltic units from total depth at 4566 m to 3570 m. Within this interval, some tuffaceous units are indicated by the Canstrat log, but the majority of the cuttings are described as basaltic with amygdales and a green-grey-brown colour, as well as calcite veins and zeolite minerals. A shallow-water depositional setting is also consistent with the presence of these tuffaceous units, as pyroclastic material can accumulate in shallow-water settings (e.g. Ayres et al., 1991). Miller and D'Eon (1987) suggested an inner shelf setting, which is consistent with the present authors' interpretation.

This section of the well sampled by core 3 was dated as Selandian (middle Paleocene) by Williams (2007a) and early Paleocene by Nøhr-Hansen et al. (2016), both based on cuttings analyses; however, an Ar-Ar age of 48.7 ± 1.3 Ma by Williamson and Villeneuve (2002) places the core in the late Ypresian. This younger age is inconsistent with biostratigraphic results from the overlying Thanetian sedimentary rocks (Nøhr-Hansen et al., 2016), which would have improved palynomorph recovery compared to the basalt intervals, so the Ar-Ar age could be suspect, possibly due to the alteration noted above.

## Herjolf M-92

Herjolf M-92 was drilled in the Hopedale Basin, offshore Labrador (Fig. 1), in 1976 to test Lower Cretaceous rocks of an equivalent age to the gas-bearing interval in Bjarni

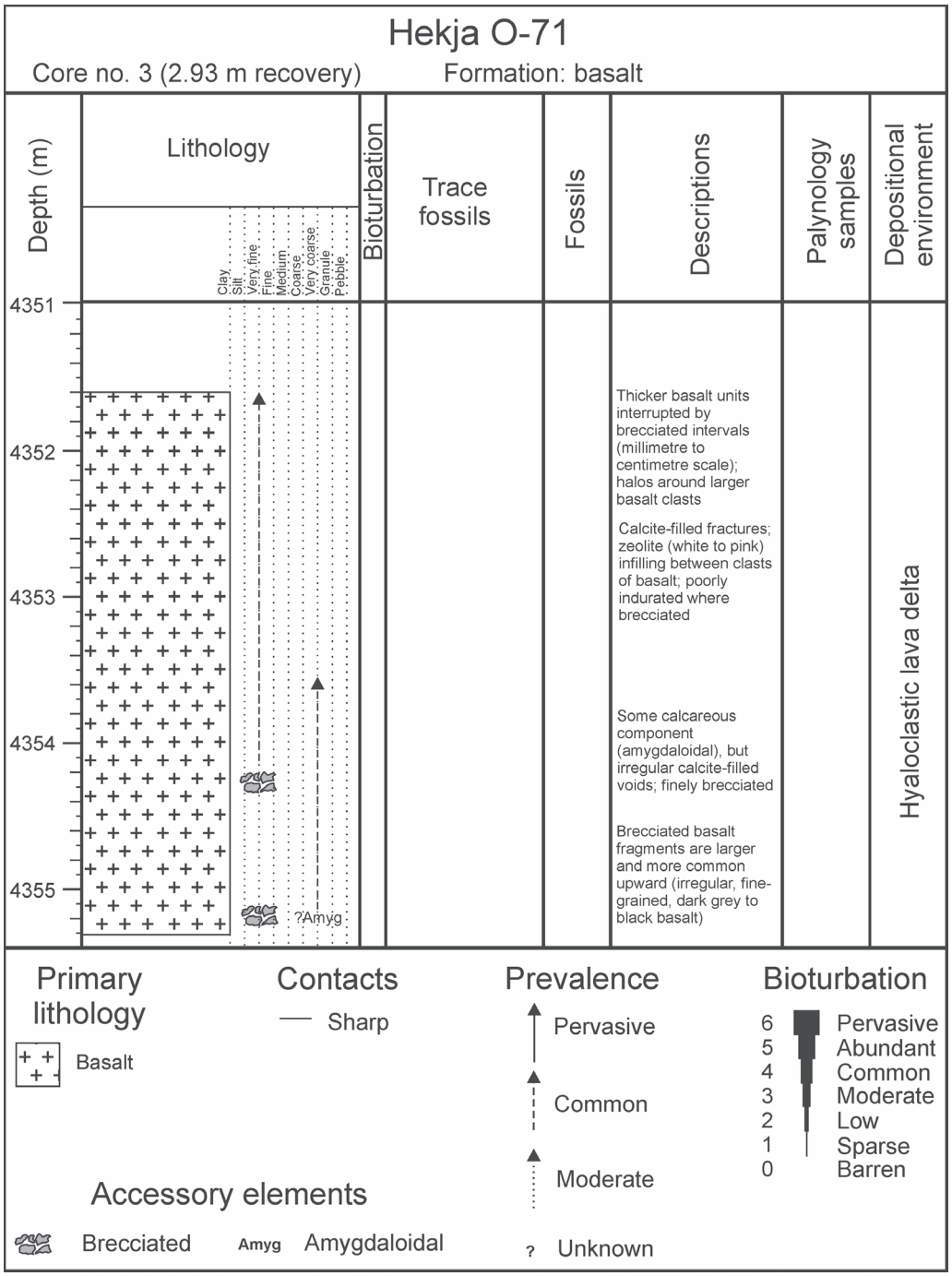


**Figure 29.** Log of core 3 from Hekja O-71. Much of the core comprises brecciated fragments.


**Figure 30.** Photograph of core 3, Hekja O-71. Scale bar = 10 cm. NRCan photo 2019-363. Photograph by L.T. Dafoe.

H-81 (Total Eastcan Exploration Ltd., 1977); total depth was 4086.1 m. Core intervals were collected within the Bjarni Formation (cores 1 and 2), Alexis Formation basalt units (core 3), and Precambrian basement (core 4).

## *Core 1: coarse-grained sandstone and thin shale (2632.28–2639.9 m)*

### *Core description and interpretation*

Core 1 of the Herjolf M-92 well includes two facies from the Bjarni Formation: 1) a medium- to coarse-grained, granule- and pebble-bearing sandstone, and 2) a heterolithic facies with interbedded fine-grained sandstone and dark grey shale (Fig. 32, 33). The sandstone facies is light grey and ranges from a moderately to well sorted, medium- to coarse-grained sandstone to a comparatively poorly sorted sandstone with abundant granules and small pebbles comprised of quartzite, orthoclase feldspar, and dark chert (<1 cm in diameter; Fig. 34a, b, c). Sedimentary structures include planar laminations and tabular crossbedding, but the unit is primarily massive, especially in coarser grained intervals (Fig. 34a, b, c). Organic detritus and coal fragments are present in association with thin mudstone laminae (Fig. 34a). Pyrite is rare, and no bioturbation was observed within these sandstone units.

The second, heterolithic, facies comprises light grey sandstone that is fine- to medium-grained and with interbedded dark grey shale or mudstone (Fig. 34d, e, f, g). Fining-upward and coarsening-upward intervals are present, as well as sharp and palimpsest boundaries (those overprinted by discrete trace fossils within a stiff substrate; Fig. 34e). Granules and pebbles are less common than the sandstone-dominated facies, but are often composed of quartzite. Mudstone units are typically planar laminated (Fig. 34d, e, f), and the sandstone may preserve tabular crossbedding, current ripples (Fig. 34g), and microfaults (Fig. 34f). Organic detritus is scattered throughout, and mudstone laminae are common within thicker sandstone beds. Pyrite and siderite are rare (Fig. 34e). Bioturbation was noted only in discrete intervals with 2–20% internal reworking of the sediment (Fig. 34d, e, f). Trace fossils include rare *Planolites*, *Chondrites*, and *Thalassinoides*, with one *Thalassinoides* filled with medium-grained sandstone from the overlying bed (Fig. 34e).

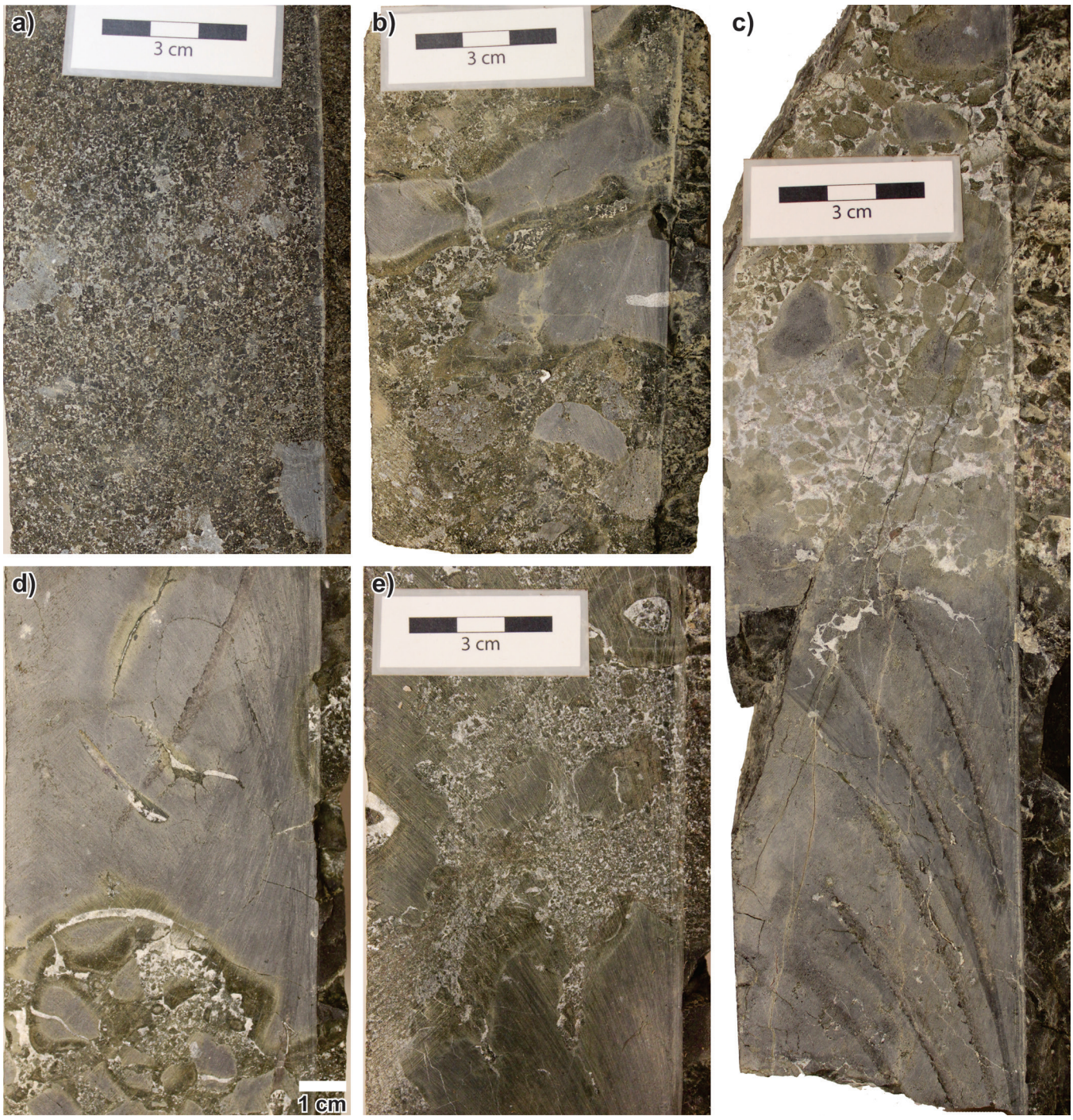


**Figure 31.** Photographs of core 3, Hekja O-71. **a)** Finely brecciated basalt fragments with some calcareous cement. NRCan photo 2019-364. **b)** Large rimmed basalt fragments in a finely commuted matrix of basalt. NRCan photo 2019-365. **c)** A basalt flow capped by brecciated fragments and a zeolite mineral matrix. NRCan photo 2019-366. **d)** Another solid basalt interval above brecciated fragments. NRCan photo 2019-367. **e)** Large brecciated and fractured basalt fragments with rimmed zones within a matrix of smaller basalt fragments. NRCan photo 2019-368. All photographs by L.T. Dafoe.

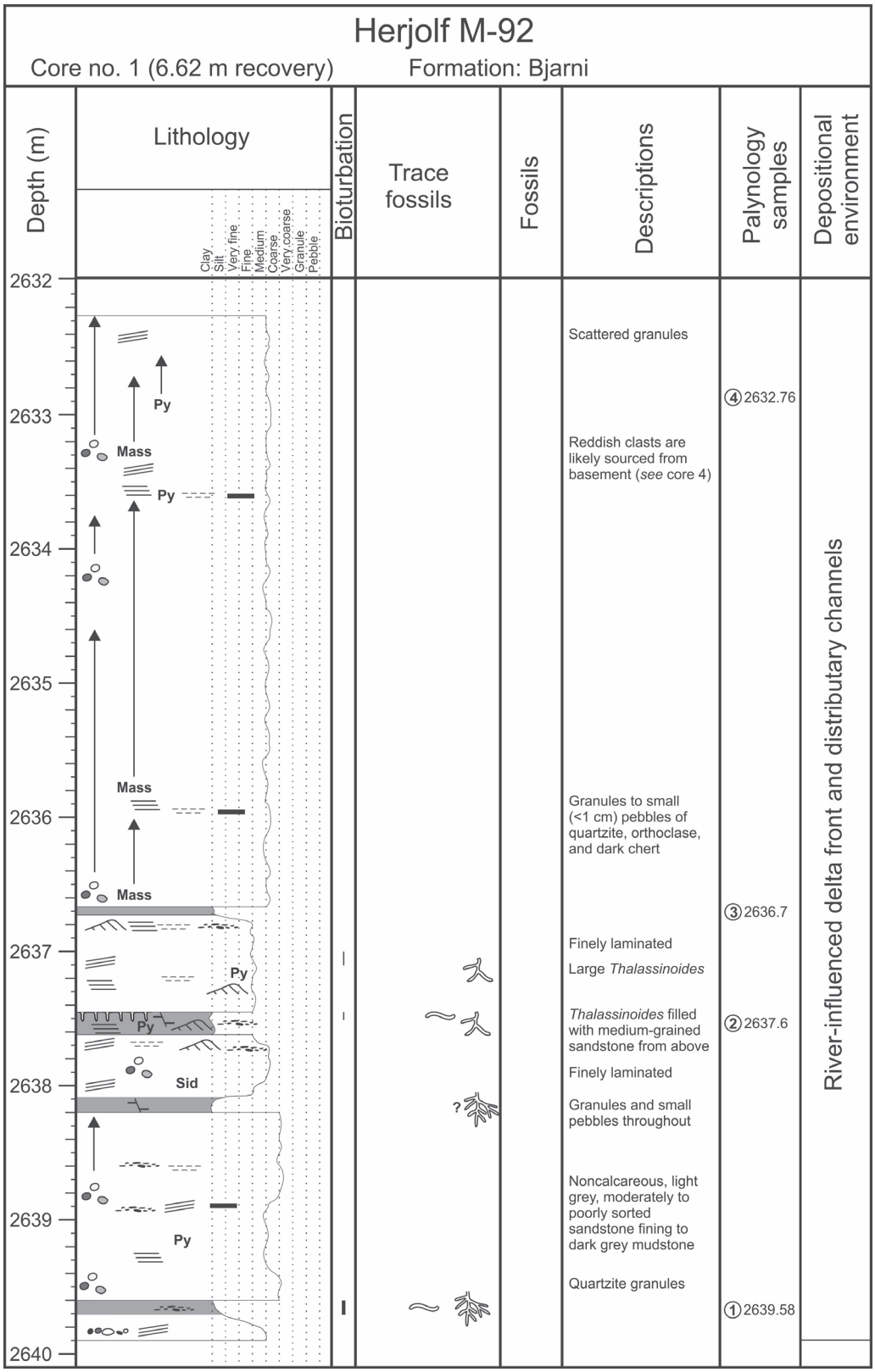


**Figure 32.** Log of core 1 from Herjolf M-92.

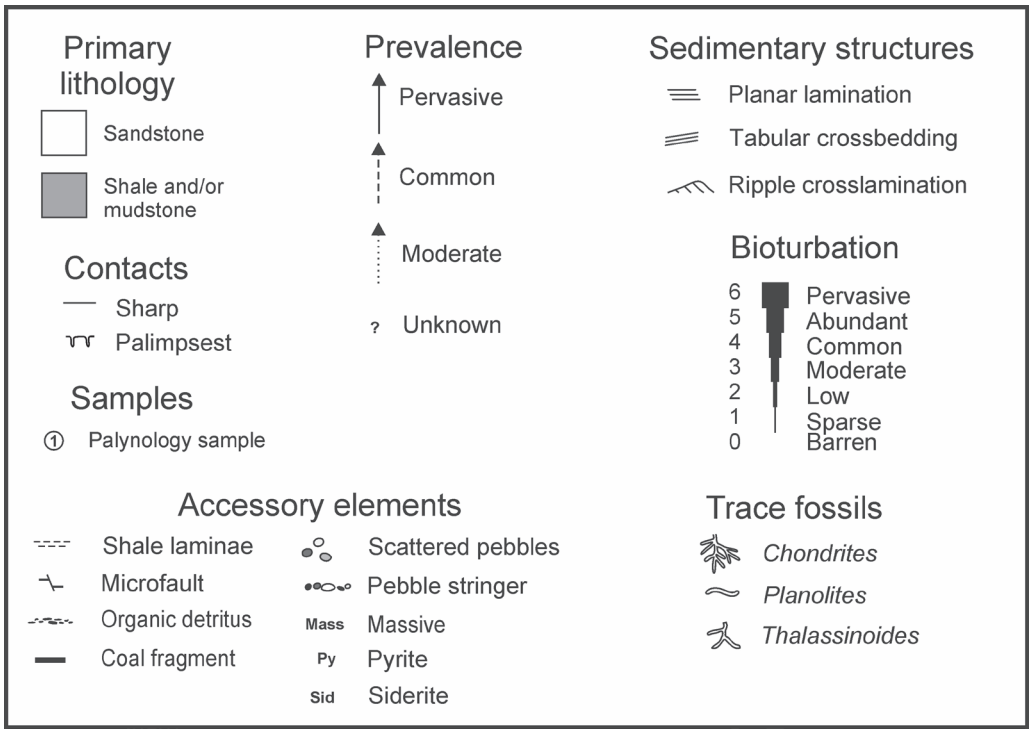


**Figure 32.** (cont.)


**Figure 33.** Photographs of core 1, Herjolf M-92, showing the two major facies of blocky, pebbly sandstone (much of the core) and interbedded sandstone and shale (two intervals in the lower part of the core). Scale bar = 10 cm. NRCan photo 2019-369, 2019-370. Both photographs by L.T. Dafoe.

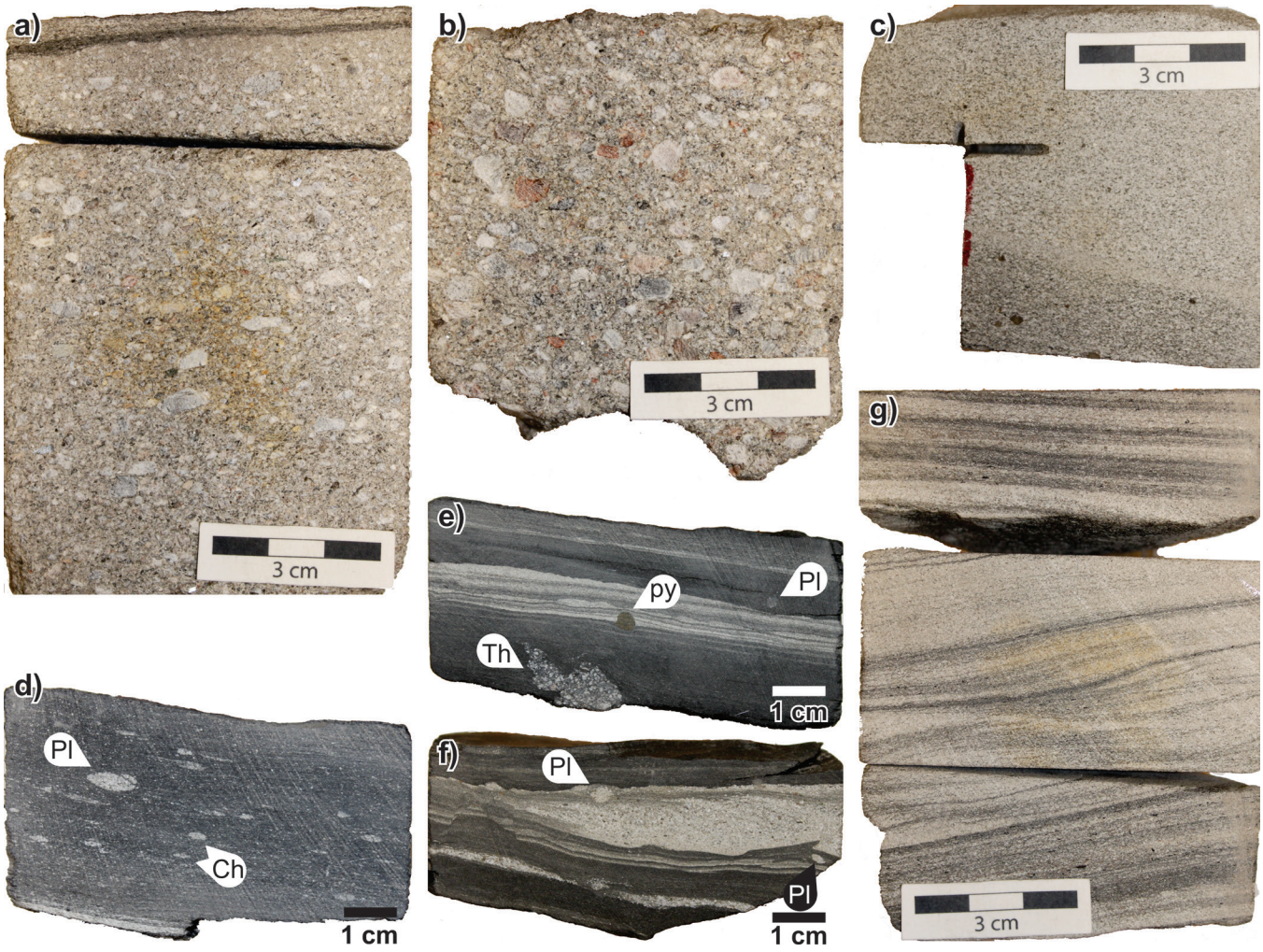


**Figure 34.** Photographs of core 1, Herjolf M-92. **a)** Coarse-grained sandstone with granules and small pebbles. A thin carbonaceous mudstone lamina is present near the top of the massive bed. NRCan photo 2019-371. **b)** Pebble- and granule-bearing sandstone with reddish orthoclase feldspar clasts likely sourced from core 4–equivalent basement rock. NRCan photo 2019-372. **c)** Tabular crossbedded, medium-grained sandstone. NRCan photo 2019-373. **d)** Sandy laminated mudstone with *Chondrites* (Ch) and *Planolites* (Pl) traces. NRCan photo 2019-374. **e)** Interlaminated sandstone and shale with pyrite (py), *Planolites* (Pl), and palimpsest *Thalassinoides* (Th) where the coarse-grained sand is derived from the overlying sandstone bed (not shown). NRCan photo 2019-375. **f)** Interlaminated sandstone and shale with a microfault (left) and current ripple crosslamination (right side of photo), bioturbated with rare *Planolites* (Pl). NRCan photo 2019-376. **g)** Tabular crossbedded, planar-laminated, and current-rippled, fine-grained sandstone with organic-rich layers. NRCan photo 2019-377. All photographs by L.T. Dafoe.

The sandstone facies shows evidence of unidirectional currents (crossbedding), high sedimentation rates (massive bedding), and strong current flow (as indicated by overall grain size). Organic detritus and coal fragments suggest a fluvial or shallow-marine setting. The thin mudstone laminae, a lack of trace fossils, and interbedding with the shalier facies are considered to indicate deltaic deposition, possibly within distributary channels. The heterolithic facies shows evidence of unidirectional currents and reduced current strength. Specimens of *Chondrites* support marine deposition; however, the trace fossil suite is representative of a highly stressed expression of the archetypal *Cruziana* Ichnofacies (comprised mostly of deposit-feeding structures), with unexpectedly low abundance and diversity of trace fossils considering the fine-grained nature of the mudstone beds. The dark colour of the mudstone probably represents high organic content, which can result in poorly oxygenated conditions at the seafloor (Tonkin, 2012), consistent with a lack of bioturbation. Much of the colonization appears to be opportunistic and confined to discrete beds. Sedimentology and ichnology for the heterolithic facies is consistent with deposition in a river-influenced delta front, in which sedimentation rates are relatively high, and with deposition of mudstone of possible hypopycnal or homopycnal origin (MacEachern et al., 2005). The absence of traces of inferred suspension-feeding animals indicates that there was likely enhanced turbidity and suspended sediment in the water column, preventing suspension-feeding behaviours.

### *Palynology*

Four samples were processed and analyzed for palynomorphs from core 1. The lowermost, at 2639.58 m, contains the dinocyst *Chichaouadinium vestitum*, which is restricted to the Albian (Stover et al., 1996). All the other palynomorphs are miospores, primarily bisaccates. These include *Abiespollenites, Piceapollenites, Pinuspollenites, Parvisaccites radiatus*, and *Vitreisporites*. As noted earlier, Nøhr-Hansen et al. (2016) placed the last or youngest occurrence of the pollen *Parvisaccites radiatus* toward the top of the Aptian. The presence of the single specimen of *Chichaouadinium*, however, indicates an Albian age and a setting that was marginal marine to inner neritic. The present authors assign importance to the presence of the single specimen of *Chichaouadinium vestitum* because the sample is from a conventional core, indicating that the miospores (*Parvisaccites radiatus* and *Vitreisporites*) may be reworked.

The sample from 2637.6 m has a sparse palynomorph assemblage, with the miospore *Parvisaccites radiatus* and the dinocyst *Nyktericysta davisii*. Presumably, the age is Albian, based on the presence of *Chichaouadinium vestitum* in the sample immediately below at 2639.58 m. The presence of both miospores and of *Nyktericysta* could indicate a brackish or freshwater paleoenvironment (Bint, 1986; Leckie and Singh, 1991), whereas others have concluded that ceratiacean cysts of this morphological type were associated with nonmarine to marginal marine environments (Nøhr-Hansen, 1992, 2008; Nøhr-Hansen et al., 2016). Therefore, the present authors consider the paleoenvironment as determined from the dinocyst to be coastal or marginal marine.

As in the underlying sample, the one at 2636.7 m also includes the bisaccate *Parvisaccites (Parvisaccites amplus and Parvisaccites radiatus*) and the dinocyst *Nyktericysta.* By applying the same logic, this sample is also concluded to be Albian and the paleoenvironment is coastal or marginal marine.

The highest sample at 2632.76 m predominantly contains miospores, including the taxa *Cerebropollenites*, *Foveotriletes*, *Ischyosporites*, *Parvisaccites radiatus*, *Pinuspollenites*, *Rugutriletes*, *Sculptisporis aulosenensis*, *Vitreisporites pallidus*, and *Vitreisporites* sp. Singh, 1971. One specimen of *Nyktericysta* and four specimens of the acritarch genus *Micrhystridium* were also recorded. This sample is also presumed to be Albian and from a coastal or marginal marine setting.

### *Summary*

This interval, which was cored near the top of the sandstone-dominated Bjarni Formation, was considered to be late Albian to Cenomanian by Williams (1979c) and Ainsworth et al. (2014) from cuttings; however, the present study constrains the age to Albian. Previous paleoenvironmental interpretations by Miller and D'Eon (1987) indicated a marginal marine to inner shelf proximal delta front or alluvial fan delta. This interpretation is consistent with the interpretation presented here of a river-influenced delta front and distributary channels and with the palynology that indicates a coastal or marginal marine setting.

## *Core 2: brown-grey shale (3561.02–3564.07 m)*

### *Core description and interpretation*

The second core recovered from Herjolf M-92 consists of 3.05 m of dark brown to grey shale of the Bjarni Formation (Fig. 35, 36). The shale is weakly fissile, indurated, and possesses shiny fractured surfaces, indicating reorientation of mica grains due to deep burial. Fine- to medium-grained sand and rare granules are scattered throughout the core, which is, overall, finely planar laminated (Fig. 37a). Thin, very fine-grained sandstone laminae are present (Fig. 37b), as well as siderite-cemented beds (Fig. 37c) and rare coal fragments. A 10 cm thick, sharp-based sandstone with soft-sediment deformation at its upper boundary occurs near the top of the core (Fig. 37c). This sandstone bed is tabular crossbedded with small siderite nodules. Overall, bioturbation is minimal (locally 2–10% of the core), and rare trace fossils were noted from sandier intervals, including rare *Chondrites* (Fig. 37b) and *Helminthopsis*. The overall homogeneous nature of the sediment may reduce the visibility of trace fossils; however, disruption to the laminated fabric appears to be minimal.

The planar laminated nature of the shale indicates a low-energy setting with little current or wave activity. Thin sandstone beds and a thicker crossbedded sandstone suggest intermittent influxes of coarse-grained clastic material. Small coal fragments indicate a nearby source of vegetation. These rocks could represent a lacustrine setting, but the presence of marine trace fossils (albeit rare) suggests a marine setting. The trace fossils are diminutive, and low in diversity and abundance, indicating a highly stressed environmental setting. The colour of the shale may indicate high organic content that could have produced dysoxic to anoxic conditions at the sediment surface (Tonkin, 2012). The sparse trace-fossil suite is consistent with a brackish-water setting. Based on the lack of wave-formed structures, a quiet, restricted marine bay with intermittent distal deltaic sand pulses is the interpreted depositional setting.

### *Palynology*

Three samples were processed and analyzed for palynomorphs from core 2. The lowest, from 3563.8 m, contains a varied miospore assemblage and three dinocysts, one of which is *Nyktericysta*. Miospores include *Aequitriradites* cf. *verrucosus* and *Callialasporites dampieri*.Nøhr-Hansen et al. (2016) placed the last or youngest occurrence of

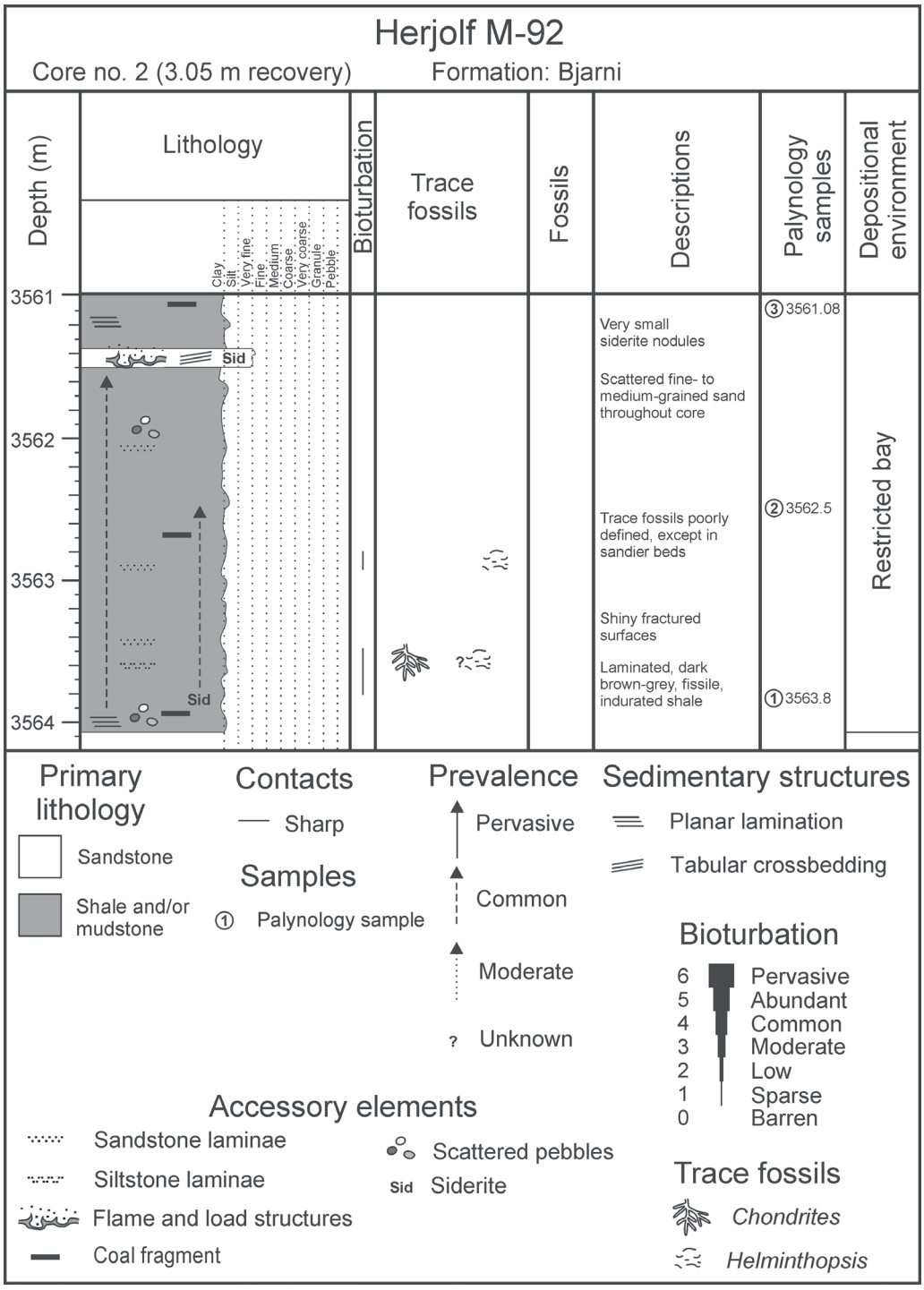


**Figure 35.** Log of core 2 from Herjolf M-92. The shale is consistently planar laminated and rare trace fossils are present in sandier intervals.


**Figure 36.** Photograph of core 2, Herjolf M-92. Scale bar = 10 cm. NRCan photo 2019-378. Photograph by L.T. Dafoe.

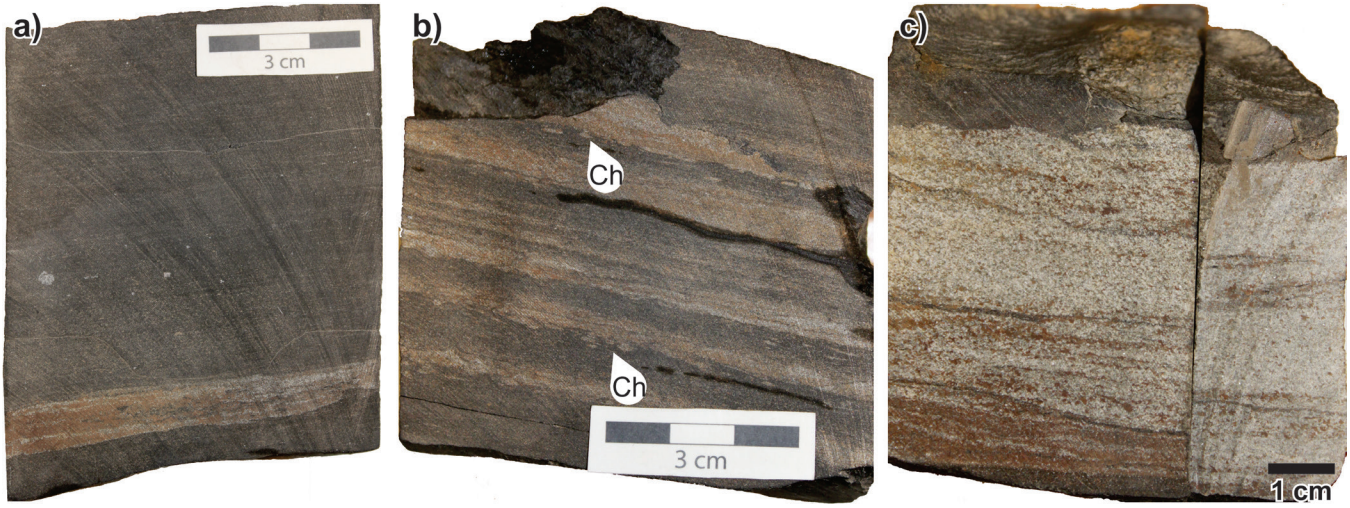


**Figure 37.** Photographs of core 2, Herjolf M-92. **a)** Planar-laminated shale with small siderite nodules in a fine-grained sandstone bed near the base of the core. Sand grains and granules are scattered in the shale. NRCan photo 2019-379. **b)** Thin sandstone beds and *Chondrites* (Ch). NRCan photo 2019-380. **c)** Tabular crossbedded sandstone with small siderite nodules near the top of the core. NRCan photo 2019-381. All photographs by L.T. Dafoe.

*Callialasporites dampieri* within the Aptian, whereas Williams (2003) considered the last or youngest occurrence of this species in the Skua E-41 well in the Carson Basin to be within the Barremian. This evidence suggests that the sample is close to the base of the Aptian; however, the presence of *Nyktericysta* suggests the age could be Barremian–Albian. This is based on Stover et al. (1996), who plotted the stratigraphic range of the closely related genus *Vesperopsis* as Barremian–early Cenomanian; however, since overlying samples are considered Barremian–Aptian (*see* below), this sample cannot extend into the Albian. The presence of *Nyktericysta* indicates a marginal marine paleoenvironment.

A second sample from 3562.5 m has only a few miospores, with *Aequitriradites*, *Cerebropollenites*, and *Cicatricosisporites*. In a study of Labrador Shelf microfossils, Gradstein and Williams (1976) defined a Barremian–Aptian *Cerebropollenites mesozoicus* assemblage. The evidence is weak because of the few miospores, but these indicate an age no younger than Barremian–Aptian. A single specimen of the dinocyst *Nyktericysta*, indicates that the paleoenvironment was marginal marine.

The highest sample, at 3561.08 m, includes the miospores *Aequitriradites* and *Cerebropollenites*. The authors date this sample Barremian–Aptian, similar to the sample described above from 3562.5 m. An absence of dinocysts suggests a nonmarine paleoenvironment for this uppermost sample.

#### *Summary*

Based on cuttings of the Bjarni Formation, Williams (1979c) and Ainsworth et al. (2014) considered the age of this interval to be Barremian–Aptian, which is consistent with the findings of the present study. Miller and D'Eon (1987) suggested a nonmarine, lacustrine delta-front to -slope setting. These previous results are inconsistent with the current analyses from both the core and palynology that generally indicate a marginal marine setting or restricted bay. A lack of dinocysts in the palynology sample from 3561.08 m may indicate highly brackish conditions that are not conducive to dinoflagellates, as implied by the depauperate trace fossil assemblage. Brackish conditions and the presence of only subtle marine indicators likely account for previous interpretations, suggesting nonmarine deposition. Possibly, this core interval represents a phase of marine inundation during lower Bjarni Formation deposition.

### *Core 3: green-brown basalt (3789.93–3790.84 m)*

#### *Core description and interpretation*

Core 3 of the Herjolf M-92 well is in poor condition, with one box sleeve comprising bags of rubbly core material (Fig. 38a). The core, which is representative of the Alexis Formation, consists of green-brown basalt with calcite veins (stained red-brown; Fig. 38b, c). The aphanitic texture is consistent with basalt flows. A K-Ar age of 121 ± 5 Ma was determined for this core (Umpleby, 1979).

#### *Palynology*

A single sample at 3790.84 m was processed for palynology and, surprisingly, contained two pollen grains, one *Piceaspollenites* and one *Abiespollenites*. Whereas these pollen grains probably reflect contamination considering the poor condition of the core, shale interbeds are noted from the Canstrat log for the Alexis Formation. No age or paleoenvironment could be interpreted based on the limited assemblage.

### *Core 4: granodiorite (4084.37–4086.32 m)*

#### *Core description and interpretation*

The lowermost core of Herjolf M-92 was recovered from pre-rift basement rock comprising orthoclase-rich granodiorite (Fig. 39). Wasteneys et al. (1996) described this basement rock as fine- to medium-grained granodiorite–quartz monzonite with a relict K-feldspar porphyritic texture. The age of crystallization based on U-Pb dates is 1801.4 ± 5 Ma, with metamorphism occurring later (Wasteneys et al., 1996). This granodiorite has been equated with the onshore Makkovik Orogen (Fig. 1; Wasteneys et al., 1996). Clasts of this material can be identified in the sandstone of core 1, suggesting that exposures of Makkovik Orogen granodiorite were a local source of sediment during deposition of the Bjarni Formation.

## Hopedale E-33

Hopedale E-33 was drilled in 1978 in the Hopedale Basin, offshore Labrador (Fig. 1), as a wildcat well (Chevron Standard Ltd., 1978); its total depth was 2072.2 m. The Bjarni Formation was sampled by a single core interval.

### *Core 1: dark grey shale (1957.0–1964.7 m)*

#### *Core description and interpretation*

Much of the material comprising core 1 of the Bjarni Formation from Hopedale E-33 is in a rubbly state (Fig. 40), and the upper portion of the core appears to consist of bedrock fragments encased in drilling mud. Despite this poor condition, two facies could be discerned: a buff sandstone and a dark grey shale (Fig. 41). The sandstone occurs at the base of the core, is less than 1 m thick, and is in a rubbly state, making interpretations of the sedimentary features difficult; however, mudstone laminae were noted in addition to wavy, parallel-laminated beds. Coal fragments are present

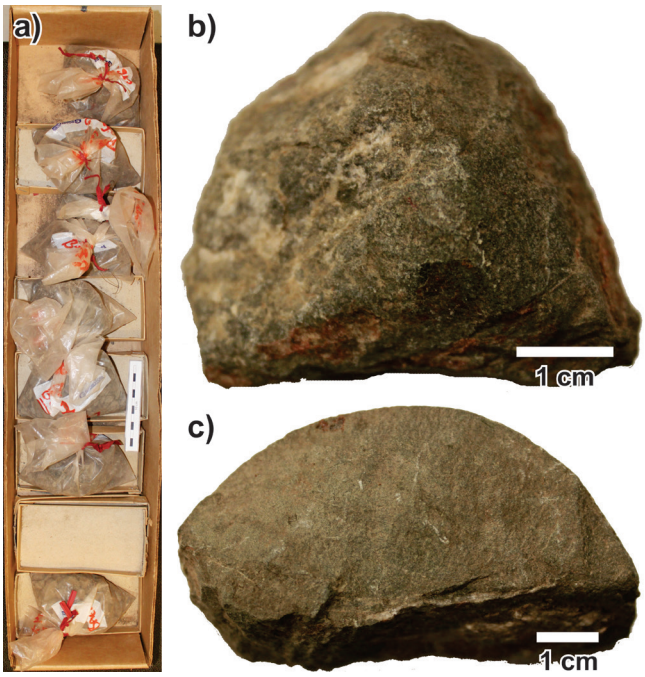


**Figure 38.** Photographs of core 3, Herjolf M-92. **a)** Core box showing bagged core materials (scale bar = 10 cm). NRCan photo 2019-382. **b)**, **c)** Green-brown, finely crystalline basalt with some reddish coloration on the fragment shown in Figure 38b. NRCan photo 2019-383, NRCan photo 2019-384. All photographs by L.T. Dafoe.

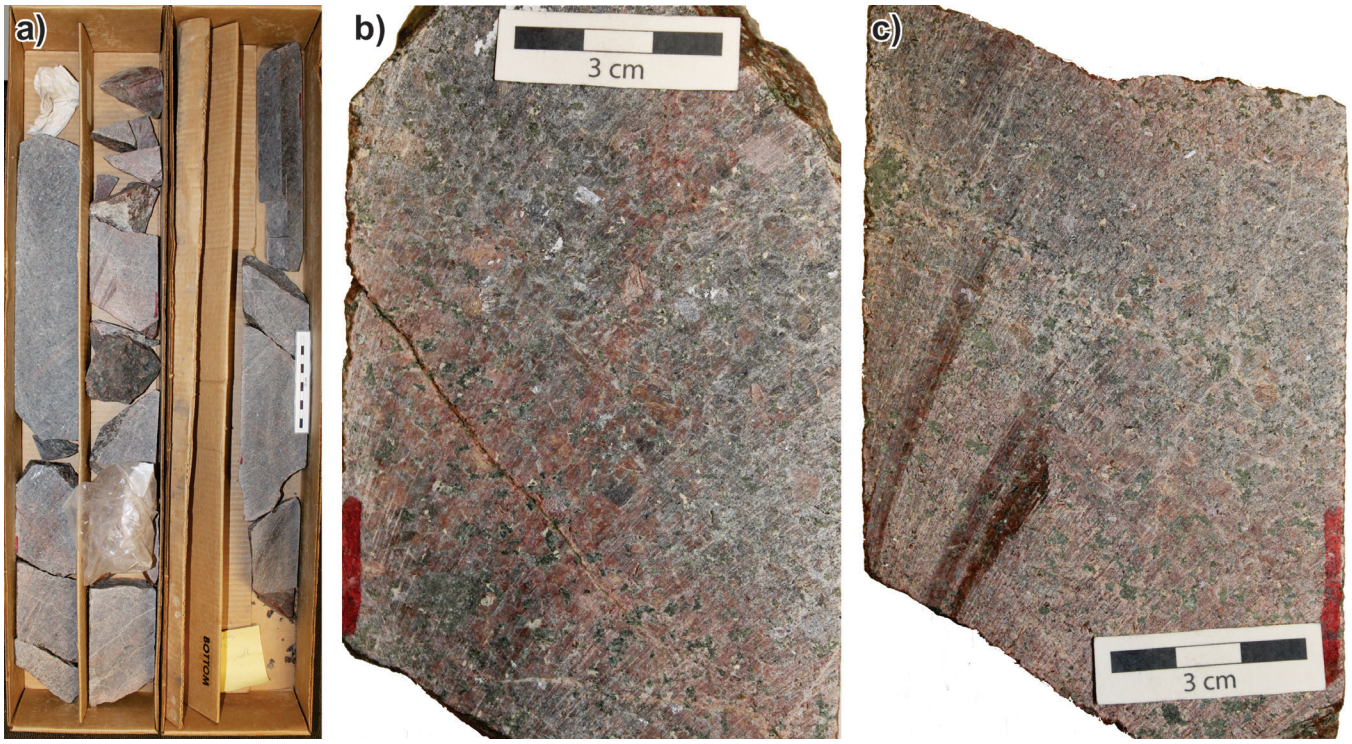


**Figure 39.** Photographs of core 4, Herjolf M-92. **a)** Core boxes showing the granodiorite basement core (scale bar = 10 cm). NRCan photo 2019-385. **b)**, **c)** Examples of the granodiorite with a composition rich in orthoclase, and fine fractures and subtle banding are seen in Figure 39c. NRCan photo 2019-386, 2019-387. All photographs by L.T. Dafoe.

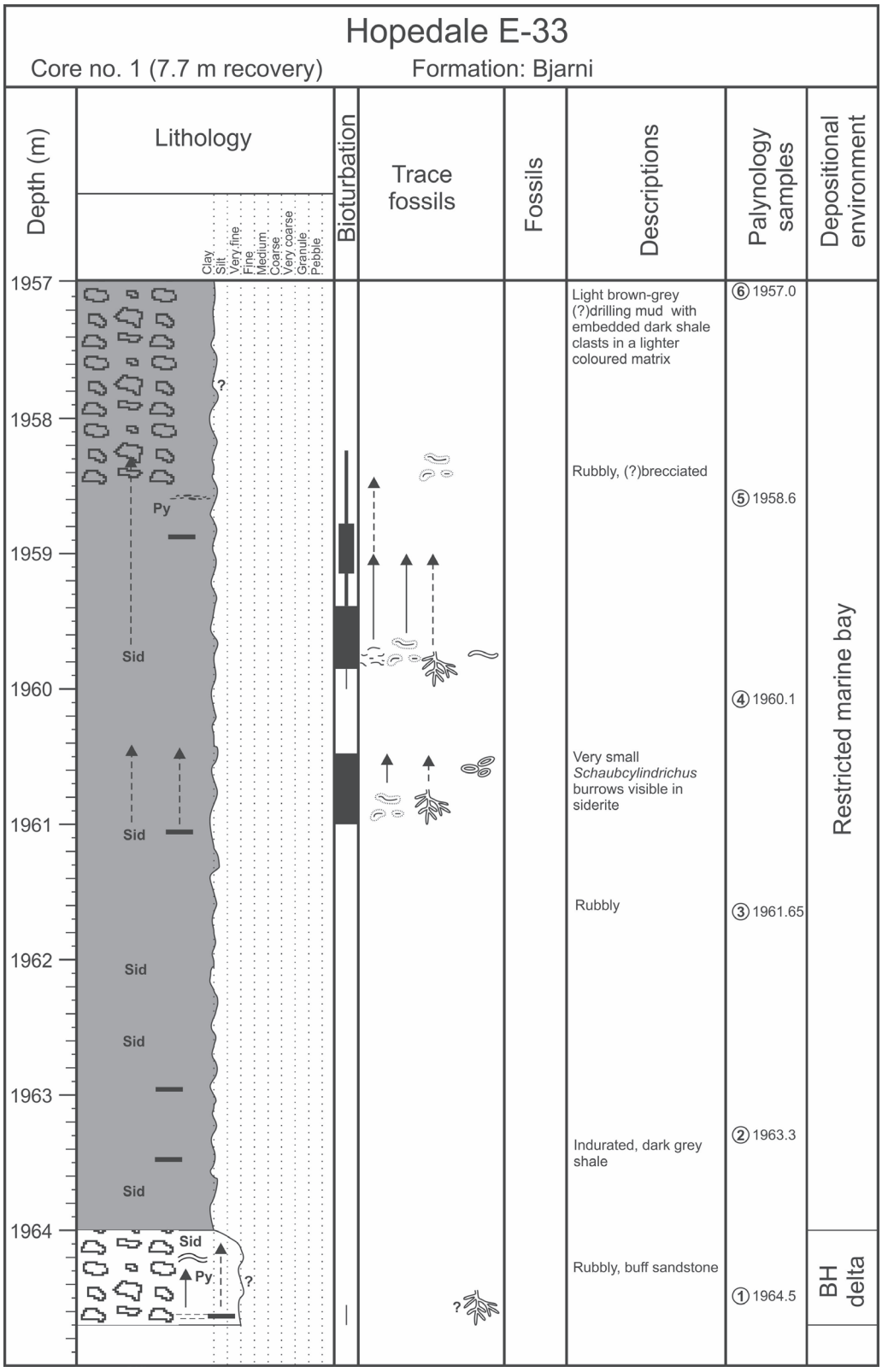


**Figure 40.** Log of core 1 from Hopedale E-33. Note that identification of sedimentary structures and trace fossils was difficult given the rubbly nature of most of the core interval. BH = Bayhead.

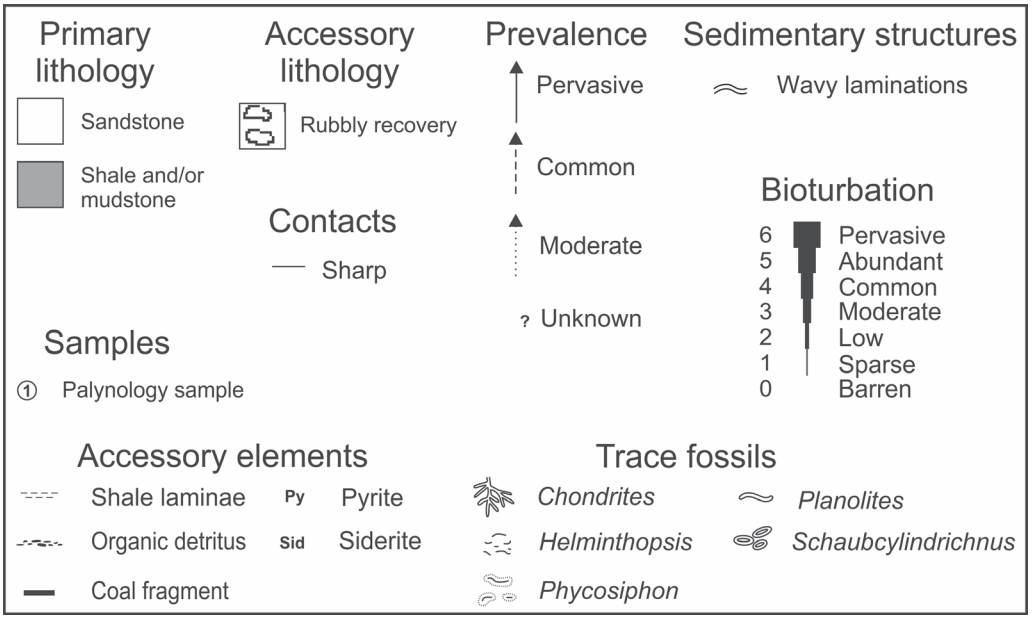


**Figure 40.** (cont.)

throughout, and pyrite and siderite are both rare (Fig. 42a, b). Possible *Chondrites* characterize the muddy interval at the very base of the core (Fig. 42a) with about 10% bioturbation of the sediment there.

The dark grey shale facies is indurated, and much of it comprises rubbly material, except for sideritized intervals (Fig. 42). Siderite (Fig. 42d, e, f) and coal fragments (Fig. 42c) are common throughout the facies, and rare pyrite and organic detritus were noted near the top of the core. The uppermost portion of the facies appears to comprise fragmented shale encased in drilling mud (Fig. 42g). Trace fossils can be identified in thick sideritized intervals, where sideritization highlights slight contrasts in lithology and fabric (Fig. 42d, e, f). The diversity and abundance of the trace-fossil suite are both very low, with bioturbation ranging from 0–100% of the facies. Homogenized units are characterized by common *Phycosiphon* and *Helminthopsis*, moderate numbers of *Chondrites*, and rare *Planolites* and *Schaubcylindrichus* (Fig. 42d, e). The one example of *Schaubcylindrichus* was notably very small (about 2 mm in cross-section).

There is no evidence of wave-reworking in the fine-grained, dark grey shale facies. A quiet-water, shallow-marine setting is indicated by the fine-grained nature of the sediment combined with the presence of consistent coal fragments and marine trace fossils. The trace-fossil suite is representative of a stressed expression of the *Zoophycos* Ichnofacies, dominated by grazing traces and, combined with the sedimentology, is interpreted to represent a brackish, restricted marine bay with low wave energy. Organic-rich, terrestrial-sourced mud can result in enhanced siderite formation through bacterially facilitated precipitation (Coleman, 1993), and high sedimentation rates can lead to sulphate reduction that also promotes siderite precipitation (Gautier, 1982). Based on this interpretation for the shale, the sandstone at the base of the core is consistent with a bayhead deltaic setting, especially considering the amount of coal material and presence of *Chondrites*.

## *Palynology*

Six samples from core 1 were processed for palynomorphs. In the bottommost sample at 1964.5 m, the spores include *Plicatella jansonii*, *Callialasporites dampieri*, *Cerebropollenites macroverrucatus*, *Pilosisporites trichopapillosus*, *Ruffordiaspora australiensis*, and *Podocarpidites* sp. Williams (2003, 2007b) placed the last or youngest occurrence of the genus *Callialasporites* within the Barremian, but Nøhr-Hansen et al. (2016) considered *Callialasporites* and the species *Cerebropollenites macroverrucatus* to extend into the Aptian. Williams (2007b) recorded *Ruffordiaspora australiensis* from an interval in the Snorri J-90 well that he considered to be Barremian. This was, however, modified in Nøhr-Hansen et al. (2016) wherein they considered the interval to be Aptian. Williams (1975) erected a *Pilosisporites trichopapillosus* Zone, which he considered was early Aptian. Accordingly, the present authors consider this sample to be early Aptian. The absence of dinocysts conforms with the interpretation of a nonmarine paleoenvironment.

Dinocysts are also absent from the sample at 1963.3 m. Miospores include *Callialasporites* sp., *Ruffordiaspora australiensis*, *Cicatricosisporites hallei*, *Ischyosporites punctatus*, *Parvisaccites radiatus*, and *Impardecispora apiverrucatus*. Because of the similarities to the sample at 1964.5 m, this sample is considered to be no younger than


**Figure 41.** Photographs of core 1, Hopedale E-33. There are two boxes for every interval intended to represent the opposing slabs of the core. Scale bar = 10 cm. NRCan photo 2019-388, 2019-389, 2019-390, 2019-391, 2019-392, 2019-393, 2019-394, 2019-395, 2019-396, 2019-397, 2019-398. All photographs by L.T. Dafoe.


**Figure 41.** (cont.)


**Figure 42.** Photographs of core 1, Hopedale E-33. **a)** Buff sandstone facies, with mudstone laminae, *Chondrites* (Ch), and coal fragments (cf). NRCan photo 2019-399. **b)** Sandstone facies with distinct heterolithic composition, coal fragments (cf) and pyrite (py). NRCan photo 2019-400. **c)** Massive dark grey shale facies with coal fragments (cf). NRCan photo 2019-401. **d)** Sideritized interval within the shale facies with thorough bioturbation by *Chondrites* (Ch), *Helminthopsis* (He), and *Phycosiphon* (Ph). NRCan photo 2019-402. **e)** Siltier mudstone interval with intense bioturbation, including *Helminthopsis* (He), *Chondrites* (Ch), and *Phycosiphon* (Ph). NRCan photo 2019-403. **f)** Mudstone interval with a possible gutter cast structure outlined by the white dotted line, as well as *Chondrites* (Ch). NRCan photo 2019-404. **g)** Uppermost part of the core that appears to consist of fragments of bedrock within drilling mud. NRCan photo 2019-405. All photographs by L.T. Dafoe.

early Aptian. The absence of dinocysts is again suggestive of a nonmarine setting. Similarly, *Pilosisporites trichopapillosus* and the pollen *Callialasporites trilobatus* are present in the sample at 1961.65 m. For the reasons noted above, this sample is also considered to be early Aptian and from a nonmarine paleoenvironment.

The sample at 1960.1 m is also devoid of dinocysts; however, there are several miospore taxa, including *Aequitriradites verrucosus*, *Appendicisporites problematicus, Callialasporites turbatus*, *Contignisporites cooksoniae*, *Maculatisporites undulatus*, *Osmundacidites* sp., *Pilosisporites trichopapillosus, Ruffordiaspora australiensis, Saxetia* sp., and *Vitreisporites* sp. sensu Singh, 1971. Williams (2007b) recorded *Ruffordiaspora australiensis* from an interval in Snorri J-90 that he considered to be Barremian. This was, however, modified in Nøhr-Hansen et al. (2016), where they considered the interval to be Aptian. Also, Williams (2003, 2007b) placed the last or youngest occurrence of the genus *Callialasporites* within the Barremian, but Nøhr-Hansen et al. (2016) considered *Callialasporites* to extend into the Aptian. The presence of *Pilosisporites trichopapillosus* indicates that the sample is likely early Aptian. The absence of dinocysts again indicates a nonmarine paleoenvironment.

The sample at 1958.6 m is also devoid of dinocysts. Miospores are *Aequitriradites* cf. *verrucosus*, *Cicatricosisporites* sp., *Ischyosporites* sp., *Parvisaccites* sp., and *Impardecispora apiverrucatus*. The assemblage indicates an Albian or older age, based on the findings of Williams (1975). More specifically, the present authors consider the absence of species of the pollen *Rugubivesiculites* to suggest an early Albian or older age. Although not the most reliable way to determine ages, the absence of key species can be used; in this case *Rugubivesiculites* is usually common in the late Albian of this region. An absence of dinocysts and acritarchs conforms with the interpretation of a nonmarine paleoenvironment.

The uppermost sample, at 1957 m, shows a marked change from the underlying samples in having a diverse dinocyst assemblage, including *Cerodinium diebelii*, *Cribroperidinium* sp., *Impagidinium* cf. *victorianum*, *Isabelidinium cooksoniae*, *Palaeoperidinium pyrophorum*, *Sepispinula huguoniotii*, *Spinidinium uncinatum*, and *Surculosphaeridium convocatum*. Nøhr-Hansen et al. (2016) considered the last or youngest occurrences of *Impagidinium* cf. *victorianum* and *Isabelidinium cooksoniae* to be within the Maastrichtian; and *Heterosphaeridium bellii* and *Surculosphaeridium convocatum* have their last or youngest occurrences in the Campanian. Both McIntyre (1974) and Nøhr-Hansen et al. (2016) considered *Cerodinium diebelii* to have its first or oldest occurrence at the base of the Maastrichtian, however, there are conflicting opinions on this. For instance, Williams et al. (2004) plotted the first or oldest occurrence for *Cerodinium diebelii* within the middle Campanian in Northern Hemisphere mid-latitudes. Based on the convincing evidence regarding the last or youngest occurrences of *Heterosphaeridium bellii* and *Surculodinium convocatum* in the Campanian, the present authors consider this assemblage to be late Campanian; however, the presence of bedrock fragments encased in drilling mud at this level in the core (Fig. 42g) suggests that the assemblage may not be in place due to contamination. Judging by the presence of *Impagidinium* cf. *victorianum*, the sediments at this horizon were apparently deposited in an open-ocean paleoenvironment, but this sample is contaminated.

### *Summary*

Williams (1981) gave the age of the interval based on cuttings as Barremian–Aptian. The new results indicate a slightly younger age of early Aptian to early Albian or older for this interval of the Bjarni Formation, such that an Aptian age is most likely. Previous interpretations of the paleoenvironment include lower bathyal (Bujak Davies Group, 1989d) and lacustrine (delta slope, alluvial fan delta, turbidite sequences and/or debris flows; Miller and D'Eon, 1987). Results from the core from the present study indicate a brackish, restricted marine bay with bayhead delta progradation, whereas the palynomorphs denote a nonmarine paleoenvironment between 1964.5 m and 1958.6 m. Since the sedimentological and ichnological interpretation of the core material is rather conclusive, that interpretation is preferred. A highly brackish, restricted marine bay may have significantly deterred dinoflagellate habitation, giving rise to the apparent nonmarine paleoenvironmental signature.

## Karlsefni A-13

Karlsefni A-13 was drilled in the southern part of the Saglek Basin, offshore Labrador (Fig. 1) in 1975–1976; the total depth was 4148.9 m. The objective was to test the rocks draping a basement structure (Eastcan Exploration Ltd., 1975a). Two core intervals were recovered, the upper core from the Cartwright Formation, and the lower core from within Precambrian basement.

### *Core 1: sandy mudstone (3325.1–3333.94 m)*

#### *Core description and interpretation*

Core 1 consists of grey-brown, very fine- to fine-grained sandy mudstone of the Cartwright Formation that is mostly homogenized by bioturbation (Fig. 43, 44), but contains some dark grey, unbioturbated mudstone laminae scattered throughout the core (Fig. 45). Sedimentary structures in this core interval include scattered planar laminations and current ripples (Fig. 45d, f), rare wavy laminations, and soft-sediment deformation features (convoluted bedding and flame structures). Accessory features include siderite nodules (Fig. 45f), siderite beds, and possible syneresis cracks. Trace fossils dominate

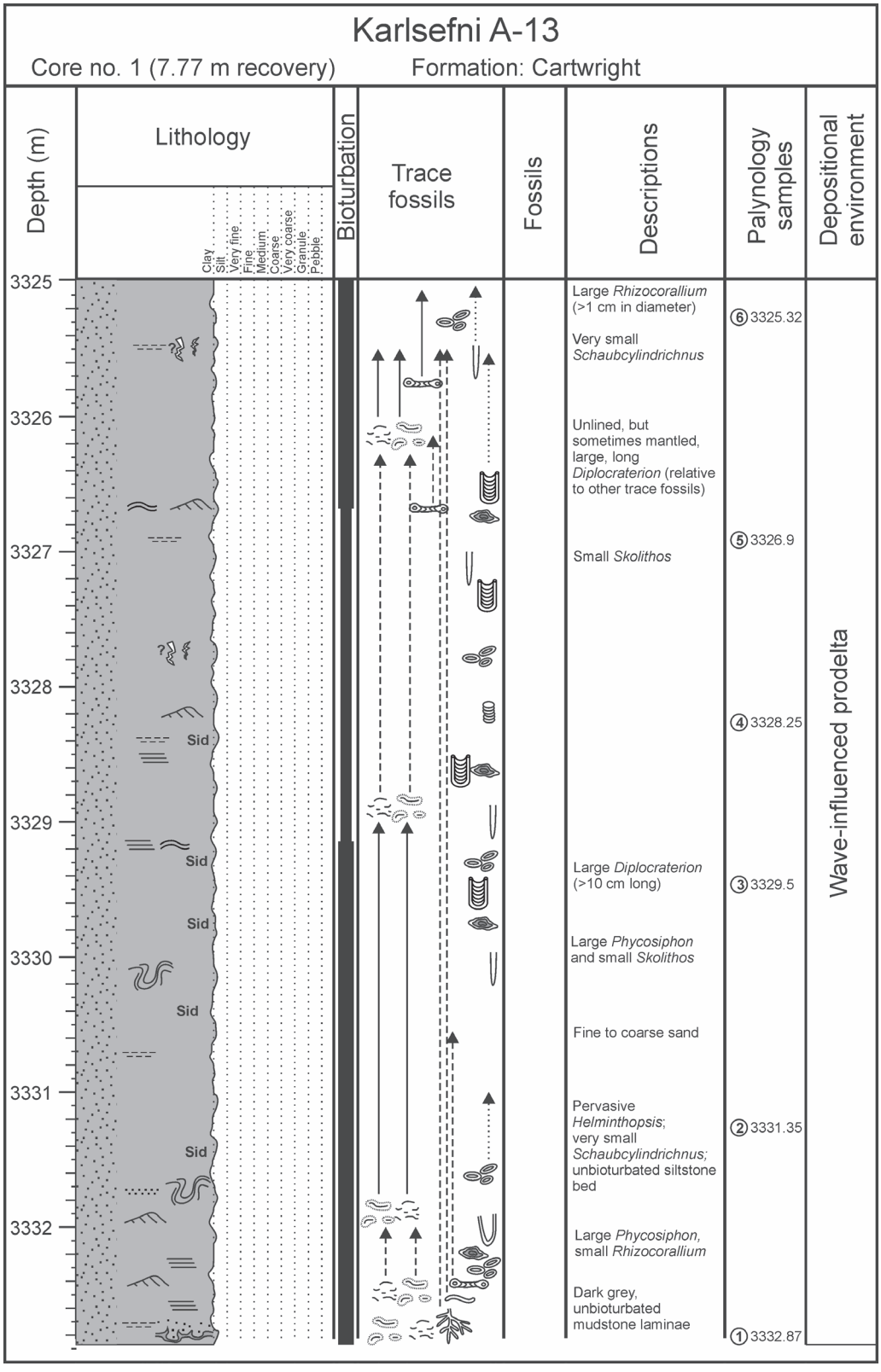


**Figure 43.** Log of core 1 from Karlsefni A-13, showing a consistently bioturbated, sandy mudstone lithology.

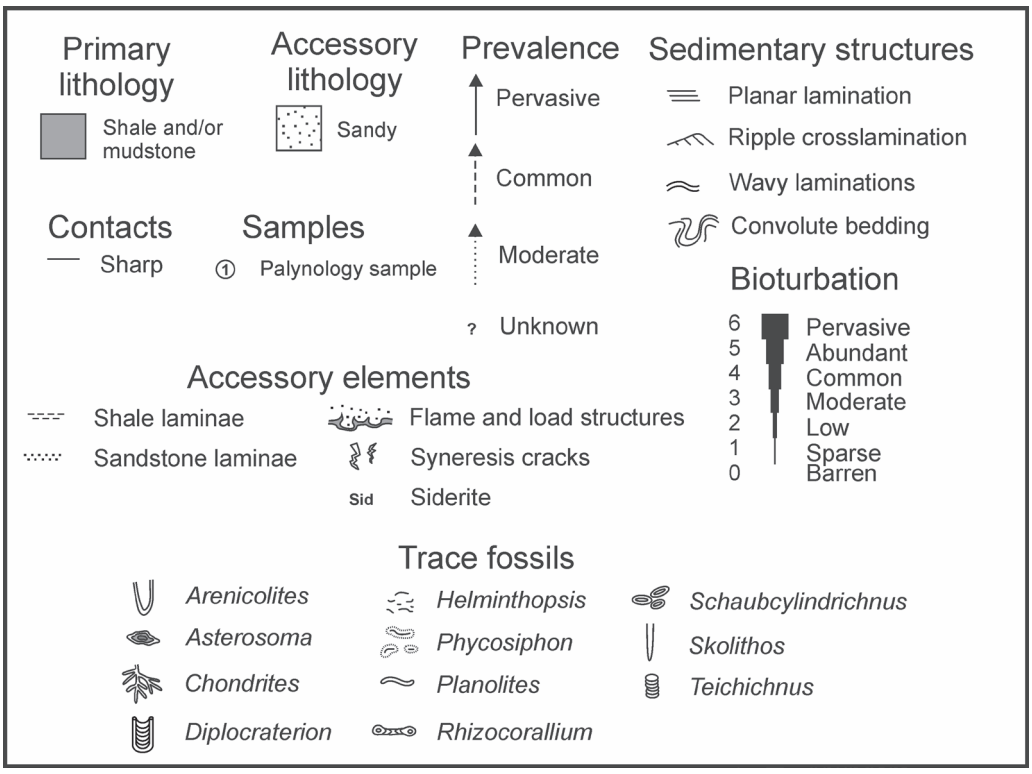


**Figure 43.** (cont.)


**Figure 44.** Photographs of core 1, Karlsefni A-13. Scale bars = 10 cm. NRCan photo 2019-406, 2019-407. Both photographs by L.T. Dafoe.

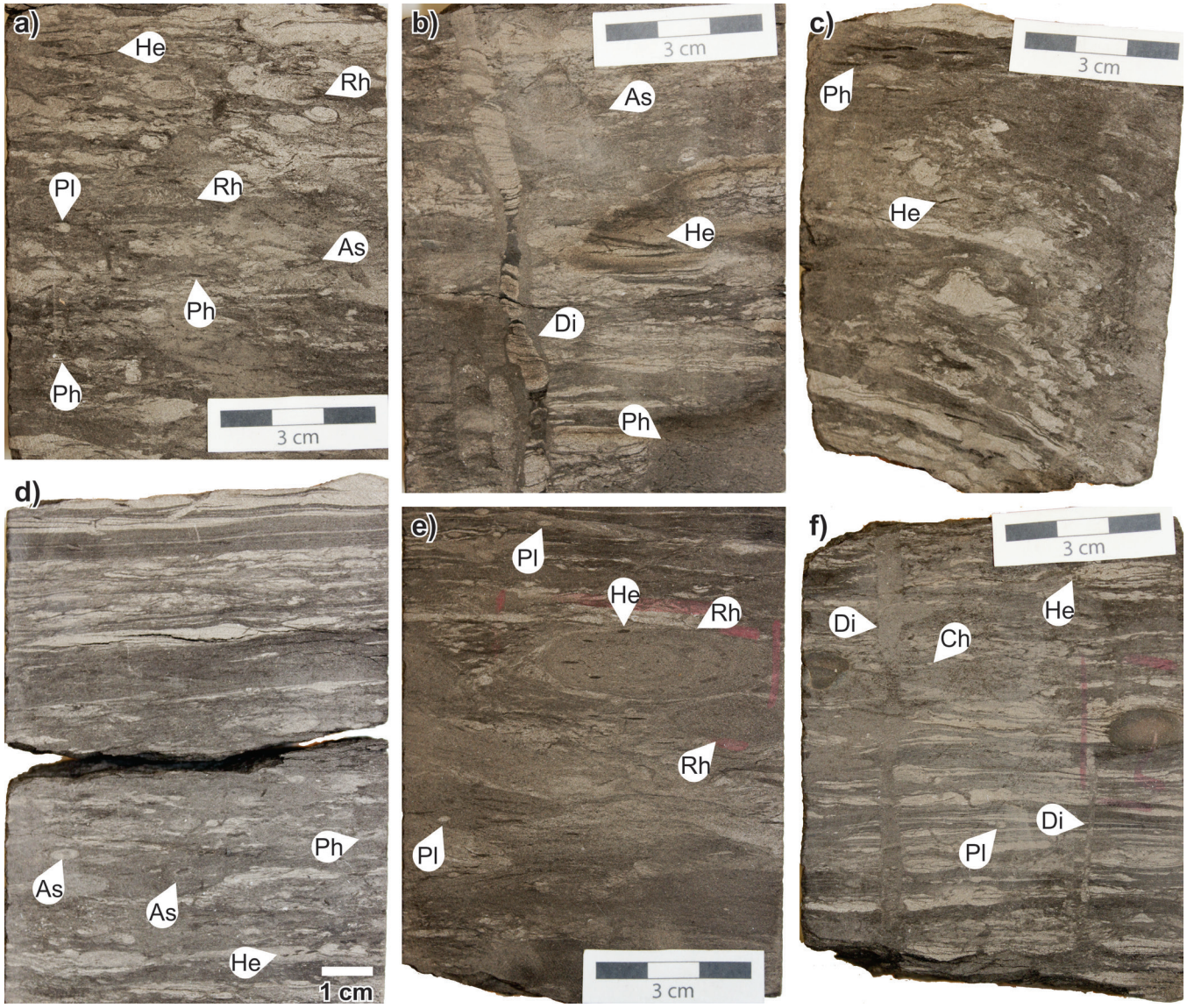


**Figure 45.** Photographs of core 1, Karlsefni A-13. **a)** Bioturbated sandy mudstone with *Phycosiphon* (Ph), *Planolites* (Pl), *Rhizocorallium* (Rh), *Asterosoma* (As), and *Helminthopsis* (He). NRCan photo 2019-408. **b)** Large *Diplocraterion* (Di) crosscutting partially burrowed and partially laminated sediments with *Helminthopsis* (He), *Asterosoma* (As), and *Phycosiphon* (Ph). Note that the *Diplocraterion* trace is partially thickly lined with mud. NRCan photo 2019-409. **c)** Convoluted bedding in sandy mudstone with grazing traces *Helminthopsis* (He) and *Phycosiphon* (Ph). NRCan photo 2019-410. **d)** Laminated to burrowed sediment with common *Asterosoma* (As), *Phycosiphon* (Ph), and *Helminthopsis* (He). NRCan photo 2019-411. **e)** Large *Rhizocorallium* (Rh), reburrowed by *Helminthopsis* (He), and with *Planolites* (Pl). NRCan photo 2019-412. **f)** Planar-laminated to weakly current-rippled sandstone and mudstone relatively less bioturbated than the rest of the core interval. *Diplocraterion* (Di) crosscuts the fabric, which also includes *Chondrites* (Ch), *Helminthopsis* (He), and *Planolites* (Pl). NRCan photo 2019-413. All photographs by L.T. Dafoe.

the succession, with bioturbation ranging from 60% to 80% of the rock (Fig. 45). Ichnofossils include pervasive to common *Helminthopsis* and *Phycosiphon*; common *Chondrites*, *Rhizocorallium*, *Asterosoma*, and *Planolites*; *Diplocraterion* and *Schaubcylindrichnus* in moderate numbers; and rare *Teichichnus*, *Arenicolites*, and *Skolithos*. Some unusual trace-fossil occurrences include larger than typical *Phycosiphon* and *Rhizocorallium* (Fig. 45e), as well as some diminutive examples of *Rhizocorallium*, *Schaubcylindrichnus*, and *Skolithos*. *Diplocraterion* can be a decimeter or more in length and are generally unlined, although some have muddy linings (Fig. 45b, d).

The consistently sandy nature of the mudstone, with 50% or more sand locally, and prevalence of bioturbation suggests a shelfal depositional setting; however, the trace-fossil suite reveals additional information about the paleoenvironmental conditions during deposition. In this core, there is a high abundance and diversity of marine trace fossils, indicating an overall normal marine suite. Whereas the large size of some ichnofossils suggests typical normal marine conditions or opportunistic behaviour, the diminutive nature of others implies some degree of environmental stress. In addition, the lack of bioturbation in some intervals, especially those containing dark mudstone, suggest more rapid depositional rates, possibly associated with low oxygenation, reducing the decomposition of organic matter. These dark mudstone units are interpreted to represent hyperpycnal flows from a fluvial source. The presence of soft-sediment deformation features further suggests rapid sedimentation rates combined with 'soupy' or water-laden sediments typical of deltaic settings. In addition, the presence of vertical trace fossils indicates that water turbidity was moderate, such that suspension-feeding animals could maintain their filter-feeding behaviours. The overall trace-fossil assemblage is characteristic of a weakly stressed expression of the archetypal *Cruziana* Ichnofacies. This, and the sedimentological characteristics suggest a wave-influenced prodeltaic setting, where wave activity mitigates some stresses associated with deltaic deposition (turbidity, suspended sediment concentrations, and reduced salinity).

## Palynology

Six samples from core 1 were processed for palynomorphs. The lowest sample, at 3332.87 m, has few palynomorphs, but a single specimen of *Palaeocystodinium bulliforme,* a significant dinocyst marker, is present. Nøhr-Hansen et al. (2016) considered the last or youngest occurrence of this species to be at the top of the Selandian. Also present are the dinocysts *Cerodinium diebelii* and *Cerodinium* cf. *speciosum*. *Cerodinium diebelii* is generally considered to have its last or youngest occurrence in the Danian, but can extend into the early Selandian in mid-latitudes of the Northern Hemisphere (Williams et al., 2004). The pollen *Momipites wyomingensis*, which Nichols and Ott (1978) restricted to their Paleocene P2 and P3 zones, also occurs in the sample. Extrapolation suggests that the P3 zone equates in part with the Selandian. The two dinocysts observed, both peridinioids, indicate a marine paleoenvironment, but the present authors cannot be any more precise.

Pollen grains in the sample at 3331.35 m are rare: one is a specimen of *Alnipollenites verus*, which is generally considered to be restricted to the Cenozoic. The one dinocyst encountered belongs to the ubiquitous species *Spiniferites ramosus*, indicating that the paleoenvironment was marine.

Dinocysts and miospores are sparse in the sample at 3329.50 m. The former comprise one specimen each of *Areoligera gippingensis* and *Hystrichosphaeridium quadratum*, the latter having shorter processes than the type. According to Fensome et al. (2016), who erected the species, *Hystrichosphaeridium quadratum* last occurs in the Selandian. That agrees with the age of the overlying sample at 3228.25 m. The paleoenvironment was marine, possibly inner neritic.

One of the unusual aspects of the sample at 3228.25 m is the occurrence of the triprojectate pollen *Aquilapollenites* sp. and the oculate pollen *Azonia* sp., normally found in Upper Cretaceous sediments. Other pollen taxa are *Abiespollenites*, *Alnipollenites verus*, *Pinuspollenites*, *Pterocaryapollenites*, and *Taxodiaceaepollenites*. Only two dinocyst species were recorded: *Glaphyrocysta ordinata* and *Impletosphaeridium apodastum*. The latter species has been recorded only from the Selandian of the Labrador–Baffin Seaway (Fensome et al., 2016), which gives good evidence for the age of this sample. The presence of a few dinocysts and the dominance of pollen indicates that the paleoenvironment was presumably coastal.

Dinocysts recorded from the sample at 3226.9 m include *Alterbidinium* sp., *Areoligera gippingensis*, *Glaphyrocysta ordinata*, and *Isabelidinium*? cf. *viborgense*. Also present is the nonmarine coenobial green alga *Pediastrum*. In a study of the Faroe-Shetland Basin, Mudge and Bujak (2001) stated that *Areoligera gippingensis* had its last or youngest occurrence in the Thanetian; however, Williams et al. (2004) placed the last or youngest occurrence of *Isabelidinium*? *viborgense* within the Selandian. Since the present study recorded *Isabelidinium*? cf. *viborgense* rather than *Isabelidinium*? *viborgense*, this occurrence cannot be relied on heavily so perhaps the sample should be considered as Thanetian, but allow for the possibility that it can be Selandian. The abundance of pollen is suggestive of an inner neritic to possibly marginal marine setting. This is supported by the few dinocyst specimens, none of which are outer-neritic forms. Also the presence of one *Pediastrum* specimen is possibly suggestive of a coastal location.

The topmost sample at 3325.32 m contains the miospores *Coryluspollenites*, *Hazaria*, *Retitriletes*, *Pinuspollenites*, and *Taxodiaceaepollenites* and the acritarch *Micrhystridium*.

An age could not be determined from this assemblage, but the presence of *Micrhystridium* indicates that the paleoenvironment was possibly shallow marine.

### *Summary*

Within cuttings samples, Ainsworth et al. (2016) interpreted the interval of the Cartwright Formation containing core 1 as Thanetian, which is slightly different from that of Fensome (2015), who considered it to be at the Thanetian–Ypresian boundary. Present analyses of conventional core 1 indicate that it is older, Selandian to Thanetian near the top. Previous findings concerning the paleoenvironment range from mostly shallow neritic (Gradstein, 1980) to bathyal (Miller and D'Eon, 1987). The present palynological studies support Gradstein's (1980) findings, in that the setting was inner neritic to marginal marine. The sedimentology and ichnology indicate a wave-influenced prodelta setting, a conclusion not inconsistent with the palynological results. Whereas the trace-fossil assemblage indicates only a weak environmental stress, dinocyst diversity is comparatively limited, possibly suggesting that the latter has a greater sensitivity to fluvial influx in deltaic settings as compared to infaunal organisms.

## *Core 2: gneiss (4145.94–4148.99 m)*

### *Core description and interpretation*

The lowermost core from Karlsefni A-13 consists of grey, variably banded gneiss with some fracturing and scattered garnet-bearing intervals (Fig. 46). Wasteneys et al. (1996) described the material as garnet-biotite, quartzofeldspathic gneiss representing an amphibolite-facies metapsammitic rock. Wasteneys et al. (1996) found the age of the rock to be 2680 Ma based on U-Pb isotopic age dating with detrital zircon grains showing ages consistent with the onshore Nain Province (Fig. 1).

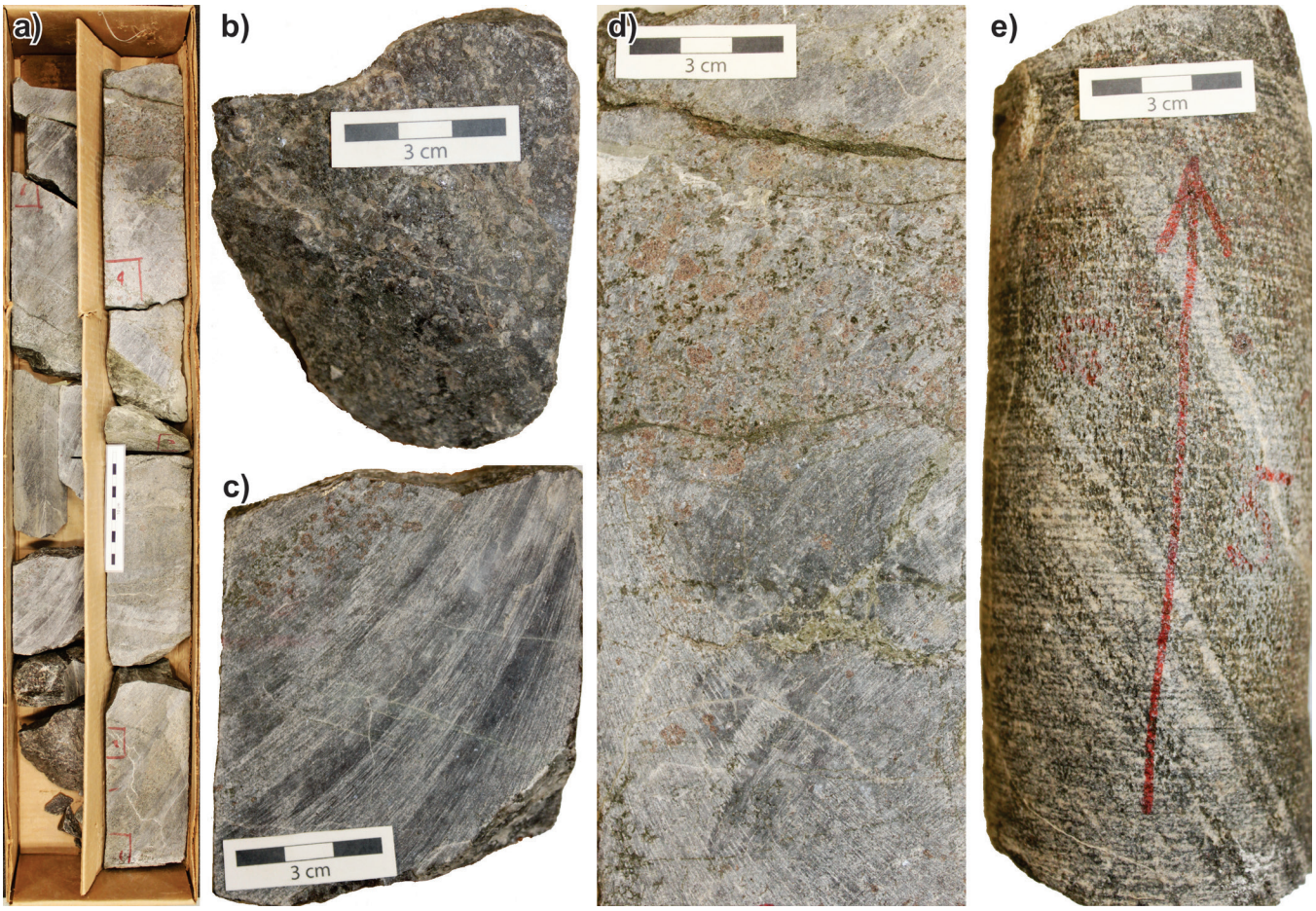


**Figure 46.** Photographs of core 2, Karlsefni A-13. **a)** Photographs showing the total recovered gneissic core (scale bar = 10 cm). NRCan photo 2019-414. **b)** Close-up of a coarser grained interval. NRCan photo 2019-415. **c)** Another coarse-grained interval with dark minerals. NRCan photo 2019-416. **d)** Fractures and possible garnet crystals within the gneiss. NRCan photo 2019-417. **e)** High-angle gneissic banding showing alternating light and dark mineralogy. NRCan photo 2019-418. All photographs by L.T. Dafoe.

## North Bjarni F-06

North Bjarni F-06 is in the Hopedale Basin on the Labrador margin (Fig. 1) and was originally drilled in 1980, and later re-entered in 1981 and 1983; total depth is 2813 m. The objective was to test the hydrocarbon potential of the Bjarni Formation in a dip closure formed by a basement high (Petro-Canada Exploration Inc., 1980a). A single core interval was recovered from within the Bjarni Formation.

### *Core 1: massive pebbly sandstone (2452.0–2458.0 m)*

#### *Core description and interpretation*

Core 1 of North Bjarni F-06 recovered 1.5 m of massive pebbly sandstone from the Bjarni Formation (Fig. 47). The sandstone is poorly sorted, light buff to white, and primarily medium- to coarse-grained (Fig. 48). Granules and small pebbles (up to 1.7 cm diameter) occur throughout the core; clasts include quartzite, granite, volcanic rock, orthoclase fragments, and syenite (Fig. 48b, c). Bioturbation and sedimentary structures other than massive bedding are lacking, and there is minimal variation in grain size.

Without sedimentary structures or trace fossils, only broad paleoenvironmental interpretations can be made. The depositional setting was likely high energy based on the coarse-grained nature of the sandstone. The overall sedimentation rate was high, explaining the massive bedding and lack of other physical structures. A fluvial, alluvial, or deltaic setting could explain the rapid sedimentation rates and high-energy setting.

#### *Palynology*

A single sample from 2452.40 m was processed for palynomorphs. The sample contains the dinocysts *Hystrichosphaerina schindewolfii, Gardodinium* sp., *Lagenorhytis* sp., and *Systematophora complicata*; the bisaccate pollen *Parvisaccites amplus* and *Vitreisporites* sp. sensu Singh, 1971; the spore *Ruffordiaspora* sp.; and some fungal structures. According to Stover et al. (1996), *Hystrichosphaerina schindewolfii* has a stratigraphic range of Valanginian to early Albian and *Gardodinium*

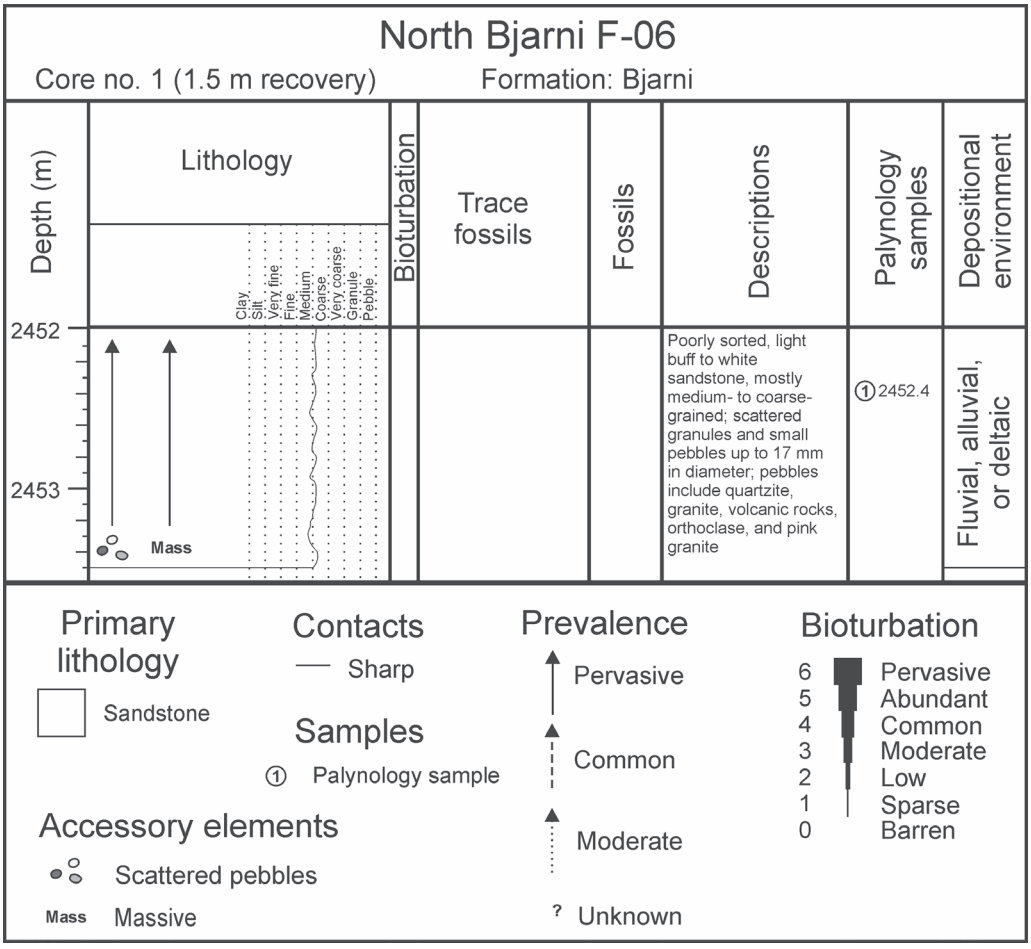


**Figure 47.** Log of core 1 from North Bjarni F-06, showing the limited core recovery of massively bedded, pebbly sandstone.

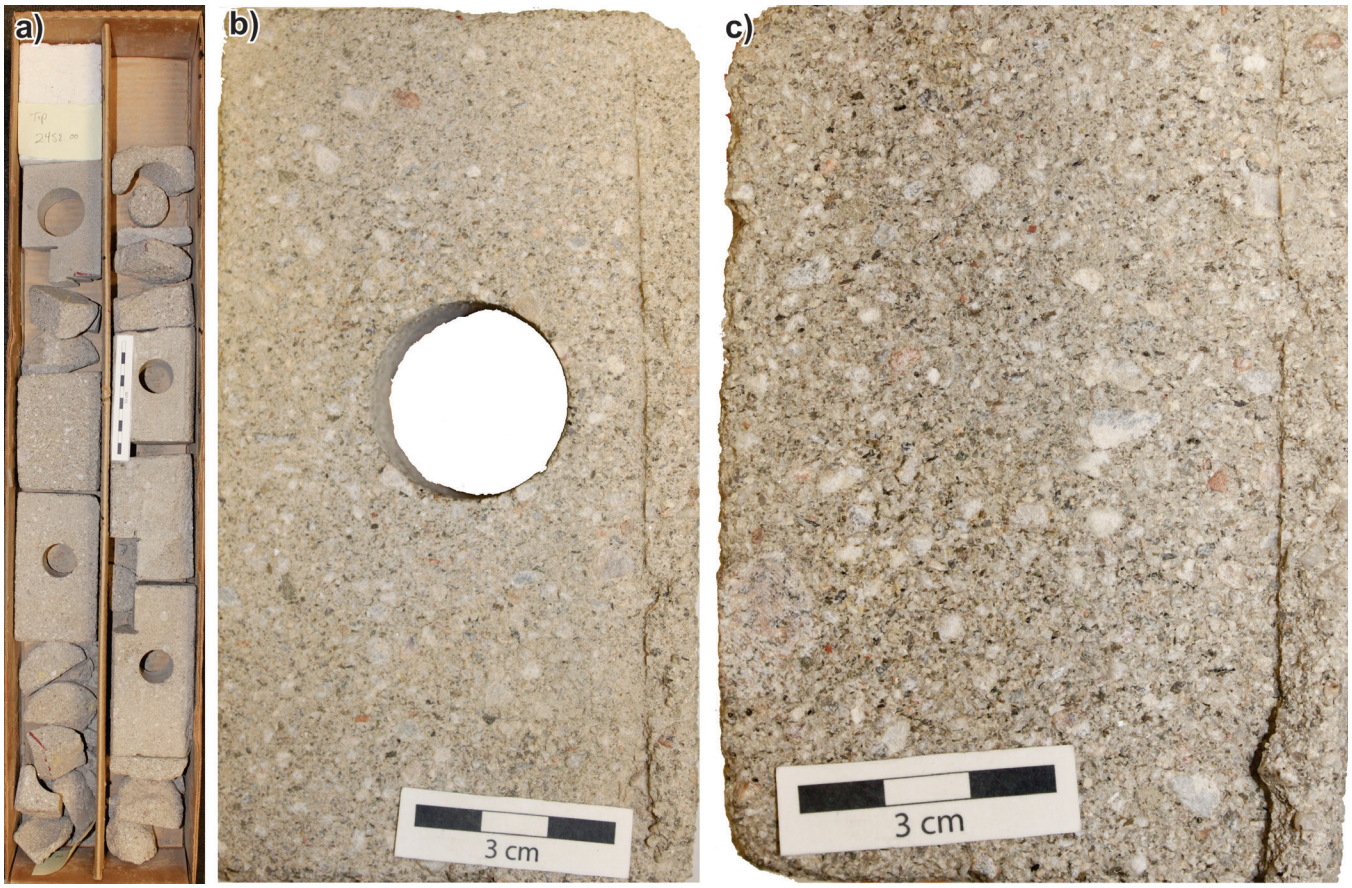


**Figure 48.** Photographs of core 1, North Bjarni F-06. **a)** Core box (scale bar = 10 cm). NRCan photo 2019-419. **b)**, **c)** Examples of the granule- and pebble-bearing sandstone with massive bedding. NRCan photo 2019-420, 2019-421. All photographs by L.T. Dafoe.

*trabeculosum*, the type for the genus *Gardodinium*, ranges from the Hauterivian to the Aptian. This, and the absence of the pollen *Rugubivesiculites*, indicates an age for the sample of early Albian or older. The mixed assemblage is dominated by miospores including fern spores, suggesting a marginal marine paleoenvironment.

### *Summary*

The palynomorph assemblage suggests an early Albian or older age for this part of the Bjarni Formation, which is relatively consistent with the late Albian age of Ainsworth et al. (2014) and Albian interpreted by Duff (1981) from cuttings. Bujak Davies Group (1989e), however, suggested a Turonian–Coniacian age for the interval sampled by the core. Previous paleoenvironmental interpretations from cuttings samples at the same depth as the core have included marginal marine to inner shelf settings (Ainsworth et al., 2014) and nonmarine to transitional (Miller and D'Eon, 1987). Samples from the core reveal a marine influence based on the presence of dinocysts as the sedimentology does not provide a conclusive paleoenvironmental interpretation. Combining the two analyses, a deltaic setting is the most plausible depositional environment. More specifically, comparison to the other Bjarni Formation cores from nearby wells (e.g. Herjolf M-92) suggests a similar river-influenced deltaic setting is possible.

## North Leif I-05

North Leif I-05 is in the Hopedale Basin on the Labrador Shelf (Fig. 1). The well was drilled in 1980 and re-entered in 1981 to test the Bjarni Formation onlapping a northward-plunging anticlinal nose (Petro-Canada Exploration Inc., 1980b); total depth is 3513 m. Two vertically adjacent core intervals were recovered from within the Bjarni Formation.

### *Core 1: heterolithic sandstone, siltstone, and shale (3110–3113.5 m)*

#### *Core description and interpretation*

Core 1 of the North Leif I-05 well consists of buff to grey, silty, fine-grained sandstone with interbedded shale in a heterolithic succession from the Bjarni Formation (Fig. 49, 50). Sedimentary structures include planar and wavy laminations, with some tabular crossbedding

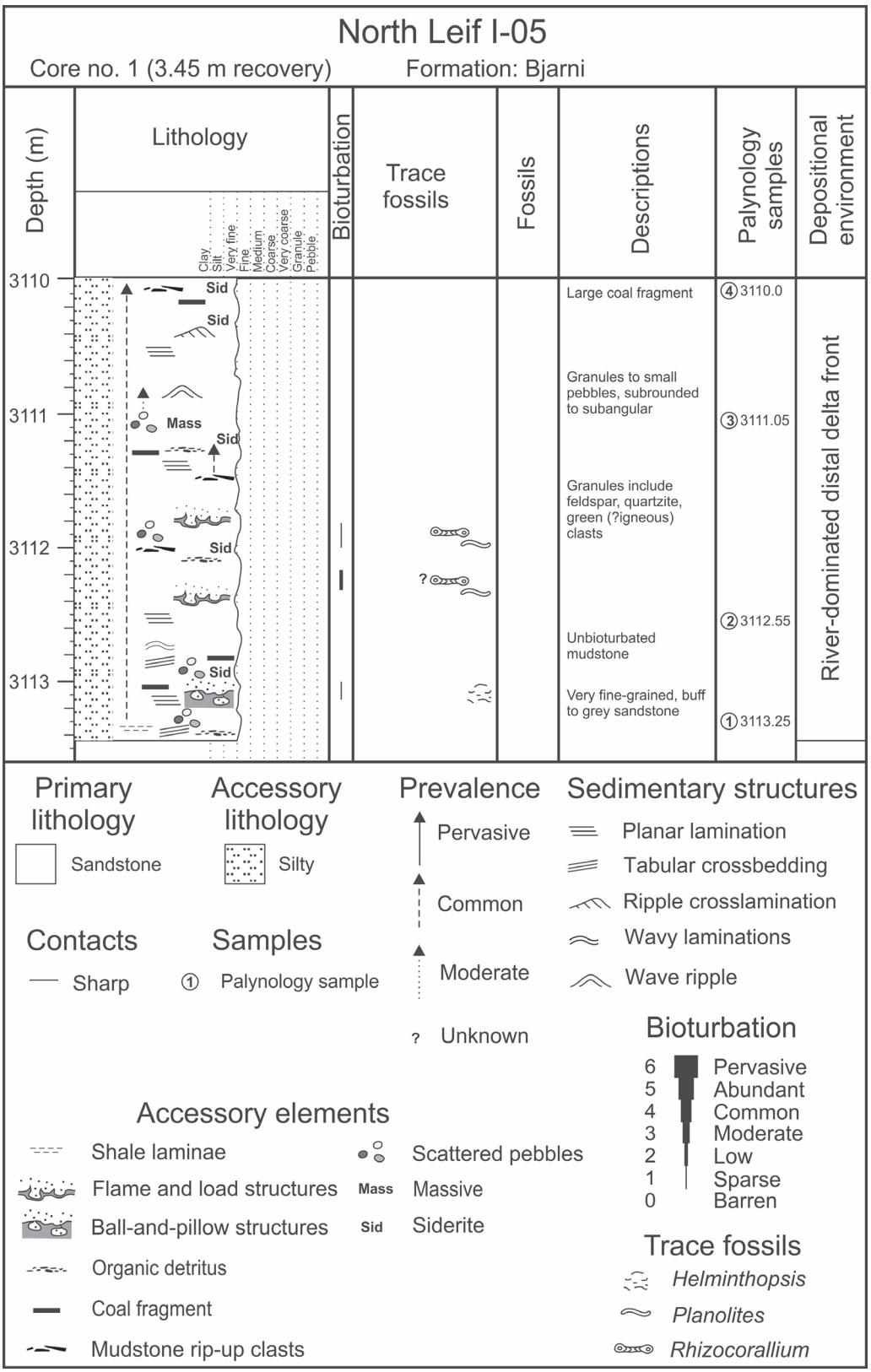


**Figure 49.** Log of core 1 from North Leif I-05 comprising silty sandstone with interbedded shale.


**Figure 50.** Photographs of core 1, North Leif I-05 (scale bar = 10 cm). NRCan photo 2019-422. Photograph by L.T. Dafoe.

(Fig. 51a), convoluted bedding (Fig. 51e), massive bedding (Fig. 51b), and rare current-ripple crosslaminations. Feldspar, quartzite, and green (possibly igneous) granules and small pebbles are common, as well as mudstone rip-up clasts (Fig. 51a, b, c), coal fragments (Fig. 51a, c), siderite (Fig. 51a, b, c), soft-sediment deformation features (flame and load structures and pillow structures; Fig. 51g), and organic detritus. Trace fossils are restricted to discrete bioturbated intervals with up to 20% reworking of the sediment, and include *Rhizocorallium*, *Planolites*, *Chondrites*, and rare *Helminthopsis* (Fig. 51d, e, f).

The fine-grained nature of the sandstone, presence of silty beds, lack of prominent massive or crossbedded intervals, prevalence of soft-sediment deformation, abundant mudstone rip-up clasts, and scattered coal fragments suggest a deltaic setting near a terrestrial source where high sedimentation rates prevail. Thick, fining-upward silty intervals may be consistent with deposition from hypopycnal plumes. The trace-fossil suite is sparse, but characterized by marine forms (e.g. *Rhizocorallium*). The low abundance and diversity of ichnofossils is consistent with a highly stressed assemblage of the archetypal *Cruziana* Ichnofacies composed mostly of deposit-feeding structures. The lack of vertical traces of inferred suspension-feeding animals suggests high sedimentation rates (also indicated by soft-sediment deformation) and significant water turbidity (also indicated by deposition of thick, fining-upward units). Overall, the setting is consistent with the distal delta front of a river-dominated, deltaic succession. Here, erosion of interfluves may source the coal and mudstone fragments seen in the core.

## *Palynology*

In core 1, four samples were processed for palynomorphs. *Pinuspollenites* is common in the sample from 3113.25 m, which also contains one specimen of each of the following: *Ischyosporites foveolatus*, *Parvisaccites radiatus*, and *Rugubivesiculites rugosus*. The authors conclude that the presence of *Parvisaccites radiatus* and *Rugubivesiculites rugosus* in the same sample are indicative of a middle to late Albian age, based on the following reasoning. Pedersen and Nøhr-Hansen (2014) placed the first or oldest occurrence of the genus *Rugubivesiculites* within the Albian. Nøhr-Hansen et al. (2016) considered the last or youngest occurrence of *Parvisaccites radiatus* to be around the top of the Aptian; however, the Bujak Davies Group (1989a) defined a *Parvisaccites amplus* Zone, which they considered early Albian. Key index species were *Parvissacites amplus* and *Parvisaccites radiatus*. Oldest occurrences are usually

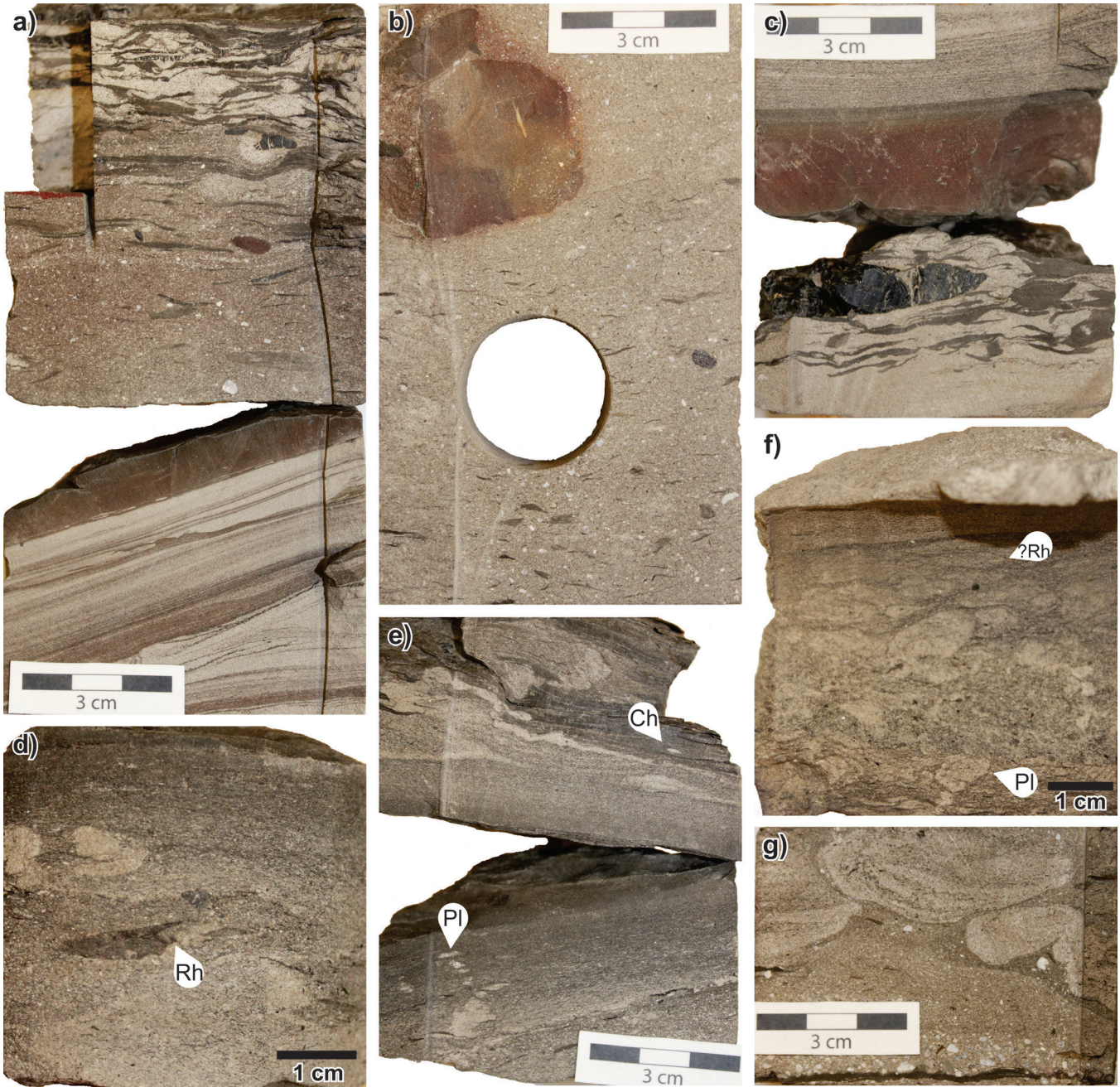


**Figure 51.** Photographs of core 1, North Leif I-05. **a)** Silty sandstone showing contrast between tabular crossbedded sandstone and a mudstone rip-up and coal fragment-dominated massive unit. NRCan photo 2019-423. **b)** Small mudstone rip-up clasts, sideritized clast, and overall massive bedding. NRCan photo 2019-424. **c)** Mudstone rip-up and coal fragments below a siderite band and finely laminated silty sandstone. NRCan photo 2019-425. **d)** Fining-upward unit with *Rhizocorallium* (Rh). NRCan photo 2019-426. **e)** Same section of core as in Figure 51d with *Planolites* (Pl) and *Chondrites* (Ch) in soft-sediment deformed silty sandstone with shale interbeds. NRCan photo 2019-427. **f)** Bioturbated silty sandstone with possible *Rhizocorallium* (?Rh) and *Planolites* (Pl). NRCan photo 2019-428. **g)** Pillow structures in a silty, fine-grained sandstone with organic fragments and granules. NRCan photo 2019-429. All photographs by L.T. Dafoe.

more reliable as they reflect an evolutionary event that is not duplicated; however last or youngest occurrences can vary considerably depending on the region, as demonstrated by refugian taxa. The most reliable evidence on which to base the age is the first or oldest occurrence of *Rugubivesiculites,* indicating that the sample is middle to late Albian, and the paleoenvironment is probably nonmarine given the absence of marine elements.

Bisaccates dominate the sample at 3112.55 m, forming more than 50% of the assemblage and including *Abiespollenites*, *Parvisaccites amplus*, *Parvisaccites radiatus*, *Piceapollenites*, *Pinuspollenites*, and *Rugubivesiculites rugosus*. As noted above, the presence of *Rugubivesiculites rugosus* leads to the conclusion that the age of the sample is middle to late Albian. Based on the absence of dinocysts, the authors interpret the paleoenvironment as nonmarine.

Sample 3 at 3111.05 m contains specimens of the pollen *Eucommiidites troedssonii*, *Rugubivesiculites reductus*, and *Rugubivesiculites rugosus* and the spore *Appendicisporites bilateralis*. Singh (1971) described *Appendicisporites bilateralis* from the Albian of Alberta and it has not been recorded from younger rocks in offshore wells of eastern Canada. As noted above, *Rugubivesiculites* first occurs in the middle to late Albian, the age to which the present authors assign this sample. From the absence of dinocysts, it would appear that the paleoenvironment was nonmarine.

The uppermost sample, at 3110 m, contains primarily bisaccate pollen, including *Parvisaccites amplus*, *Rugubivesiculites reductus*, and *Rugubivesiculites rugosus*. Also present are the miospores *Appendicisporites bilateralis* and *Distaltriangularis perplexus*. As noted above, the authors conclude that the presence of *Appendicisporites bilateralis*, *Parvisaccites amplus*, *Rugubivesiculites reductus,* and *Rugubivesiculites rugosus* in the same sample are indicative of a middle to late Albian age. As with the other samples, the paleoenvironment is interpreted as nonmarine.

### *Summary*

There have been various age assignments for the portion of the Bjarni Formation in the North Leif I-05 well sampled by core 1. The Bujak Davies Group (1989f) considered to it be late Aptian; Nøhr-Hansen et al. (2016) assigned it a late Albian to Cenomanian age; and Dafoe and Williams (2020) consider it to be Albian. The present study's results indicate that the age is middle to late Albian, suggesting a thicker Albian unit in this well. The paleoenvironment was previously interpreted as nonmarine (marsh-swamp setting; Petro-Canada Exploration Inc., 1981) or marginal marine (deltaic or tidal; Miller and D'Eon, 1987). The palynology also indicates a nonmarine setting, but the conventional core interpretations are consistent with deposition in a river-dominated distal delta front in a setting that would have been environmentally harsh as a result of fluvial discharge. Accordingly, a brackish setting would explain the absence of dinocysts.

## *Core 2: dark grey shale (3113.5–3117.1 m)*

### *Core description and interpretation*

In the North Leif I-05 well, core 2, also from the Bjarni Formation, lies directly under core 1, but is dominated by medium grey shale that is moderately fissile and friable (Fig. 52). The shale contains very fine-grained sandstone beds (Fig. 53a) with soft-sediment deformation features (Fig. 54b, c), convoluted bedding (Fig. 54b), rare current-ripple crosslamination (Fig. 54e), siderite (Fig. 54b, d, e), and coal fragments (Fig. 54b). The shale itself (Fig. 54f) also contains siderite bands, organic detritus, coal fragments, and wavy parallel laminations with possible syneresis cracks near the base of the core. Trace fossils are restricted to specific intervals with up to 5% reworking, and include *Chondrites* and fewer *Planolites*, *Rhizocorallium*, and *Asterosoma*.

The fine-grained nature of the core material and inclusion of sandy beds similar to those in core 1 suggest a prodeltaic setting. Coal fragments indicate proximity to a fluvial source, whereas convoluted or soft-sediment deformed units suggest high sedimentation rates. An overall lack of trace fossils in such a fine-grained unit is consistent with harsh environmental stresses that likely included reduced salinity, high sedimentation rates, and elevated water turbidity. The trace-fossil suite is similar to core 1 and would represent a highly stressed assemblage of the archetypal *Cruziana* Ichnofacies. Overall, the core material is consistent with a prodeltaic setting of a river-dominated delta. Furthermore, this setting fits with the interpretation of the overlying core and would indicate overall deltaic progradation from deposition of core 2 to the overlying core 1.

### *Palynology*

There were only slight variations in the composition of the palynomorph assemblages in the three samples from core 2 that were processed for palynomorphs. The assemblage in the bottommost sample, at 3116.50 m, comprises primarily bisaccate pollen, although there are rare spores such as *Cicatricosisporites augustus* and *Ischyosporites foveolatus*. The bisaccates include *Pinuspollenites*, *Parvisaccites radiatus*, *Rugubivesiculites convolutus*, *Rugubivesiculites rugosus*, and *Vitreisporites* sp. sensu Singh, 1971. The presence of *Rugubivesiculites convolutus* and *Rugubivesiculites rugosus* leads to the conclusion that the sample is middle to late Albian. The dominance of the bisaccates and the absence of dinocysts are considered to indicate a nonmarine paleoenvironment, although bisaccate pollen can also be transported far offshore.

In the sample at 3115.0 m, bisaccate pollen include *Parvisaccites radiatus*, *Rugubivesiculites rugosus, Vitreisporites pallidus*, and *Vitreisporites* sp. sensu Singh, 1971. There are also several spores, including

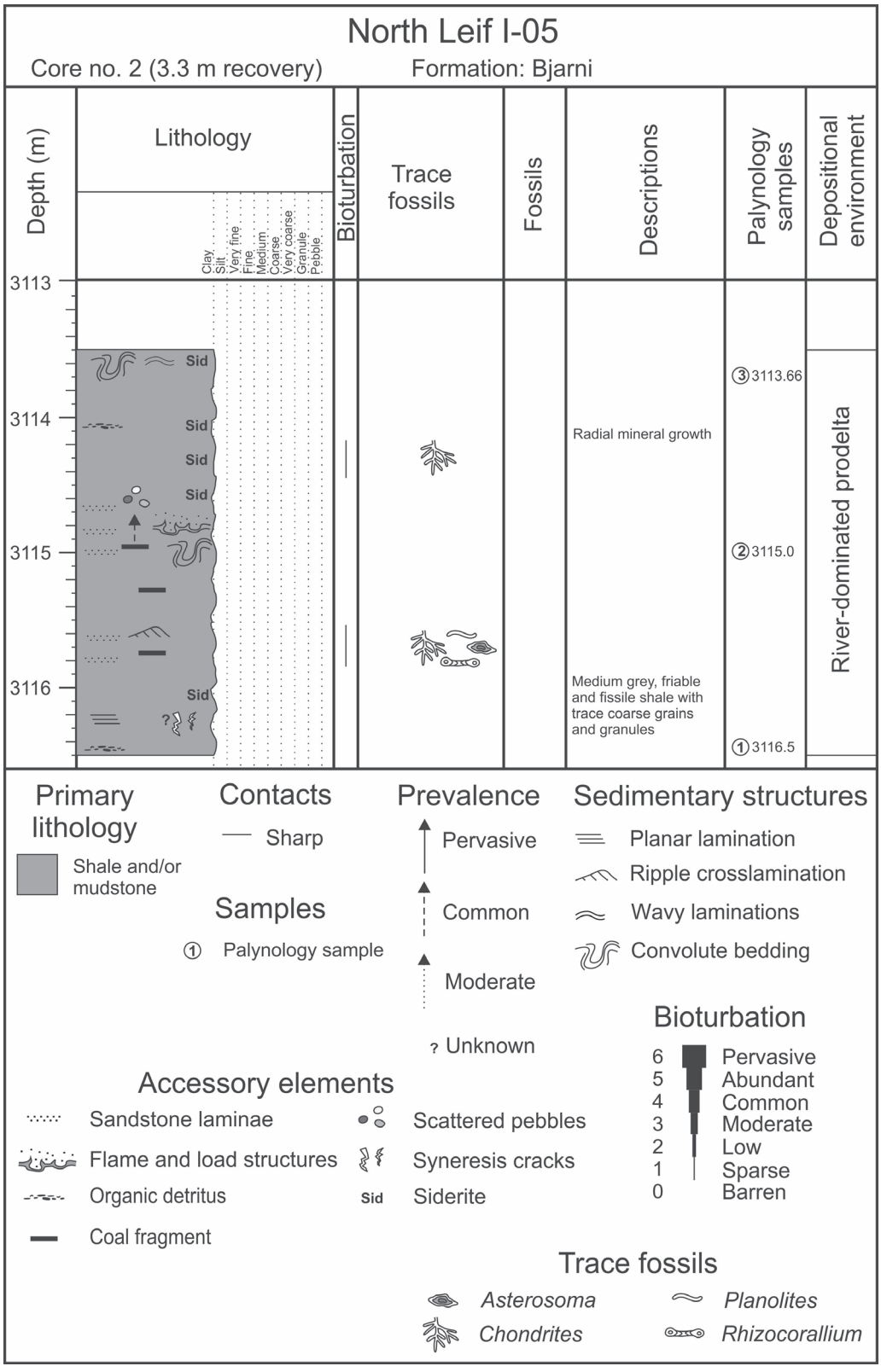


**Figure 52.** Log of core 2 from North Leif I-05, showing a shale-dominated succession.


**Figure 53.** Photographs of core 2, North Leif I-05. **a)** The entire core (scale bar = 10 cm). NRCan photo 2019-430. **b)** Sandy mudstone with convoluted bedding, mudstone rip-up clasts, and coal fragments near the top. NRCan photo 2019-431. **c)** Sandstone bed with *Rhizocorallium* (Rh) cutting through and evidence of soft-sediment deformation at the base of the bed. Coarser grained sandstone and mudstone rip-up clasts are present in the upper part of the core section. NRCan photo 2019-432. **d)** Siderite and sideritized mudstone fragments containing *Chondrites* (Ch) traces. NRCan photo 2019-433. **e)** Current-rippled, fine-grained sandstone, siderite, and *Chondrites* (Ch) traces. NRCan photo 2019-434. **f)** Typical shale comprising much of core 2. NRCan photo 2019-435. All photographs by L.T. Dafoe.

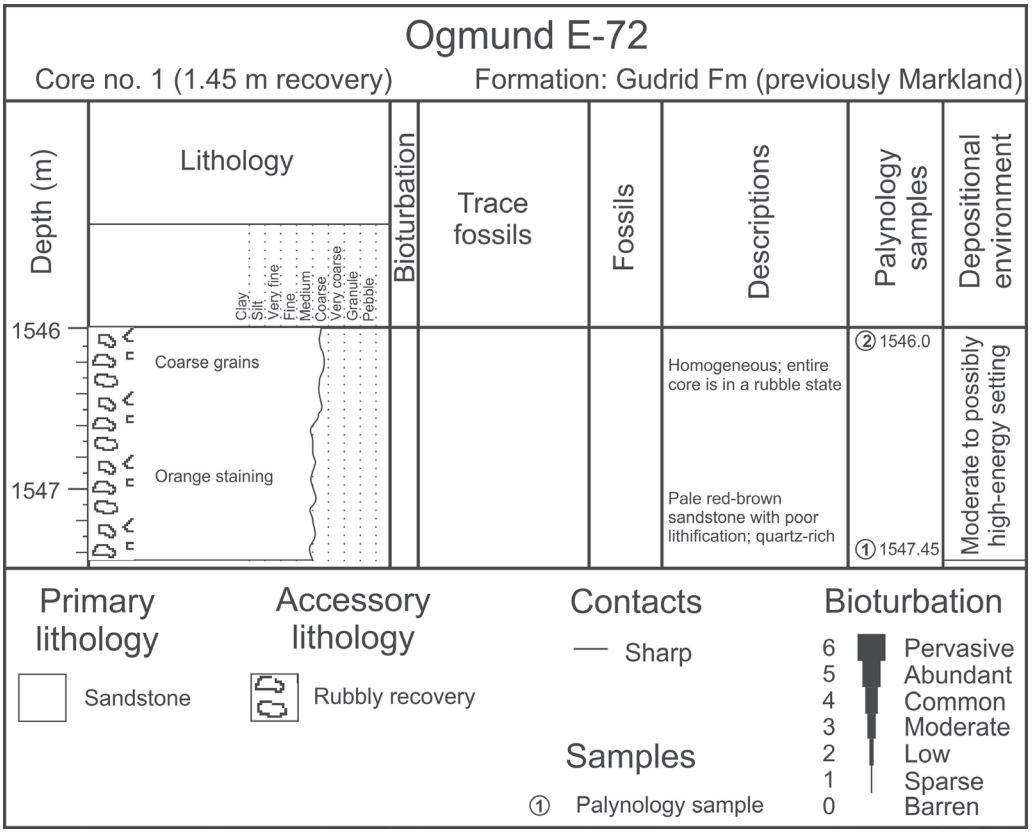


**Figure 54.** Log of core 1, Ogmund E-72 showing a subtly coarsening-upward sandstone.

*Appendicisporites bifurcatus*, *Cicatricosisporites hallei*, *Cicatricosisporites* sp. cf. *Anemia exilioides* sensu Singh 1971, *Concavissimisporites* sp., *Distaltriangulisporites* sp., *Gleicheniidites senonicus, Nodosisporites* sp., and *Trilobosporites* sp. The authors date the sample as middle to late Albian because of the presence of *Rugubivesiculites rugosus*. The dominance of the bisaccates is taken to indicate a nonmarine paleoenvironment. One surprise is the presence of a chitinozoan; chitinozoa are organic-walled microfossils that are restricted to the Ordovician to Devonian, and clearly reworked here. Some Labrador Shelf wells contain sedimentary rocks predating rifting thought to be Paleozoic, such as Hopedale E-33 (Williams, 1981), Roberval K-92 (Williams et al., 1990), and Tyrk P-100 (Robertson Research Canada Ltd., 1979) that locally form basement in the region that predates rifting and are likely the source of the chitinozoan.

The uppermost sample, at 3113.66 m, contained predominantly pollen, including *Abiespollenites*, *Parvisaccites amplus*, *Piceapollenites*, *Pinuspollenites*, *Rugubivesiculites reductus*, and *Rugubivesiculites rugosus*. The authors also recorded single specimens of the spores *Cicatricosisporites* sp., *Contignisporites cooksoniae*, and *Gleicheniidites* sp. *Pinuspollenites* is particularly abundant. From the composition of the assemblage and following the logic used to date the samples in core 1, the age was considered to be middle to late Albian. Based on the presence of miospores and the absence of dinocysts, the paleoenvironment is presumably nonmarine.

### *Summary*

As in core 1, the age of the Bjarni Formation succession sampled by core 2 (from cuttings) is late Aptian (Bujak Davies Group, 1989f) or late Albian to Cenomanian (Nøhr-Hansen et al., 2016). The new results above indicate a middle to late Albian succession. Previous paleoenvironmental findings are the same as core 1 of this well. The river-dominated prodeltaic setting is again compatible with the nonmarine interpretation from the palynology, considering the highly brackish nature of the paleoenvironment that likely explains the lack of dinocysts.

## Ogmund E-72

Ogmund E-72 is in the northern part of the Hopedale Basin, offshore Labrador (Fig. 1). The well was drilled in 1980 to test the hydrocarbon potential of both the Freydis and Bjarni sandstone units in a graben structure (Petro-Canada Exploration Inc., 1980c); total depth was 3094 m. Three core intervals were recovered: core 1 was from the Markland Formation, and cores 2 and 3 are from the underlying Bjarni Formation.

## *Core 1: homogeneous sandstone (1546–1556 m)*

### *Core description and interpretation*

Core 1 consists of rubbly sandstone fragments of moderate consolidation, characterizing the Freydis Member of the Markland Formation (Fig. 54, 55). Only 1.45 m of section was recovered, and due to the nature of the fragments, interpretation of the unit is limited. The core shows a very subtle coarsening-upward trend from lower medium- to upper medium-grained pale red-brown sandstone (Fig. 54). In overall composition, the sandstone appears to be quartz-rich and relatively homogeneous. No sedimentary structures or fossil material were observed (Fig. 55b, c).

The sandstone is consistent with deposition in a moderate to possibly high-energy setting in which finer grained material (clay and silt) remained in suspension. A lack of sedimentary structures and fossil material precludes a detailed interpretation of this core interval.

### *Palynology*

Two samples were processed for palynomorphs from core 1; however, there was no recovery from the sample at 1547.45 m. The upper sample, at 1546 m, contains both dinocysts and pollen. Dinocysts include *Apectodinium parvum*, *Dapsilidinium pastielsii*, *Glaphyrocysta ordinata*, and *Xenikoon*. Pollen are *Alnipollenites verus*, *Pterocaryapollenites*, and *Retitricolpites vulgaris*. Harland (1979) restricted *Apectodinium parvum* to the late Thanetian; however, Nøhr-Hansen et al. (2016) placed the last or youngest occurrence of that species within the basal Ypresian. Because of the presence of *Glaphyrocysta ordinata*, the present authors consider the age of the sample to be basal Ypresian. Reworked Early Cretaceous miospores and dinocysts form a small percentage of the assemblage. Miospores are the dominant palynomorphs, constituting 98%, with dinocysts representing only 2%, which is consistent with a coastal paleoenvironment.

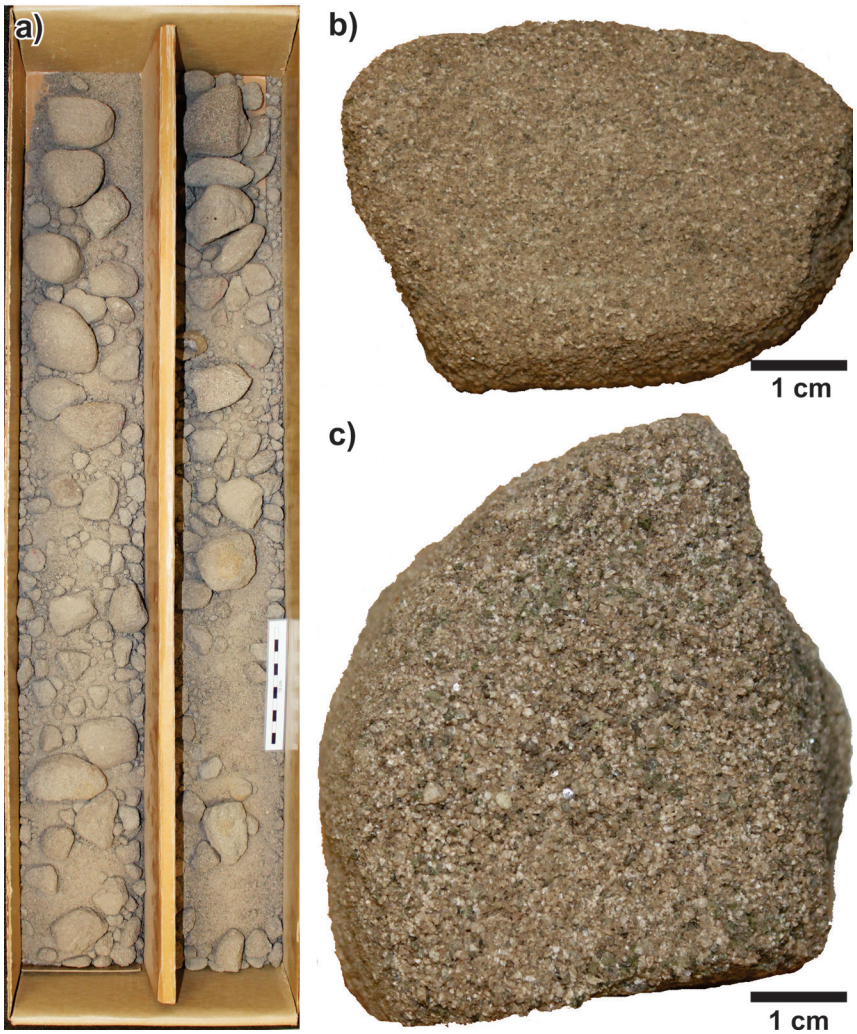


**Figure 55.** Photographs of core 1, Ogmund E-72. **a)** Core box showing the rubbly nature of the core (scale bar = 10 cm). NRCan photo 2019-436. **b)** Lower medium-grained sandstone with no defining features. NRCan photo 2019-437. **c)** Upper medium-grained sandstone showing variation in clasts, but dominated by quartz grains. NRCan photo 2019-438. All photographs by L.T. Dafoe.

### *Summary*

Based on analyses of cuttings, the interval sampled by core 1 lies between the (?)Turonian–Campanian and Campanian–Maastrichtian of Ainsworth et al. (2014) and in the late Maastrichtian of Nøhr-Hansen et al. (2016) and Bujak Davies Group (1989f). This study's findings of a Ypresian age contrast with these earlier results; however, Bujak Davies Group (1989f) found that lower Eocene sediments overlaid the Maastrichtian section at 1515–1535 m, with no Paleocene present. One possible explanation for the different interpretations is that considerable reworking of Late Cretaceous palynomorphs occurred in the Paleogene, a situation perhaps reflected in the probable absence of Paleocene rocks. This would indicate that the core belongs to the Gudrid Formation rather than the underlying Markland Formation. Ainsworth et al. (2014) suggested that the interval sampled by core 1 represents deposition within an inner neritic setting, but a marginal marine environment was also postulated (beach, possible barrier; Miller and D'Eon, 1987). Palynological results of the present study indicate a coastal setting, which is relatively consistent with previous interpretations, but observations from the core only suggest a high-energy setting. Gamma-ray log signatures and grain-size variations in under- and overlying sediments indicate 30–50 m coarsening-upward cycles separated by siltier horizons within an overall coarsening-upward profile from about 1610 m to 1500 m (Wielens and Williams, 2009). Based on the various lines of evidence above, this core likely represents a prograding shoreface or delta-front setting.

## *Core 2: heterolithic sandstone and mudstone (2234–2240 m)*

### *Core description and interpretation*

Core 2 in Ogmund E-72 (Fig. 56) is from the Bjarni Formation and comprises centimetre-scale sandstone beds with interbedded millimetre- to centimetre-scale, mudstone beds or laminae (Fig. 57, 58). The sandstone is very fine- to coarse-grained and primarily consists of medium-grained, buff sandstone that is overall well sorted (Fig. 56). One interval, from 2238.6–2239.1 m, is well indurated and possibly altered, possessing a fabric that is inconsistent with the rest of the core (Fig. 58d). Sedimentary features and structures in this core interval include occasional planar laminations, scattered granules, scattered soft-sediment deformation features (Fig. 58e; including flame structures), scattered organic detritus, rare coal fragments, and rare trough or planar tabular crossbedding. One 6 cm diameter quartzite pebble was encountered at 2235.42 m. Bioturbation ranges from unbioturbated (barren) intervals to bioturbated zones with 5–40% reworking. Trace fossils include locally moderate abundances of *Planolites* and *Helminthopsis*, with fewer *Palaeophycus*, *Rhizocorallium*, and *Asterosoma* (Fig. 58a, b, c, e, f). Rare (?)*Ophiomorpha*, *Thalassinoides*, *Chondrites*, and *Skolithos* are also present (Fig. 58b, c, e).

The sedimentary structures, presence of organic detritus and heterolithic nature of the sediment is consistent with a deltaic setting. Interbedding of sandstone with mudstone beds and laminae indicates changing flow conditions and relatively rapid sedimentation rates, which are required to bury clay material that would otherwise be reworked or remain in suspension within a shoreface setting. Soft-sediment deformation features are indicative of high sedimentation rates, especially sand being deposited above soupy mud layers. It is unknown what may have caused the altered zone described above, but it could relate to faulting or a diagenetic process. The trace-fossil suite is consistent with a moderately stressed archetypal expression of the *Cruziana* Ichnofacies, with a dominance of deposit-feeding structures and lesser grazing traces and structures of inferred suspension feeders. In regard to the trace fossils, diversity is moderate and abundance is low to moderate, indicating that environmental stresses affected the infaunal community. These would have included high sedimentation rates, water turbidity, and a likely reduction in salinity; however, the presence of rare *Skolithos* and the heterolithic nature of the sediment suggests some wave mitigation of environmental stresses. Accordingly, the trace-fossil suite is consistent with a wave-influenced, distal delta-front setting.

### *Palynology*

Four samples from core 2 were processed for palynomorphs. The bottommost sample, at 2238.6 m, contains only miospores, primarily bisaccates, although there were a few trilete spores. One of the bisaccates was identified as a questionable *Parvisaccites*, but there were no specimens of *Rugubivesiculites*, which suggests that the age is early Albian or older. The absence of dinocysts indicates a nonmarine paleoenvironment.

Vitrinite dominates the sample from 2236.28 m, and all the miospores present are bisaccates. *Pinuspollenites* is common, but other taxa are single specimens (*Abiespollenites*, *Parvisaccites radiatus*, and *Piceapollenites*). Based on the presence of *Parvisaccites radiatus* and the absence of *Rugubivesiculites*, the authors consider this sample to be no younger than early Albian, with the absence of *Rugubivesiculites* suggesting that it is early Albian. It is difficult to interpret the paleoenvironment, but the absence of dinocysts seems to denote a nonmarine setting. The abundance of vitrinite and carbonized wood is suggestive of fluvial or perhaps even deltaic deposits.

The sample at 2235.20 m contains only a single specimen of the bisaccate pollen *Pinuspollenites* and a questionable specimen of the dinocyst *Subtilisphaera*.

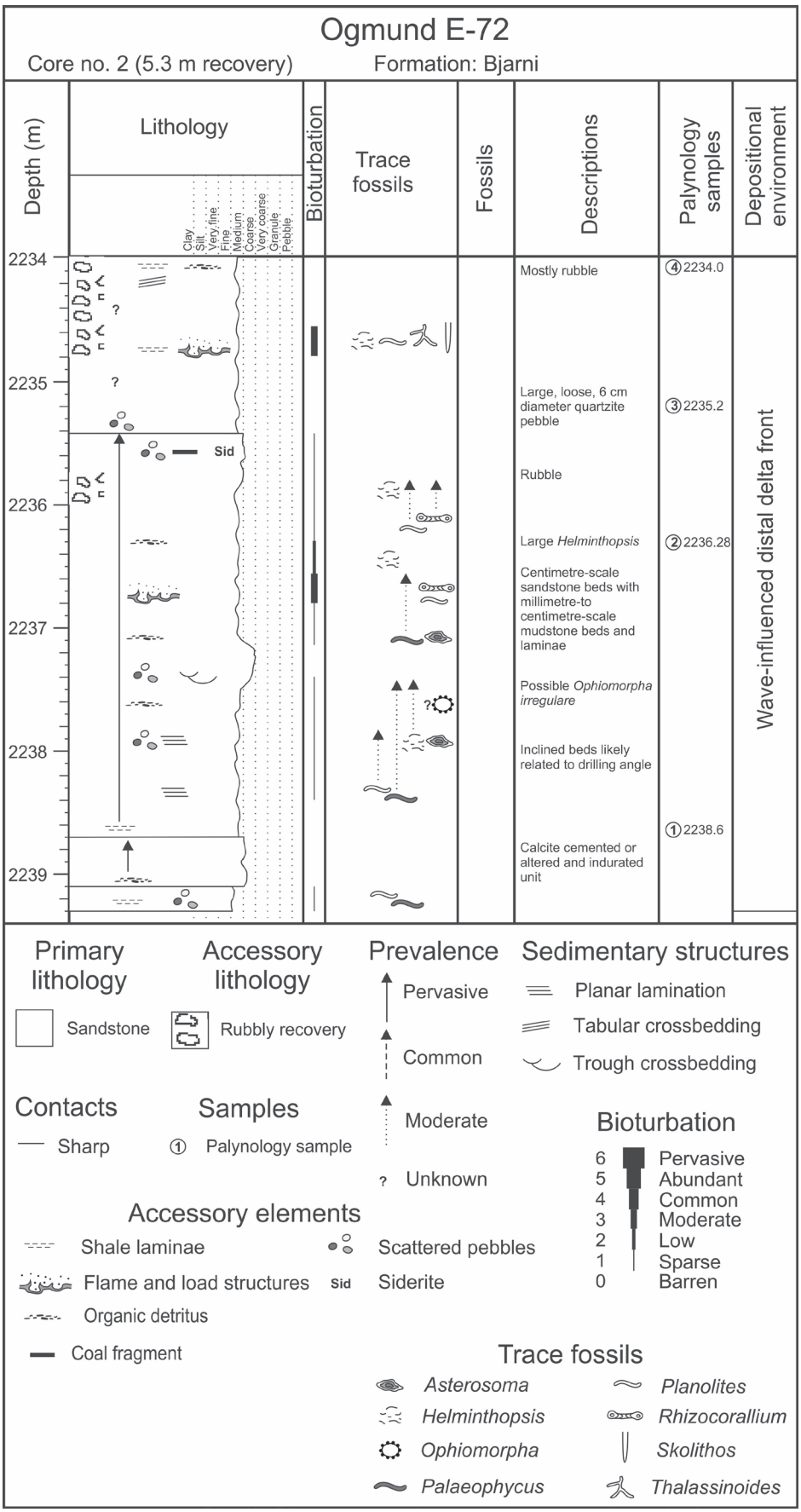


**Figure 56.** Log of core 2, Ogmund E-72, showing bioturbated zones in medium-grained sandstone.


**Figure 57.** Photographs of core 2, Ogmund E-72 showing the cemented zone near the base and a rubbly section near the top of the core. Scale bars = 10 cm. NRCan photo 2019-439, 2019-440, 2019-441. All photographs by L.T. Dafoe.

This information is too sparse to draw a conclusion regarding the age of the sample, but the dinocyst would seem to indicate a marginal marine setting.

Miospores dominate the assemblage in the uppermost sample from core 2 at 2234 m. Trilete spores are *Cicatricosisporites* sp., *Ischyosporites* sp., and *Fisciniasporites (as Cicatricosisporites) potomacensis.* Bisaccate pollen include *Piceapollenites*, *Parvisaccites amplus*, *Pinuspollenites*, and *Rugubivesiculites rugosus*. Most surprising is the occurrence of two specimens of the dinocyst *Nyktericysta*, one of which is *Nyktericysta nebulosa*. Singh (1971) gave a stratigraphic range for *Fisciniasporites potomacensis* of Barremian to Albian. As noted earlier in the palynological discussion for core 1 from North Leif I-05, the present authors consider the presence of the bisaccates *Parvisaccites radiatus*, *Rugubivesiculites reductus*, and *Rugubivesiculites rugosus* in the same sample as indicative of a middle to late Albian age. The presence of *Nyktericysta nebulosa*, the sole dinocyst, generally indicates a nonmarine to marginal marine paleoenvironment.

### *Summary*

Ainsworth et al. (2014) considered the age of the Bjarni Formation interval sampled by the core to be late Aptian to late Albian. Nøhr-Hansen et al. (2016) dated it as middle Albian, and Bujak Davies Group (1989f) assigned an early–middle Albian age. From our palynological analysis, the present study determined the age of the sample at 2234 m to be middle to late Albian and the lower samples to be early Albian, which is partially in agreement with previous studies. The paleoenvironment from palynomorphs is interpreted as nonmarine to marginal marine. Ainsworth et al. (2014) considered the depositional setting to be nonmarine to transitional, which is consistent with the above interpretation, but Miller and D'Eon (1987) interpreted it as an alluvial fan setting. The sedimentological and ichnological interpretation is, however, of a wave-influenced, distal delta-front setting, which broadly agrees with palynological results of the present study.

## *Core 3: matrix-supported conglomerate (3093–3094.05 m)*

### *Core description and interpretation*

In Ogmund E-72, the lowermost core of the Bjarni Formation comprises 1.05 m (Fig. 59) of matrix-supported conglomerate. The buff rocks include a mostly fine- to coarse-grained sandstone matrix (Fig. 60). Pebbles are subangular to rounded, can be in excess of 6 cm in diameter (Fig. 60b), and include feldspar, granite, quartzite, volcanic, and sandstone clasts likely representing source-rock lithologies. The cement is calcareous and rare fractures are present.

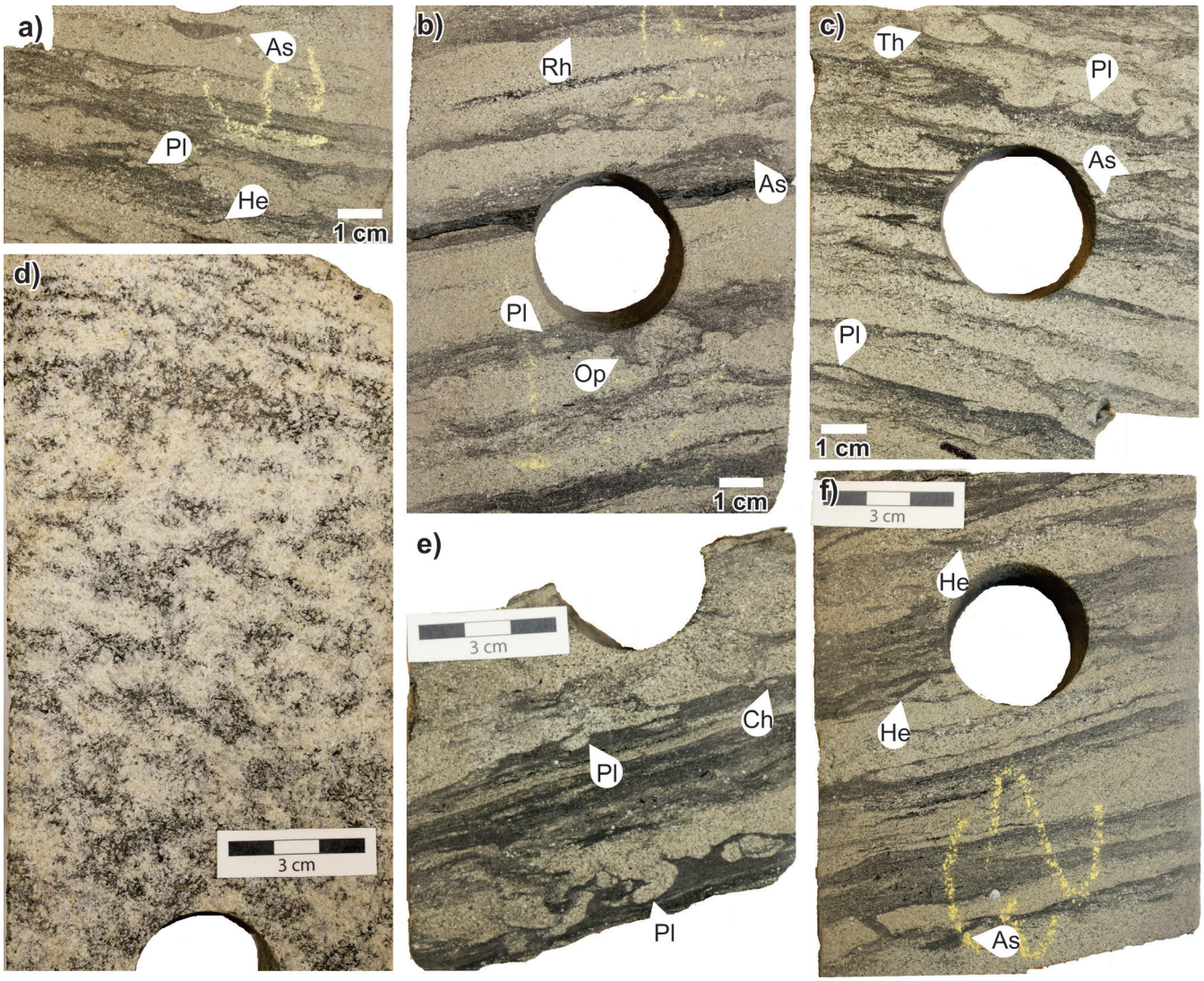


**Figure 58.** Photographs of core 2, Ogmund E-72. **a)** Sandstone with mudstone laminae and trace fossils including *Asterosoma* (As), *Planolites* (Pl), and *Helminthopsis* (He). NRCan photo 2019-442. **b)** Sandstone with apparently inclined laminae (due to drilling angle) and coaly horizons through the centre with *Planolites* (Pl), *Ophiomorpha* (Op), *Asterosoma* (As), and *Rhizocorallium* (Rh). NRCan photo 2019-443. **c)** Moderately burrowed zone showing *Thalassinoides* (Th), *Planolites* (Pl), and *Asterosoma* (As). NRCan photo 2019-444. **d)** Mottled zone near the base of the core interval that is calcite cemented and possibly diagenetically modified. NRCan photo 2019-445. **e)** Mudstone-dominated unit with flame structures at the base and *Planolites* (Pl) and *Chondrites* (Ch). NRCan photo 2019-446. **f)** Weakly burrowed and thinly bedded unit with *Helminthopsis* (He) and *Asterosoma* (As). NRCan photo 2019-447. All photographs by L.T. Dafoe.

Proximity to the source area is suggested by the coarse-grained nature of this core interval; however, rounding of the clasts indicates some degree of transport, but more competent, quartz-rich lithologies appear to be more angular than others. There are no sedimentary structures or trace fossils to further aid interpretation. The lack of imbrication and matrix-supported nature of the conglomerate suggests that sedimentation was likely rapid and not directly tied to a consistent current such as in a fluvial system. Accordingly, the conglomerate likely represents alluvial deposition.

## *Palynology*

The sample from core 3 at 3093.44 m contains a sparse assemblage of palynomorphs, with one dinocyst specimen and two pollen grains. The sole dinocyst is *Cerbia tabulata*. Williams (1975) defined *Cerbia tabulata* (as *Cyclonephelium attadalicum*) as the index species of an early Aptian zone in the Scotian Basin. Subsequent studies (e.g. Williams, 2003) confirmed that the last or youngest occurrence of *Cerbia tabulata* is a consistent marker for the Aptian. There is some supporting evidence in the two bisaccate pollen species, *Parvisaccites radiatus* and *Vitreisporites*

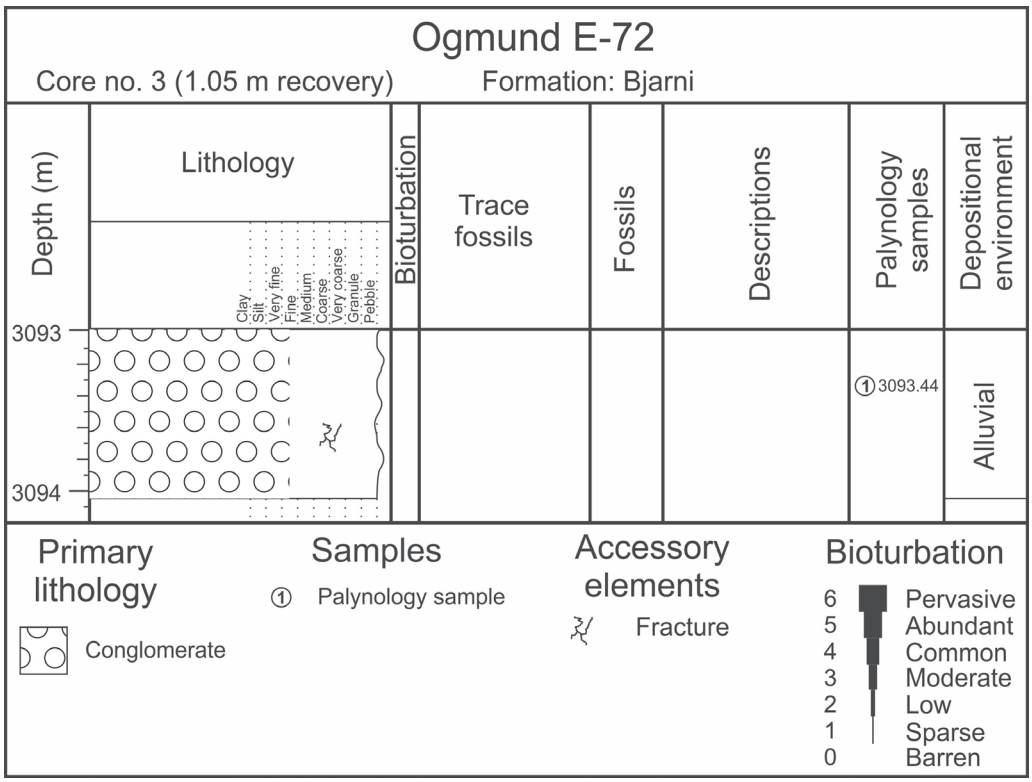


**Figure 59.** Log of core 3, Ogmund E-72.

*pallidus*, that occur in the sample. Nøhr-Hansen et al. (2016) placed the last or youngest occurrence of *Parvisaccites* at the Aptian–Albian boundary; however, this study has shown that *Parvisaccites* can occur in the same samples as the genus *Rugubivesiculites*, which has its first or oldest occurrence in the middle Albian. Based on the presence of *Cerbia tabulata*, assuming it is not reworked, the present authors are dating this sample as Aptian. From the above assemblage, the paleoenvironment was presumably marginal marine.

### *Summary*

Bujak Davies Group (1989f) and Ainsworth et al. (2014) considered the age of the interval sampled by core 3 as Barremian to early Aptian; Nøhr-Hansen et al., (2016) assigned a late (?)Aptian–early Albian age. The present palynological analysis indicates that the interval of the Bjarni Formation is Aptian. These sediments have only been defined as nonmarine in nature (Ainsworth et al., 2014), and were further suggested to be braided fluvial deposits by Miller and D'Eon (1987). An alluvial origin is indicated by this study's sedimentological observations, but marginal marine conditions are indicated by the palynomorphs, suggesting that the setting was likely a high-energy shoreface or delta front with high sedimentation rates.

## Roberval K-92

Roberval K-92, located in the southern part of the Hopedale Basin, offshore Labrador (Fig. 1), was drilled in 1978 and was re-entered multiples times between 1979 and 1982; total depth was 3874 m. The well was intended as a test of the potential for additional Paleozoic reserves near the Gudrid H-55 well (Total Eastcan Exploration Ltd., 1978a). A total of seven core intervals were recovered, of which core 1 from the Markland Formation and core 2 from the Bjarni Formation are discussed below. Additional cores within the Alexis Formation were not evaluated, and cores 6 and 7 within Paleozoic sedimentary rocks are middle to late Ordovician (Bingham-Koslowski et al., 2019).

### *Core 1: dark grey shale (3014–3017 m)*

#### *Core description and interpretation*

In the Roberval K-92 well, core 1 intersected dark grey, fissile and friable shale with about 2.79 m of recovery from 3014–3017 m within the Markland Formation (Fig. 61). The grey shale (Fig. 62) becomes more reddish and silty toward the top of the core and is planar laminated throughout (Fig. 63). Green nodular mineralizations, possibly glauconitic and potentially related to bioturbation are present at the base of the core (Fig. 63a), and a bentonite horizon is located near the middle (Fig. 63e). The bentonite horizon is

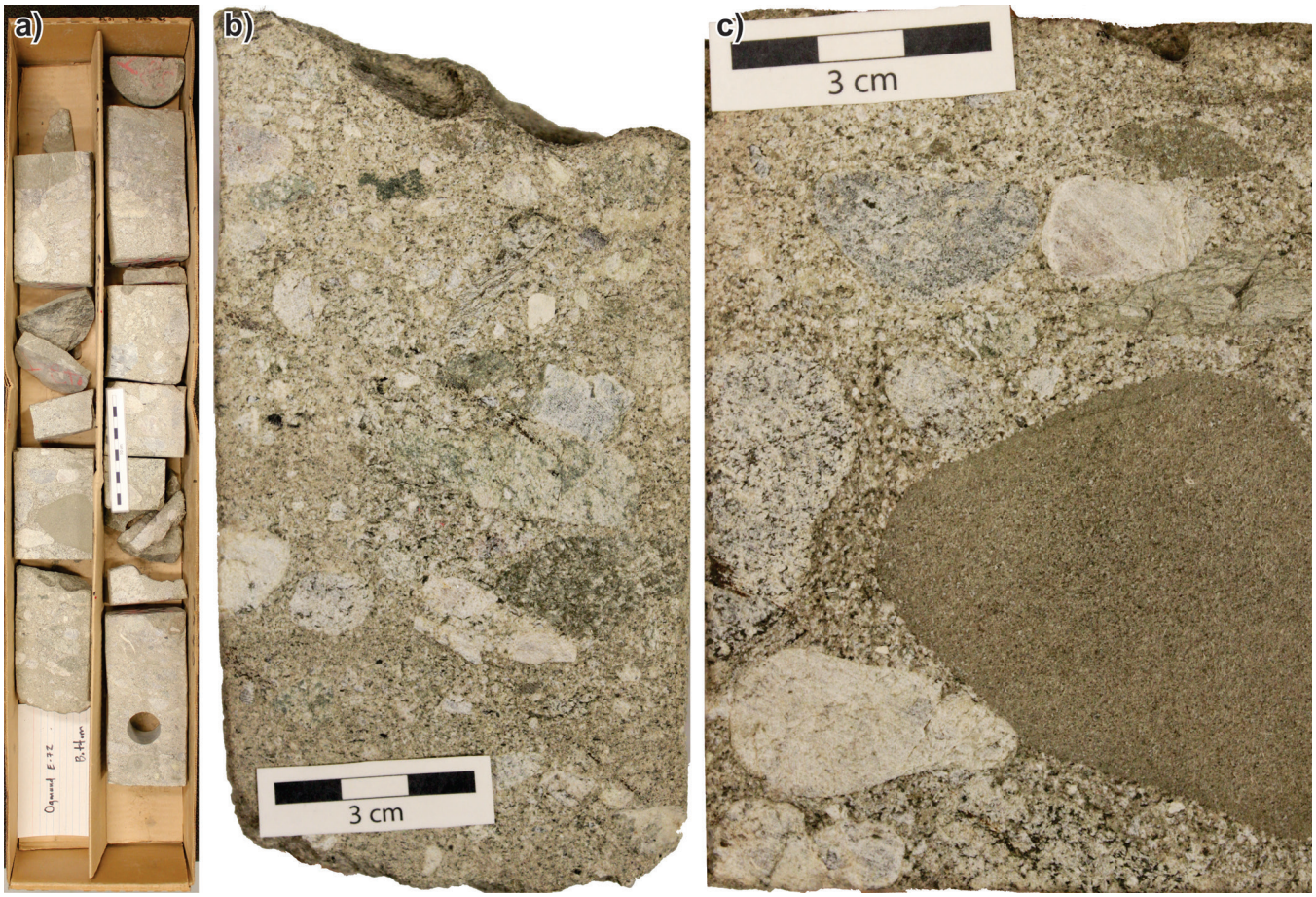


**Figure 60.** Photographs of core 3, Ogmund E-72. **a)** Core box showing highly subsampled conglomerate (scale bar = 10 cm). NRCan photo 2019-448. **b)** Matrix-supported conglomerate near the base. NRCan photo 2019-449. **c)** Large subrounded to rounded clasts in the conglomerate. NRCan photo 2019-450. All photographs by L.T. Dafoe.

about 8 cm thick, soft, and swells with the addition of water. Slickensides were also noted near the top of the core, and a calcite-filled fracture occurs near the bentonite (Fig. 63b). The core is barren of fossil and trace-fossil material aside from a possible tooth (black, triangular fossil fragment, with longitudinal striations; Fig. 63d).

Core 1 contains minimal amounts of organic detritus and fossil and trace-fossil material. This may be explained by either a distal setting far removed from the shoreline and beyond the shelf, perhaps in a slope-equivalent paleowater depth, or a proximal, stressed environmental setting in which oxygenation and salinity were very low. The lack of terrestrial influence precludes a lacustrine setting. An absence of sand-sized grains or evidence of wave-formed structures suggests a deep-marine setting beyond storm wave base. The green nodular mineralizations may have developed in reducing conditions under low oxygenation and were perhaps formed within burrow structures based on their morphology. Overall, the depositional setting appears to be consistent with a slope-equivalent water depth (Fig. 3).

## *Palynology*

Three samples were processed for palynomorphs from core 1. The bottommost, at 3016.75 m, has a rich dinocyst assemblage and occasional miospores. The dinocysts include *Adnatosphaeridium* sp. sensu Ioannides 1986, *Aptea* spp., *Cerbia* cf. *tabulata*, *Coronifera oceanica*, *Heterosphaeridium bellii, Heterosphaeridium difficile*, *Hystrichodinium pulchrum*, *Hystrichosphaeridium bowerbankii*, *Hystrichosphaeridium quadratum*, *Hystrichosphaeridium salpingophorum*, *Impagidinium* sp., *Isabelidinium cretaceum*, *Kleithriasphaeridium loffrense*, *Laciniadinium williamsii*, *Manumiella* sp., *Microdinium ornatum*, *Odontochitina costata*, *Palaeoperidinium pyrophorum*, *Spiniferella* sp., *Spiniferites ramosus*, and *Spiniferites scabrosus*. Also present is the triprojectate pollen *Aquilapollenites*. Nøhr-Hansen et al. (2016) plotted the last or youngest occurrence of *Odontochitina costata* at the Campanian–Maastrichtian boundary and the first or oldest occurrence of *Aquilapollenites* at the base of the Campanian; however, Nichols and Sweet (1993) placed the first or oldest occurrence of triprojectate pollen in the Coniacian–Santonian. *Heterosphaeridium difficile* has its

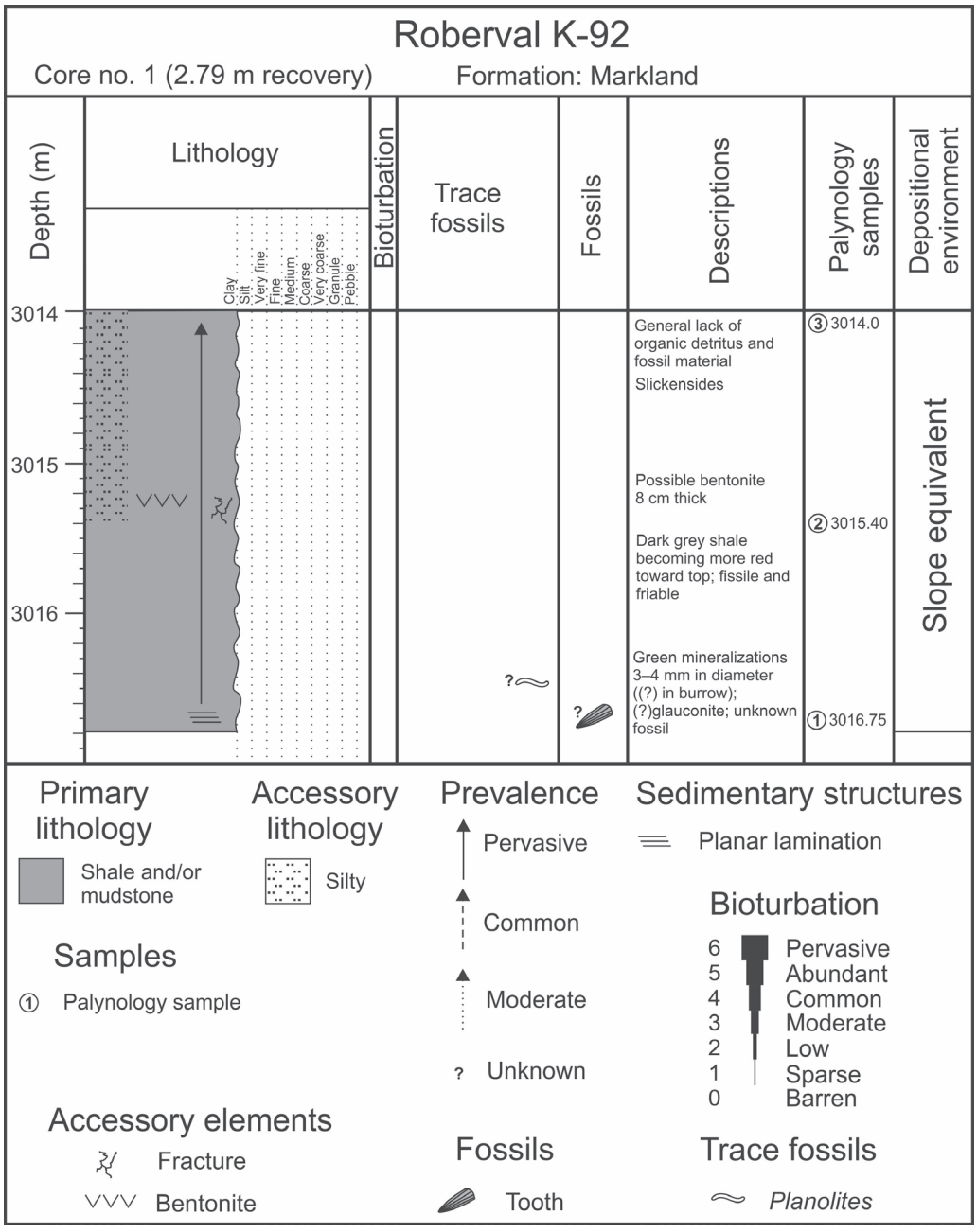


**Figure 61.** Log of core 1, Roberval K-92. The shale to silty shale preserves only one fossil fragment and notably contains green mineralizations (possibly glauconite) and a possible bentonite horizon.

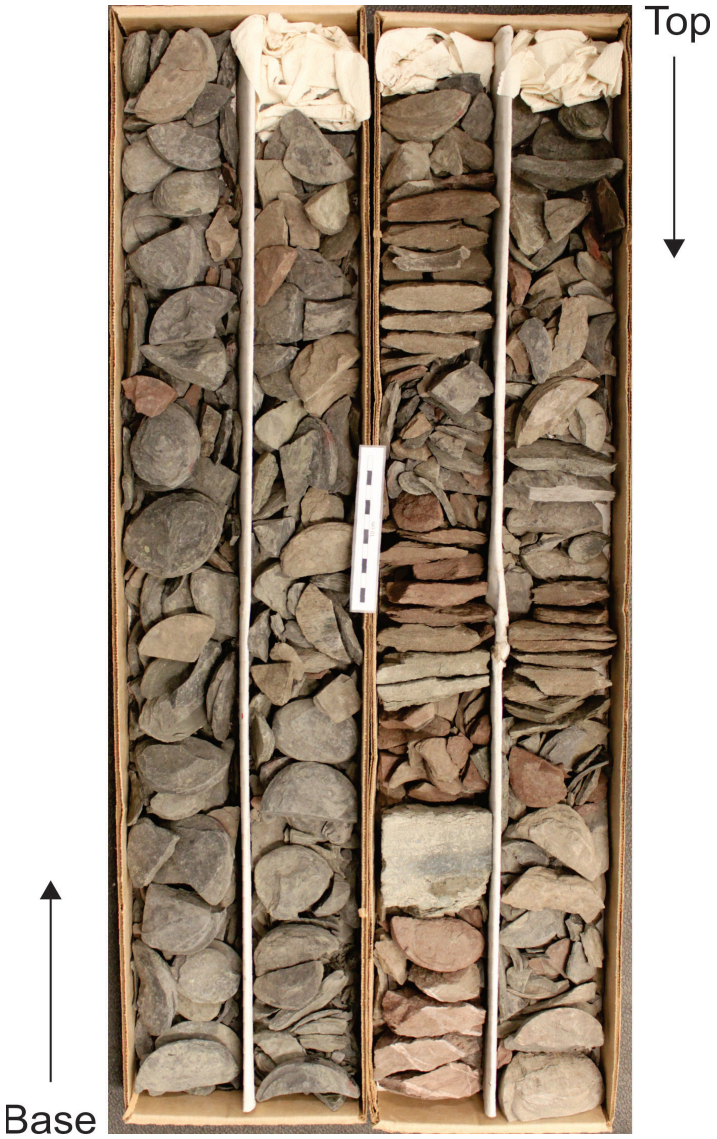


**Figure 62.** Photograph of core 1, Roberval K-92. Scale bar = 10 cm. NRCan photo 2019-451. Photograph by L.T. Dafoe.

last or youngest occurrence in the early Campanian, according to Williams et al. (2004). J.P. Bujak (pers. comm., 1987) has proposed a zonation for the Cretaceous of Arctic Canada based on the last or youngest occurrences of palynomorphs and especially dinocysts. He recognized a *Eurydinium glomeratum* Zone of middle Turonian to early Coniacian age and a *Chatangiellla verrucosa* Zone of middle to late Coniacian age. Bujak stated that "Species of *Canningia* occur commonly in the *Eurydinium glomeratum* Zone and include several forms that have not been previously described. This genus was evolving rapidly during the Cenomanian to Coniacian and several stratigraphically useful species occur in this and the overlying *C. verrucosa* Zone." One of the characteristic features of this sample is the high number of *Canningia* species and specimens present. Thus, the evidence seems to indicate that the age of this sample is Coniacian. As noted by Wall et al. (1977) and Sluijs et al. (2005), open-ocean paleoenvironments are characterized by the occurrence of the dinocyst genus *Impagidinium*. The presence of several specimens of this genus in the sample is indicative of such a paleoenvironment, presumably reflecting deeper water.

Several dinocysts were recorded in the sample from 3015.40 m, including *Achomosphaera ramulifera*, *Cordosphaeridium* sp., *Elytrocysta druggii*, *Hystrichosphaeridium quadratum*, *Impagidinium* sp., *Oligosphaeridium pulcherrimum*, *Sepispinula huguoniotii*, *Spiniferites scabrosus*, and *Tenua* cf. *hystrix,* which has penitabular processes (recorded as *Cerbia* cf. *tabulata* in some wells, e.g. Williams (2003)). *Tenua* cf. *hystrix* has been recorded from the Campanian of other Labrador Shelf wells including South Labrador N-79 and Roberval K-92 (Williams, 2017), so its last or youngest occurrence appears to have some validity as an index marker for this stage. In samples from the related sections on Bylot Island, the first or oldest occurrences of *Elytrocysta druggii* and *Spiniferites scabrosus* were in the early

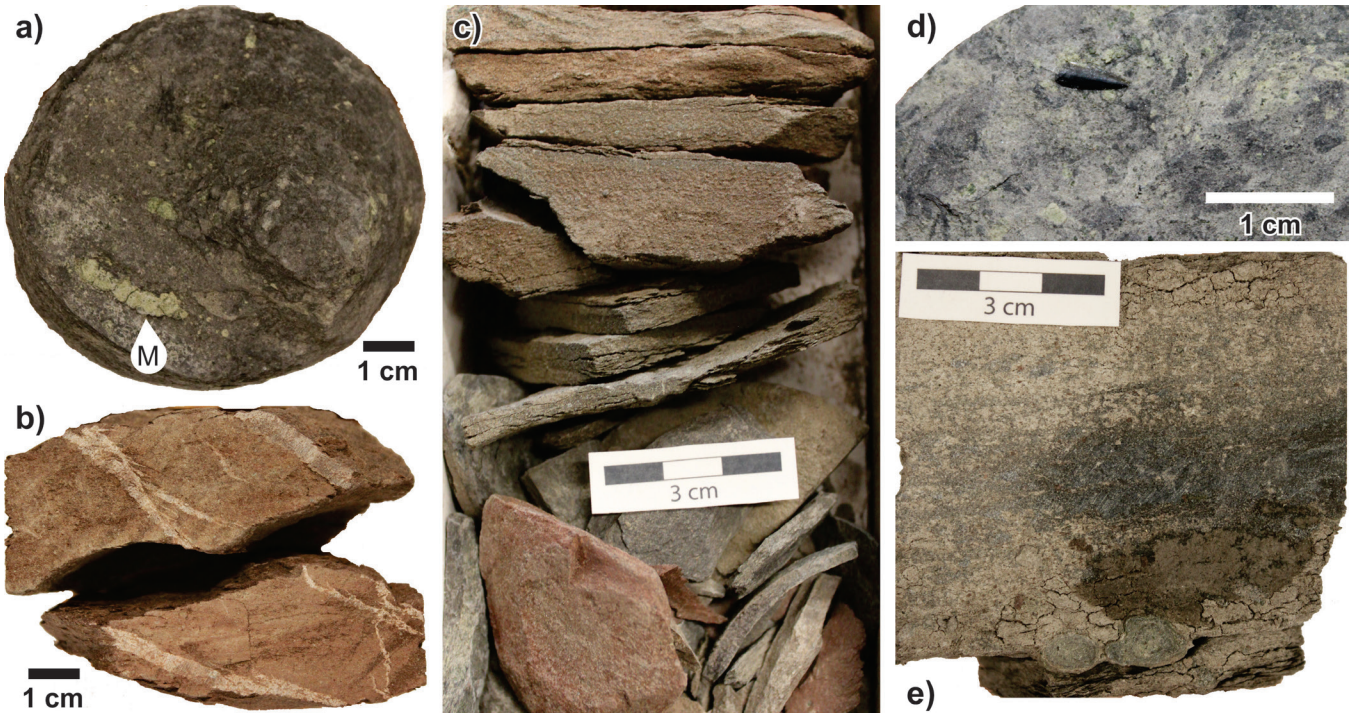


**Figure 63.** Photographs of core 1, Roberval K-92. **a)** Plan view of dark grey shale with green mineralizations, possibly related to prediagenetic burrowing. NRCan photo 2019-452. **b)** Red friable shale with calcite-filled fractures. NRCan photo 2019-453. **c)** Variably coloured shale layers that are fissile and friable. NRCan photo 2019-454. **d)** Small tooth-like fossil in plan view. NRCan photo 2019-455. **e)** Possible bentonite horizon at approximately 3015.25 m depth. NRCan photo 2019-456. All photographs by L.T. Dafoe.

Campanian (G.L. Williams, work in progress, 2020). The age was confirmed by Sweet (2015). Perhaps one significant line of evidence is the absence of species of *Canningia*, suggesting that the age is younger than Coniacian and that it is Santonian–early Campanian, but more likely the latter. The presence of *Impagidinium* indicates that the paleoenvironment was open ocean, deeper water.

The topmost sample, at 3014.0 m, contains a single palynomorph, a specimen of the dinocyst *Spiniferites ramosus*. There is an overwhelming abundance of vitrinite. An age for the sample could not be determined, but it can be considered marine with an influx of terrestrial plant material.

### *Summary*

Ainsworth et al. (2014) dated all the interval of Markland Formation sampled by core 1 as Santonian; Bujak Davies Group (1989g) considered it to be Campanian; and Williams (2017) proposed an age of early Campanian. New results from the present study indicate a Coniacian age for the lowermost sample, although it could be as young as early Campanian, and a Santonian–early Campanian for the sample at 3015.40 m. There is no evidence for a major stratigraphic break in the cored interval between the lowermost two samples, so an early Campanian age seems most likely. Previous interpretations from cuttings have suggested that this interval was part of an upper to middle bathyal (Ainsworth et al., 2014), open ocean, deeper water (Williams, 2017) to outer shelf setting (Miller and D'Eon, 1987). These are all consistent with the present authors' slope-equivalent environment and open ocean, deeper water interpretations above. The presence of abundant vitrinite in the uppermost sample indicates an influx of plant material that may reflect a distal expression of fluvial flooding whereby detritus is carried by currents or turbidity flows into deeper water.

## *Core 2: heterolithic sandstone and siltstone (3095–3112.5 m)*

### *Core description and interpretation*

Core 2 from Roberval K-92 intersected the Bjarni Formation and comprises two facies: a buff, fine- to coarse-grained sandstone and a sandy siltstone and/or mudstone to muddy and/or silty sandstone facies (Fig. 64, 65). The sandstone is poorly to well sorted, quartz-rich and contains feldspar grains. It is also noncalcareous with scattered granules (Fig. 66a) and pebbles up to 3 cm in diameter that are composed of quartzite and rounded coal fragments. Sedimentary structures include massive bedding (Fig. 66a), planar lamination, and rare tabular crossbedding (Fig. 66b). Mudstone laminae are present (Fig. 66b), as well as organic detritus, coal

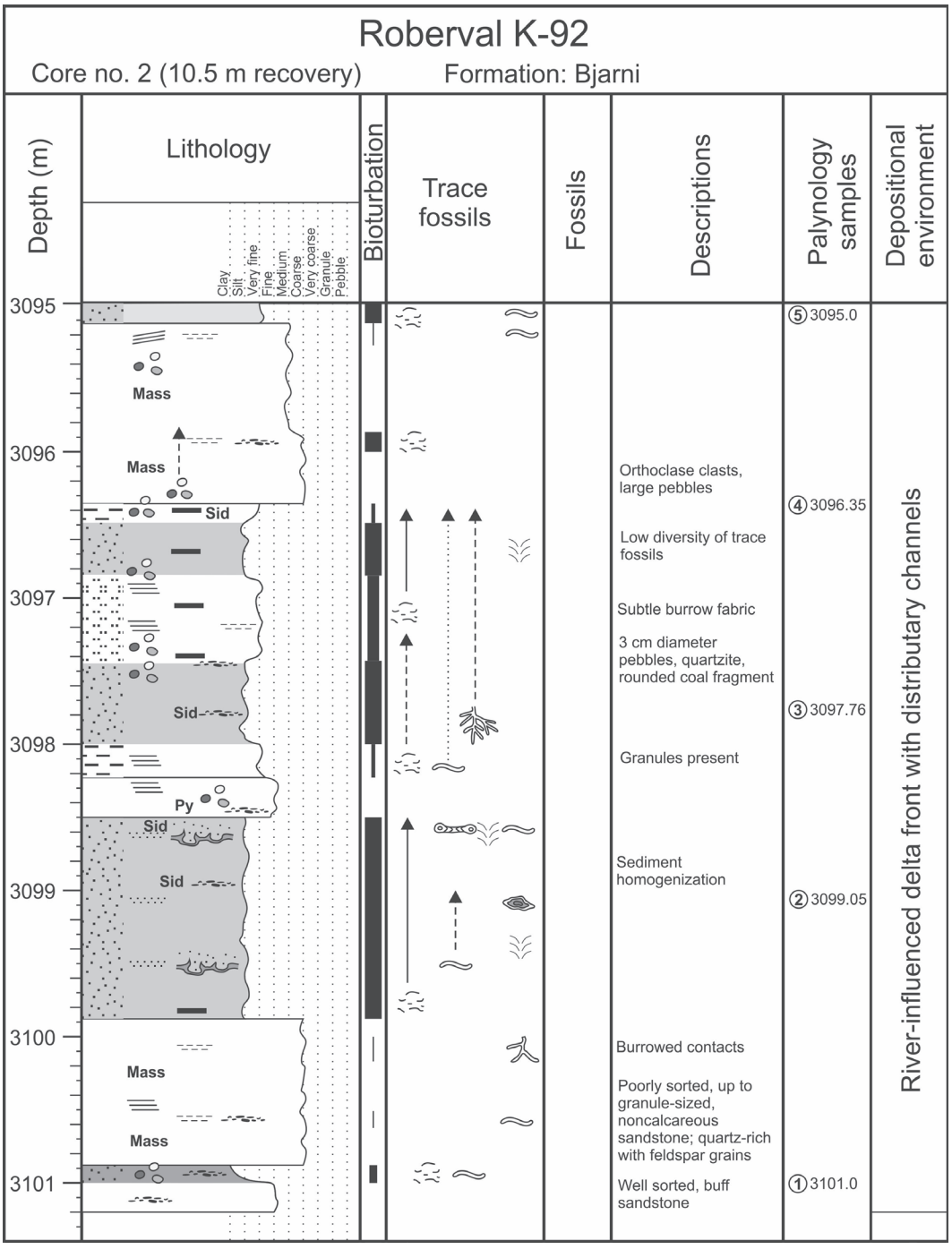


**Figure 64.** Log of core 2, Roberval K-92 showing mixed sandstone and sandy mudstone and/or siltstone intervals.

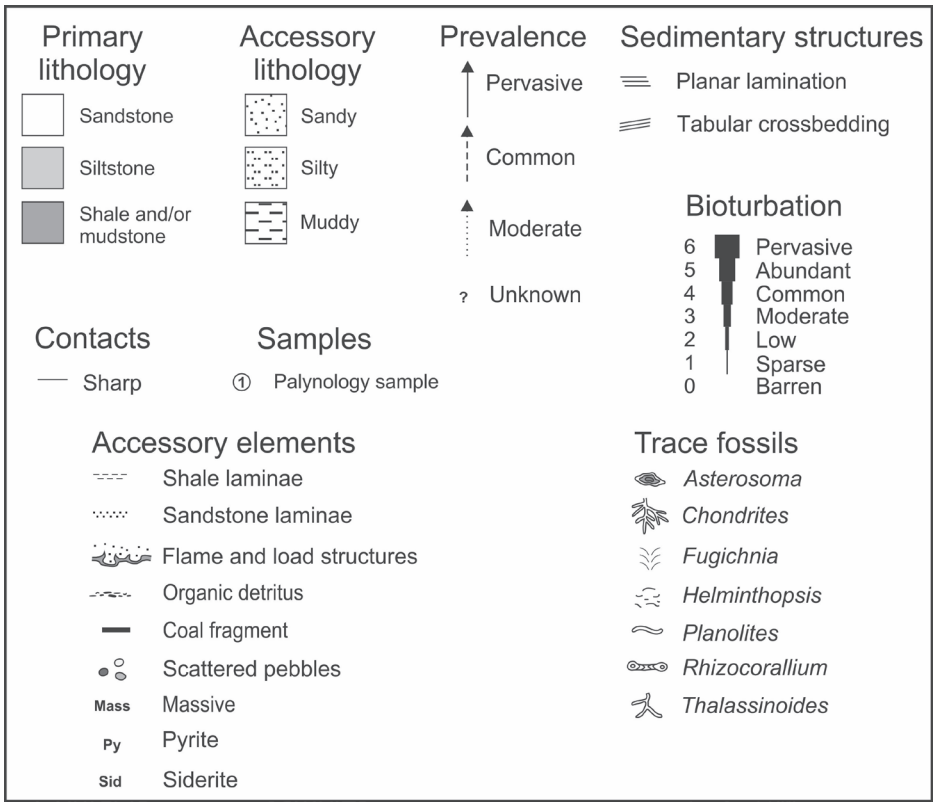


**Figure 64.** (cont.)


**Figure 65.** Photographs of core 2, Roberval K-92. Scale bar = 10 cm. NRCan photo 2019-457, 2019-458. Both photographs by L.T. Dafoe.

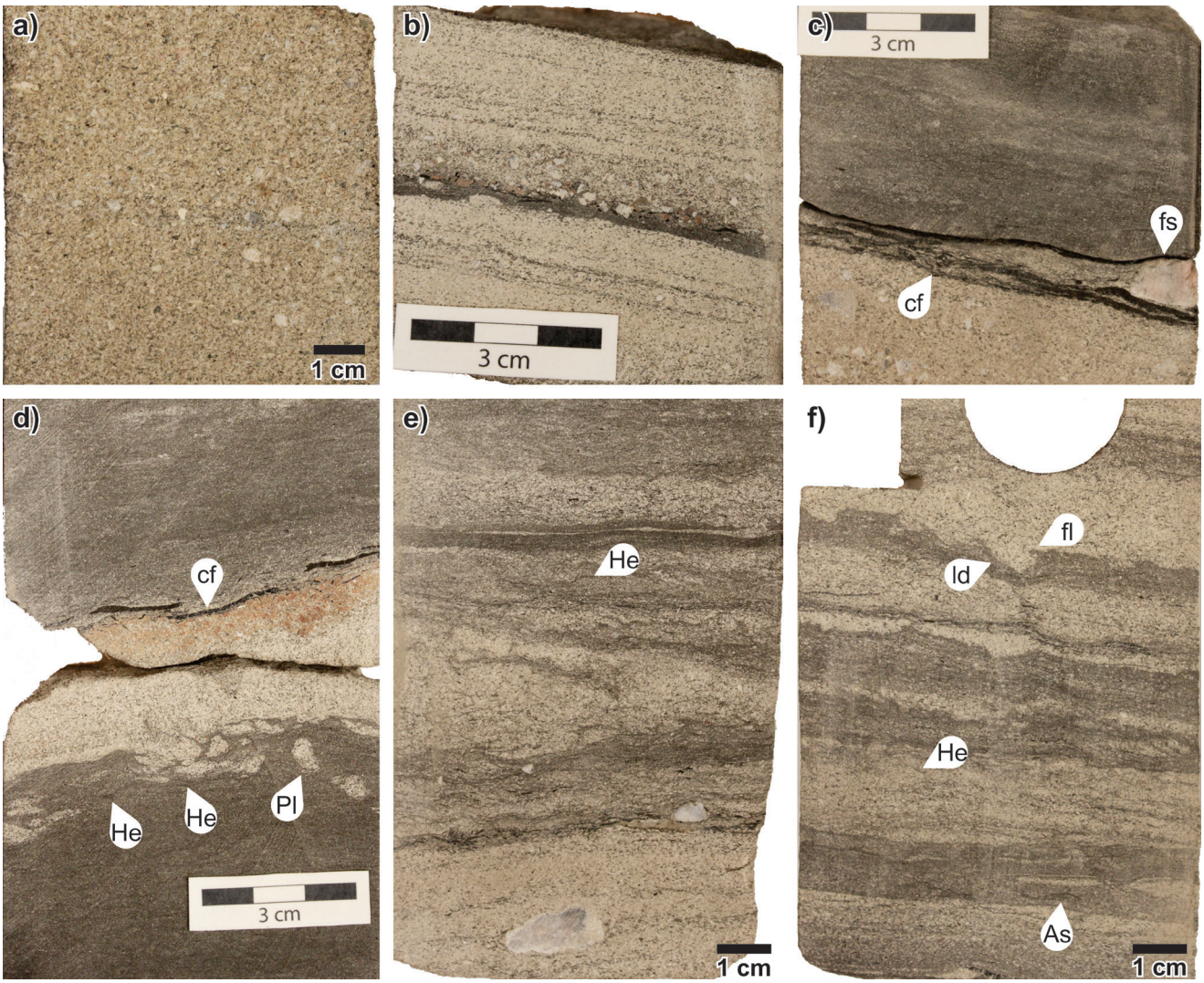


**Figure 66.** Photographs of core 2, Roberval K-92. **a)** Coarse-grained sandstone with granules. NRCan photo 2019-459. **b)** Planar to low-angle crossbedded, fine- to medium-grained sandstone with carbonaceous mudstone laminae and granules. NRCan photo 2019-460. **c)** Contact between a sandstone and siltstone bed with coal fragments (cf) and an orthoclase feldspar pebble (fs). NRCan photo 2019-461. **d)** Siltstone facies with a thin sandstone bed. The sandstone allows for lithological contrast and identification of trace fossils, including *Helminthopsis* (He) and *Planolites* (Pl). The sandstone is capped by siderite and coal fragments (cf). NRCan photo 2019-462. **e)** Silty sandstone with quartzite pebbles, carbonaceous layers, and *Helminthopsis* (He) traces. NRCan photo 2019-463. **f)** Muddy sandstone with soft-sediment deformation: load (ld) and flame (fl) structures. Trace fossils include *Helminthopsis* (He) and *Asterosoma* (As). NRCan photo 2019-464. All photographs by L.T. Dafoe.

fragments (Fig. 66c), and rare siderite and pyrite. Bioturbation in this facies ranges from 0–80%, but trace fossils can only be rarely identified and include *Planolites* and *Thalassinoides*.

The sandstone facies is interbedded with a finer grained sandy siltstone and/or mudstone and muddy and/or silty sandstone facies (Fig. 64). The medium grey siltstone and/or mudstone deposits are characterized by 10–20% buff sand grains. Sandier intervals comprise very fine-grained sandstone (Fig. 66d). Sedimentary structures include planar lamination (Fig. 66e) and soft-sediment deformation (Fig. 66f). Granules and small pebbles are also scattered in this facies, but are less prevalent than in the coarser grained sandstone facies (Fig. 66e). These deposits also contain organic detritus, siderite, and common coal fragments (Fig. 66d). Bioturbation comprises 20–80% of the core; however, a lack of lithological contrast locally hampers identification of trace-fossil genera (Fig. 66d). Trace fossils represent a low-diversity, low-abundance suite, including common *Helminthopsis*, moderate numbers of *Chondrites* and *Planolites*, and rare fugichnia, *Asterosoma*, and *Rhizocorallium* (Fig. 66d, e, f).

The massive and crossbedded, coarse-grained nature of the sandstone facies suggests rapid deposition by high-energy currents. The presence of trace fossils and coal

fragments and association with the finer grained facies suggest a shallow-marine origin. The limited trace-fossil suite is consistent with a highly stressed expression of the *Cruziana* Ichnofacies, reflecting a brackish depositional setting. Thick sandstone may represent distributary channels, especially where coarser grained clasts are found at the base of fining-upward beds. Thick silty and/or muddy beds of the second facies, with moderate degrees of bioturbation, may represent hypopycnal deposits in a delta-front environment. Despite the fine-grained nature of the sediment, the abundance and diversity of trace fossils are both low, representing a stressed expression of the archetypal *Cruziana* Ichnofacies, dominated by structures formed by grazing and deposit-feeding organisms. Overall, the absence of vertical structures of inferred suspension feeders suggests that environmental conditions were brackish with high concentrations of suspended sediment, precluding filter-feeding behaviours. This evidence, combined with thick hypopycnal deposits, is consistent with a river-influenced delta-front setting where fluvial influx would reduce salinity and supply ample sediment.

### *Palynology*

Five samples from core 2 were processed for palynomorphs. The bottommost sample, at 3101.0 m, contains two bisaccate pollen grains, one of which is *Parvisaccites radiatus*. Thus, the sample is presumably early Albian or older (Bujak Davies Group, 1989g; Nøhr-Hansen et al., 2016). The absence of dinocysts suggests that the paleoenvironment was nonmarine.

*Cicatricosisporites hallei* (identification was based on the illustrations of this species in Singh, 1971), a trilete spore, and the bisaccate pollen *Podocarpidites* and *Vitreisporites* sp. sensu Singh, 1971 occur in the sample from 3099.05 m. There is also a single fungal hypha. Singh (1971), gave a stratigraphic range of Early Cretaceous to Cenomanian for *Cicatricosisporites hallei*. The evidence therefore points to an Albian or older age because of the absence of dinocysts, but is not conclusive. Again, the absence of dinocysts suggests that the paleoenvironment was nonmarine.

A sample from 3097.76 m contains an equally sparse assemblage with only three specimens, all miospores. These are *Parvisaccites*, *Pinuspollenites*, and *Taxodiaceaepollenites*. The authors are assuming that the presence of *Parvisaccites* indicates an age no younger than early Albian (*see* above). This seems to be supported by the absence of *Rugubivesiculites*. As in the sample above, the paleoenvironment is considered nonmarine.

Only single specimens of the spore *Ischyosporites pseudoreticulatus* and the pollen *Vitreisporites* sp. sensu Singh, 1971 were recorded from the sample at 3096.35 m. This evidence is insufficient on which to base an age; however, the absence of dinocysts can be used to suggest that the paleoenvironment was nonmarine.

The uppermost sample at 3095.0 m contains the pollen *Pinuspollenites* and a spore *Baculatisporites*. What appeared to be a specimen of the dinocyst genus *Subtilisphaera* was also identified. Although it is not possible to determine the age of this sample, the assemblage seems to indicate that the paleoenvironment was marginal marine.

### *Summary*

The age of the core 2 interval of the Bjarni Formation has been previous reported as late–(?)middle Albian (Ainsworth et al., 2014) or Aptian (Williams, 2017) from cuttings. Results of the present study indicate an age no younger than early Albian for the core. Previous interpretations suggested nonmarine to transitional (Ainsworth et al., 2014), marginal (?)marine and/or alluvial fan (?)delta (Miller and D'Eon, 1987), and inner shelf and nonmarine (Williams, 2017) settings. The nonmarine and lesser marginal-marine setting from palynological analysis generally agree with the previous results and with core observations from the present study that indicate a river-influenced delta-front setting. A more pronounced nonmarine signature, resulting from the lack of dinocysts, is likely due to the influx of fresh water.

## Skolp E-07

Skolp E-07 is located within the southern part of the Saglek Basin, offshore Labrador (Fig. 1). The well was drilled in 1978 to test sedimentary units absent in Karlsefni A-13 (Total Eastcan Exploration Ltd., 1978b); total depth is 2992 m. Conventional cores were taken from seven intervals, with one in Precambrian basement, one in the Bjarni Formation, and five in the Markland Formation (some intersecting the Freydis Member).

## *Cores 1 and 2: medium grey shale (1276.3–1276.5 m and 1276.5–1280.0 m)*

### *Core description and interpretation*

Cores 1 and 2 (Fig. 65) are vertically adjacent to one another, with only 0.2 m of recovery from core 1 and 2.65 m of recovery from core 2, in total spanning the interval 1276.3–1279.35 m within the Markland Formation; part of the section in core 2 is also missing (Fig. 67). The cores are characterized by two facies: a muddy grey sandstone and a medium grey shale (Fig. 67, 68). The lowermost part of core 2 is characterized by the muddy sandstone comprising moderately sorted, fine-grained sandstone, with interspersed coarse-grained quartzose sand grains (Fig. 69a). This interval is 90% bioturbated, but trace fossils are difficult to identify due to the coarse-grained nature of the facies. Muddy *Rhizocorallium* and *Asterosoma* dominate the trace-fossil fabric, with *Palaeophycus*, rare *Planolites*, and possible *Skolithos* (Fig. 69a). This facies is

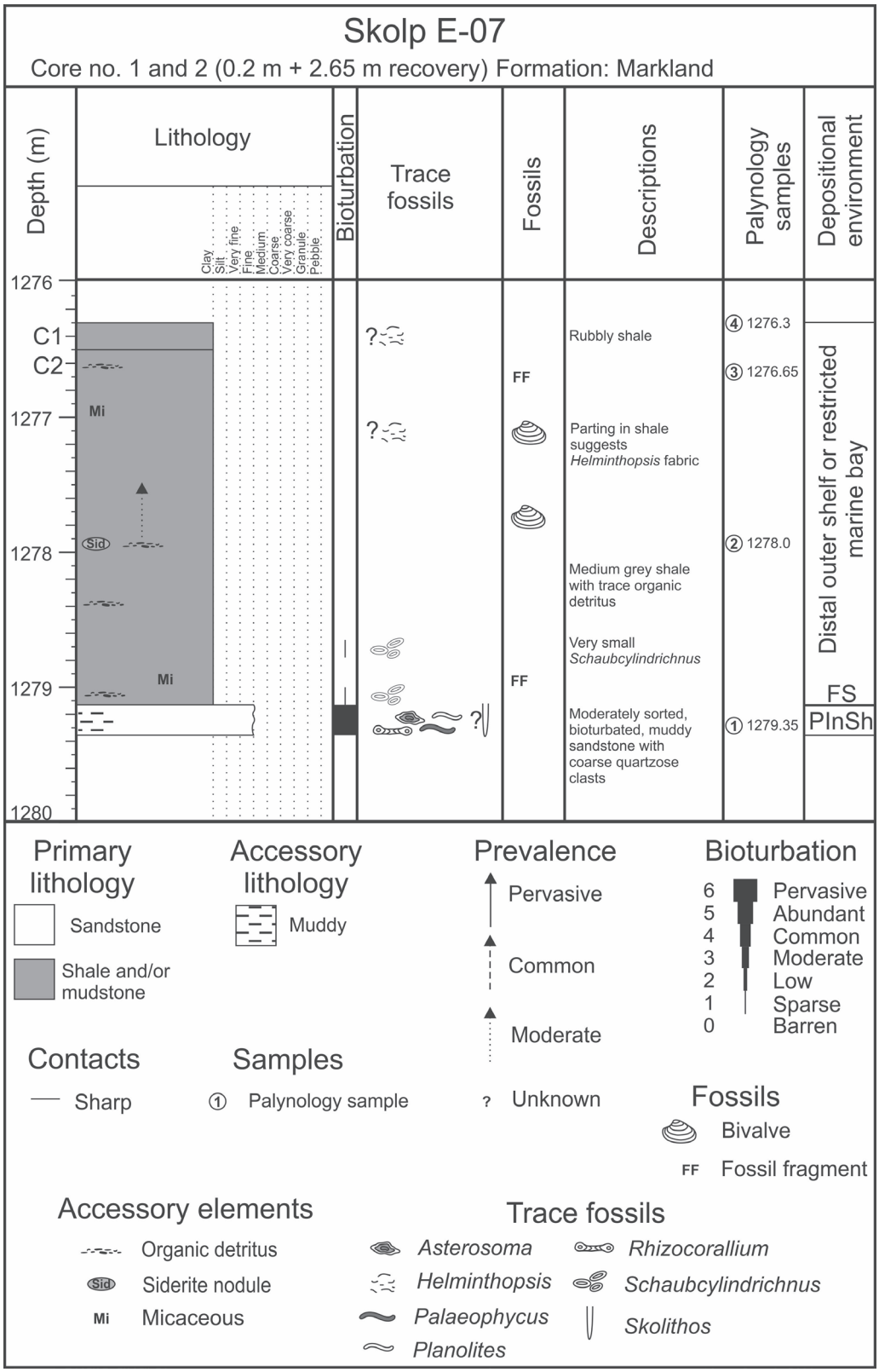


**Figure 67.** Log of cores 1 and 2 from Skolp E-07. The cores are differentiated as C1 and C2 on the left side of the log. A significant flooding surface (FS) separates the muddy sandstone at the base of core 2 from the overlying shales. PInSh = proximal inner shelf.


**Figure 68.** Photograph of cores 1 and 2, Skolp E-07 well. Note the small amount of recovered material in core 1 (top right). The base of the core 2 begins in the lower left and the top of the section is at the top right. Scale bar = 10 cm. NRCan photo 2019-465. Photograph by L.T. Dafoe.

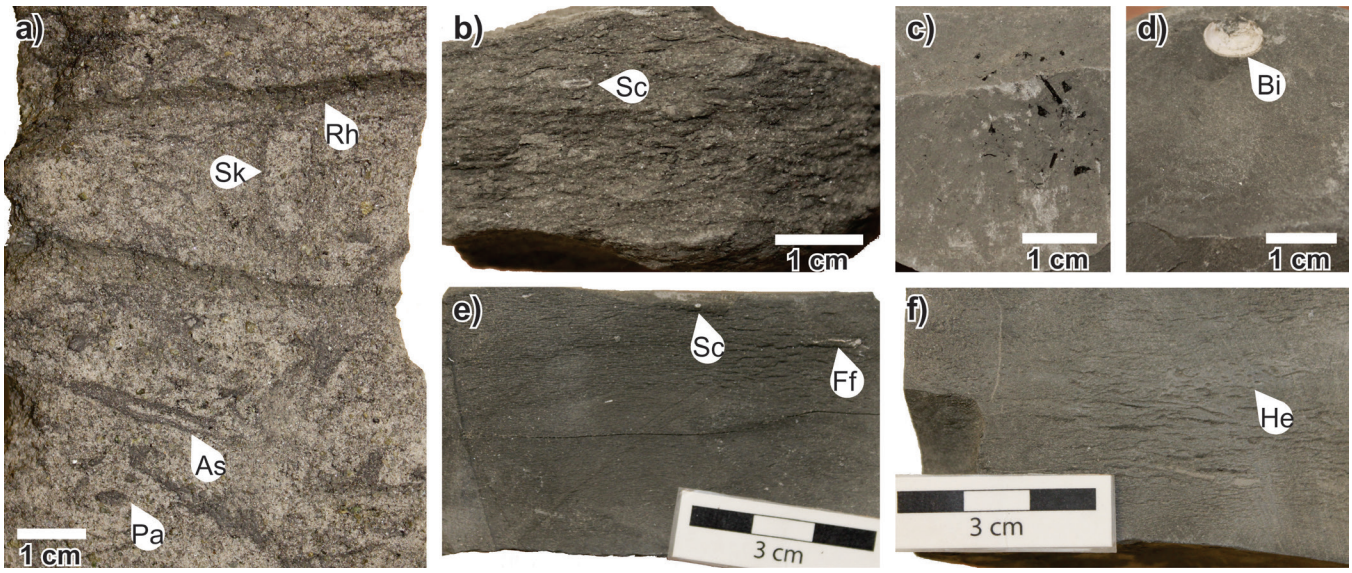


**Figure 69.** Photographs from core 2 of Skolp E-07. Muddy sandstone and medium grey shale facies from the Skolp E-07 cores 1 and 2. **a)** Muddy sandstone with *Rhizocorallium* (Rh), *Skolithos* (Sk), *Asterosoma* (As), and *Palaeophycus* (Pa). NRCan photo 2019-466. **b)** Solitary *Schaubcylindrichnus* (Sc) in shale. NRCan photo 2019-467. **c)** Fine organic detritus along a bedding surface in the shale. NRCan photo 2019-468. **d)** A bivalve (Bi) found in shale partings. NRCan photo 2019-469. **e)** A very small *Schaubcylindrichnus* (Sc) and some fossil fragments (Ff). NRCan photo 2019-470. **f)** Possible *Helminthopsis* (He) that may suggest additional reworking by organisms that cannot be otherwise seen in the homogeneous sediment. NRCan photo 2019-471. All photographs by L.T. Dafoe.

sharply overlain by laminated medium grey shale of the second facies (Fig. 69b, c, d, e, f). The shale contains scattered, fine organic detritus (Fig. 69c), micaceous material, and siderite nodules. Bioturbation is apparently rare, although shale partings in places suggest a possible *Helminthopsis* ichnofabric (Fig. 69f). Rare, small *Schaubcylindrichnus* (Fig. 69b, e) were noted, as well as unidentified fossil fragments and rare bivalve shells (Fig. 69d).

The bioturbated muddy sandstone facies suggests a well oxygenated, low-energy, but relatively proximal setting consistent with a proximal inner shelf. Although little core exists through this facies, the trace-fossil assemblage is consistent with an archetypal expression of the *Cruziana* Ichnofacies dominated primarily by deposit-feeding structures. Conversely, the lack of trace fossils in the shale-dominated facies, aside from small *Schaubcylindrichnus* and possible *Helminthopsis*, may be due to the homogeneous clay composition and lack of lithological contrast. The presence of diminutive *Schaubcylindrichnus* and very rare fossil material may indicate low oxygenation or otherwise stressful environmental conditions during deposition. Organic detritus and coarse-grained sand grains occur throughout, suggesting proximity to a shoreline and possible transport of this material into a more distal setting by storms. The depositional setting for the shale facies is therefore likely consistent with the distal outer shelf or possibly a restricted marine bay under poor water circulation and a lack of clastic influx.

## *Palynology*

The short length and mutual proximity of cores 2 (1280–1276.5 m) and 1 (1276.5–1276.3 m) explains why the palynological analyses are treated together below. Three samples were processed from core 2 and one from core 1. The bottommost sample in core 2, at 1279.35 m, contains unidentified dinocysts as well as *Cannosphaeropsis utinensis*, *Hystrichosphaeridium quadratum*, *Impagidinium* sp*., Isabelidinium cooksoniae*, and *Spiniferites ramosus*. *Densoisporites* and *Matonisporites*, forms of two trilete spore genera, and the acritarch *Fromea glabella* are also in the sample. These spores are generally found in Lower Cretaceous or older rocks, so it is assumed that they are reworked. According to Williams et al. (2004), *Cannosphaeropsis utinensis* is restricted to the Maastrichtian, giving good control on the age of this sample. Despite the presence of a single specimen of *Impagidinium*, the paleoenvironment is interpreted as inner to middle neritic, based on the dominance of miospores.

The sample at 1278.0 m yielded the dinocysts *Elytrocysta druggii*, *Hystrichosphaeridium quadratum*, *Isabelidinium cooksoniae*, and *Spiniferites ramosus*, as well as the acritarch *Fromea fragilis*. One surprise is the presence of a scolecodont, a detached element from the compound jaw apparatus of a polychaetous annelid (Szaniawski, 1996). Scolecodonts are most abundant in Ordovician rocks, but their range extends to today. The presence of *Isabelidinium cooksoniae* indicates that the sample is Turonian to Maastrichtian (Costa and Davey, 1992; Nøhr-Hansen et al., 2016), and the dinocyst/miospore ratio indicates that the paleoenvironment was neritic.

In the uppermost sample from core 2, at 1276.65 m, dinocysts species include *Alterbidinium* sp., *Elytrocysta druggii*, *Isabelidinium cooksoniae*, *Membranosphaera* sp., and *Spiniferites ramosus*. Species of the acritarch genus *Fromea* include *F. glabella* and *F. chytra*. There were no spores and few pollen grains, the most notable being *Extratriporopollenites* sp. *Elytrocysta druggii* was originally described from the Danian of California by Drugg (1967), but on Bylot Island appears to extend down into the Santonian (G.L. Williams and R.A. Fensome, unpub. data, 2020). Specimens of *Isabelidinium cooksoniae* are common in the sample. It is difficult to determine a precise age, but from a study of the cuttings samples, Dafoe and Williams (2020) consider it early Maastrichtian. The presence of several dinocysts with a preponderance of peridiniaceans suggests an inner neritic paleoenvironment.

The extremely short length of core 1 meant that only one sample, from 1276.3 m, was processed. The sparse palynomorph assemblage includes the dinocysts *Cerodinium diebelii*, *Circulodinium distinctum*, *Hystrichosphaeridium quadratum, Isabelidinium*, and *Odontochitina costata*. As noted earlier, *Odontochitina costata* has its last or youngest occurrence at the Campanian–Maastrichtian boundary, but is commonly reworked into the Maastrichtian. This is the case within some of the Bylot Island sections (G.L. Williams and R.A. Fensome, unpub. data, 2020) where the recorded specimen is an operculum. *Cerodinium diebelii* has its first occurrence in the upper Campanian, but is more frequent in the Maastrichtian. Other palynomorphs in the section are the acritarch *Veryhachium trispinosum* and the pollen *Caryapollenites* and *Extratriporopollenites*. *Caryapollenites* generally has a first or oldest occurrence in the Paleocene. Collectively, the assemblage supports a Maastrichtian age. The dominance of the miospores and the low number of dinocysts make it difficult to predict the paleoenvironment, other than to conclude it is neritic.

## *Summary*

The Markland Formation interval encompassing these two cores from cuttings was previously dated as later early Maastrichtian (Williams, 1980; Dafoe and Williams, 2020) or early late Maastrichtian (Nøhr-Hansen et al., 2016). A Maastrichtian age is confirmed by the present palynological analysis. Miller and D'Eon (1987) suggested a mid- to inner shelf paleoenvironment, which is generally consistent with the present authors' interpretation from the lithology as proximal inner shelf to distal outer shelf, and the palynomorphs further confirm these findings. The possibility of a restricted marine bay does not seem likely based on the diversity of dinocysts in the samples.

## *Core 3: medium grey shale and bioturbated mudstone (1280–1289 m)*

### *Core description and interpretation*

Located immediately below core 2 in the Markland Formation, core 3 recovered 9 m of section from 1280 m to 1289 m (Fig. 70). The core consists of similar facies to cores 1 and 2: a medium grey shale and a muddy sandstone to sandy mudstone (Fig. 70, 71). Alternation between the shale and sandy mudstone and/or muddy sandstone suggests minor, but continuous paleoenvironmental shifts (Fig. 70). The medium grey laminated shale is quite rubbly at the base of the core, with abundant gypsum crystals covering the surfaces of shale fragments, which formed following core recovery, likely from the drilling fluids. As in the overlying cores, fine, black, organic detritus fragments are scattered throughout the facies (Fig. 72a), and micaceous minerals occur rarely. Only one unidentified fossil fragment was observed. This facies is barren of trace fossils, except in association with small influxes of sand or at transitions to the sandier facies (Fig. 72f). In these cases, bioturbation can be 5 to 40% of the core and includes common *Chondrites*, fewer *Helminthopsis* and *Planolites*, and rare *Thalassinoides* and *Rhizocorallium*. Contacts between the medium grey shale and the sandier facies are gradational, with one example of a burrowed contact characterized by distinct *Thalassinoides* (at about 1284.6 m depth; Fig. 70, 72b).

Fine-grained, moderately sorted sandstone comprises the muddy sandstone facies. This unit is bioturbated, typically comprising a fabric dominated by *Helminthopsis* (and possibly *Phycosiphon* as well) with moderate *Rhizocorallium* and rare *Chondrites* (Fig. 72c). Organic detritus is scattered throughout the sandy mudstone, which contains 10 to 40% fine-grained sand particles. The facies is highly bioturbated (80–100%) through the common occurrences of *Rhizocorallium* (Fig. 72d), moderate numbers of *Chondrites* and *Helminthopsis*, and rare *Asterosoma*, *Planolites*, *Schaubcylindrichnus*, *Skolithos*, and *Thalassinoides*. Notably, a few of the *Rhizocorallium* are quite large (>1 cm in height) and orientation of organic material is seen in the meniscate structures (Fig. 72e). Observed *Skolithos* and *Schaubcylindrichnus* are notably small (Fig. 72e).

The medium grey shale contains both organic detritus and, where present, a trace-fossil suite consistent with a *Cruziana* Ichnofacies dominated by deposit-feeding traces such as *Chondrites* and *Rhizocorallium*. In contrast, the muddy sandstone and/or sandy mudstone units are highly bioturbated by a relatively diverse and abundant ichnofossil suite, with a clear lack of structures of inferred suspension-feeders. In this facies, a lack of sedimentary structures suggests quiet, normal marine conditions with little storm activity. Furthermore, the predominance of structures formed by deposit-feeding organisms suggests suites representative of the archetypal *Cruziana* Ichnofacies. Based on the lack of sedimentary structures, persistence of organic detritus, and the nature of the trace-fossil suites, core 3 is interpreted to represent fluctuations between distal inner shelf (sandier facies) and distal outer shelf (shale facies) settings.

### *Palynology*

Seven samples were processed from core 3. The lowest sample, at 1289 m, is one of the most productive in the core; it contains the dinocysts *Circulodinium distinctum*, *Elytrocysta* sp., *Hystrichosphaeridium quadratum*, *Isabelidinium cooksoniae*, *Membranilarnacia* sp., *Oligosphaeridium complex*, and *Spiniferites ramosus*. Miospores include the spores *Distaltriangularis mutabilis*, *Laevigatisporites, Osmundacidites*, and *Retitriletes* and the pollen *Caryapollenites*. One acritarch, *Fromea madurensis,* is also present. Nøhr-Hansen et al. (2016) placed the last or youngest occurrence of *Isabelidinium cooksoniae* at approximately the top of the early Maastrichtian, whereas Sweet (2015) dated the interval in which *Hystrichosphaeridium quadratum* had its first or oldest occurrence as Campanian in the Maud Bight section of Bylot Island. Therefore, the presence of these two taxa is indicative of a Campanian–early Maastrichtian age. The paleoenvironment was marine with the high percentage of miospores indicating that this location was marginal marine, and possibly in the vicinity of a delta or estuary.

The sample from 1287.5 m contains several dinocysts, a miospores, and a fungal spore. The dinocysts are *Achomosphaera ramulifera*, *Hystrichosphaeridium quadratum*, *Isabelidinium cooksoniae*, *Membranophoridium* sp., *Oligosphaeridium complex*, *Stiphrosphaeridium dictyophorum*, and *Tanyosphaeridium xanthiopyxides*. One unusual occurrence is the prasinophycean genus *Tasmanites*. Determining an age for the sample is difficult, but the absence of Campanian markers inclines the authors to consider it as Maastrichtian. The dominance of the miospores and the presence and nature of the dinocysts indicates an inner neritic paleoenvironment, possibly in the vicinity of a delta or estuary.

*Cerodinium diebelii* occurs in the sample from 1285.65 m. Other dinocyst species are *Cribroperidinium wetzelii* and *Hystrichosphaeridium quadratum*. Both McIntyre (1974) and Nøhr-Hansen et al. (2016) considered *Cerodinium diebelii* to have its first or oldest occurrence at the base of the Maastrichtian in higher northern latitudes. One pollen grain, assigned to *Aquilapollenites augustus*, is present; Nichols and Sweet (1993) considered this species to be representative of their Assemblage 9, which they considered to be probably late Maastrichtian. Therefore, based on the occurrence of *Cerodinium diebelii* and *Aquilapollenites augustus*, a Maastrichtian age is assigned to the sample. The paleoenvironment must have been marine, presumably neritic.

In the sample from 1284.17 m, pollen include *Caryapollenites*, *Coryluspollenites*, *Extratriporopollenites*, and *Momipites*. Dinocysts with restricted stratigraphic ranges

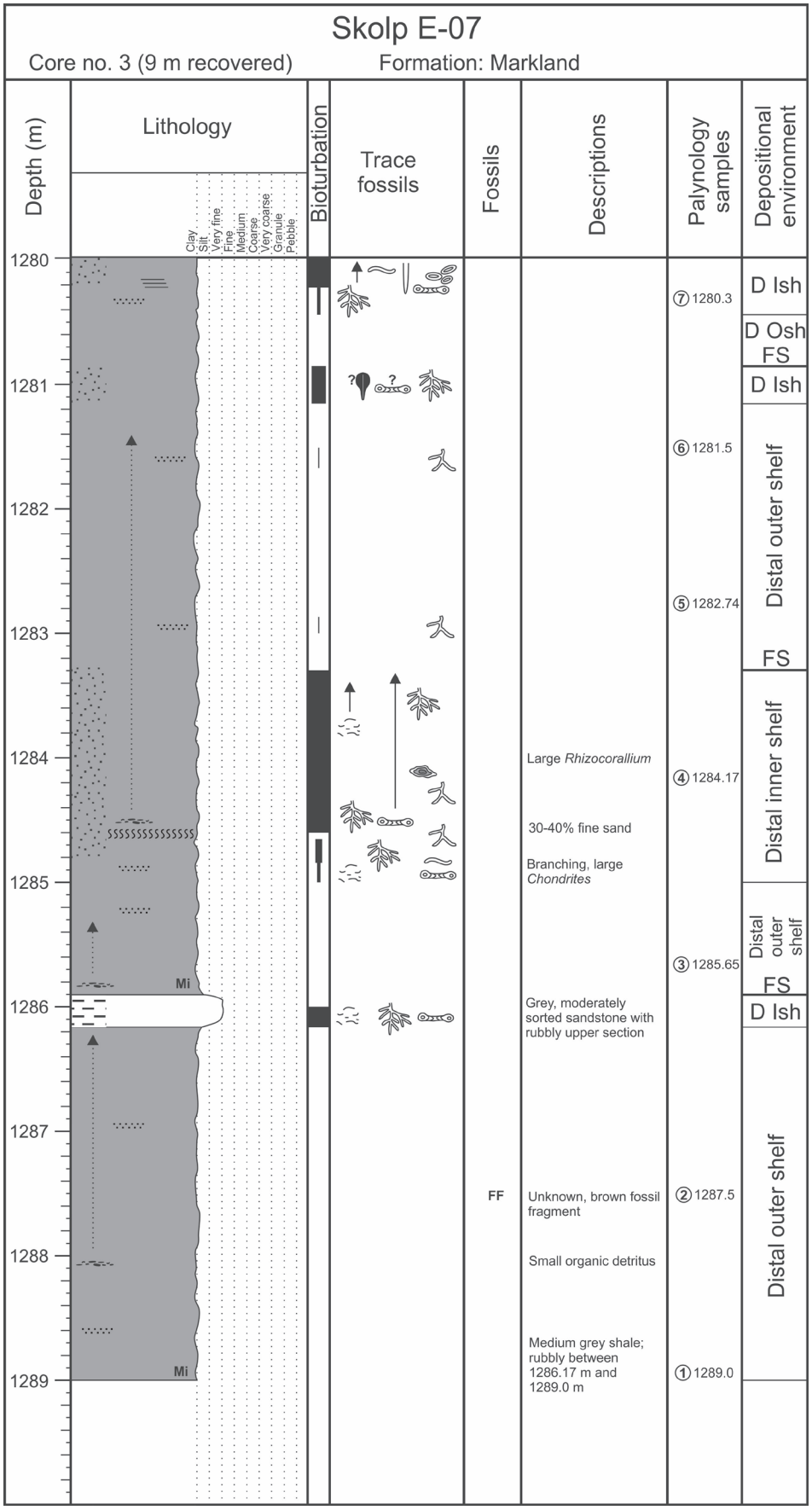


**Figure 70.** Log of core 3 from Skolp E-07. The change in sandstone content and degree of bioturbation highlight the cyclic nature of sedimentation with intervals deposited in outer to inner shelf conditions and separated by flooding surfaces (FS). Note the increased bioturbation in sandy intervals. D Ish = distal inner shelf, D Osh = distal outer shelf.

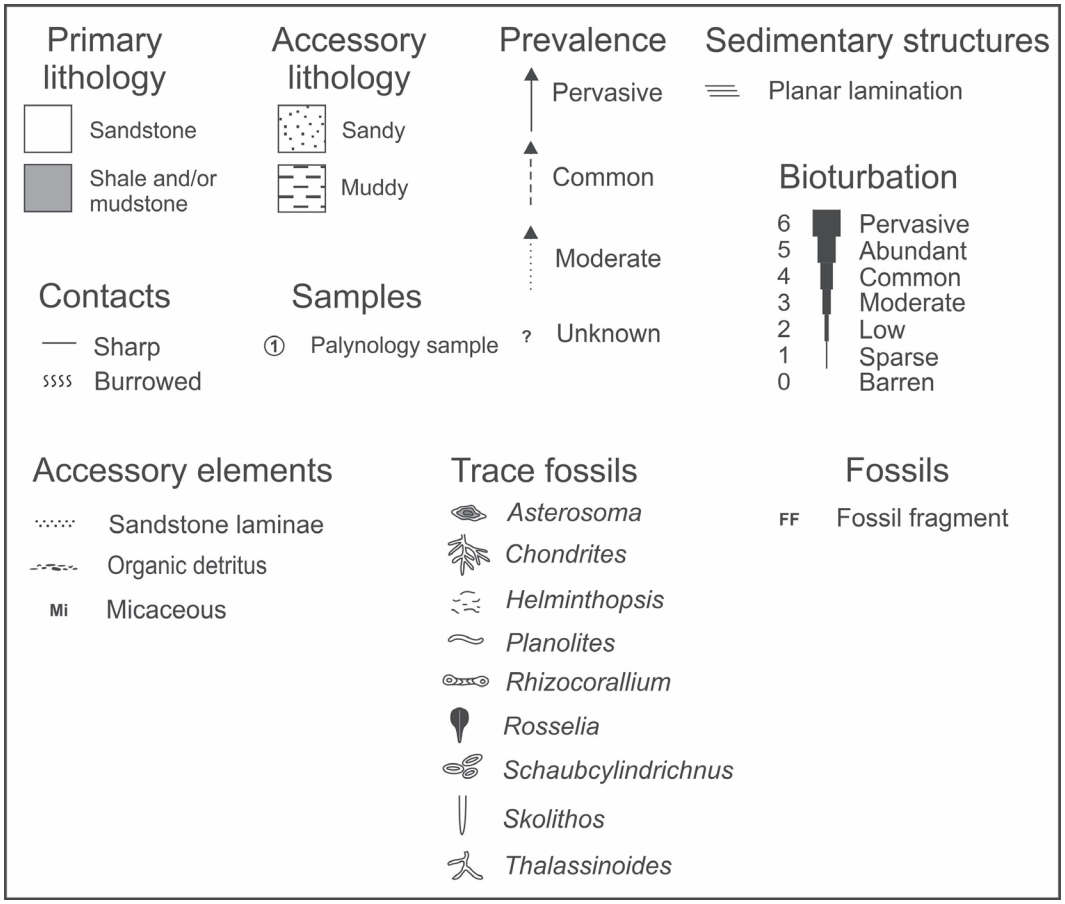


**Figure 70.** (cont.)

are *Hystrichosphaeridium quadratum* and *Palaeoperidinium pyrophorum*. Williams et al. (2004) placed the first or oldest occurrence of *Palaeoperidinium pyrophorum* at 73.7 Ma in mid-northern latitudes, close to the Campanian–Maastrichtian boundary. If *Momipites* is in place, the sample can be no older than Maastrichtian; however, the specimen could represent contamination, as most palynologists consider the genus to have its first or oldest occurrence in the Paleocene. Thus, the age is considered to be Maastrichtian. The paleoenvironment was neritic, with the somewhat reduced amounts of vitrinite compared to the sample at 1282.74 m, indicating a change in the setting, perhaps simply a decline in fluvial influx.

Sample 5 at 1282.74 m has several dinocysts including *Cleistosphaeridium*, *Distatodinium*, *Hystrichosphaeridium quadratum*, *Microdinium*, and *Palaeoperidinium pyrophorum*, and the acritarch *Fromea glabella*. Also present are the spores *Laevigatosporites* and *Retitriletes* and the pollen *Extratriporopollenites*, *Momipites*, and *Pinuspollenites*. Based on the rationale for the above sample, the age is also considered to be Maastrichtian. The paleoenvironment was determined to be a deltaic setting based on the abundance of vitrinite and carbonized wood.

The sixth sample, at 1281.5 m, contains the dinocysts *Circulodinium distinctum*, *Elytrocysta druggii*, *Hystrichosphaeridium quadratum*, *Isabelidinium cooksoniae*, *Microdinium* sp., and *Palaeoperidinium pyrophorum,* and the acritarchs *Fromea chytra* and *Fromea madurensis*. Nøhr-Hansen et al. (2016) placed the last or youngest occurrence of *Isabelidinium cooksoniae* at approximately the top of the early Maastrichtian. Based on this, this sample is considered to be early Maastrichtian. The sample also contains abundant vitrinite and carbonized wood, but has several dinocysts, suggesting a distal delta-front setting.

The uppermost sample at 1280.3 m yielded only one palynomorph, the trilete spore *Camarozonosporites*. Determining the age is therefore not possible. The presence of abundant vitrinite and carbonized wood, coupled with the absence of dinocysts, suggests a deltaic setting, but more evidence is needed for a reliable conclusion.


**Figure 71.** Photographs of core 3, Skolp E-07, showing the core boxes. The rubbly core materials recovered from the base of the core barrel have been bagged. Scale bars = 10 cm. NRCan photo 2019-472, 2019-473. Both photographs by L.T. Dafoe.

*Summary*

This core interval also falls within the later part of the early Maastrichtian of Dafoe and Williams (2020) or early part of the late Maastrichtian (Nøhr-Hansen et al., 2016) of the Markland Formation. The presence of *Cerodinium diebelii* in the sample from 1285.65 m indicates that the core is Maastrichtian, with the presence of the dinocyst *Isabelidinium cooksoniae* indicating an early Maastrichtian age. Miller and D'Eon (1987) suggested that this interval was deposited within a mid- to inner shelf setting. This is consistent with the distal inner-shelf to distal outer-shelf settings suggested by the present core observations. Some of the palynological results from this study, however, indicate a strong deltaic influence and more marginal marine conditions. To explain this discrepancy, reworking of nearby deltaic deposits via prevailing currents could have transported plant detritus to the area from a nearby terrestrial or deltaic source. Alternating inner- and outer-shelf settings indicate minor marine flooding events as sedimentation kept pace with subsidence.

## *Core 4: fine-grained, bioturbated sandstone (1388–1397 m)*

*Core description and interpretation*

Core 4 from Skolp E-07 (also in the Markland Formation) had poor recovery (1 m), and much of the material is in a rubbly state (Fig. 73, 74a). The core transitions from fine- to medium-grained sandstone, which is moderately sorted with some coarse grains present, to a muddy (40%) sandstone. The sandstone is buff and quartz-rich with some organic detritus (Fig. 74b). At the base of the core the sandstone is apparently massive, whereas the muddy sandstone is 80% bioturbated with few sedimentary structures preserved (Fig. 74c, d). Trace fossils include common *Helminthopsis*, moderate *Rhizocorallium*, and lesser *Asterosoma* and *Chondrites*. A greenish coloration was noted, which may indicate the presence of glauconite.

With a lack of identifiable sedimentary structures, trace fossils play a key role in the interpretation of this core interval. In combination with the lithology, the archetypal *Cruziana*


**Figure 72.** Photographs of core 3, Skolp E-07. **a)** Medium grey shale with organic detritus on a bedding plane surface. NRCan photo 2019-474. **b)** Transition from the medium grey shale to sandy mudstone and *Thalassinoides* (Th; highlighted by the white dotted line) infilled with sand-sized material from the overlying facies (a palimpsest horizon). Other trace fossils include *Rhizocorallium* (Rh), *Chondrites* (Ch), and *Helminthopsis* (He). NRCan photo 2019-475. **c)** Muddy sandstone dominated by small, muddy *Helminthopsis* (He) traces, and *Chondrites* (Ch) and *Rhizocorallium* (Rh) are also present. NRCan photo 2019-476. **d)** Prominent *Rhizocorallium* (Rh) ichnofossils with *Planolites* (Pl), *Chondrites* (Ch), and *Helminthopsis* (He). NRCan photo 2019-477. **e)** A large *Rhizocorallium* trace fossil at the top of the core piece with oriented organic detritus fragments and *Schaubcylindrichnus* (Sc) within the spreite. *Chondrites* (Ch) are also present. NRCan photo 2019-478. **f)** A *Chondrites* (Ch)-rich fabric with a clear branching structure in the lower right of the image. NRCan photo 2019-479. All photographs by L.T. Dafoe.

Ichnofacies comprised mostly of deposit-feeding to grazing traces suggests deposition within a proximal inner-shelf paleoenvironment. The transition from clean sandstone to muddy sandstone may represent a minor transgressive event from a shoreface to inner-shelf setting; although, the lack of core recovery makes detailed interpretations difficult.

## *Palynology*

Two samples from core 4 were analyzed for palynomorphs, with the lower at 1389.9 m containing the pollen *Betulaepollenites*, *Caryapollenites*, and *Retitricolpites vulgaris*. An age could not be determined for this sample, but the absence of dinocysts suggests a nonmarine paleoenvironment. The upper sample, at 1388.3 m, is barren.

## *Summary*

Core 4 is from an interval of the Markland Formation dated as early Maastrichtian by Williams (1980), Nøhr-Hansen et al. (2016), and Dafoe and Williams (2020)) based on cuttings, but conclusive ages could not be drawn from the core samples. Miller and D'Eon (1987) suggested

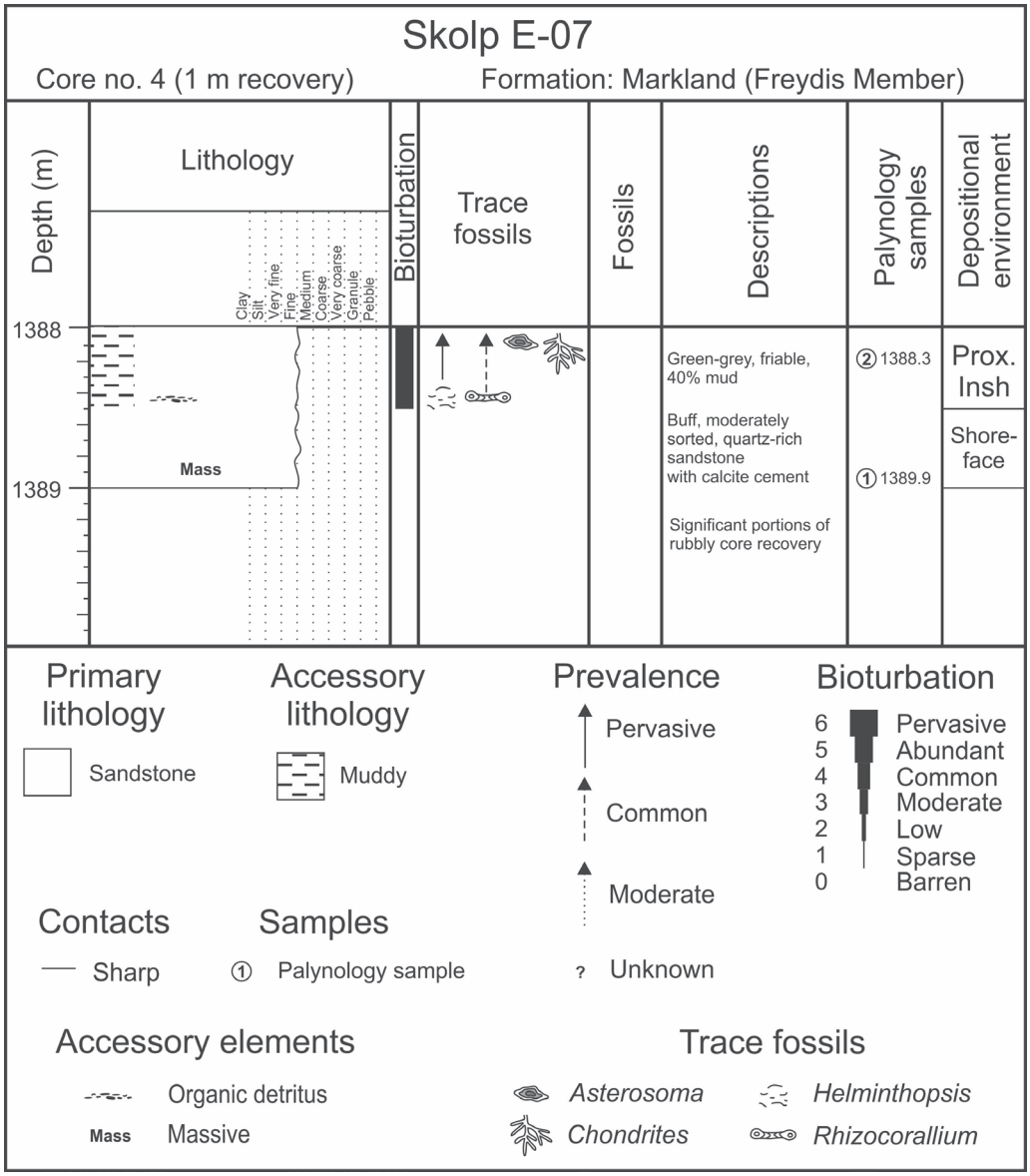


**Figure 73.** Log of core 4 from Skolp E-07. Prox. Insh = proximal inner shelf.

that this interval represents deposition within a marginal marine to inner-shelf setting (prograding alluvial fan delta); this is consistent with the shoreface to inner-shelf environment interpreted in the present study. The lack of dinocysts suggests a nonmarine setting, but could be explained by poor recovery within a sandstone-dominated core interval.

## *Core 5: dark grey, sandy mudstone (1450–1454.32 m)*

### *Core description and interpretation*

Only about 50% of core 5 was recovered, representing the oldest Markland Formation core, or 4.32 m of the 9 m interval (Fig. 75). The entire core consists of one facies, a dark grey sandy mudstone that is friable and moderately fissile with rare siderite (Fig. 76, 77). Very fine- to fine-grained sand makes up about 20% of this core, but, in general the lack of lithological contrast hampers identification of discrete ichnogenera. The trace-fossil assemblage consists of moderate numbers of *Helminthopsis*, which — as mud-cored burrows within a mudstone matrix — are difficult to identify. Scattered throughout the core are also *Schaubcylindrichnus*, *Rhizocorallium*, *Chondrites*, and *Planolites* (Fig. 77). The *Schaubcylindrichnus* are notably diminutive (Fig. 77).

The fine-grained nature of the core and the trace fossil assemblage suggest a shelf environment. The lack of organic detritus and wave-formed sedimentary structures denotes quiescence, beyond the storm-wave base. Overall, the ichnofossil suite is low in diversity and abundance, possibly due to the homogeneous nature of the sediment;

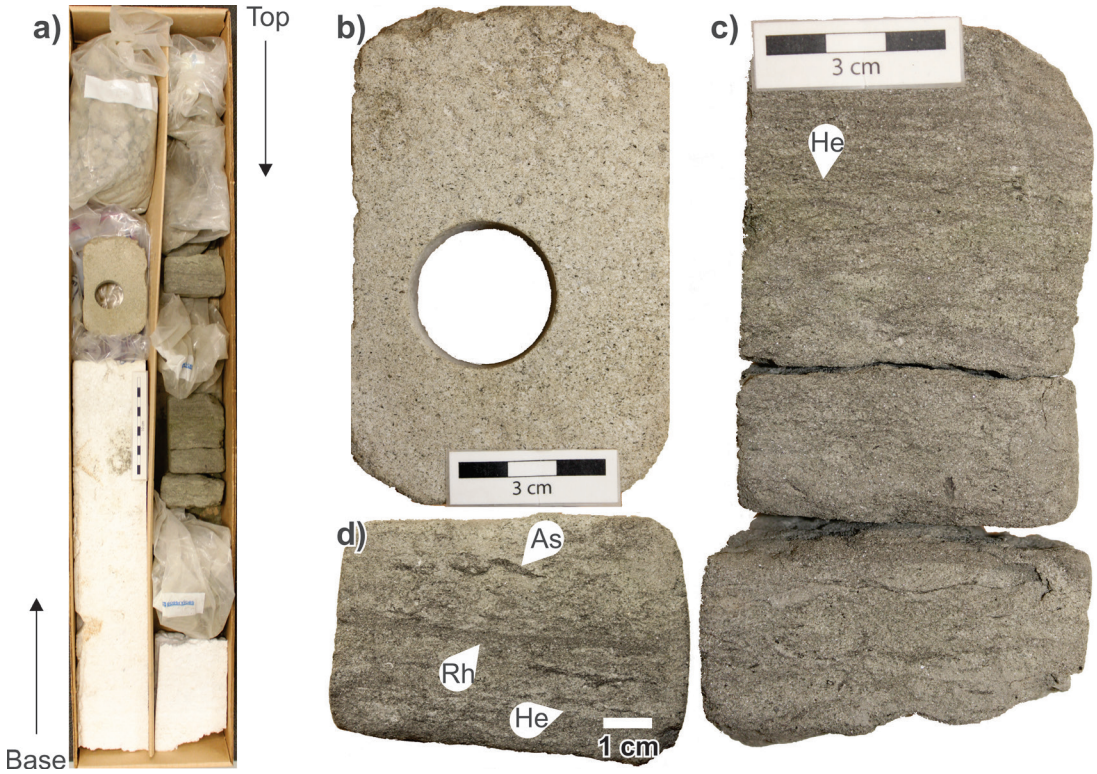


**Figure 74.** Photographs of core 4, Skolp E-07. **a)** The core box for core 4 showing missing core and bags of rubbly core. Scale bar = 10 cm. NRCan photo 2019-480. **b)** Buff, massive sandstone. NRCan photo 2019-481. **c)** Muddy sandstone with *Helminthopsis* (He). NRCan photo 2019-482. d) Muddy sandstone with *Asterosoma* (As), *Rhizocorallium* (Rh), and *Helminthopsis* (He). NRCan photo 2019-483. All photographs by L.T. Dafoe.

however, the suite represents a distal expression of the *Cruziana* Ichnofacies, dominated by grazing traces such as *Helminthopsis*. Accordingly, core 5 is interpreted to reflect a proximal outer-shelf setting beyond the storm wave base where very small amounts of sand and terrigenous material are transported.

## *Palynology*

Four samples from core 5 were processed for palynomorphs. In the lowermost sample, from 1454.32 m, miospores include *Costatoperforosporites fistulosus* (presumably reworked since it is an Early Cretaceous species) and *Pinuspollenites.* Identifiable dinocysts are *Gillinia hymenophora* and *Hystrichosphaeridium quadratum.* Two acritarchs are observed, both are forms of *Fromea*. Stover et al. (1996) assigned an age of late Campanian to Maastrichtian for *Gillinia hymenophora*. Thus, the age of the sample must fall within that range. Based on the high concentrations of vitrinite and carbonized wood (not observed in macroscale), the paleoenvironment appears to have been neritic, not too far from shore, and possibly in the vicinity of a delta.

In the sample from 1452.5 m, dinocysts are rare and the only pollen is *Pinuspollenites*. The identifiable dinocysts are *Hystrichosphaeridium quadratum, Microdinium* sp., and *Xenascus* sp. There are some acritarchs, assignable to the genera *Micrhystridium* and *Fromea*, and one scolecodont. The presence of *Hystrichosphaeridium quadratum* indicates that the sample is no older than Campanian. Based on the high concentrations of vitrinite and carbonized wood, the paleoenvironment appears to have been neritic, not too far from shore, and possibly in the vicinity of a delta.

Several dinocysts and miospores are present in the sample at 1451.2 m. The miospores include forms of *Abiespollenites*, *Extratriporopollenites*, and *Pinuspollenites*. Dinocysts include *Gillinia hymenophora*, *Heterosphaeridium bellii, Hystrichosphaeridium quadratum*, and *Odontochitina costata*. Radmacher et al. (2014) gave a range for *Heterosphaeridium bellii* of late Campanian to Maastrichtian, whereas Nøhr-Hansen et al. (2016) restricted the species to the late Campanian. *Gillinia hymenophora* is common in the Campanian of Bylot Island (G.L. Williams and R.A. Fensome, work in progress, 2020). Thus, the age of this sample is considered to be late Campanian. The paleoenvironment is neritic, with the high concentration of vitrinite suggesting deposition was in the vicinity of a delta and not too far from shore.

The uppermost sample, at 1450 m, contains a diverse dinocyst assemblage comprising *Gillinia* sp., *Hystrichosphaeridium quadratum*, *Impagidinium* sp.,

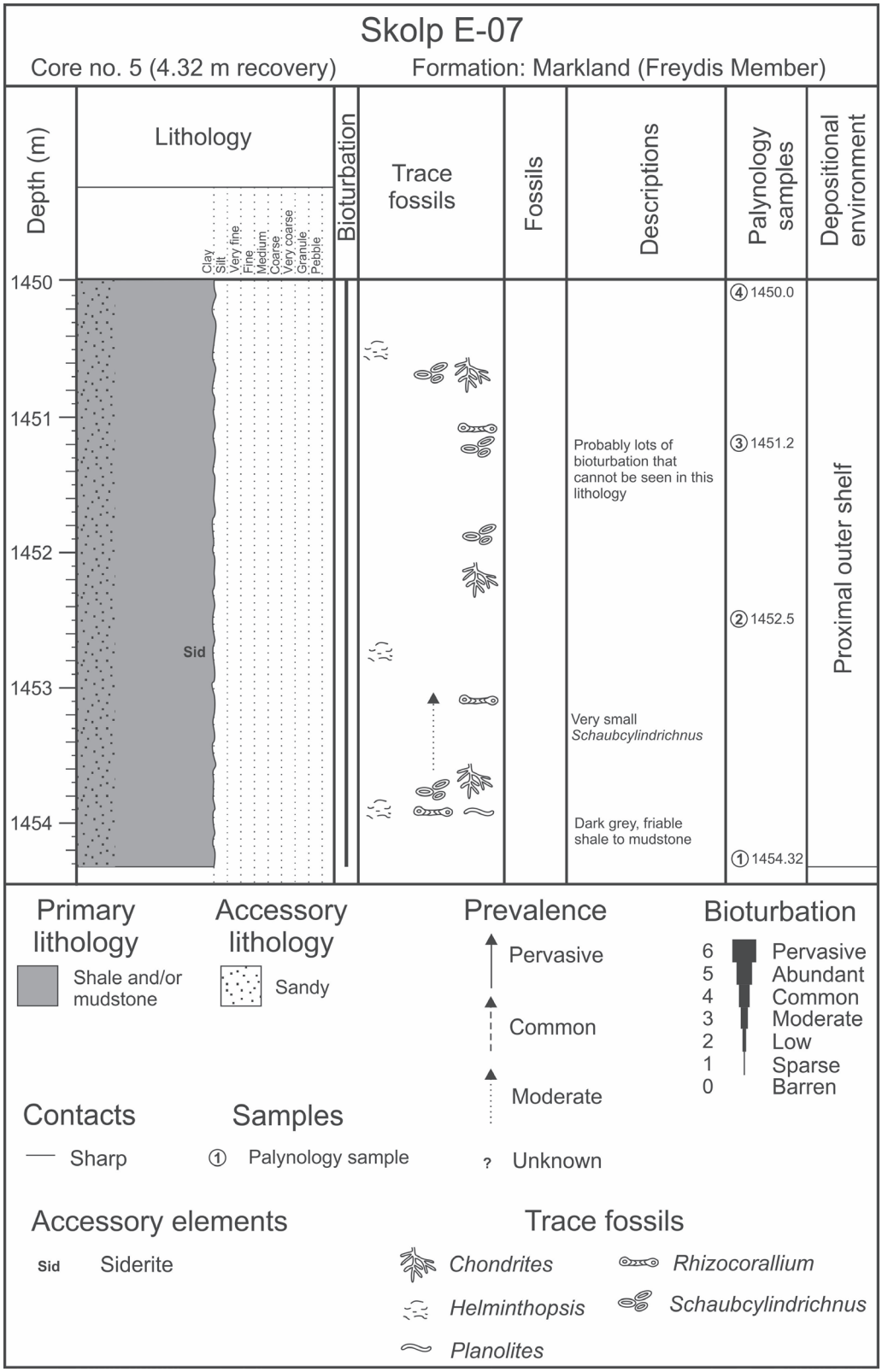


**Figure 75.** Log of core 5, Skolp E-07. The sandy mudstone shows a consistent moderate degree of bioturbation.


**Figure 76.** Photograph of core 5, Skolp E-07 well. Scale bar = 10 cm. NRCan photo 2019-484. Photograph by L.T. Dafoe.

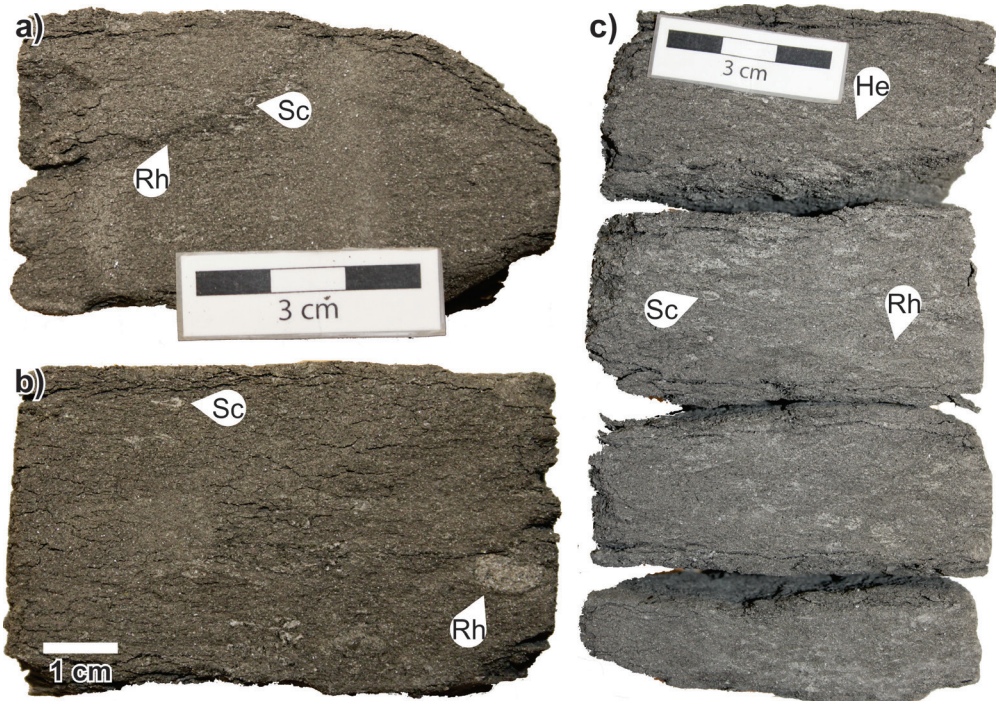


**Figure 77. a)**, **b)**, **c)** Photographs of core 5, Skolp E-07 showing the homogeneous sandy mudstone with trace fossils, including *Rhizocorallium* (Rh), *Schaubcylindrichnus* (Sc), and *Helminthopsis* (He). NRCan photo 2019-485, 2019-486, 2019-487, respectively. All photographs by L.T. Dafoe.

*Odontochitina costata*, *Odontochitina* sp., *Oligosphaeridium complex*, *Pterodinium* sp., *Senoniasphaera rotundata*, and *Spiniferites scabrosus*. A Campanian age is indicated by the presence of *Gillinia* and *Odontochitina costata*: the last or youngest occurrence of the latter species roughly equates with the Campanian–Maastrichtian boundary according to Nøhr-Hansen et al. (2016). Further proof is the presence of *Senoniasphaera rotundata*, which has a last or youngest occurrence in the late Campanian, according to Williams et al. (2004). The general composition of the assemblage indicates a neritic paleoenvironment with the high concentration of vitrinite, suggesting that deposition was in the vicinity of a delta and not too far from shore; however, the presence of a single specimen of *Impagidinium* may indicate deeper water conditions (Dale, 1996).

### *Summary*

In an analysis of this well based on cuttings by Williams (1980), core 5 falls within an interpretation gap of the Markland Formation between the Campanian and early Maastrichtian, but within the latest part of the late Campanian (Dafoe and Williams, 2020). The results of the present study also indicate a late Campanian age. Miller and D'Eon (1987) suggested that this interval was within a marginal marine to inner shelf setting (prograding alluvial fan delta). Current observations from this core, in contrast, indicate a deeper, proximal outer shelf setting relatively consistent with the neritic interpretation from palynomorphs; however, the palynological analyses suggest proximity to a delta, which is not implied by the core observations from this core or the sandier core intervals in this well. Again, prevailing current redistribution of terrigenous detritus from a nearby deltaic setting may explain the abundance of vitrinite and carbonized wood noted.

## *Core 6: sandstone and conglomerate (2915.5–2918.77 m)*

### *Core description and interpretation*

At 2915.5–2921.8 m in the Skolp E-07 well, core 6 was collected from deeper in the well within the Bjarni Formation. Only 3.27 m were retrieved and it includes some poorly recovered, rubbly sections (Fig. 78, 79). Three distinct facies were recognized. From oldest to youngest, they are: a medium- to coarse-grained sandstone; a matrix-supported conglomerate; and a fining-upward, fine-grained, muddy sandstone to sandy mudstone (Fig. 78). The sandstone in the first facies is white to buff and moderately to poorly sorted, with scattered pebbles up to 3 cm in diameter throughout. Bedding is massive, planar laminated, and tabular crossbedded, with calcite cement and scattered pyrite (Fig. 80a, b). The abruptly overlying conglomerate of the second facies is matrix-supported with the matrix resembling the medium-grained, buff sandstone of the underlying facies (Fig. 80c, d). Bedding is massive to tabular crossbedded, with trace pyrite and mudstone laminae and rip-up clasts also present. Pebbles are subrounded to rounded and primarily composed of quartzite (Fig. 80c), but also include gneiss, granite, and volcanic rock. This second facies grades upward into the muddy sandstone and/or sandy mudstone facies above. This third facies is characterized by a clearly fining-upward unit (Fig. 80e). Sedimentary structures in the fine-grained facies include current-ripple crosslaminations, trough crossbedding, planar laminations, and possible wave ripples (Fig. 80f). Pyrite and organic detritus are also present in the uppermost facies. There is no evidence of bioturbation or rooting in any of the facies.

The coarse-grained nature of both the sandstone and conglomerate suggests a high-energy setting, and the relative rounding of the pebbles suggest reworking and long-distance transport. Crossbedding indicates unidirectional current flow, with a sudden change in the current regime toward the top of the core accounting for finer grained deposition. This core is interpreted as a fluvial succession representing dune migration with an increase in flow strength represented by the conglomeratic unit. A change to low-energy, but still aquatic conditions is seen in the uppermost fine-grained unit that likely reflects channel abandonment or stagnation. The lack of plant remains is curious; only small amounts of organic detritus occur in the fine-grained unit, suggesting a terrestrial or, based on the presence of possible symmetrical wave ripples, perhaps a nearshore-marine setting, although, symmetrical ripples can form in nonmarine shallow, aquatic settings such as lake beaches (Baas, 2003).

### *Palynology*

Three samples from core 6 were processed for palynomorphs. The bottommost sample, at 2918.77 m, contains *Hazaria, Parvisaccites radiatus*, and *Pinuspollenites.* The presence of *Parvisaccites radiatus* and absence of *Rugubivesiculites* indicates an early Albian or older age. The sample also contains the pollen *Coryluspollenites* and *Momipites wyomingensis*, which are found in situ in Paleocene or younger rocks, so they are presumably contaminants here. The paleoenvironment is interpreted as nonmarine based on a lack of dinocysts.

A second sample, at 2917.1 m, contains miospores only, including *Callialasporites dampieri* and *Vitreisporites pallidus* (both pollen), and *Camarozonosporites* sp. (a spore). Nøhr-Hansen et al. (2016) placed the last or youngest occurrence of *Callialasporites dampieri* at the top of the Aptian. Based on this evidence, the present authors date this sample as Aptian. The absence of dinocysts indicates that the paleoenvironment was nonmarine.

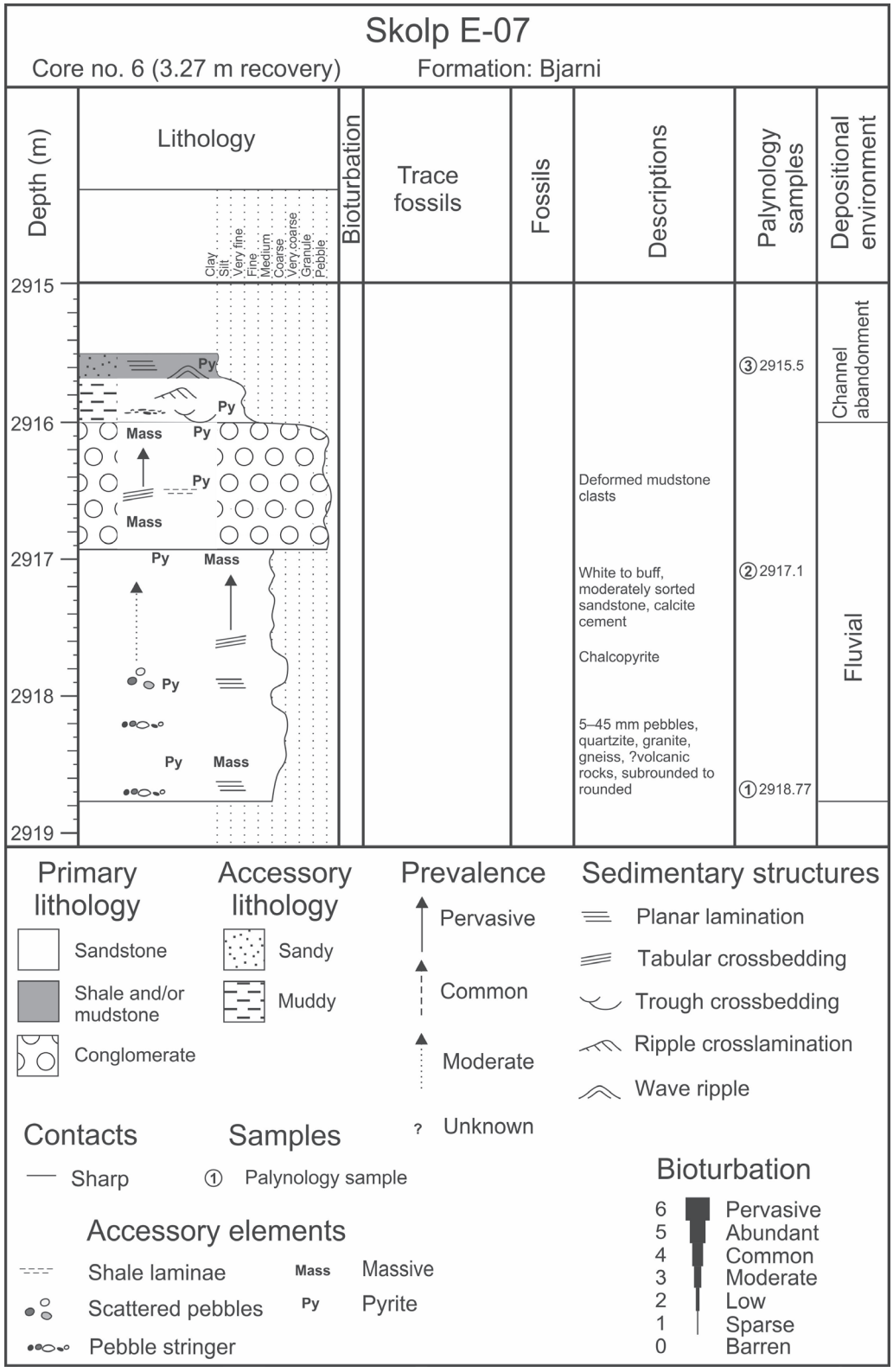


**Figure 78.** Log of core 6, Skolp E-07.

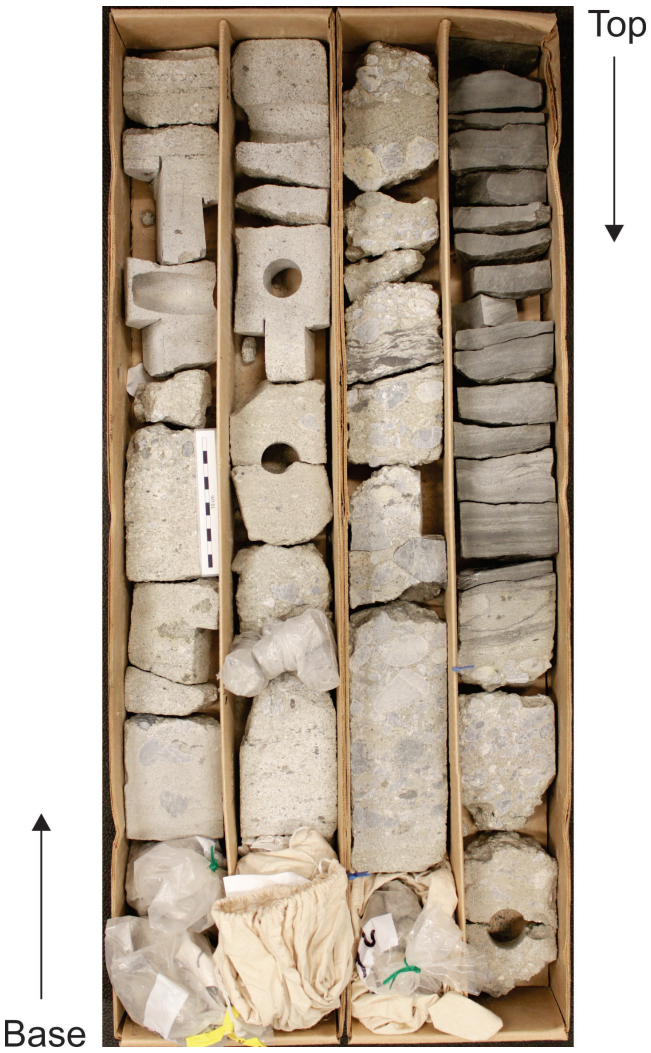


**Figure 79.** Photograph of core 6, Skolp E-07. Scale bar = 10 cm. NRCan photo 2019-488. Photograph by L.T. Dafoe.

The highest sample, at 2915.5 m, was barren, but contained high amounts of vitrinite and carbonized wood. The authors cannot speculate on the age, but the paleoenvironment is assumed to be nonmarine.

*Summary*

Williams (1980) considered the interval of the Bjarni Formation from which this core derives as within the (?) Barremian–Aptian; Nøhr-Hansen et al. (2016) considered it Albian–Cenomanian (Nøhr-Hansen et al., 2016). The present study supports that it is Aptian. Fluvial interpretation from the core is supported by the nonmarine interpretation from palynomorphs. The interpretation is also consistent with previous work by Miller and D'Eon (1987), who suggested a nonmarine, meandering fluvial-alluvial succession; and by Price and Thorne (1978), who suggested a continental origin.

### *Core 7: gneiss (2988–2992 m)*

*Core description and interpretation*

The lowermost core of Skolp E-07, from 2988 m to 2992 m, recovered 3.96 m of gneiss (Fig. 81, 82). This gneiss is variably banded and primarily consists of mafic bands (Fig. 83). Quartz-filled fractures are also present (Fig. 83a). The material is described as migmatitic quartz diorite gneiss correlated with the onshore Nain Province, and U-Pb age dating places the magmatic precursor at about 3213 (+21/-3.6) Ma (Wasteneys et al., 1996). Possible anatectic melting may have occurred at 2552 (+3.6/-21) Ma and regional cooling at 2504.3 ± 3.6 Ma, postdating migmatization (Wasteneys et al., 1996).

## Snorri J-90

Snorri J-90, located in the northern part of the Hopedale Basin, on the Labrador Shelf (Fig. 1), was drilled in 1975 and re-entered in 1976. The well, which has a total depth of 3209.8 m, was planned to test the informally named Bjarni and Cartier sandstone units (Eastcan Exploration Ltd., 1975b). Two core intervals were recovered: one within Precambrian gneiss and the other within the Gudrid Formation. The upper core from the Gudrid Formation is described below.

### *Core 1: bioturbated sandstone (2496.04–2504.54 m)*

*Core description and interpretation*

The interval 2496.04–2504.54 m is sampled by core 1 within the Gudrid Formation and comprises bioturbated, very fine-grained sandstone (Fig. 84). The core can be divided into two facies based on the trace-fossil suites and general degree of bioturbation (Fig. 85).

The lowermost facies is a very fine-grained, light brown to buff sandstone (Fig. 86). Sedimentary structures are common and include tabular crossbedding (Fig. 86a), planar laminations (Fig. 86a, c, e, f), and lesser current-ripple crosslaminations (Fig. 86c), as well as rare trough crossbedding (Fig. 86b), combined flow ripples (Fig. 86c), and wavy parallel laminations (Fig. 86d, f). Thin mudstone laminae and mudstone rip-up clasts (Fig. 86a) are sometimes present, as well as organic detritus or thin, organic-rich laminae (Fig. 86c). Pyrite, coal fragments, micaceous minerals, and soft-sediment deformation are also rarely observed. Overall, the sandstone is quartz-rich and clean with some orange (possibly siderite) grains and is noncalcareous. The degree of bioturbation varies from unbioturbated or scarcely bioturbated (5%) to pervasively bioturbated (70–80%). Trace fossils include moderately numerous to common *Helminthopsis*, moderately numerous *Chondrites*, scattered *Planolites*, *Palaeophycus*, *Phycosiphon*, *Schaubcylindrichnus*,

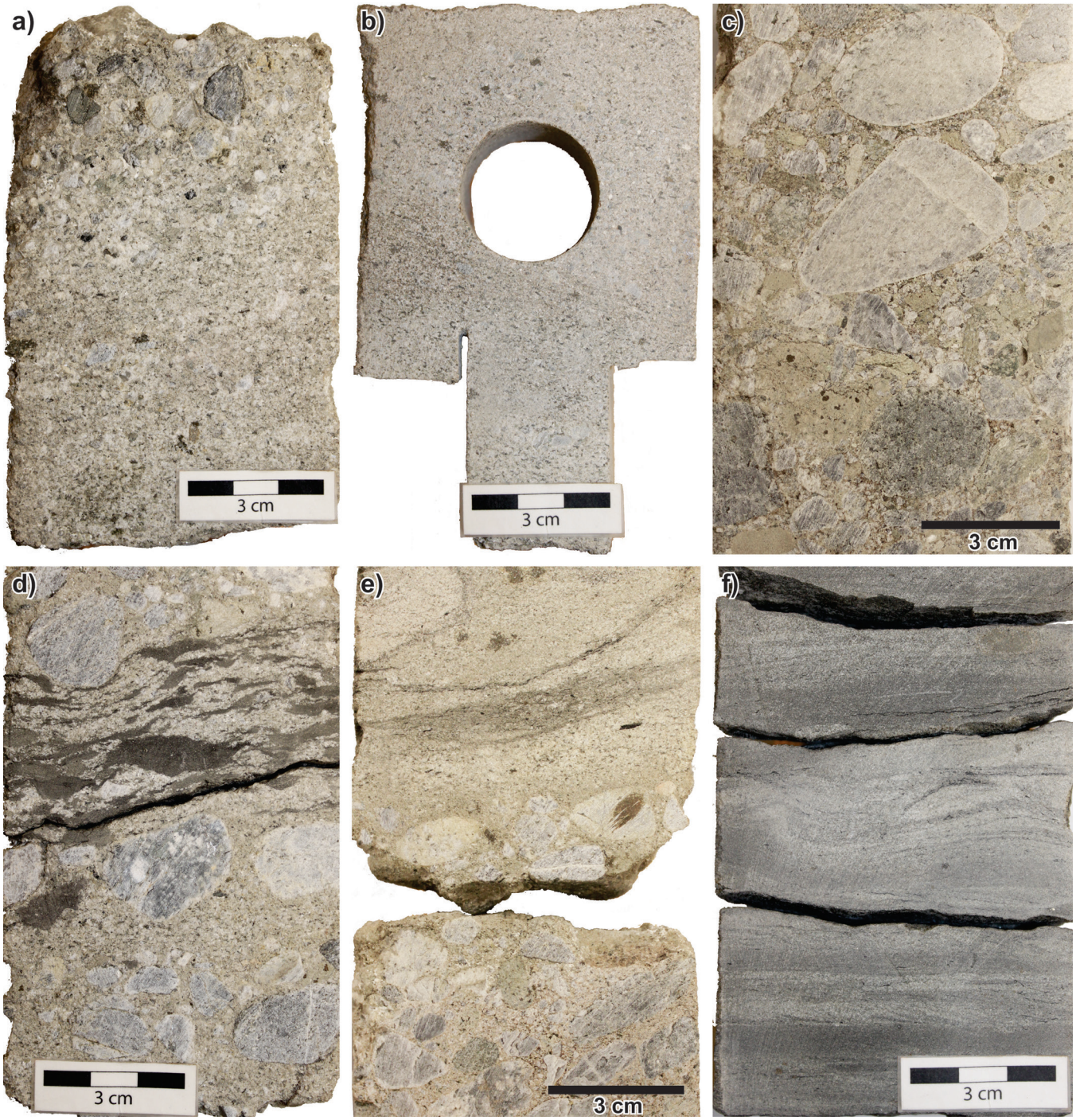


**Figure 80.** Photographs of core 6, Skolp E-07. **a)** Buff, poorly sorted sandstone, and **b)** crossbedded sandstone (dipping from left to right). NRCan photo 2018-489, 2019-490. **c)**, **d)** Matrix-supported conglomerate with large quartzite pebbles and mudstone rip-up clasts (in Fig. 80d). NRCan photo 2019-491, 2019-492. **e)** The transition from conglomerate into the fine-grained uppermost facies. NRCan photo 2019-493. **f)** The fine-grained facies with current ripple crosslamination and a possible wave ripple in the centre of the core. NRCan photo 2019-494, All photographs by L.T. Dafoe.

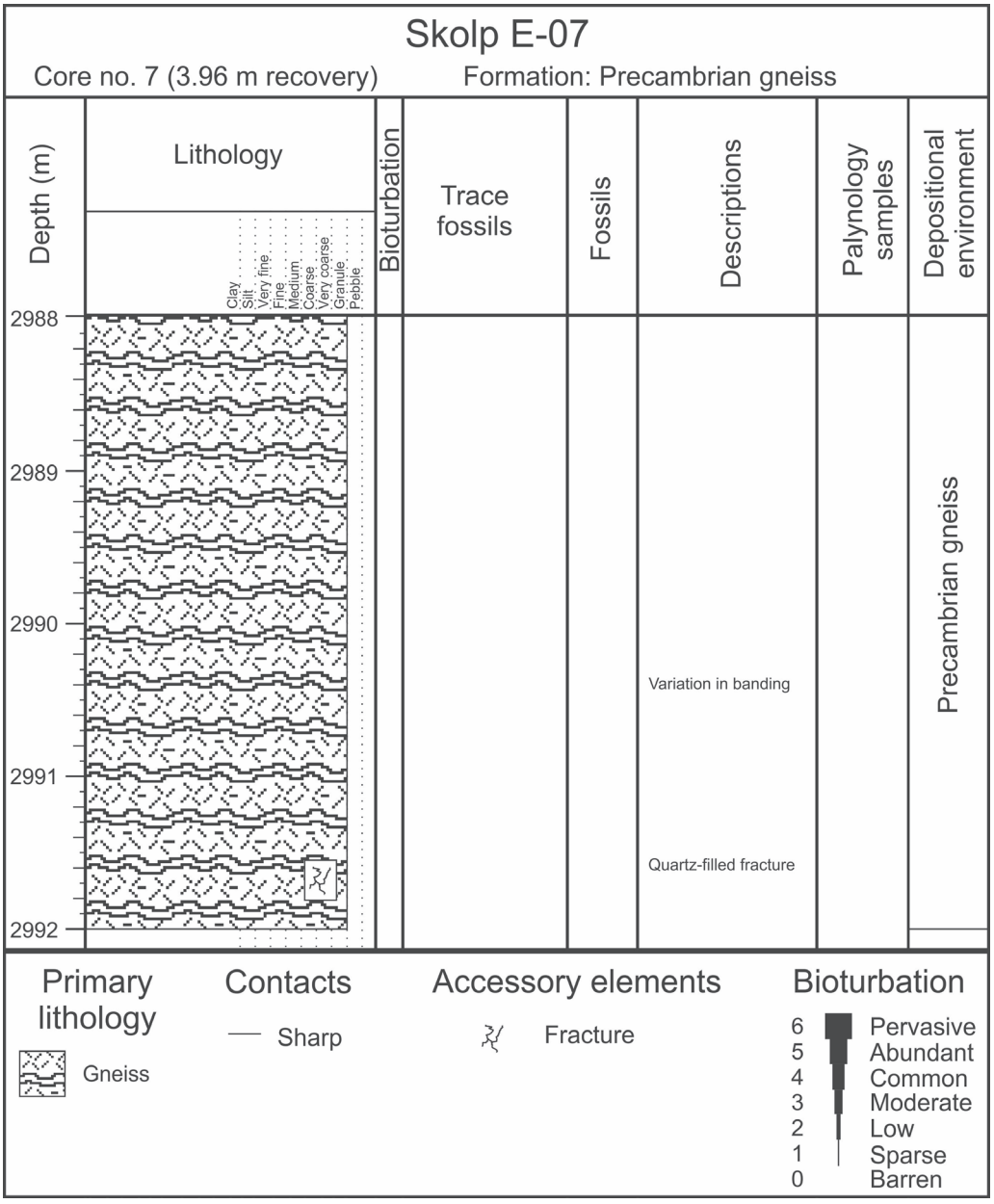


**Figure 81.** Log of core 7, Skolp E-07.


**Figure 82.** Photograph of core 7, Skolp E-07, showing the Precambrian gneissic basement rock and variation in banding. NRCan photo 2019-495. Photograph by L.T. Dafoe.

*Asterosoma*, *Thalassinoides*, and *Rhizocorallium,* and rare *Skolithos*. Notably, scattered *Macaronichnus* were observed only from discrete intervals (Fig. 86c, e) and at the gradational transition to the overlying facies.

The uppermost facies also consists of buff, very fine-grained sandstone, but has more common bioturbation and a prevalence of the trace fossil *Macaronichnus* (Fig. 87) like the few seen in the lowermost facies. Sedimentary structures include planar laminations (Fig. 87b), lesser tabular and trough crossbedding (Fig. 87a, b), and rare, wavy parallel laminations. Organic detritus and coal fragments are scattered throughout the facies, as well as millimetre-scale siderite nodules. Pyrite and mudstone rip-up clasts are rare. Bioturbation ranges from rare unbioturbated intervals to 20–80% bioturbation. Trace fossils are predominated by *Macaronichnus* and *Helminthopsis* with moderate occurrences of *Asterosoma* and *Spirophyton* (Fig. 87g, h, i). Other traces include scattered *Planolites*, *Palaeophycus*, *Rhizocorallium*, *Cylindrichnus*, and *Arenicolites* (Fig. 87). *Macaronichnus* are primarily horizontal and relatively consistent at 4 mm in diameter, with some intervals characterized by smaller, 2 mm diameter burrows (Fig. 87c, d). These traces are preferentially infilled with quartzose sand grains and some appear to have a mantled structure (Fig. 87e; as in *Macaronichnus simplicatus*) and even possible backfilling. *Spirophyton* are uncommon traces and fit the description presented in Miller (1991) whereby whorls may be curved upward, forming a dish-like shape to the lamina. Lamellae are rarely visible due to the thin nature of lamina and the vertical axial shaft. The examples from Snorri J-90 have clear axial shafts often infilled with the very fine-grained sandstone-host substrate (Fig. 87h). Whorls are highly irregular and sometimes dish-shaped and primarily curve upward, although some downward-curving whorls are also noted (Fig. 87g, h). The whorls are muddy and thin (millimetres or less in scale). Traces can be 8 cm in height and vary in their width and mudstone content, perhaps as a result of variation in sedimentation rates. The top of the core is heavily reworked by *Macaronichnus* with vertical structures that appear to be *Cylindrichnus* or perhaps rhizoliths with carbonaceous linings (Fig. 87i).

The lowermost facies in core 1 of Snorri J-90 is characterized by moderate degrees of bioturbation with sedimentary structures suggestive of unidirectional flow. Subtle wave-rippled strata combined with planar to low-angle laminations (possibly hummocky cross-stratification) suggest possible marine deposition. Trace fossils are dominated by grazing traces (*Helminthopsis*) and other deposit-feeding to dwelling structures dominated by marine forms. This suite is characteristic of a marine, archetypal *Cruziana* Ichnofacies with only moderate diversity and relatively low abundance,

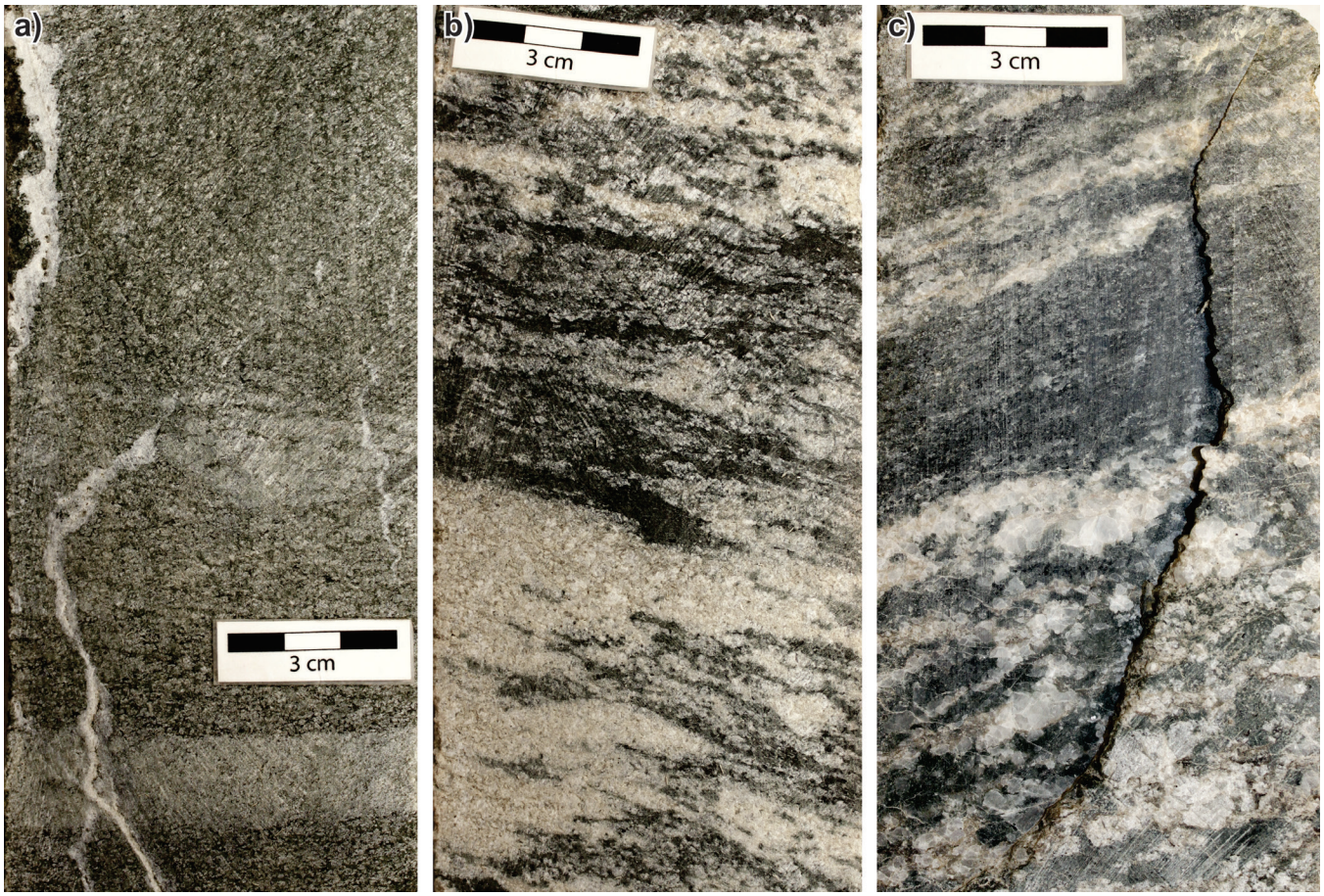


**Figure 83.** Photographs of the gneissic basement rock from core 7 of Skolp E-07, showing mostly mafic mineral banding, as well as **a)** fractures, **b)** more localized felsic-rich bands, and **c)** a coarse mineral texture. NRCan photo 2019-496, 2019-497, 2019-498, respectively. All photographs by L.T. Dafoe.

suggesting some environmental stress. Carbonaceous mudstone laminae and beds suggest possible hyperpycnal flows, whereas crossbedding indicates a high-energy setting. Some unbioturbated mudstone indicates rapid sedimentation, as do soft-sediment deformation features. A lack of vertical trace fossils of suspension feeding and/or dwelling trace makers typical of a high-energy shoreface indicates that suspended sediment concentrations may have been high. The overall low abundance and diversity suggest that salinity may have been reduced and that this facies reflects a brackish setting. Based on the sedimentary structures, presence of possible hyperpycnal mud deposition, and the trace-fossil suite, this facies likely represents storm-dominated, delta-front deposition.

The overlying facies is lithologically very similar, but shows minimal crossbedding and more abundant bioturbation. Coal fragments and organic detritus still attest to a shoreline-proximal setting; however, the current regime is quieter, with planar lamination dominating the succession where bioturbation is slightly reduced. The trace-fossil suite is dominated by *Macaronichnus*, which is often found within high-energy nearshore settings (Pemberton et al., 2001). *Spirophyton* has been reported from similar fluvial-marine transitions where the trace maker was opportunistic in colonizing brackish environmental settings (Miller and Johnson, 1981; Miller, 1991). The overall trace-fossil suite is more abundant and diverse than the underlying facies, suggesting a reduction in the overall energy of the depositional setting. The trace-fossil suite is consistent with an archetypal *Cruziana* Ichnofacies with very rare vertical traces of inferred suspension feeders. The predominance of *Spirophyton* and association of this trace to opportunistic colonization, as well as the overwhelming presence of *Macaronichnus,* suggest continued environmental stress. Again, the lack of vertical traces in sandy, proximal substrate suggests that suspended sediment, sedimentation rates, and/or reduced salinity were likely environmental factors. This facies is interpreted to represent a distal delta-front setting, indicating a slight rise in relative sea level relative to the underlying facies or delta-lobe switching and reduced influx of sand. The presence of possible rhizoliths at the top of the core may indicate a return to shallower water, with near-subaerial conditions allowing for colonization by plants in a tidal or nearshore setting. This type of deltaic setting is most consistent with a storm-dominated environment where stresses

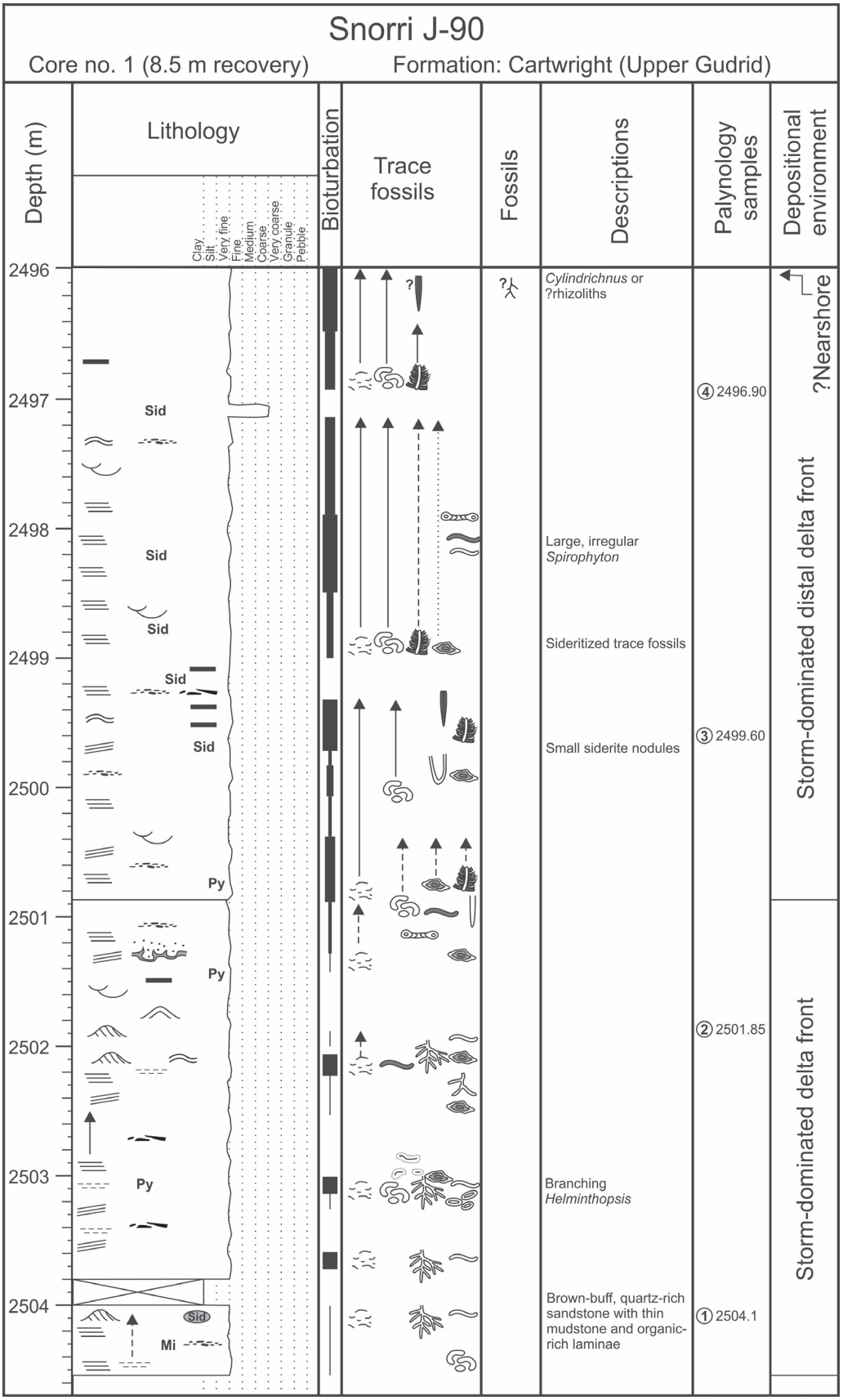


**Figure 84.** Log of core 1, Snorri J-90. Note the distinct change in facies between the lower and upper halves of the core.

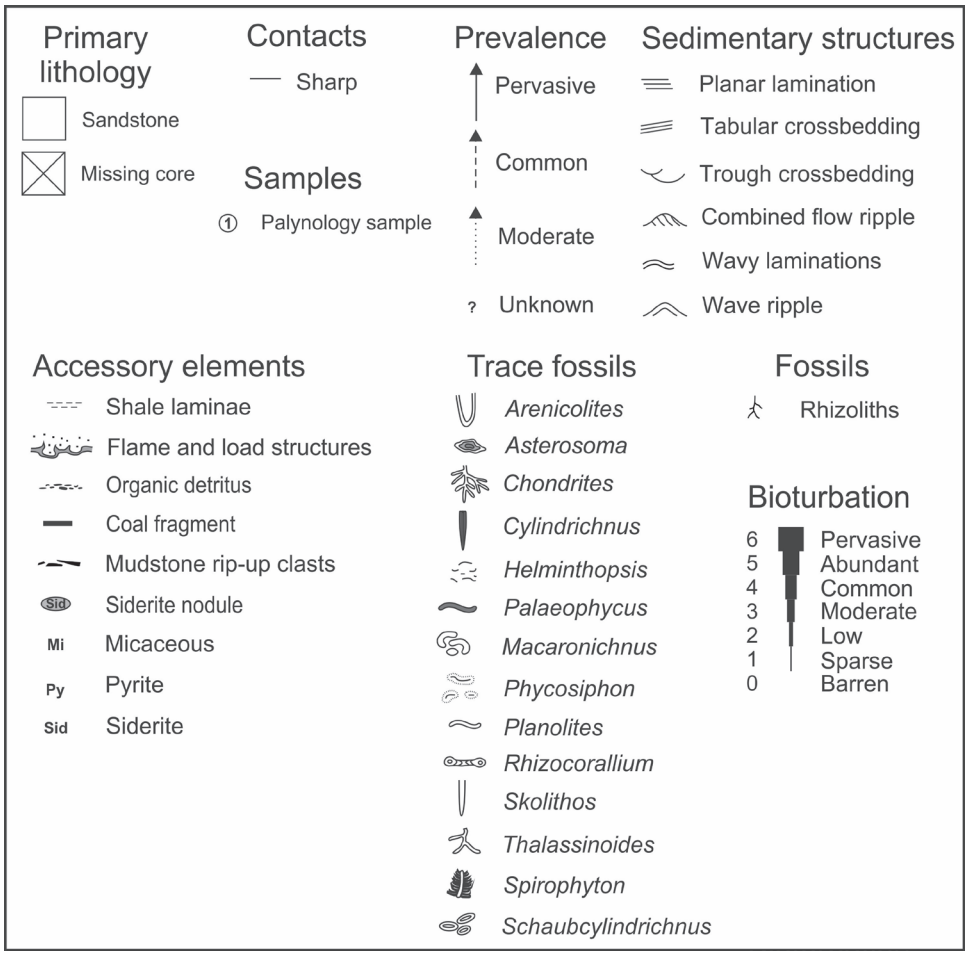


**Figure 84.** (cont.)

of fluvial discharge are mitigated, and unbioturbated intervals represent thick storm deposits that are interbedded with fair-weather, bioturbated intervals.

## *Palynology*

Four samples from core 1 were processed for palynomorphs. The bottommost sample, at 2504.1 m, has several dinocysts, including *Apectodinium homomorphum*, *Apectodinium parvum*, *Apectodinium quinquelatum*, *Areoligera gippingensis*, *Areoligera* cf. *gippingensis*, *Glaphyrocysta divaricata*, and *Glaphyrocysta ordinata*. Also present are the pollen *Betulaepollenites* and *Pinuspollenites*, and fragments of the free-floating, freshwater fern *Azolla*. Harland (1979) restricted *Apectodinium parvum* to the late Thanetian; however, Nøhr-Hansen et al. (2016) placed the last or youngest occurrence within the basal Ypresian. The present authors follow Harland and hence consider the age of this sample to be late Thanetian. Based on the presence of *Apectodinium* specimens and the dominance of miospores over dinocysts, the paleoenvironment is interpreted to be inner neritic. The occurrence of several specimens of *Apectodinium* has significance for interpreting climatic conditions. Crouch et al. (2001) showed that the earliest appearance of *Apectodinium*-dominated assemblages seems to be synchronous on a global scale, with one occurring at the Paleocene–Eocene Thermal Maximum (PETM). This supports dating of the samples from this core by the present authors as late Thanetian to basal Ypresian.

Although miospores, including *Trudopollis*, dominate the palynomorph assemblages in the sample from 2501.85 m, excellent dinocyst markers occur. These include *Apectodinium paniculatum*, *Apectodinium parvum*, *Apectodinium quinquelatum*, and *Areoligera gippingensis*. Harland (1979) restricted both *Apectodinium paniculatum* and *Apectodinium parvum* to the late Thanetian; however, Nøhr-Hansen et al. (2016) placed the last or youngest occurrences of both species within the basal Ypresian. *Chatangiella victoriensis*, *Hystrichodinium* sp., and *Stiphrosphaeridium anthophorum,* which are also present, are reworked Late Cretaceous species. They demonstrate erosion of rocks of this age somewhere on the Labrador margin and transportation into the vicinity of Snorri J-90. Although there is a slight contradiction, the age of this sample is considered to be late Thanetian, based on the two *Apectodinium* species. The paleoenvironment is interpreted as inner neritic.


**Figure 85.** Photographs of core 1, Snorri J-90. Scale bars = 10 cm. NRCan photos 2019-499, 2019-500, 2019-501, 2019-502, 2019-503. All photographs by L.T. Dafoe.

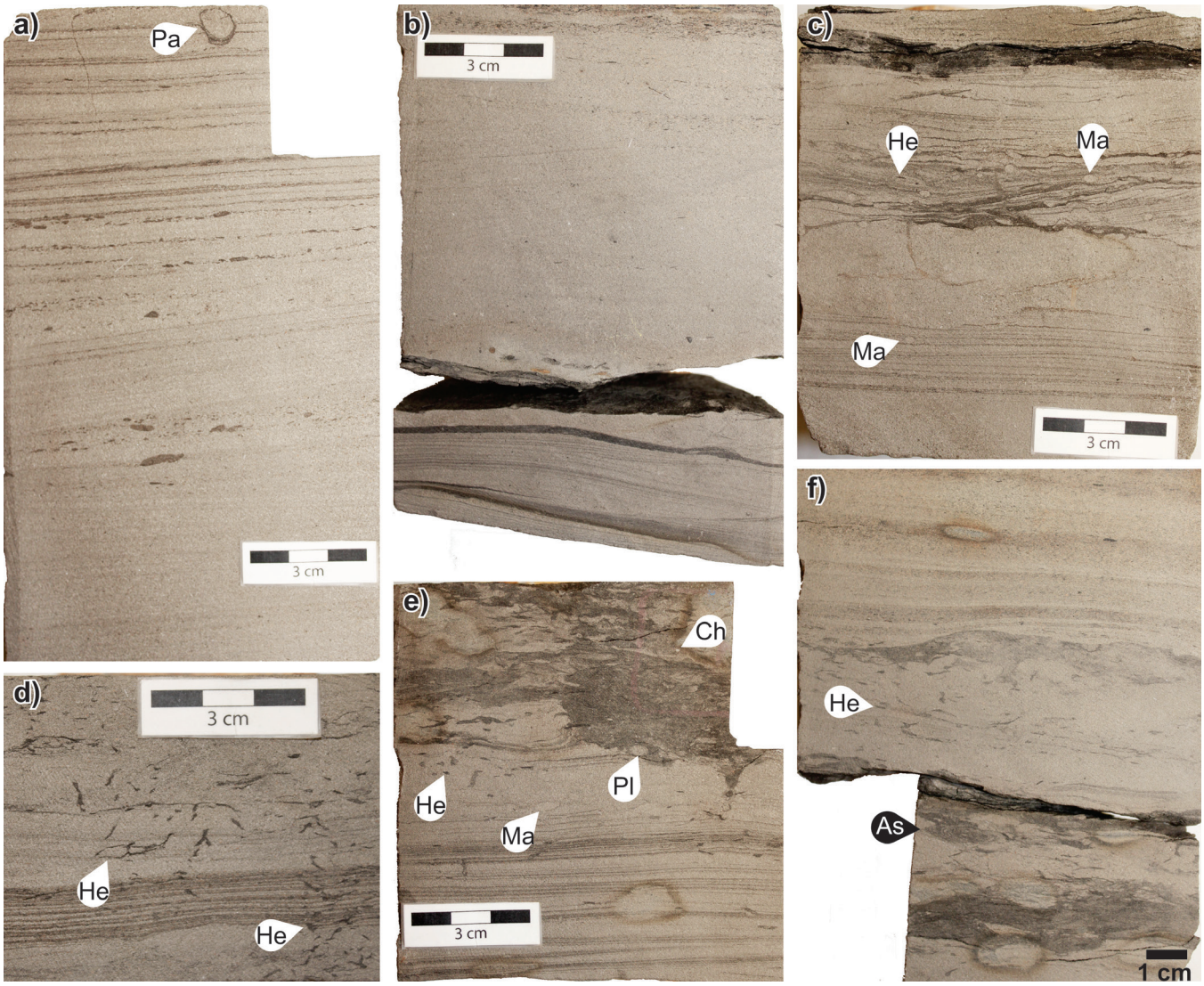


**Figure 86.** Photographs of core 1, Snorri J-90, showing the basal facies in the core: variably bioturbated, very fine-grained sandstone. **a)** Planar-laminated to low-angle tabular crossbedded sandstone with thin, organic-rich, muddy laminae and small mudstone rip-up clasts. *Palaeophycus* (Pa) at the top of the core. NRCan photo 2019-504. **b)** Trough crossbedded sandstone above wave-rippled sandstone with mudstone drapes and small rip-up clasts. NRCan photo 2019-505. **c)** Planar to wavy laminated sandstone with a carbonaceous mudstone bed. Trace fossils include small *Macaronichnus* (Ma) and *Helminthopsis* (He). NRCan photo 2019-506. **d)** *Helminthopsis* in a wavy parallel-laminated sandstone near the top of the facies. NRCan photo 2019-507. **e)** Planar-laminated sandstone with *Helminthopsis* (He), *Planolites* (Pl), *Macaronichnus* (Ma), and *Chondrites* (Ch). NRCan photo 2019-508. **f)** Bioturbated muddy sandstone overlain by low-angle crossbedded sandstone. Traces include *Helminthopsis* (He) and *Asterosoma* (As). NRCan photo 2019-509. All photographs by L.T. Dafoe.

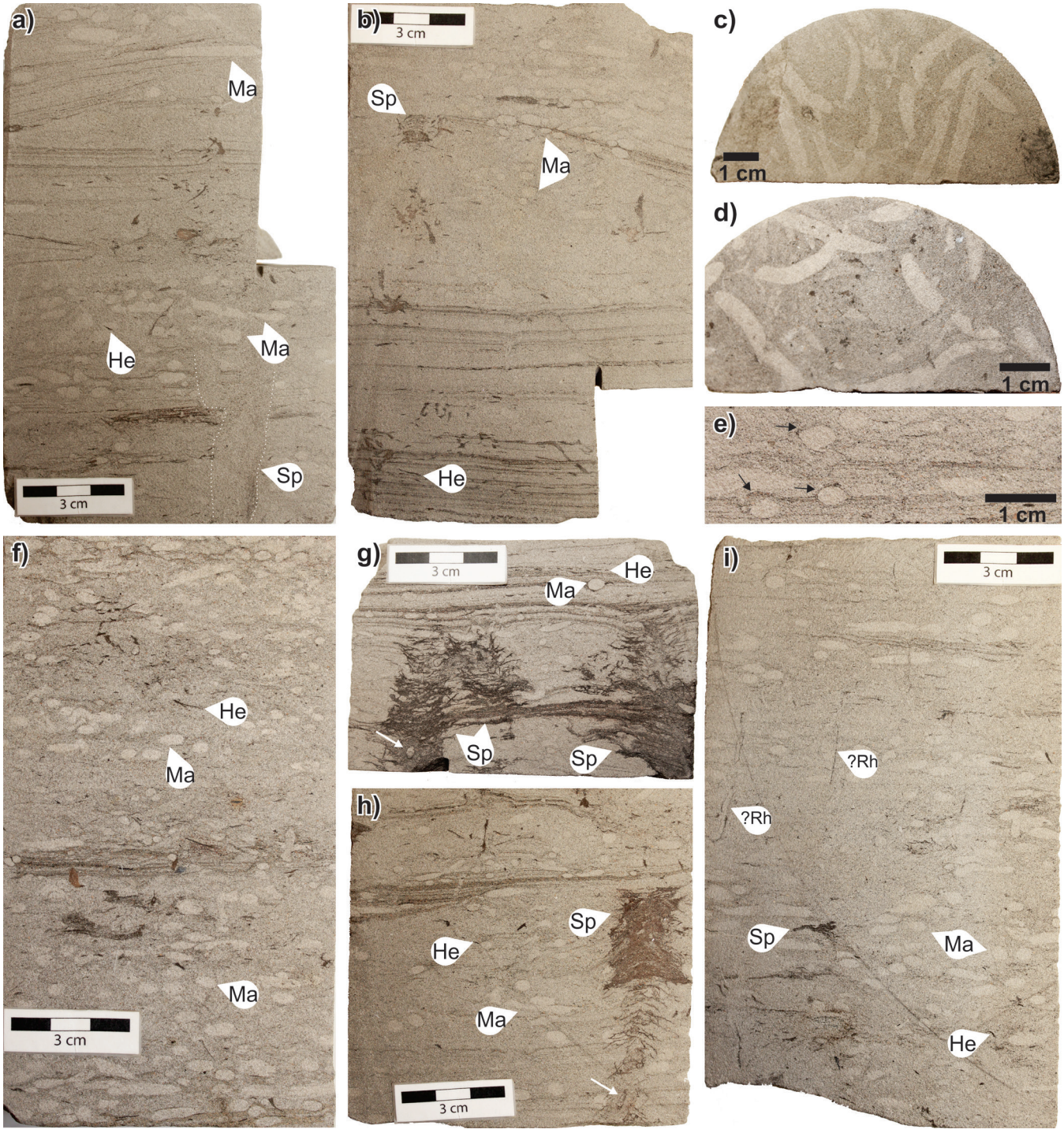


**Figure 87.** Photographs of core 1, Snorri J-90, showing the uppermost facies consisting of bioturbated sandstone. **a)** Trough cross-bedded sandstone characterized by *Macaronichnus* (Ma), *Helminthopsis* (He), and a possible *Spirophyton* (Sp) trace indicated by the white dotted line. NRCan photo 2019-510. **b)** Planar-laminated to trough crossbedded sandstone with subtle *Macaronichnus* (Ma), small *Spirophyton* (Sp), and *Helminthopsis* (He). NRCan photo 2019-511. **c**), **d)** *Macaronichnus* in plan view on the slabbed core showing the meandering and predominantly horizontal burrow fabric with some false branching. NRCan photo 2019-512, 2019-513, respectively. **e)** Close-up of *Macaronichnus*, showing mantling by the darker and/or more organic-rich material in the sandstone. NRCan photo 2019-514. **f)** Abundant *Macaronichnus* (Ma) with *Helminthopsis* (He). NRCan photo 2019-515. **g)** Well developed *Spirophyton* (Sp) with the axial shaft indicated by a white arrow. *Macaronichnus* (Ma) and *Helminthopsis* (He) are also present. NRCan photo 2019-516. **h)** Another *Spirophyton* (Sp) with axial shaft indicated by a white arrow. Variously sized *Macaronichnus* (Ma) and *Helminthopsis* (He). NRCan photo 2019-517. **i)** Abundant *Macaronichnus* (Ma) with *Helminthopsis* (He), poorly developed *Spirophyton* (Sp) and vertical structures that could represent rhizoliths (?Rh) or possible *Cylindrichnus*. NRCan photo 2019-518. All photographs by L.T. Dafoe.

Recovery is poor in the sample from 2499.60 m. The assemblage includes the pollen *Alnipollenites verus*, *Betulaepollenites*, *Caryapollenites imparalis*, and *Pinuspollenites*. Dinocysts present are *Areoligera gippingensis* and *Glaphyrocysta ordinata*, the latter species having its last or youngest occurrence in the early Lutetian according to Bujak and Mudge (1994). Nichols and Ott (1978) considered *Caryapollenites imparalis* to be an index species for their Paleocene P4 zone in Wyoming. This, coupled with the stratigraphic range of *Areoligera gippingensis* as outlined above, suggests a later Paleocene to early Eocene age. The paleoenvironment is neritic.

The topmost sample at 2496.9 m contains the pollen *Abiespollenites*, *Pinuspollenites*, and *Pterocaryapollenites*. The dinocysts *Areoligera* cf. *medusettiformis* and *Areoligera* cf. *gippingensis* were also recorded. Jolley (1992) described the species *Areoligera gippingensis* from the late Paleocene of the British Isles; however, he did not include in synonymy the identical form that Williams and Downie (1966) described from the Ypresian of southern England and which they identified as *Areoligera* cf. *medusettiformis*. Williams et al. (2004) gave the stratigraphic range of *Areoligera gippingensis* as late Selandian to mid-Thanetian. Based on this range and the findings of Williams and Downie (1966), the present authors have concluded that the age of this sample must be latest Selandian to Ypresian. The dominance of the miospores indicates that the paleoenvironment was inner neritic.

### *Summary*

The Snorri J-90 core 1 of the Gudrid Formation sampled a very thin (about 20 m) sandstone unit that, based on previous analyses of cuttings, is late Paleocene (Thanetian) to basal Ypresian (Early Eocene) with the basal Ypresian beginning around 2499 m (Williams, 1979b, 2007b). The present study results indicate a late Thanetian to earliest Ypresian age, which is consistent with the findings from cuttings. Williams (2007b) reported the paleoenvironment of this section to be inner to outer neritic, passing to outer neritic at 2499.67 m; Ainsworth et al. (2014) considered the entire interval encompassed by the core to be upper bathyal. In contrast, the present authors' interpretation from the core indicates a storm-dominated delta-front to distal delta-front setting that is relatively consistent with the inner-neritic interpretation from the palynomorphs. To explain the discrepancy with previous studies, the attenuated nature of the sandstone interval sampled by core 1 could result in cavings from overlying deep-water units masking the shallow nature of the Gudrid Formation when studied by cuttings.

## Tyrk P-100

The Tyrk P-100 well, located in the southern part of the Hopedale Basin on the Labrador Shelf (Fig. 1), was drilled to test the Lower Cretaceous sequence seen in nearby wells and to determine if Paleozoic strata were present and whether they held any hydrocarbon potential (Total Eastcan Exploration Ltd., 1979c); total depth was 1739 m. Two core intervals were recovered: one within Precambrian granite and the other within the Gudrid Formation (as defined by Moir, 1989).

### *Core 1: medium grey shale (1185–1190 m)*

#### *Core description and interpretation*

The upper core (core 1) from Tyrk P-100 lies within the Gudrid Formation of Moir (1989), but the interval has also been interpreted as part of the Markland Formation (C-NLOPB, 2007). The core sampled 4.5 m of shale between 1185 m and 1190 m with about 0.5 m of missing core (Fig. 88, 89), and comprises medium grey shale that is relatively homogeneous, friable, and consistently planar laminated (Fig. 90). Very fine-grained sandstone beds are dispersed throughout the core, but are rare, as are organic detritus fragments and siderite (Fig. 90c). Pyrite is more commonly observed and is well disseminated. One medium-grained sandstone bed was noted and the topmost part of the core consists of rubbly material. One wavy laminated bed was observed and there is a low degree of overall bioturbation; however, between 1187 m and 1186 m, intermittent bioturbation (5–80%) occurs where siltier and sandier beds are present (Fig. 90b). Possibly more bioturbation is present than can be seen in a homogeneous shale lithology. Trace fossils are thus rare and include primarily *Planolites* and lesser *Helminthopsis* and rare *Schaubcylindrichnus* (Fig. 90b, d).

The fine-grained nature of the sediment and presence of marine trace fossils suggest either a shelf or shallow-marine, quiet-water (embayment or lagoonal) setting. The trace-fossil suite is low in diversity and abundance and represents a stressed archetypal expression of the *Cruziana* Ichnofacies, which may be related to the lack of lithological contrast or stressful environmental conditions such as reduced salinity. The lack of wave-formed structures suggests either deposition beyond the storm wave base consistent with distal outer-shelf deposition or low overall wave energy in a restricted marine bay.

#### *Palynology*

Four samples from core 1 were processed for palynomorphs. The bottommost sample, at 1189 m, has an abundance of *Pinuspollenites*. Other bisaccate taxa are

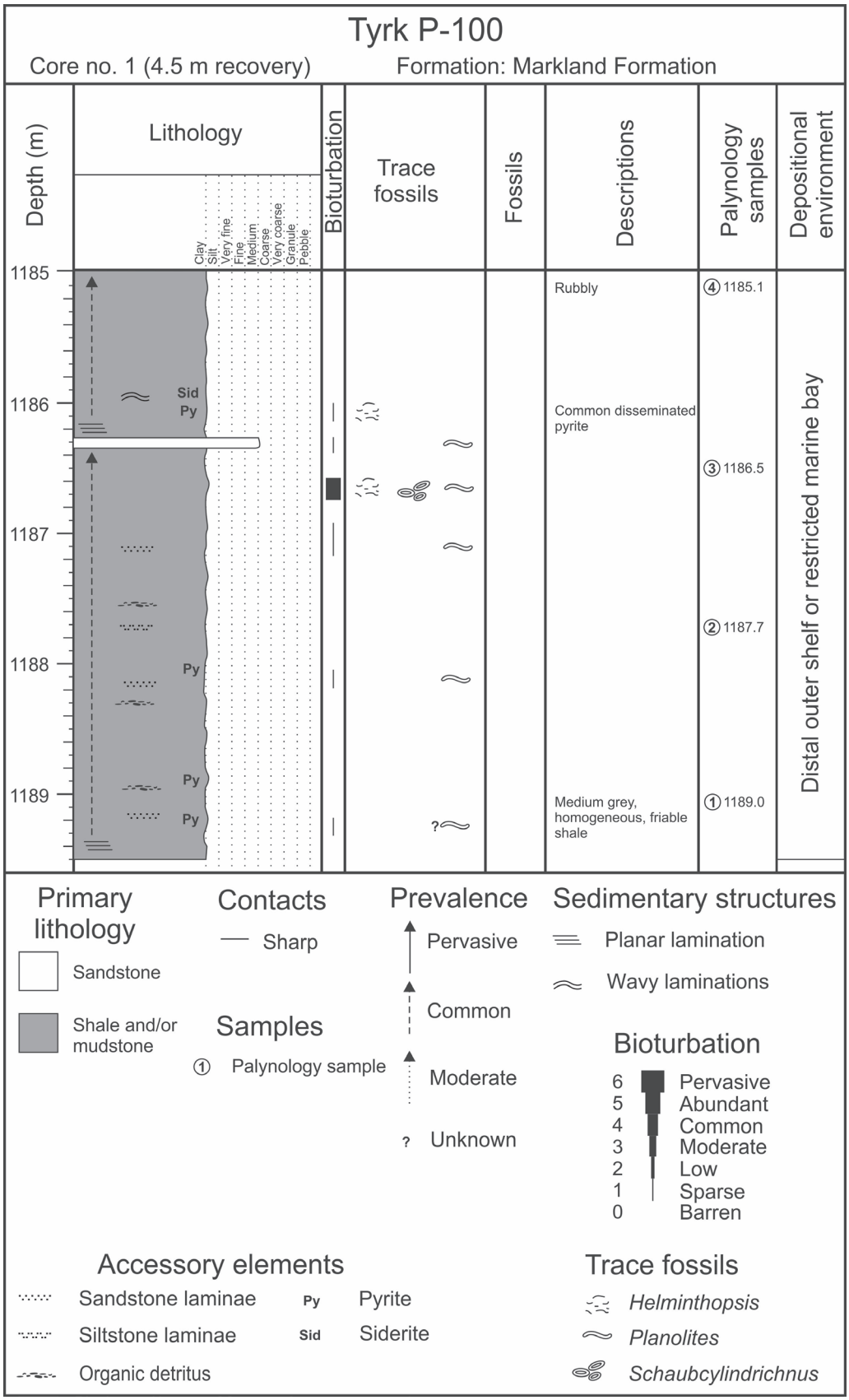


**Figure 88.** Log of core 1, Tyrk P-100.


**Figure 89.** Photographs of core 1, Tyrk P-100. Scale bar = 10 cm. NRCan photos 2019-519, 2019-520, 2019-521. All photographs by L.T. Dafoe.

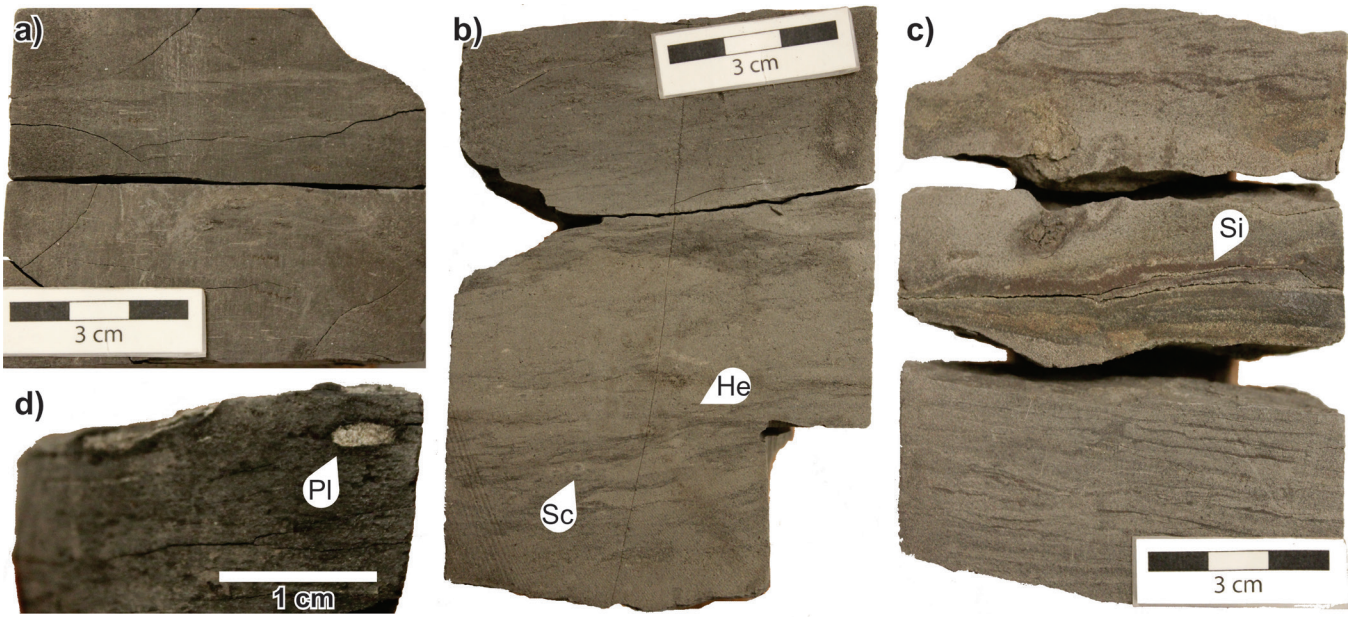


**Figure 90.** Photographs of core 1, Tyrk P-100. **a)** Homogeneous, laminated, medium grey shale. NRCan photo 2019-522. **b)** Bioturbated silty mudstone with small *Schaubcylindrichnus* (Sc) and *Helminthopsis* (He). NRCan photo 2019-523. **c)** Laminated silty mudstone with siderite (Si) and some wavy parallel laminations possibly related to subsequent diagenesis. NRCan photo 2019-524. **d)** *Planolites* filled with medium-grained sandstone from the overlying thin sandstone bed. NRCan photo 2019-525. All photographs by L.T. Dafoe.

*Abiespollenites*, *Piceapollenites*, *Rugubivesiculites convolutus*, *Rugubivesiculites reductus,* and *Rugubivesiculites rugosus*. Trilete spores include *Distaltriangulisporites irregularis* and *Retitriletes* sp. Singh (1971) cited the stratigraphic range of *Distaltriangulisporites irregularis* as middle to late Albian. The present authors regard the presence of *Distaltriangulisporites irregularis* and *Rugubivesiculites* to denote a middle to late Albian age. The absence of dinocysts indicates a nonmarine paleoenvironment.

Miospores in the sample from 1187.7 m include the bisaccate pollen *Pinuspollenites*, *Rugubivesiculites convolutes, Rugubivesiculites reductus*, *Rugubivesiculites rugosus*, and *Vitreisporites* sp. Singh, 1971. One significant trilete spore is *Plicatella jansonii*, which Singh (1971) considered to have a stratigraphic range of Barremian–Albian. Also present are the trilete spores *Appendicisporites* sp. and *Cicatricosisporites hallei*. As the sample also contains species of *Rugubivesiculites*, it has to be considered as middle to late Albian and nonmarine, the latter conclusion based on the absence of dinocysts (Nøhr-Hansen et al., 2016).

The sample at 1186.5 m contains the bisaccate pollen *Rugubivesiculites convolutus*, *Rugubivesiculites rugosus, Vitreisporites pallidus*, and *Vitreisporites* sp. (Singh, 1971). One of the few trilete spores is *Costatoperforsporites foveolatus*, which Singh (1971) considered to be late Aptian to Albian. Therefore, the age of the sample has to be considered as middle to late Albian, and the absence of dinocysts indicates a nonmarine paleoenvironment.

Sample four at 1185.10 m contains a rich miospore assemblage with abundant *Pinuspollenites* and several *Rugubivesiculites rugosus*. Also present are *Rugubivesiculites reductus*, *Cicatricosisporites subrotundus*, *Costatoperforosporites fistulosus*, *Tricolpites crassimurus*, and *Verrucosisporites*? sp. As noted earlier, Nøhr-Hansen et al. (2016) plotted the first or oldest occurrence of *Rugubivesiculites rugosus* at about the base of the middle Albian and the last or youngest occurrence of the genus within the Turonian. Perhaps of even greater significance is that Nøhr-Hansen et al. (2016) noted that *Rugubivesiculites rugosus* is common in the late Albian. Based on the literature, Singh (1971) considered *Tricolpites crassimurus* to have a stratigraphic range of Albian–Coniacian. Singh (1971) also restricted *Cicatricosisporites subrotundus* to the Albian and *Costatoperforosporites fistulosus* to the Aptian–Albian. Based on the above evidence, this sample is considered to be late Albian. From the absence of dinocysts, the suggested paleoenvironment was nonmarine.

### *Summary*

According to previous work involving cuttings samples, this interval falls in the early–middle Albian (Bujak Davies Group, 1989h), late Albian–Cenomanian (Robertson Research Canada Ltd., 1979), and Albian (Caro et al., 1980). A middle to late Albian age was confirmed by recent analyses of the conventional core with late Albian in the uppermost sample. Accordingly, the core should be considered as part of the Bjarni Formation rather than the Gudrid or Markland formation. Previous interpretations of the depositional environment include transitional (Robertson Research Canada Ltd., 1979), continental (Caro et al., 1980), and distal turbidite deposits in a bathyal setting (Miller and D'Eon, 1987). A nonmarine setting is suggested by the present study's palynological analyses based on the lack of dinocysts. Combined with the presence of a limited marine trace-fossil suite, the palynological evidence suggests a nearshore, but brackish depositional setting. Therefore, the lack of sand and wave reworking is consistent with a restricted marine bay or lagoonal setting.

## *Core 2: granite (1736–1738 m)*

### *Core description and interpretation*

Core 2 was recovered from the base of Tyrk P-100 and is composed of granite (Fig. 91, 92) dominated by orthoclase feldspar and a significant proportion of mafic minerals. Only 2 m were recovered from the 1736–1739 m interval. The texture is phaneritic with mineral grains in the millimetre to centimetre range (Fig. 92b). In places, elongate orthoclase feldspar crystals occur, but some alteration (metamorphism) may have taken place. Fractures are present and are typically filled with pyrite or, less commonly, with quartz (Fig. 92b, c). In places, some 'void' spaces appear to have been filled with pyrite (Fig. 92c), but it is unclear if these voids reflect weathering of exposed basement material. It appears that this granitic interval extends above the cored section of the well, up to 1706 m (Moir, 1989). Weathering at this depth into the granite is unlikely, but the pyrite is most likely diagenetic in nature due to hydrothermal fluids flowing within fractures. This cored interval was interpreted as Precambrian (Moir, 1989). Wasteneys et al. (1996) interpreted it as alkali-feldspar granite–granitic gneiss and provided U-Pb age dates of 1864.4 ± 3.1 Ma and 1839.1 ± 4.7 Ma, but were unable to obtain a precise age date, suggesting that these ages were more likely consistent with migmitization; however, the core could be correlated as an offshore extension of the Makkovik Orogen.

# SYNOPSIS

The Hopedale and Saglek basins preserve a record of the opening of the Labrador Sea as Greenland separated from North America in the Early Cretaceous. The lithostratigraphic units include strata of the Alexis and Bjarni formations formed during rifting, late rift Upper Cretaceous strata of the Markland Formation and sandy Freydis Member, and a succession postdating the rifting that begins with the mid-Paleocene to basal Eocene Gudrid and Cartwright formations. These strata were sampled in conventional cores within exploration wells along the Labrador and southeast Baffin shelves.

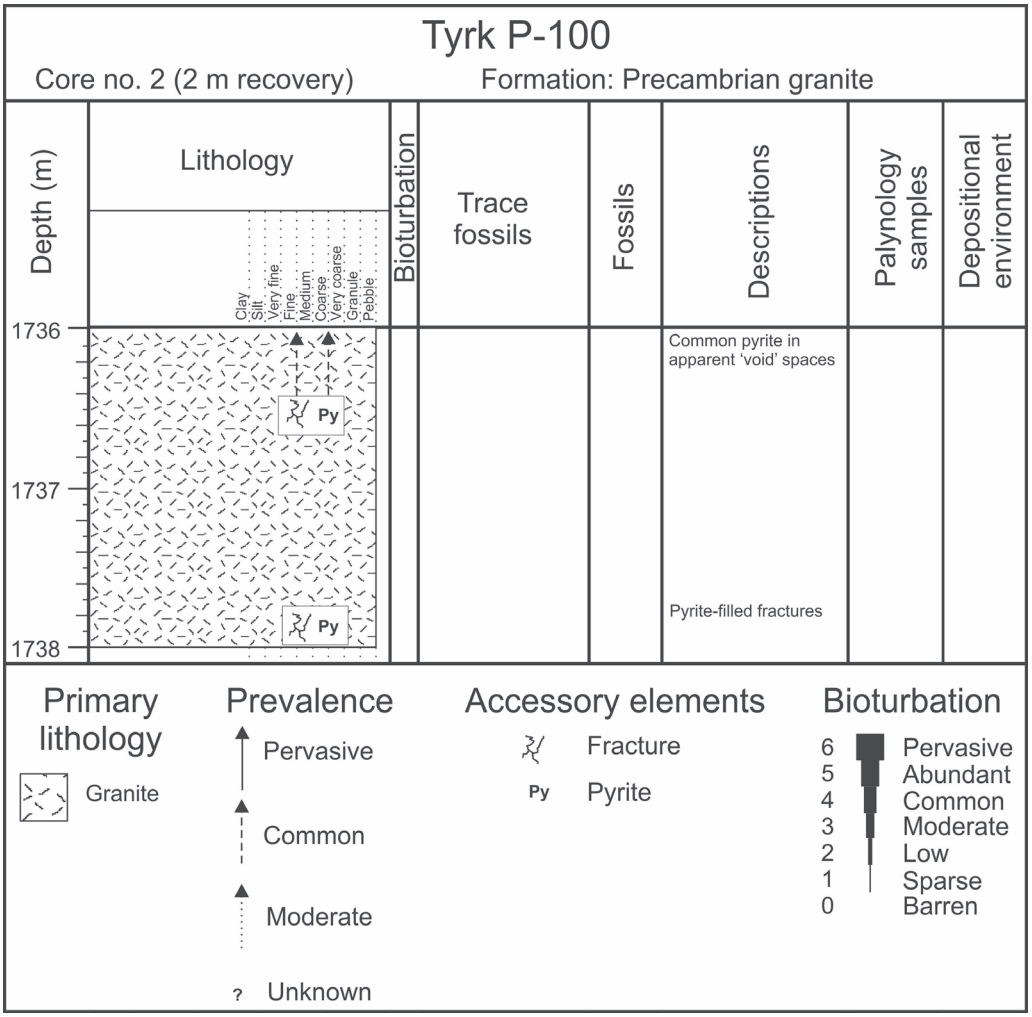


**Figure 91.** Log of core 2, Tyrk P-100.

This study's lithological, sedimentological, ichnological, and palynological analysis of 37 conventional core intervals from 15 wells provide new insights into the depositional paleoenvironments and age of these Mesozoic to lower Cenozoic sedimentary deposits, as well as volcanic rocks formed during rifting and underlying crystalline basement. The present approach differs from previous studies in that core observations are integrated with palynological analyses to provide a more robust interpretation of the paleoenvironment, in addition to a biostratigraphic age from in situ strata.

In basement rocks that predate rifting, five intervals are recognized comprised of gneissic and granitic rock. In the Saglek Basin, three of these are gneiss units that have a similar appearance. Wasteneys et al. (1996) dated these as Archean and related them to the onshore Saglek Block of the Nain Province or North Atlantic Craton. The granitic rocks from the Hopedale Basin are orthoclase feldspar–dominated with an overall similar appearance. These Proterozoic rocks represent offshore extensions of the onshore Makkovik Province, but their ages could be overprinted by younger events such as migmitization (Wasteneys et al., 1996). These rocks provide information about local sediment sources, especially during deposition of the Bjarni Formation that accumulated during early rifting and deposition when fault blocks would have supplied local sediment into grabens and half grabens.

A selection of three Alexis Formation basalt cores were described from the adjacent Bjarni H-81 and Herjolf M-92 wells. The basalt from Bjarni H-81 reflects solidification of subaerial, gas-bearing flow deposits that show some evidence of subaerial exposure and weathering. Existing K-Ar age dates from cores 2 and 3 of this well are Aptian and Valanginian, respectively. These cores are only 300 m apart within the well, suggesting a suspect nature to the ages. Pollen grains recovered from the rubbly, green-brown Herjolf M-92 basalt core could not provide an age determination, but a previous K-Ar age date indicated Aptian.

Of the 14 cores from the Bjarni Formation, strata are interpreted to be as old as Barremian–Aptian to as young as middle Albian–Cenomanian. As many of these cores are derived from upper portions of the Bjarni Formation preserved in the wells, an Albian age is expected. The lithology varies and includes:

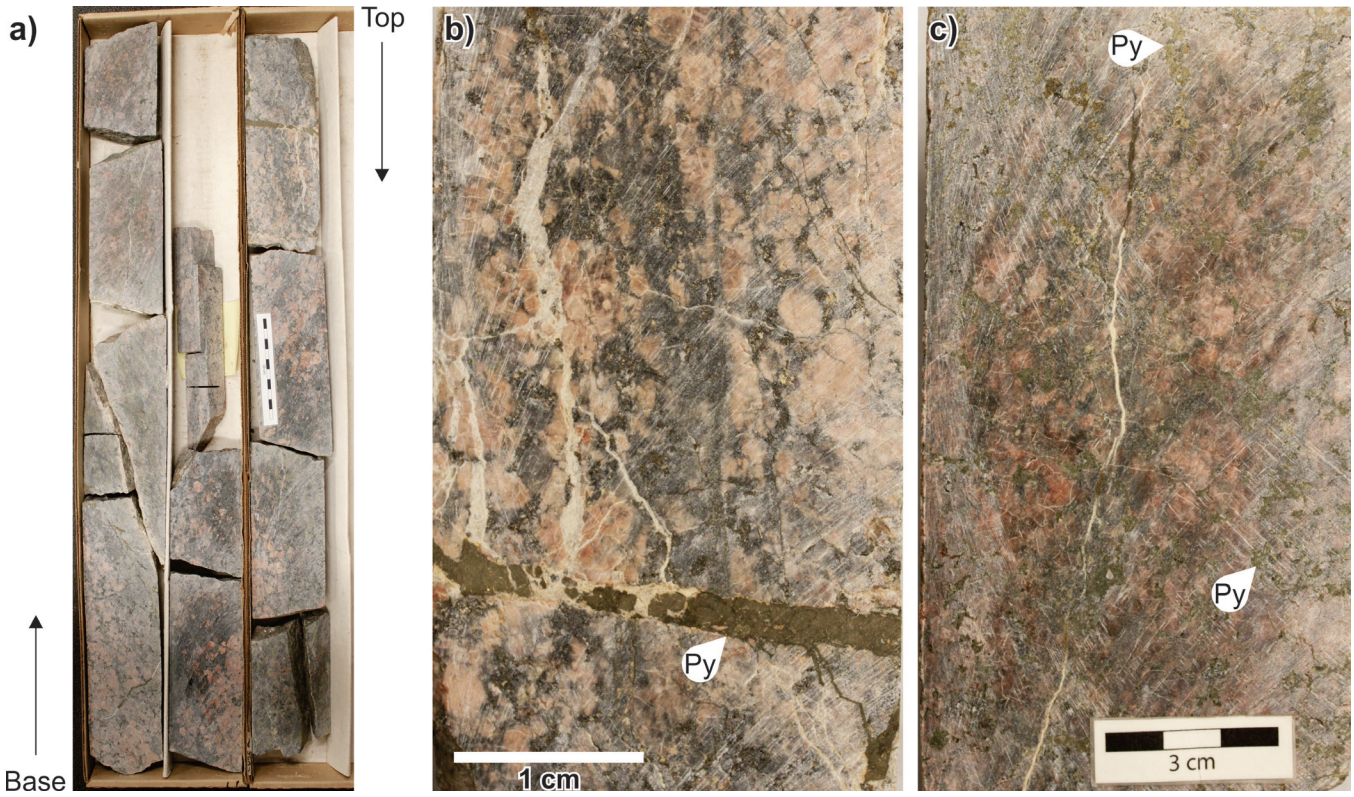


**Figure 92.** Photographs of core 2, Tyrk P-100. **a)** The entire core 2 interval (scale bar = 10 cm). NRCan photo 2019-526. **b)**, **c)** Close-up images of the granite showing the phaneritic texture and quartz and pyrite-filled fractures. Pyrite (Py) is present throughout this upper section of the core (in Fig. 92c) filling apparent 'voids' in the granite. NRCan photo 2019-527, 2019-528, respectively. All photographs by L.T. Dafoe.

sandstone, shale and/or mudstone, conglomerate, and volcanic rocks. The core intervals overwhelmingly represent shallow-marine deltaic settings (nine cores) including mostly river-influenced and lesser river-dominated and wave-influenced settings. One core was determined to reflect nonmarine, fluvial deposition in the Barremian–Aptian and three others are indicative of restricted marine bay or lagoonal settings. The final core, thought to be contaminated by drilling mud, appears to reflect shallow-marine volcanic accumulations apparently related to the Bjarni Formation. Core observations provide the most detail in terms of specific paleoenvironmental settings, but some cores greatly benefited from dinocyst identifications that confirmed a marginal marine setting where core observations were inconclusive.

Within the overlying Markland Formation and Freydis Member, eight lower Campanian through Maastrichtian cores were interpreted. The Markland Formation is comprised of shale and sandy mudstone, reflecting more distal marine settings: distal inner-shelf to distal outer-shelf settings and open-ocean, slope-equivalent water depths. The Freydis Member reflects more proximal conditions and is characterized by heterolithic sandstone and mudstone and/or shale and bioturbated sandstone. These strata are interpreted as distributary channels and deltaic deposits (river-influenced), shoreface, and inner-shelf settings. Paleoenvironments determined from palynomorph assemblages generally agree well with core observations, but sometimes indicate a proximity to a delta and source of terrestrial detritus not noted in core observations. In other cases, rich dinocyst assemblages can sometimes suggest a more distal setting than implied by the sedimentology and trace-fossil assemblage. Notably, in Skolp E-07, thick Markland Formation (and Freydis Member) rocks show depositional cyclicity, indicating that sedimentation was keeping pace with subsidence, but with many small marine flooding events taking place in the Campanian and Maastrichtian.

The Gudrid and Cartwright formations are represented by four cores that are interpreted to be Selandian to early Ypresian. The single core of Cartwright Formation shale is consistent with wave-influenced prodelta deposition. The other cores are sandstone of the Gudrid Formation, reflecting tidal channels, shoreface and/or delta front, and storm-dominated proximal and distal delta front. Depositional settings interpreted from palynomorphs were found to agree well with core observations. From the northern part of the Saglek Basin, three core intervals from unnamed Paleocene basalt units record both subaerial flows and shallow, subaqueous hyaloclastic lava delta accumulations with weathering of the uppermost basalt evident in Hekja O-71. Existing Ar-Ar ages from Gjoa G-37 place the basalt units in the early Thanetian. The age of core 2 from Hekja O-71 is Selandian, and a previous late Ypresian Ar-Ar age of the lowermost core 3 of that

well is suspect. Based on composition of sand grains, these rocks were found to have been eroded and reworked into the overlying Gudrid Formation of the Hekja O-71 well.

In general, the biostratigraphic ages from palynomorph analyses provide improved age control over those from cuttings since both last and first occurrences can be studied. By combining evidence from the lithology, sedimentological properties, and trace-fossil occurrences within the sedimentary cores, a comprehensive interpretation of the paleoenvironment is herein provided. This is further augmented by palynological analyses that provide a separate line of evidence for paleoenvironmental interpretation of the cores. By integrating these methodologies, paleoenvironmental interpretations were refined and confirmed. The sedimentology and ichnology often provide more detailed interpretations of the depositional settings and related conditions, yet they sometimes do not contain diagnostic structures. In these cases, palynological analyses are instrumental in providing evidence to support a particular interpretation, often whether the core reflects nonmarine or shallow-marine conditions; however, caution is required when the paleoenvironment is shallow marine and brackish in nature (e.g. deltaic or lagoonal), as these settings are not conducive to dinoflagellates and may show a miospore-dominated assemblage that otherwise suggests nonmarine deposition.

Results from the conventional core intervals has refined the age and paleoenvironments of deposition of Lower Cretaceous through basal Eocene strata of the offshore Labrador (Newfoundland and Labrador) and southeast Baffin Island (Nunavut) margins. This work has future implications for understanding the stratigraphy when extrapolated within the wells, and forms the basis for future studies in the region.

## ACKNOWLEDGMENTS

The authors would like to acknowledge the Canada-Newfoundland and Labrador Offshore Petroleum Board for their assistance and co-operation in the core viewing and sampling process for the offshore Labrador core materials. Thanks to R. Fensome and N. Bingham-Koslowski for their detailed and pertinent reviews. R. Harms of Global Geolab and L. Dancey of GSC Calgary are acknowledged for undertaking the palynology processing on the core materials. Also thanks to W. MacMillan for compiling the plates showing the palynomorphs and to L. Campbell for helping to co-ordinate processing and slide organization. The authors also appreciate the assistance of the Canada-Nova Scotia Offshore Petroleum Board and the National Energy Board for permitting the viewing and sampling of the Gjoa G-37 and Hekja O-71 cores. A special thanks to D. Piper and G. Pe-Piper for their assistance with thin-section observations and for providing sections of the Bjarni O-82 core.

## REFERENCES

Ainsworth, N.R., Riley, L.A., Bailey, H.W., and Gueinn, K.J., 2014. Cretaceous–Tertiary stratigraphy of the Labrador Shelf; Riley Geoscience Ltd.; on file with the Canada-Newfoundland and Labrador Offshore Petroleum Board, St. John's, Newfoundland and Labrador, 56 p.

Ainsworth, N.R., Riley, L.A., Bailey, H.W., and Gueinn, K.J., 2016. Cretaceous–Tertiary stratigraphy of the Labrador Shelf; Riley Geoscience Ltd.; on file with the Canada-Newfoundland and Labrador Offshore Petroleum Board, St. John's, Newfoundland and Labrador, 31 p.

Aquitaine Company of Canada Ltd., 1980. Well history report Aquitaine et al Hekja O-71; on file with the Canada-Newfoundland and Labrador Offshore Petroleum Board, St. John's, Newfoundland and Labrador, 88 p.

Ayres, L.D., Van Wagoner, N.A., and Ferreira, W.S., 1991. Voluminous shallow-water to emergent phreatomagmatic basaltic volcaniclastic rocks, Proterozoic (~1886 Ma) Amisk Lake composite volcano, Flin Flon Greenstone Belt, Canada; *in* Sedimentation in Volcanic Settings, (ed.) R.V. Fisher and G.A. Smith; Society for Sedimentary Geology Special Publication 45, p. 175–187. https://doi.org/10.2110/pec.91.45.0175

Baas, J.H., 2003. Ripple, ripple mark, ripple structure; *in* Encyclopedia of Sediments and Sedimentary Rocks, (ed.) G.V. Middleton; Springer, Dordrecht, The Netherlands, p. 565–568.

Balkwill, H.R., 1987. Labrador basin: structural and stratigraphic style; *in* Sedimentary Basins and Basin-Forming Mechanisms, (ed.) C. Beaumont and A.J. Tankard; Canadian Society of Petroleum Geologists, Memoir, v. 12, p. 17–43.

Balkwill, H.R. and McMillan, N.J., 1990. Mesozoic-Cenozoic geology of the Labrador Shelf, Chapter 7 (part 1); *in* Geology of the Continental Margin of Eastern Canada, volume 2, (ed.) M.J. Keen and G.L. Williams; Geological Survey of Canada, Geology of Canada, p. 295–324 (*also* Geological Society of America, The Geology of North America, V. I-1).

Barss, M.S., 1981. Palynological analysis of core samples from Eastcan et al. Roberval K-92; Atlantic Report EPGS-PAL. 16-81MSB, BASIN database, Geological Survey of Canada. <https://basin.gdr.nrcan.gc.ca/wells/index_e.php> [accessed April 13, 2017]

Bell, J.S., 1989. Labrador Sea; East Coast Basin Atlas Series, Geological Survey of Canada, 135 p. https://doi.org/10.4095/127152

Bingham-Koslowski N., Miller, M.A., McCartney,T., and Carey, J.S., 2019. Revised biostratigraphic and thermal alteration interpretations for the Paleozoic of the Hopedale Basin, offshore Labrador, Canada; Bulletin of Canadian Petroleum Geology, v. 67, no. 3, p. 185–214.

Bint, A.N., 1986. Fossil ceratiaceae: a restudy and new taxa from the mid-Cretaceous of the western interior, USA; Palynology, v. 10, p. 135–180. https://doi.org/10.1080/01916122.1986.9989307

Brewer, T.S., Harvey, P.K., Lovell, M.A., Haggas, S., Williamson, G., and Pezard, P., 1998. Ocean floor volcanism: constraints from the integration of core and downhole logging measurements; *in* Core-Log Integration, (ed.) P.K. Harvey and M.A. Lovell; Geological Society of London, Special Publication 136, p. 341–362. https://doi.org/10.1144/GSL.SP.1998.136.01.28

Bujak, J.P. and Mudge, D., 1994. A high-resolution North Sea Eocene dinocyst zonation; Journal of the Geological Society, v. 151, p. 449–462. https://doi.org/10.1144/gsjgs.151.3.0449

Bujak Davies Group, 1989a. Biostratigraphy and maturation of 17 Labrador and Baffin Shelf wells, volume 1: scope, methodology, format and recommendations; Geological Survey of Canada, Open File 1929, 92 p. https://doi.org/10.4095/130622

Bujak Davies Group, 1989b. Biostratigraphy and maturation of 17 Labrador and Baffin Shelf wells, volume 2: Bjarni O-82 and Corte Real P-85; Geological Survey of Canada, Open File 1930, 68 p. https://doi.org/10.4095/130623

Bujak Davies Group, 1989c. Biostratigraphy and maturation of 17 Labrador and Baffin Shelf wells, volume 3: Gilbert F-53 and Gjoa G-37; Geological Survey of Canada, Open File 1931, 65 p. https://doi.org/10.4095/130624

Bujak Davies Group, 1989d. Biostratigraphy and maturation of 17 Labrador and Baffin shelf wells, volume 4: Hekja O-71 & Hopedale E-3; Geological Survey of Canada, Open File 1932, 54 p. https://doi.org/10.4095/130625

Bujak Davies Group, 1989e. Biostratigraphy and maturation of 17 Labrador and Baffin Shelf wells, volume 5: Leif M-48 and North Bjarni F-06; Geological Survey of Canada, Open File 1933, 63 p. https://doi.org/10.4095/130626

Bujak Davies Group, 1989f. Biostratigraphy and maturation of 17 Labrador and Baffin Shelf wells, volume 6: North Leif I-05 & Ogmund E-72; Geological Survey of Canada, Open File 1934, 35 p. https://doi.org/10.4095/130627

Bujak Davies Group, 1989g. Biostratigraphy and maturation of 17 Labrador and Baffin Shelf wells, volume 8: Roberval K-92 and Rut H-11; Geological Survey of Canada, Open File 1936, 67 p. https://doi.org/10.4095/130629

Bujak Davies Group, 1989h. Biostratigraphy and maturation of 17 Labrador and Baffin Shelf wells, volume 10: Tyrk P-100; Geological Survey of Canada, Open File 1938, 22 p. https://doi.org/10.4095/130631

Canada-Newfoundland and Labrador Offshore Petroleum Board, 2007. C-NLOBP schedule of wells: St. John's, Newfoundland. <https://www.cnlopb.ca/> [accessed November 2018]

Caro, J., Fediaevsky, A., Jourdan, A., and Villain, J.-M., 1980. Biostratigraphic study of the Tyrk P100 Eastcan well; total – C.F.P.; on file with the Canada-Newfoundland and Labrador Offshore Petroleum Board, St. John's, Newfoundland and Labrador, 13 p.

Chevron Standard Ltd., 1978. Well history report Chevron et al Hopedale E-33; on file with the Canada-Newfoundland and Labrador Offshore Petroleum Board; St. John's, Newfoundland and Labrador, 29 p.

Coleman, M.L., 1993. Microbial processes: controls on the shape and composition of carbonate concretions; *in* Marine Sediments, Burial, Pore Water Chemistry, Microbiology and Diagenesis, (ed.) R.J. Parkes, P. Westbroek, and J.W. de Leeuw; Marine Geology, v. 113, p. 127–140. https://doi.org/10.1016/0025-3227(93)90154-N

Corgnet, J.L. and McWhae, J.R.H., 1973. Well History Report Eastcan et al Bjarni H-81; Eastcan Exploration Ltd.; on file with the Canada-Newfoundland and Labrador Offshore Petroleum Board, St. John's, Newfoundland and Labrador, 45 p.

Costa, L.I. and Davey, R.J., 1992. Dinoflagellate cysts of the Cretaceous system; *in* A Stratigraphic Index of Dinoflagellate Cysts, (ed.) A.J. Powell; British Micropalaeontological Society Publication Series, p. 99–153.

Crouch, E.M., Heilmann-Clausen, C., Brinkhuis, H., Morgans, H.E.G., Rogers, K.M., Egger, H., and Schmitz, B., 2001. Global dinoflagellate event associated with the late Paleocene thermal maximum; Geology, v. 29, no. 4, p. 315–318. https://doi.org/10.1130/0091-7613(2001)029%3c0315:GDEAWT%3e2.0.CO%3b2

Dafoe, L.T. and Williams, G., 2020. Palynological analysis of the two Labrador Shelf wells, Petro-Canada et al. North Leif I-05 and Total Eastcan et al. Skolp E-07, offshore eastern Canada: new age, paleoenvironmental and lithostratigraphic interpretations; Geological Survey of Canada, Open File 8670, 103 p. https://doi.org/10.4095/321502

Dale, B., 1996. Dinoflagellate cyst ecology: modelling and geological applications; *in* Palynology: Principles and Applications 3, (ed.) J. Jansonius and D.C. McGregor; American Association of Stratigraphic Palynologists Foundation, Dallas, Texas, p. 1249–1275.

Dickie, K., Keen, C.E., Williams, G.L., and Dehler, S.A., 2011. Tectonostratigraphic evolution of the Labrador Margin, Atlantic Canada; Marine and Petroleum Geology, v. 28, p. 1663–1675. https://doi.org/10.1016/j.marpetgeo.2011.05.009

Drugg, W.S., 1967. Palynology of the Upper Moreno Formation (Late Cretaceous-Paleocene) Escarpado Canyon, California; Palaeontographica, Abteilung B, Paläophytologie, v. 120, no. 4, p. 1–71.

Duff, D.E., 1981. Well history report Petro-Canada et al North Bjarni F-06 (Geological File); Petro-Canada Exploration Inc.; on file with the Canada-Newfoundland and Labrador Offshore Petroleum Board, St. John's, Newfoundland and Labrador, 110 p.

Eastcan Exploration Ltd., 1975a. Well history report Eastcan et al Karlsefni H-13; on file with the Canada-Newfoundland and Labrador Offshore Petroleum Board, St. John's, Newfoundland and Labrador, 52 p.

Eastcan Exploration Ltd., 1975b. Well history report Eastcan et al Snorri J-90; on file with the Canada-Newfoundland and Labrador Offshore Petroleum Board, St. John's, Newfoundland and Labrador, 67 p.

Esso Exploration Ltd., 1979. Esso HB Gjoa G-37 final well report; on file with the Canada-Newfoundland and Labrador Offshore Petroleum Board, St. John's, Newfoundland and Labrador, 363 p.

Fensome, R.A., 2015. Palynology analysis of two Labrador Shelf wells: Petro Canada et al. Rut H-11 and Eastcan et al. Karlsefni A-13; Geological Survey of Canada, Open File 7738, 21 p. https://doi.org/10.4095/295616

Fensome, R.A., Nøhr-Hansen, H., and Williams, G.L., 2016. Cretaceous and Cenozoic dinoflagellate cysts and other palynomorphs from the western and eastern margins of the Labrador-Baffin Seaway; Geological Survey of Denmark and Greenland, Bulletin 36, 141 p.

Frederiksen, N.O. and Christopher, R.A., 1978. Taxonomy and biostratigraphy of Late Cretaceous and Paleogene triatriate pollen from South Carolina; Palynology, v. 2, p. 113–145. https://doi.org/10.1080/01916122.1978.9989168

Gautier, D.L., 1982. Siderite concretions: indicators of early diagenesis in the Gammon Shale (Cretaceous); Journal of Sedimentary Petrology, v. 52, p. 859–871.

Gradstein, F.M., 1980. Labrador Shelf foraminiferal stratigraphy I – supplement, Eastcan et al., Karlsefni A-13, Labrador Shelf; Geological Survey of Canada, Atlantic Report EPGS-PAL.21-80FMG, BASIN database, Geological Survey of Canada. <https://basin.gdr.nrcan.gc.ca/wells/index_e.php> [accessed April 13, 2017]

Gradstein, F.M. and Williams, G.L., 1976. Biostratigraphy of the Labrador Shelf, part 1; Geological Survey of Canada, Open File 349, 39 p. https://doi.org/10.4095/100443

Gradstein, F.M., Ogg, J.G., Schmitz, M., and Ogg, G., 2012. The Geologic Time Scale 2012; Elsevier B.V., Oxford, United Kingdom, 1144 p.

Harland, R., 1973. Dinoflagellate cysts and acritarchs from the Bearpaw Formation (Upper Campanian) of southern Alberta, Canada; Palaeontology, v. 16, p. 665–706.

Harland, R., 1979. The *Wetzeliella* (*Apectodinium*) *homomorphum* plexus from the Palaeogene/earliest Eocene of north-west Europe; *in* Fourth International Palynology Conference, Lucknow, 1976–1977; Proceedings, v. 2, p. 59–70.

Harris, I., 1980. Basement rocks cored in Roberval C-02 and Gilbert F-53; Petro-Canada Internal Memorandum; on file with the Canada-Newfoundland and Labrador Offshore Petroleum Board, St. John's, Newfoundland and Labrador, 1 p.

Jauer, C., Wielens, H., and Williams, G., 2009. Hydrocarbon prospectivity of Davis Strait and Labrador Shelf: seismic setting and stratigraphy for Gjoa G-37, Hekja O-71, Rut H-11, Gilbert F-53, Karlsefni A-13, and Skolp E-07; Geological Survey of Canada, Open File 5910, 6 sheets. https://doi.org/10.4095/247336

Jauer, C.D., Oakey, G.N., Williams, G., and Wielens, H.J.B.W., 2014. Saglek Basin in the Labrador Sea, east coast Canada; stratigraphy, structure and petroleum systems; Bulletin of Canadian Petroleum Geology; Baffin Bay, v. 62, special issue, p. 232–260. https://doi.org/10.2113/gscpgbull.62.4.232

Jolley, D.W., 1992. A new species of the dinoflagellate genus *Areoligera* Lejeune-Carpentier from the Late Palaeocene of the eastern British Isles; Tertiary Research, v. 14, no. 1, p. 25–32.

Keen, C.E., Dickie, K., and Dehler, S., 2012. The volcanic margins of the northern Labrador Sea: insights to the rifting process; Tectonics, v. 31, cit. no. TC1011. https://doi.org/10.1029/2011TC002985

Keen, C.E., Dickie, K., and Dafoe, L.T., 2018a. Structural characteristics of the ocean-continent transition along the rifted continental margin, offshore central Labrador; Marine and Petroleum Geology, v. 89, p. 443–463. https://doi.org/10.1016/j.marpetgeo.2017.10.012

Keen, C.E., Dickie, K., and Dafoe, L.T., 2018b. Structural evolution of the rifted margin off northern Labrador: the role of hyperextension and magmatism; Tectonics, v. 37, p. 1955–1972. https://doi.org/10.1029/2017TC004924

Leckie, D.A. and Singh, C., 1991. Estuarine deposits of the Albian Paddy Member (Peace River Formation) and lowermost Shaftesbury Formation, Alberta, Canada; Journal of Sedimentary Petrology, v. 61, no. 5, p. 825–849.

Lee, J.K.W., 2014. Ar-Ar and K-Ar dating; *in* Encyclopedia of Scientific Dating Methods, (ed.) W.J. Rink and J. Thompson; Springer, 27 p. https://doi.org/10.1007/978-94-007-6326-540-1

MacEachern, J.A., Bann, K.L., Bhattacharya, J.P., and Howell, C.D., Jr., 2005. Ichnology of deltas: organism responses to the dynamic interplay of rivers, waves, storms and tides; *in* River Deltas—Concepts, Models, and Examples, (ed.) L. Giosan and J.P. Bhattacharya; Society for Sedimentary Geology Special Publication 83, p. 49–85. https://doi.org/10.2110/pec.05.83.0049

MacEachern, J.A., Pemberton, S.G., Gingras, M.K., and Bann, K.L., 2010. Ichnology and facies models; *in* Facies Models 4, (ed.) N.P. James and R.W. Dalrymple; Geological Association of Canada, St. John's, Newfoundland and Labrador, p. 19–58.

Manum, S.B. and Cookson, I.C., 1964. Cretaceous microplankton in a sample from Graham Island, arctic Canada, collected during the second "Fram" expedition (1898-1902); with notes on microplankton from the Hassel Formation, Ellef Ringnes Island; Norske Videnskaps-Akademi i Oslo. I. Matematisk-Naturvidenskapelig Klass Skrifter; Ny Serie, v. 17, p. 1–36.

McIntyre, D.J., 1974. Palynology of an Upper Cretaceous section, Horton River, District of Mackenzie, Northwest Territories; Geological Survey of Canada, Paper 74-14, p. 1–57. https://doi.org/10.4095/103304

McIntyre, D.J., 1975. Morphologic changes in *Deflandrea* from a Campanian section, District of Mackenzie, N.W.T., Canada; Geoscience and Man, v. 11, p. 61–76. https://doi.org/10.1080/00721395.1975.9989756

McWhae, J.R.H., 1980. Structure and spreading history of the northwestern Atlantic region from the Scotian Shelf to Baffin Bay; *in* Geology of the North Atlantic Borderlands, (ed.) J.W. Kerr, A.J. Fergusson, and L.C. Machan; Canadian Society of Petroleum Geologists, Memoir 7, p. 299–332.

McWhae, J.R.H., Elie, R., Laughton, K.C., and Gunther, P.R., 1980. Stratigraphy and petroleum prospects of the Labrador Shelf; Bulletin of Canadian Petroleum Geology, v. 28, p. 460–488.

Miller, M.F., 1991. Morphology and paleoenvironmental distribution of Paleozoic *Spirophyton* and *Zoophycos*: implications for the *Zoophycos* Ichnofacies; Palaios, v. 6, p. 410–425. https://doi.org/10.2307/3514966

Miller, M.F. and Johnson, K.G., 1981. *Spirophyton* in alluvial-tidal facies of the Catskill deltaic complex: possible biological control of ichnofossil distribution; Journal of Paleontology, v. 55, p. 1016–1027.

Miller, P.E. and D'Eon, G.J., 1987. Labrador Shelf–paleoenvironments; Geological Survey of Canada, Open File 1722, 186 p. https://doi.org/10.4095/130598

Moir, P.N., 1987a. Stratigraphic picks, Aquitaine et al. Hekja O-71; Geological Survey of Canada Atlantic, Report EPGS-STRAT.33-87PNM, BASIN database, Geological Survey of Canada. <https://basin.gdr.nrcan.gc.ca/wells/index_e.php> [accessed April 13, 2017]

Moir, P.N., 1987b. Stratigraphic picks, Esso H.B. Gjoa G-37; Geological Survey of Canada Atlantic, Report EPGS-STRAT.34-87PNM, BASIN database, Geological Survey of Canada. <https://basin.gdr.nrcan.gc.ca/wells/index_e.php> [accessed April 13, 2017]

Moir, P.N., 1989. Lithostratigraphy 1: review and type sections; *in* East Coast Basin Atlas Series, Labrador Sea (co-ord.) J.S. Bell; Geological Survey of Canada; p. 26–27. https://doi.org/10.4095/127166

Mudge, D.C. and Bujak, J.P., 2001. Biostratigraphic evidence for evolving palaeoenvironments in the Lower Paleogene of the Faeroe-Shetland Basin; Marine and Petroleum Geology, v. 18, p. 577–590. https://doi.org/10.1016/S0264-8172(00)00074-X

Nichols, D., 2003. Palynostratigraphic framework for age determination and correlation of the nonmarine Lower Cenozoic of the Rocky Mountains and Great Plains region; *in* Cenozoic Systems of the Rocky Mountain Region, (ed.) R.G. Raynolds and R.M. Flores; Rocky Mountain Section, Society for Sedimentary Geology (SEPM), Denver, Colorado, p. 107–134.

Nichols, D.J. and Ott, H.L., 1978. Biostratigraphy and evolution of the *Momipites-Caryapollenites* lineage in the early Tertiary in the Wind River Basin, Wyoming; Palynology, v. 2, p. 93–112. https://doi.org/10.1080/01916122.1978.9989167

Nichols, D.J. and Sweet, A.R., 1993. Biostratigraphy of Upper Cretaceous non-marine palynofloras in a north-south transect of the Western Interior Basin; *in* Evolution of the Western Interior Basin, (ed.) W.G.E. Caldwell and E.G. Kauffman; Geological Association of Canada, Special Paper 39, p. 539–584.

Nøhr-Hansen, H., 1992. Cretaceous marine and brackish (?) dinoflagellate cysts, West Greenland; 8th International Palynological Congress, Aix-en-Provence, 6–12 September, 1992, p. 107 (abstract).

Nøhr-Hansen, H., 2008. Morphological variability within brackish water to marginal marine dinoflagellate cyst assemblages from mid-Cretaceous, West Greenland; DINO8 – 8th International conference on modern and fossil dinoflagellates, Montreal, 4–10 May, 2008, GEOTOP-Université de Québec à Montréal, p. 41–42 (abstract).

Nøhr-Hansen, H., Williams, G.L., and Fensome, R.A., 2016. Biostratigraphic correlation of the western and eastern margins of the Labrador—Baffin Seaway and implications for the regional geology; Geological Survey of Denmark and Greenland Bulletin, v. 37, 74 p.

Oakey, G.N. and Chalmers, J.A., 2012. A new model for the Paleogene motion of Greenland relative to North America: plate reconstructions of the Davis Strait and Nares Strait regions between Canada and Greenland; Journal of Geophysical Research, v. 117, cit. no. B10401. https://doi.org/10.1029/2011JB008942

Pearce, M., 2010. New organic-walled dinoflagellate cysts from the Cenomanian to Maastrichtian of the Trunch borehole, UK; Journal of Micropalaeontology, v. 29, p. 51–72. https://doi.org/10.1144/jm.29.1.51

Pedersen, G.K. and Nøhr-Hansen, H., 2014. Sedimentary successions and palynoevent stratigraphy from the non-marine Upper Cretaceous of the Nuussuaq Basin, West Greenland; Bulletin of Canadian Petroleum Geology, v. 62, no. 4, p. 261–288. https://doi.org/10.2113/gscpgbull.62.4.261

Pemberton, S.G., Spila, M., Pulham, A.J., Saunders, T., MacEachern, J.A., Robbins, D., and Sinclair, I.K., 2001. Ichnology & Sedimentology of Shallow to Marginal Marine Systems: Ben Nevis & Avalon Reservoirs, Jeanne d'Arc Basin; Geological Association of Canada, Short Course 15, 343 p.

Petro-Canada Exploration Inc., 1980a. Well history report Petro-Canada et al North Bjarni F-06; on file with the Canada-Newfoundland and Labrador Offshore Petroleum Board, St. John's, Newfoundland and Labrador, 27 p.

Petro-Canada Exploration Inc., 1980b. Well history report Petro-Canada et al North Leif I-05; on file with the Canada-Newfoundland and Labrador Offshore Petroleum Board, St. John's, Newfoundland and Labrador, 30 p.

Petro-Canada Exploration Inc., 1980c. Well history report Petro-Canada et al Ogmund E-72; on file with the Canada-Newfoundland and Labrador Offshore Petroleum Board, St. John's, Newfoundland and Labrador, 258 p.

Petro-Canada Exploration Inc., 1981. Well history report Petro-Canada et al North Leif I-05; on file with the Canada-Newfoundland and Labrador Offshore Petroleum Board, St. John's, Newfoundland and Labrador, 222 p.

Price, R.J. and Thorne, B.V.A., 1978. The micropalaeontology, palynology and stratigraphy of the Total Eastcan Skolp E-07 well, Labrador Shelf, offshore Eastern Canada; Robertson Research, Exploration Report No. 197; on file with the Canada-Newfoundland and Labrador Offshore Petroleum Board, St. John's, Newfoundland and Labrador, 29 p.

Radmacher, W., Tyszka, J., and Mangerud, G., 2014. Distribution and biostratigraphical significance of *Heterosphaeridium bellii* sp. nov. and other Late Cretaceous dinoflagellate cysts from the south-western Barents Sea; Review of Palaeobotany and Palynology, v. 201, p. 29–40. https://doi.org/10.1016/j.revpalbo.2013.10.003

Robertson Research (North America) Ltd., 1974. Exploration Report No. 58: the micropaleontology, palynology and stratigraphy of the Eastcan et al. Bjarni H-81 well; on file with the Canada-Newfoundland and Labrador Offshore Petroleum Board, St. John's, Newfoundland and Labrador, 22 p.

Robertson Research Canada Ltd., 1979. The micropalaeontology, palynology and stratigraphy of the Total Eastcan Tyrk P-100 well; on file with the Canada-Newfoundland and Labrador Offshore Petroleum Board, St. John's, Newfoundland and Labrador, 20 p.

Robertson Research Canada Ltd., 1980. Micropaleontology, palynology and stratigraphy of the Total Eastcan Bjarni O-82 well; on file with the Canada-Newfoundland and Labrador Offshore Petroleum Board, St. John's, Newfoundland and Labrador, 23 p.

Rodrigue, G., 1980. Description of basement rocks cored in Gilbert F-53 and Roberval C-02; Petro-Canada, internal memorandum; on file with the Canada-Newfoundland and Labrador Offshore Petroleum Board, St. John's, Newfoundland and Labrador, 7 p.

Roest, W.R. and Srivastava, S.P., 1989. Sea-floor spreading in the Labrador Sea: a new reconstruction; Geology, v. 17, p. 1000–1003. https://doi.org/10.1130/0091-7613(1989)017%3c1000:SFSITL%3e2.3.CO%3b2

Singh, C., 1971. Lower Cretaceous microfloras of the Peace River area, northwestern Alberta; Research Council of Alberta Bulletin, v. 28, p. 301–542.

Sluijs, A., Pross, J., and Brinkhuis, H., 2005. From greenhouse to icehouse; organic-walled dinoflagellate cysts as paleoenvironmental indicators in the Paleogene; Earth-Science Reviews, v. 68, no. 3–4, p. 281–315. https://doi.org/10.1016/j.earscirev.2004.06.001

Srivastava, S.K., 1966. Upper Cretaceous microflora (Maestrichtian) from Scollard, Alberta, Canada; Pollen et Spores, v. 8, no. 3, p. 497–552.

St-Onge, M.R., Van Gool, J.A.M., Garde, A.A., and Scott, D.J., 2009. Correlation of Archean and Paleoproterozoic units between northeastern Canada and western Greenland: constraining the pre-collisional upper plate accretionary history of the trans-Hudson orogen; *in* Earth Accretionary Systems in Space and Time, (ed.) P.A. Cawood and A. Kroner; Geological Society, London, Special Publication 318, p. 193–235. https://doi.org/10.1144/SP318.7

Stover, L.E., Brinkhuis, H., Damassa, S.P., de Verteuil, L., Helby, R.J., Monteil, E., Partridge, A.D., Powell, A.J., Riding, J.B., Smelror, M., and Williams, G.L., 1996. Mesozoic-Tertiary dinoflagellates, acritarchs and prasinophytes; Chapter 19 *in* Palynology: Principles and Applications, 2, (ed.) J. Jansonius and D.C. McGregor; American Association of Stratigraphic Palynologists Foundation, Dallas, U.S.A., p. 641–750.

Sweet, A.R., 2015. Applied research report on 33 North Bylot Trough samples collected by Phillip Benham, Memorial University from his Section 3, Maud Bight (North Bylot) area, east coast Bylot Island (NTS Map Sheet 038-C-11); Geological Survey of Canada (Calgary), Paleontological Report, 38 p.

Szaniawski, H., 1996. Scolecodonts; Chapter 12 *in* Palynology: Principles and Applications, (ed.) J. Jansonius and D.C. McGregor; American Association of Stratigraphic Palynologists Foundation; Dallas, U.S.A., p. 337–3354.

Tonkin, N.S., 2012. Deltas; *in* Trace Fossils as Indicators of Sedimentary Environments, (ed.) D. Knaust and R.G. Bromley; Developments in Sedimentology, v. 64, p. 507–528.

Total Eastcan Exploration Ltd., 1977. Well history report Total Eastcan et al Herjolf M-92; on file with the Canada-Newfoundland and Labrador Offshore Petroleum Board, St. John's, Newfoundland and Labrador, 96 p.

Total Eastcan Exploration Ltd., 1978a. Well history report Total Eastcan et al Roberval K-92; on file with the Canada-Newfoundland and Labrador Offshore Petroleum Board, St. John's, Newfoundland and Labrador, 72 p.

Total Eastcan Exploration Ltd., 1978b. Well history report Total Eastcan et al Skolp E-7; on file with the Canada-Newfoundland and Labrador Offshore Petroleum Board, St. John's, Newfoundland and Labrador, 166 p.

Total Eastcan Exploration Ltd., 1979a. Well history report Total Eastcan et al Bjarni O-82; on file with the Canada-Newfoundland and Labrador Offshore Petroleum Board, St. John's, Newfoundland and Labrador, 197 p.

Total Eastcan Exploration Ltd., 1979b. Well history report Total Eastcan et al Gilbert F-53; on file with the Canada-Newfoundland and Labrador Offshore Petroleum Board, St. John's, Newfoundland and Labrador, 97 p.

Total Eastcan Exploration Ltd., 1979c. Well history report Total Eastcan et al Tyrk P-100; on file with the Canada-Newfoundland and Labrador Offshore Petroleum Board, St. John's, Newfoundland and Labrador, 118 p.

Umpleby, D.C., 1979. Geology of the Labrador shelf; Geological Survey of Canada, Paper 79-13, 40 p. https://doi.org/10.4095/105927

Wall, D., Dale, B., Lohmann, G.P., and Smith, W.K., 1977. The environment and climatic distribution of dinoflagellate cysts in modern marine sediments from regions in the North and South Atlantic oceans and adjacent areas; Marine Micropaleontology, v. 2, p. 121–200. https://doi.org/10.1016/0377-8398(77)90008-1

Wasteneys, H.A., Wardle, R.J., and Krogh, T.E., 1996. Extrapolation of tectonic boundaries across the Labrador shelf: U-Pb geochronology of well samples; Canadian Journal of Earth Sciences, v. 33, p. 1308–1324. https://doi.org/10.1139/e96-099

Wielens, H.J.B.W. and Williams, G.L., 2009. Stratigraphic cross section Gjoa-Snorri, Saglek – Hopedale Basin, in the Labrador Sea on the east coast of Canada, from North to South; Geological Survey of Canada, Open File 5903, 1 sheet. https://doi.org/10.4095/247636

Williams, G.L., 1975. Dinoflagellate and spore stratigraphy of the Mesozoic-Cenozoic, offshore eastern Canada; Geological Survey of Canada, Paper 74-30, v. 2, p. 107–161.

Williams, G.L., 1979a. Eastcan et al. Bjarni H-81; *in* Palynological zonation and correlation of sixty-seven wells, eastern Canada, (ed.) M.S. Barss, J.P. Bujak, and G.L. Williams; Geological Survey of Canada, Paper 78-24, p. 86–88. https://doi.org/10.4095/104894

Williams, G.L., 1979b. Eastcan et al. Snorri J-90; *in* Palynological zonation and correlation of sixty-seven wells, eastern Canada, (ed.) M.S. Barss, J.P. Bujak, and G.L. Williams; Geological Survey of Canada, Paper 78-24, p. 97–98. https://doi.org/10.4095/104894

Williams, G.L., 1979c. Palynological analysis of Eastcan et al Herjolf M-92, Labrador Shelf; Geological Survey of Canada, Atlantic, Report EPGS-PAL.29-77GLW, BASIN database, Geological Survey of Canada. <https://basin.gdr.nrcan.gc.ca/wells/index_e.php> [accessed April 13, 2017]

Williams, G.L., 1980. Palynological analysis of Eastcan et al. Skolp E-07; Geological Survey of Canada, Report EPGS-PAL. 6-80GLW, BASIN database, Geological Survey of Canada. <https://basin.gdr.nrcan.gc.ca/wells/index_e.php> [accessed April 13, 2017]

Williams, G.L., 1981. Palynological Analysis of Chevron et al. Hopedale E-33, Labrador Shelf; Geological Survey of Canada, Atlantic, Report EPGS-PAL.26-81GLW; BASIN database, Geological Survey of Canada. <https://basin.gdr.nrcan.gc.ca/wells/index_e.php> [accessed April 13, 2017]

Williams, G.L., 2003. Palynological analysis of Amoco-Imperial-Skelly Skua E-41 Carson Basin, Grand Banks of Newfoundland; Geological Survey of Canada, Open File 1658, 24 p. https://doi.org/10.4095/214540

Williams, G.L., 2007a. Palynological analysis of Aquitaine et al. Hekja O-71, Saglek Basin, Davis Strait, offshore eastern Canada; Geological Survey of Canada, Open File 5448, 19 p. https://doi.org/10.4095/224259

Williams, G.L., 2007b. Palynological analysis of Eastcan et al. Snorri J-90, Hopedale Basin, Labrador Shelf, offshore eastern Canada; Geological Survey of Canada, Open File 5447, 23 p. https://doi.org/10.4095/224258

Williams, G.L., 2007c. Palynological analysis of Esso-H.B. Gjoa G-37, Saglek Basin, Davis Strait, offshore eastern Canada; Geological Survey of Canada, Open File 5449, 19 p. https://doi.org/10.4095/224260

Williams, G.L., 2007d. Palynological analysis of Total Eastcan et al. Bjarni O-82, Hopedale Basin, Labrador Shelf, offshore Eastern Canada; Geological Survey of Canada, Open File 5439, 22 p. https://doi.org/10.4095/224256

Williams, G.L., 2007e. Palynological analysis of Total Eastcan et al. Gilbert F-53, Saglek Basin, Labrador Shelf, offshore eastern Canada; Geological Survey of Canada, Open File 5450, 24 p. https://doi.org/10.4095/224261

Williams, G.L., 2017. Palynological analysis of the two Labrador Shelf wells, Petro-Canada et al. Roberval C-02 and Total Eastcan et al. Roberval K-92, offshore Newfoundland and Labrador; Geological Survey of Canada, Open File 8183, 63 p. https://doi.org/10.4095/299645

Williams, G.L. and Downie, C., 1966. Further dinoflagellate cysts from the London Clay; *in* Studies on Mesozoic and Cainozoic Dinoflagellate Cysts, (ed.) R.J. Davey, C. Downie, W.A.S. Sarjeant, and G.L. Williams; British Museum (Natural History) Geology, Bulletin, Supplement 3, p. 215–236.

Williams, G.L., Ascoli, P., Barss, M.S., Bujak, J.P., Davies, E.H., Fensome, R.A., and Williamson, M.A., 1990. Biostratigraphy and related studies; Chapter 3 *in* Geology of the Continental Margin of Eastern Canada, (ed.) M.J. Keen and G.L. Williams; Geological Survey of Canada, Geology of Canada, no. 2, p. 87–137 (*also* Geological Society of America, The Geology of North America, V. I-1).

Williams, G.L., Brinkhuis, H., Pearce, M.A., Fensome, R.A., and Weegink, J.W., 2004. Southern Ocean and global dinoflagellate cyst events compared: index events for the Late Cretaceous–Neogene; *in* Proceedings of the Ocean Drilling Program, (ed.) N.F. Exon, J.P. Kennett, and M.J. Malone; Scientific Results, v. 189, p. 1–98.

Williams, G.L., Fensome, R.A. and MacRae, R.A., 2017. The Lentin and Williams index of fossil dinoflagellates 2017 edition, American Association of Stratigraphic Palynologists, Contributions Series, no. 48, 1097 p.

Williamson, M.-C. and Villeneuve, M.E., 2002. Age of basaltic rocks recovered from drilling in the Davis Strait, Eastern Canada; Geological Survey of Canada, report on file with the Canada-Nova Scotia Offshore Petroleum Board, St. John's, Newfoundland and Labrador, 7 p.

# APPENDIX A

# PALYNOLOGICAL TAXA

Citations for dinocysts are presented in Williams et al. (2017) and the online DINOFLAJ3 database: http://dinoflaj.smu.ca/dinoflaj3/index.php/Main_Page.

References are not included in the current reference list (unless otherwise used in text).

**Dinocysts**

*Achomosphaera ramulifera* (Deflandre 1937b) Evitt 1963

*Adnatosphaeridium* sp. sensu Ioannides 1986

*Alterbidinium* Lentin and Williams 1985

*Apectodinium* (Costa and Downie 1976) Lentin and Williams 1977b

*Apectodinium homomorphum* (Deflandre and Cookson 1955) Lentin and Williams 1977b

*Apectodinium paniculatum* (Costa and Downie 1976) Lentin and Williams 1977b

*Apectodinium parvum* (Alberti 1961) Lentin and Williams 1977b

*Apectodinium quinquelatum* (Williams and Downie 1966b) Costa and Downie 1979

*Areoligera gippingensis* Jolley 1992

*Areoligera medusettiformis* Wetzel, 1933b ex Lejeune-Carpentier 1938a

*Canningia* Cookson and Eisenack 1960b

*Cannosphaeropsis utinensis* Wetzel 1933b

*Cerbia tabulata* (Davey and Verdier 1974) Below 1981a

*Cerodinium diebelii*. (Alberti 1959) Lentin and Williams 1987

*Cerodinium* cf. *speciosum* (Alberti 1959) Lentin and Williams 1987

*Chatangiella verrucosa* (Manum 1963) Lentin and Williams 1976

*Chatangiella victoriensis* (Cookson and Manum 1964) Lentin and Williams 1976

*Chichaouadinium vestitum* (Brideaux 1971) Bujak and Davies 1983

*Circulodinium distinctum* (Deflandre and Cookson 1955) Jansonius 1986

*Coronifera oceanica* Cookson and Eisenack 1958

*Cribroperidinium wetzelii* (Lejeune-Carpentier 1939) Helenes 1984

*Cyclonephelium* sp. following Fensome et al. 2019

*Dapsilidinium pastielsii* (Davey and Williams 1966b) Bujak et al. 1980

*Distatodinium* Eaton 1976

*Elytrocysta druggii* Stover and Evitt 1978

*Endoceratium* Vozzhennikova 1965

*Eurydinium glomeratum* (Davey, 1970) Stover and Evitt 1978

*Florentinia mantellii* (Davey and Williams 1966b) Davey and Verdier 1973

*Gardodinium* Alberti 1961

*Gardodinium trabeculosum* Alberti 1961

*Gillinia* Cookson and Eisenack 1960a

*Gillinia hymenophora* Cookson and Eisenack, 1960a

*Glaphyrocysta divaricata* (Williams and Downie 1966b) Stover and Evitt 1978

*Glaphyrocysta ordinata* (Williams and Downie 1966c) Stover and Evitt 1978

*Hafniasphaera* Hansen 1977

*Heterosphaeridium bellii* Radmacher et al. 2014

*Heterosphaeridium difficile* (Manum and Cookson 1963) Ioannides 1986

*Heterosphaeridium* "*elegantulum*" informal species name

*Hystrichodinium* Deflandre 1935

*Hystrichodinium pulchrum* Deflandre 1935

*Hystrichosphaeridium* Deflandre 1937b

*Hystrichosphaeridium bowerbankii* Davey and Williams 1966b

*Hystrichosphaeridium quadratum* Fensome et al. 2016

*Hystrichosphaeridium salpingophorum* Deflandre 1935 ex Deflandre 1937b

*Hystrichosphaeridium tubiferum* (Ehrenberg 1837b) Deflandre 1937b

*Hystrichosphaerina schindewolfii* Alberti 1961

*Impagidinium* Stover and Evitt 1978

*Impagidinium victorianum* (Cookson and Eisenack 1965a) Stover and Evitt 1978

*Impletosphaeridium apodastum* Fensome et al. 2016

*Isabelidinium cooksoniae* (Alberti, 1959b) Lentin and Williams, 1977a

*Isabelidinium cretaceum* (Cookson 1956) Lentin and Williams 1977a

*Isabelidinium*? *viborgense* Heilmann-Clausen 1985

*Kleithriasphaeridium loffrense* Davey and Verdier 1976

*Laciniadinium williamsii* Ioannides 1986

*Leberidocysta chlamydata* (Cookson and Eisenack 1962b) Stover and Evitt 1978

*Manumiella seelandica* (Lange 1969) Bujak and Davies 1983

*Membranophoridium* Gerlach 1961

*Membranosphaera* Samoilovitch in Samoilovitch and Mtchedlishvili 1961

*Microdinium* Cookson and Eisenack 1960a

*Microdinium ornatum* Cookson and Eisenack 1960a

*Nyktericysta* Bint 1986

*Nyktericysta davisii* Bint 1986

*Nyktericysta nebulosa* Wan Chuanbiao and Zhang Ying 1990

*Odontochitina diducta* Pearce 2010

*Odontochitina costata* Alberti 1961

*Oligosphaeridium complex* (White 1842) Davey and Williams 1966b

*Oligosphaeridium pulcherrimum* (Deflandre and Cookson 1955) Davey and Williams 1966b

*Palaeocystodinium* Alberti 1961

*Palaeocystodinium bulliforme* Ioannides 1986

*Palaeocystodinium golzowense* Alberti 1961

*Palaeoperidinium pyrophorum* (Ehrenberg 1838 ex Wetzel 1933a) Sarjeant 1967

*Palaeotetradinium silicorum* Deflandre 1936b

*Phelodinium kozlowskii* (Gorka 1963) Lindgren 1984

*Pterodinium cingulatum* (Wetzel 1933b) Below 1981a

*Senoniasphaera rotundata* Clarke and Verdier 1967

*Sepispinula huguoniotii* (Valensi 1955a) Islam 1993

*Spinidinium echinoideum* (Cookson and Eisenack 1960a) Lentin and Williams 1976

*Spinidinium uncinatum* May 1980

*Spiniferella* Stover and Hardenbol 1994

*Spiniferites ramosus* (Ehrenberg 1838) Mantell 1854

*Spiniferites scabrosus* (Clarke and Verdier 1967) Lentin and Williams 1975

*Stiphrosphaeridium anthophorum* (Cookson and Eisenack 1958) Lentin and Williams 1985

*Stiphrosphaeridium dictyophorum* (Cookson and Eisenack 1958) Lentin and Williams 1985

*Subtilisphaera* Jain and Millepied 1973

*Surculosphaeridium convocatum* Fensome et al. 2016

*Tanyosphaeridium xanthiopyxides* (Wetzel 1933b ex Deflandre 1937) Stover and Evitt 1978

*Trichodinium castanea* Deflandre 1935 ex Clarke and Verdier 1967

*Trithyrodinium suspectum* (Manum and Cookson 1964) Davey 1969b

*Vesperopsis* Bint 1986

*Xenascus* Cookson and Eisenack 1969

**Acritarchs**

*Baltisphaeridium* Eisenack 1958a

*Fromea chytra* (Drugg 1967) Stover and Evitt 1978

*Fromea glabella* (Singh 1971) Lentin and Williams 1981

*Fromea fragilis* (Cookson and Eisenack 1962a) Stover and Evitt 1978

*Fromea madurensis* Cookson and Eisenack 1982

*Micrhystridium* Deflandre 1937b

*Micrhystridium stellatum* Deflandre 1945a

*Veryhachium europaeum* Stockmans and Willière 1960

**Miospores**

*Abiespollenites* Tiergart in Raatz ("1937") 1938

*Aequitriradites* Delcourt and Sprumont 1955

*Aequitriradites spinulosus* (Cookson and Dettmann 1958) Cookson and Dettmann 1961

*Aequitriradites verrucatus* (Cookson and Dettmann 1958) Cookson and Dettmann 1961

*Alnipollenites* Potonié 1931

*Alnipollenites verus* Potonié 1931

*Appendicisporites* Weyland and Krieger 1953

*Appendicisporites bilateralis* Singh 1971

*Appendicisporites bifurcatus* Singh 1964

*Appendicisporites problematicus* (Burger 1966) Singh 1971

*Aquilapollenites* Rouse 1957

*Aquilapollenites augustus* Srivastava 1969

*Azonia* Samoilovitch in Samoilovitch and Mtchedlishvili 1961

*Baculatisporites* Pflug and Thomson in Thomson and Pflug 1953

*Betulaepollenites* Potonié 1934 ex Potonié 1960

*Callialasporites dampieri* (Balme 1957) Dev 1961

*Camarozonosporites* Danzé-Corsin and Laveine 1963

*Caryapollenites* Raatz ("1937") 1938 ex Potonié 1960

*Caryapollenites imparalis* Nichols and Ott 1978

*Cerebropollenites mesozoicus* (Couper 1958) Nilsson 1958

*Cicatricosisporites* Potonié and Gelletich 1933

*Cicatricosisporites augustus* Singh 1971

*Cicatricosisporites hallei* Delcourt and Sprumont 1955

*Cicatricosisporites subrotundus* Brenner 1963

*Contignisporites cooksoniae* (Balme 1957) Dettmann 1963

*Coryluspollenites* Raatz ("1937") 1938

*Costatoperforosporites fistulosus* Deák 1962

*Costatoperforosporites foveolatus* Deák 1962

*Densoisporites* Weyland and Krieger 1953

*Distaltriangulisporites irregularis* (Singh 1964) Singh 1971

*Eucommiidites troedssonii* Erdtman 1948

*Extratriporopollenites* Pflug in Thomson and Pflug 1952

*Fisciniasporites potomacensis* (Brenner 1963) Dettmann and Clifford 1992

*Gleicheniidites senonicus* Ross 1949

*Hazaria* Srivastava 1971

*Ischyosporites* Balme 1957

*Ischyosporites punctatus* Cookson and Dettmann 1958

*Ischyosporites foveolatus* (Pocock 1964)

*Ischyosporites pseudoreticulatus* (Couper 1958)

*Laevigatisporites* Dybova and Jachowicz 1957

*Leiotriletes* Naumova 1939, Ishchenko 1952 ex Potonié and Kremp 1954

*Maculatisporites undulatus* Doring 1964

*Matonisporites* Couper 1958

*Momipites* Wodehouse 1933

*Momipites tenuipolus* Anderson 1960

*Momipites wyomingensis* Nichols and Ott 1978

*Osmundacidites* Couper 1953

*Parvisaccites* Couper 1958

*Parvisaccites amplus* Brenner 1963

*Parvisaccites radiatus* Couper 1958

*Piceapollenites* Potonié 1931

*Pilosisporites trichopapillosus* (Thiergart 1949) Delcourt and Sprumont 1955

*Pinuspollenites* Raatz 1938 ex Potonié 1958

*Plicatella* Maljavkina 1949

*Plicatella jansonii* (Pocock 1962)

*Podocarpidites* Cookson and Couper 1953

*Pterocaryapollenites* Raatz (1937) 1938 ex Potonié 1960

*Retitricolpites vulgaris* Pierce 1961

*Retitriletes* Pierce 1961

*Ruffordiaspora* Dettmann and Clifford 1992

*Ruffordiaspora australiensis* (Cookson 1953)

*Rugubivesiculites* Pierce 1961

*Rugubivesiculites convolutus* Pierce 1961

*Rugubivesiculites reductus* Pierce 1961

*Rugubivesiculites rugosus* Pierce 1961

*Taxodiaceaepollenites* Kremp 1949 ex Potonié 1958

*Tricolpites crassimurus* (Groot and Penny 1960) Singh 1971

*Trilobosporites* Potonié 1956

*Trilobosporites apiverrucatus* Couper 1958

*Verrucosisporites* Ibrahim 1933

*Vitreisporites* Leschik 1955

*Vitreisporites pallidus* (Reissinger) Nilsson 1958

*Vitreisporites* sp. Singh 1971

**Others**

*Azolla* Lamarck in Lamarck et al. 1783

*Palambages* Wetzel 1961

*Pediastrum* Meyen 1829

*Tasmanites* Newton 1875

# APPENDIX B

Table of taxa illustrated in the Plates with corresponding details for each specimen including: taxon name, well name, depth (in metres), external lab processing number, Geological Survey of Canada (Atlantic) (GSC-A) P-Number, fraction, co-ordinates on the slide, and GSC type number.

**Table B-1.** Table of taxa illustrated in the Plates

| Plate | Figure | Taxon | Well | Depth (m) | External lab processing no. | GSC-A P-number | Fraction | Co-ordinates | GSC type no. |
|---|---|---|---|---|---|---|---|---|---|
| 1 | 1 | *Alterbidinium* sp. | Karlsefni A-13 | 3326.90 | R3309-18 | P-50310 | Unsieved | 15.6 x 93.0 | GSC 140573 |
| 1 | 2 | *Apectodinium parvum* | Ogmund E-72 | 1546.00 | R3309-45 | P-50321 | +30 μm fraction | 10.0 x 94.0 | GSC 140574 |
| 1 | 3 | *Apectodinium parvum* | Snorri J-90 | 2501.85 | R3309-53 | P-50356 | +30 μm fraction | 8.0 x 96.7 | GSC 140575 |
| 1 | 4 | *Apectodinium quinquelatum* | Snorri J-90 | 2501.85 | R3309-53 | P-50356 | +30 μm fraction | 22.8 x 94.4 | GSC 140576 |
| 1 | 5 | *Areoligera gippingensis* | Snorri J-90 | 2501.85 | R3305-53 | P-50356 | +30 μm fraction | 20.8 x 97.2 | GSC 140577 |
| 1 | 6 | *Areoligera* cf. *gippingensis* | Snorri J-90 | 2501.85 | R3309-53 | P-50356 | +30 μm fraction | 10.0 x 99.0 | GSC 140578 |
| 1 | 7 | *Areoligera* cf. *gippingensis* | Snorri J-90 | 2501.85 | R3309-53 | P-50356 | +30 μm fraction | 20.0 x 91.4 | GSC 140579 |
| 1 | 8 | *Aptea* sp. A. | Roberval K-92 | 3016.75 | R3309-56 | P-50327 | +30 μm fraction | 16.3 x 92.3 | GSC 140580 |
| 1 | 9 | *Aptea* sp. A. | Roberval K-92 | 3016.75 | R3309-56 | P-50327 | +30 μm fraction | 16.3 x 92.3 | GSC 140581 |
| 1 | 10-11 | *Aptea* sp. A. | Roberval K-92 | 3016.75 | R3309-56 | P-50327 | +30 μm fraction | 18.7 x 93.7 | GSC 140582 |
| 1 | 12 | *Cerodinium diebelii* | Hopedale E-33 | 1957.00 | R3309-6 | P-50305 | +30 μm fraction | 5.8 x 94.1 | GSC 140583 |
| 1 | 13 | *Cerodinium* cf. *speciosum* | Karlsefni A-13 | 3332.87 | R3309-14 | P-50306 | Unsieved | 17.3 x 80.7 | GSC 140584 |
| 1 | 14 | *Chichaouadinium vestitum* | Herjolf M-92 | 2639.58 | R3309-24 | P-50292 | +30 μm fraction | 11.5 x 97.0 | GSC 140585 |
| 1 | 15 | *Cordosphaeridium* sp. | Roberval K-92 | 3015.40 | R3309-57 | P-50328 | Unsieved | 7.5 x 90.4 | GSC 140586 |
| 1 | 16 | *Cribroperidinium* sp. | Hopedale E-33 | 1957.00 | R3309-6 | P-50305 | +30 μm fraction | 8.4 x 93.5 | GSC 140587 |
| 1 | 17 | *Cyclonephelium* sp. | Gilbert F-53 | 3254.10 | R3309-37 | P-50276 | +30 μm fraction | 10.7 x 91.1 | GSC 140588 |
| 1 | 18 | *Disphaerogena* sp. | Gilbert F-53 | 3258.00 | R3309-34 | P-50273 | +30 μm fraction | 17.0 x 91.0 | GSC 140589 |
| 1 | 19 | *Distatodinium* sp. | Skolp E-07 | 1279.35 | P5331-4D | P-50335 | +30 μm fraction | 9.5 x 94.2 | GSC 140590 |
| 1 | 20 | *Tenua* sp. | Roberval K-92 | 3016.75 | R3309-56 | P-50327 | Unsieved | 16.0 x 92.2 | GSC 140591 |
| 2 | 1 | *Cleistosphaeridium*? | Gilbert F-53 | 3254.10 | R3309-37 | P-50276 | +30 μm fraction | 24.5 x 91.0 | GSC 140592 |
| 2 | 2 | *Eatonicysta* sp. | Gilbert F-53 | 3254.10 | R3309-37 | P-50276 | +30 μm fraction | 8.0 x 92.3 | GSC 140593 |
| 2 | 3 | *Elytrocysta* sp. | Gilbert F-53 | 3251.25 | R3309-39 | P-50278 | -30 μm fraction | 6.4 x 92.1 | GSC 140594 |
| 2 | 4 | *Exochosphaeridium arnace* | Gilbert F-53 | 3254.10 | R3309-37 | P-50276 | +30 μm fraction | 5.4 x 95.6 | GSC 140595 |
| 2 | 5 | *Fibrocysta vectensis* | Gilbert F-53 | 3254.10 | R3309-37 | P-50276 | +30 μm fraction | 22.0 x 92.3 | GSC 140596 |
| 2 | 6 | *Gillinia hymenophora* | Skolp E-07 | 1451.20 | P5331-15F | P-50350 | -30 μm fraction | 19.3 x 91.1 | GSC 140597 |
| 2 | 7 | *Gillinia hymenophora* | Skolp E-07 | 1454.32 | P5331-17D | P-50348 | -30 μm fraction | 15.0 x 91.3 | GSC 140598 |
| 2 | 8 | *Glaphyrocysta divaricata* | Snorri J-90 | 2504.10 | R3309-32 | P-50355 | Unsieved | 9.0 x 82.0 | GSC 140599 |
| 2 | 9 | *Gonyaulacysta* sp. | Gilbert F-53 | 3251.25 | R3309-39 | P-50278 | Unsieved | 21.4 x 91.0 | GSC 140600 |

**Table B-1.** (cont.)

| Plate | Figure | Taxon | Well | Depth (m) | External lab processing no. | GSC-A P-number | Fraction | Co-ordinates | GSC type no. |
|---|---|---|---|---|---|---|---|---|---|
| 2 | 10 | *Heterosphaeridium bellii* | Roberval K-92 | 3016.75 | R3309-56 | P-50327 | Unsieved | 4.0 x 91.1 | GSC 140601 |
| 2 | 11 | *Hystrichokolpoma* sp. | Gilbert F-53 | 3257.31 | R3305-35 | P-50274 | +30 μm fraction | 18.6 x 92.0 | GSC 140602 |
| 2 | 12 | *Hystrichosphaeridium quadratum* | Gilbert F-53 | 3257.31 | R3305-35 | P-50274 | +30 μm fraction | 18.0 x 91.0 | GSC 140603 |
| 2 | 13 | *Hystrichosphaerina schinde-wolfii* (optical section) | North Bjarni F-06 | 2452.40 | R3305-51 | P-50312 | Unsieved | 6.2 x 95.0 | GSC 140604 |
| 2 | 14 | *Hystrichosphaeridium quadratum* | Skolp E-07 | 1451.20 | P5331-15D | P-50350 | +30 μm fraction | 18.5 x 94.2 | GSC 140605 |
| 2 | 15 | *Hystrichosphaeridium tubiferum* | Gilbert F-53 | 3254.10 | R3309-37 | P-50276 | +30 μm fraction | 13.0 x 98.0 | GSC 140606 |
| 2 | 16 | *Hystrichosphaeridium* sp. | Gilbert F-53 | 3254.10 | R3309-37 | P-50276 | +30 μm fraction | 18.0 x 94.7 | GSC 140607 |
| 2 | 17 | *Hystrichosphaerina schindewolfii* | North Bjarni F-06 | 2452.40 | R3309-51 | P-50312 | Unsieved | 6.2 x 95.0 | GSC 140604 |
| 2 | 18 | *Impagidinium* sp. | Roberval K-92 | 3015.40 | R3307-57 | P-50328 | Unsieved | 14.5 x 93.2 | GSC 140608 |
| 2 | 19 | *Isabelidinium cooksoniae* | Gilbert F-53 | 3251.25 | R3309-39 | P-50278 | +30 μm fraction | 9.0 x 91.7 | GSC 140609 |
| 2 | 20 | *Isabelidinium cooksoniae* | Hopedale E-33 | 1957.00 | R3309-6 | P-50305 | +30 μm fraction | 10.6 x 94.2 | GSC 140610 |
| 3 | 1 | *Lagenorhytis* sp. | North Bjarni F-06 | 2452.40 | R3309-51 | P-50312 | Unsieved | 8.0 x 93.2 | GSC 140611 |
| 3 | 2 | *Manumiella* sp. | Roberval K-92 | 3016.75 | R3309-56 | P-50327 | Unsieved | 13.5 x 91.5 | GSC 140612 |
| 3 | 3 | *Microdinium* sp. A sensu Ioannides 1986 | Gilbert F-53 | 3251.25 | R3309-39 | P-50278 | Unsieved | 9.4 x 89.7 | GSC 140613 |
| 3 | 4 | *Microdinium* sp. A sensu Ioannides 1986 | Roberval K-92 | 3015.40 | R3309-57 | P-50328 | Unsieved | 6.0 x 90.8 | GSC 140614 |
| 3 | 5 | *Microdinium* sp. | Skolp E-07 | 1281.50 | P5331-6B | P-50344 | Unsieved | 21.7 x 82.1 | GSC 140615 |
| 3 | 6 | *Microdinium* sp. | Skolp E-07 | 1452.50 | P5331-16B | P-50349 | Unsieved | 16.6 x 80.5 | GSC 140616 |
| 3 | 7 | *Nyktericysta nebulosa* | Ogmund E-72 | 2234.00 | R3309-49 | P-50325 | +30 μm fraction | 11.6 x 92.8 | GSC 140617 |
| 3 | 8 | *Nyktericysta?* sp. | Ogmund E-72 | 2234.00 | R3309-49 | P-50325 | Unsieved | 9.3 x 81.3 | GSC 140618 |
| 3 | 9 | *Odontochitina costata* | Roberval K-92 | 3016.75 | R3309-56 | P-50327 | Unsieved | 16.0 x 92.0 | GSC 140619 |
| 3 | 10 | *Odontochitina diducta* | Gilbert F-53 | 3251.25 | R3309-39 | P-50278 | +30 μm fraction | 22.3 x 90.9 | GSC 140620 |
| 3 | 11 | *Odontochitina* sp. | Skolp E-07 | 1450.00 | P5331-14D | P-50351 | +30 μm fraction | 12.5 x 96.0 | GSC 140621 |
| 3 | 12 | *Phelodinium kozlowskii* | Gilbert F-53 | 3254.10 | R3309-37 | P-50276 | +30 μm fraction | 21.2 x 95.0 | GSC 140622 |

**Table B-1.** (cont.)

| Plate | Figure | Taxon | Well | Depth (m) | External lab processing no. | GSC-A P-number | Fraction | Co-ordinates | GSC type no. |
|---|---|---|---|---|---|---|---|---|---|
| 3 | 13 | *Pterodinium* sp. (dorsal view of dorsal surface) | Skolp E-07 | 1450.00 | P5331-14B | P-50351 | Unsieved | 9.0 x 83.5 | GSC 140623 |
| 3 | 14 | *Pterodinium* sp. (optical section) | Skolp E-07 | 1450.00 | P5331-14B | P-50351 | Unsieved | 9.0 x 83.5 | GSC 140623 |
| 3 | 15 | *Pterodinium* sp. (dorsal view of ventral surface) | Skolp E-07 | 1450.00 | P5331-14B | P-50351 | Unsieved | 9.0 x 83.5 | GSC 140623 |
| 3 | 16 | *Spinidinium echinoideum* | Gilbert F-53 | 3254.10 | R3309-37 | P-50276 | +30 μm fraction | 15.6 x 91.0 | GSC 140624 |
| 3 | 17 | *Spinidinium echinoideum* | Gilbert F-53 | 3251.25 | R3309-39 | P-50278 | -30 μm fraction | 12.0 x 90.5 | GSC 140625 |
| 3 | 18 | *Spiniferites ramosus* | Roberval K-92 | 3016.75 | R3309-56 | P-50327 | Unsieved | 21.5 x 91.4 | GSC 140626 |
| 3 | 19 | *Spiniferites scabrosus* | Roberval K-92 | 3016.75 | R3309-56 | P-50327 | +30 μm fraction | 13.0 x 92.1 | GSC 140627 |
| 3 | 20 | *Spongodinium?* sp. | Gilbert F-53 | 3408.40 | R3309-41 | P-50280 | Unsieved | 6.8 x 81.9 | GSC 140628 |
| 4 | 1 | *Stiphrosphaeridium dictyophorum* | Snorri J-90 | 2501.85 | R3309-53 | P-50356 | Unsieved | 19.0 x 90.3 | GSC 140629 |
| 4 | 2 | *Subtilisphaera* sp. | Gilbert F-53 | 3254.10 | R3309-37 | P-50276 | +30 μm fraction | 7.0 x 95.5 | GSC 140630 |
| 4 | 3 | *Subtilisphaera* sp. | Gilbert F-53 | 3254.10 | R3309-37 | P-50276 | +30 μm fraction | 16.0 x 86.0 | GSC 140631 |
| 4 | 4 | *Subtilisphaera*? sp. | Gilbert F-53 | 3408.40 | R3309-41 | P-50280 | Unsieved | 13.4 x 85.7 | GSC 140632 |
| 4 | 5 | *Systematophora complicata* | North Bjarni F-06 | 2452.40 | R3309-51 | P-50312 | Unsieved | 7.2 x 91.3 | GSC 140633 |
| 4 | 6 | *Systematophora complicata* | North Bjarni F-06 | 2452.40 | R3309-51 | P-50312 | Unsieved | 11.0 x 82.6 | GSC 140634 |
| 4 | 7 | *Trithyrodinium suspectum* | Gilbert F-53 | 3254.10 | R3309-37 | P-50276 | +30 μm fraction | 7.7 x 92.3 | GSC 140635 |
| 4 | 8 | *Alterbidinium* sp. | Gilbert F-53 | 3257.31 | P3309-35 | P-50274 | +30 μm fraction | 21.0 x 92.0 | GSC 140636 |
| 4 | 9 | *Alterbidinium* sp. | Gilbert F-53 | 3257.31 | R3309-35 | P-50274 | +30 μm fraction | 5.0 x 83.0 | GSC 140637 |
| 4 | 10 | *Fromea chytra* (an acritarch) | Skolp E-07 | 1281.50 | P5331-6F | P-50344 | -30 μm fraction | 16.0. X 91.2 | GSC 140638 |
| 5 | 1 | *Aequitriradites spinulosus* | Herjolf M-92 | 3563.80 | R3309-24 | P-50296 | +30 μm fraction | 16.1 x 97.0 | GSC 140639 |
| 5 | 2 | *Aequitriradites verrucosus* | Hopedale E-33 | 1960.10 | R3309-4C | P-50303 | +30 μm fraction | 9.5 x 93.0 | GSC 140640 |
| 5 | 3 | *Aequitriradites* cf. *verrucosus* | Herjolf M-92 | 3563.80 | R3309-24 | P-50296 | +30 μm fraction | 2.0 x 97.1 | GSC 140641 |
| 5 | 4 | *Aequitriradites* cf. *verrucosus* | Hopedale E-33 | 1958.60 | R3309-5C | P-50304 | +30 μm fraction | 15.1 x 90.7 | GSC 140642 |
| 5 | 5 | *Appendicisporites bilateralis* | North Leif I-05 | 3110.00 | R3309-10 | P-50316 | +30 μm fraction | 12.5 x 97.3 | GSC 140643 |
| 5 | 6 | *Fisciniasporites potomacensis* | Ogmund E-72 | 2234.00 | R3309-49 | P-50325 | +30 μm fraction | 9.5 x 91.0 | GSC 140644 |
| 5 | 7 | *Cicatricosisporites subrotundus* | Tyrk P-100 | 1185.10 | R3309-33 | P-50362 | Unsieved | 18.5 x 91.4 | GSC 140645 |

**Table B-1.** (cont.)

| Plate | Figure | Taxon | Well | Depth (m) | External lab processing no. | GSC-A P-number | Fraction | Co-ordinates | GSC type no. |
|---|---|---|---|---|---|---|---|---|---|
| 5 | 8 | *Cicatricosisporites hallei* | Tyrk P-100 | 1187.70 | R3309-33 | P-50360 | Unsieved | 13.7 x 91.1 | GSC 140646 |
| 5 | 9 | *Cicatricosisporites hallei* | Tyrk P-100 | 1187.70 | R3309-33 | P-50360 | Unsieved | 13.7 x 91.1 | GSC 140646 |
| 5 | 10 | *Cicatricosisporites* sp. | North Leif I-05 | 3113.66 | R3309-13 | P-50319 | Unsieved | 10.0 x 81.0 | GSC 140647 |
| 5 | 11 | *Contignisporites cooksoniae* | Hopedale E-33 | 1960.10 | R3309-4C | P-50303 | +30 μm fraction | 16.6 x 92.0 | GSC 140648 |
| 5 | 12 | *Costatoperforosporites fistulosus* | Tyrk P-100 | 1185.10 | R1185-10 | P-50362 | Unsieved | 8.3 x 91.2 | GSC 140649 |
| 5 | 13 | *Appendicisporites* sp. | Tyrk P-100 | 1187.70 | R3309-31 | P-50360 | +30 μmfraction | 12.0 x 91.7 | GSC 140650 |
| 5 | 14 | *Distaltriangularis mutabilis* | Skolp E-07 | 1289.00 | P5331-11D | P-50339 | +30 μm fraction | 7.5 x 94.2 | GSC 140651 |
| 5 | 15 | *Distaltriangulisporites perplexus* | North Leif I-05 | 3110.00 | R3309-10 | P-50316 | +30 μm fraction | 22.5 x 93.7 | GSC 140652 |
| 5 | 16 | *Distaltriangulisporites* sp. | Roberval K-92 | 3015.40 | R3309-57 | P-50328 | Unsieved | 10.7 x 87.0 | GSC 140653 |
| 5 | 17 | *Distaltriangulisporites* sp. | North Leif I-05 | 3115.00 | R3309-12 | P-50318 | Unsieved | 8.8 x 83.2 | GSC 140654 |
| 5 | 18 | *Concavissimisporites* sp. | North Leif I-05 | 3115.00 | R3309-12 | P-50318 | +30 μm fraction | 17.0 x 91.3 | GSC 140655 |
| 5 | 19 | *Ischyosporites* sp. | Hopedale E-33 | 1958.60 | P3309-5C | P-50304 | +30 μm fraction | 15.8 x 94.1 | GSC 140656 |
| 5 | 20 | *Ischyosporites foveolatus* | North Leif I-05 | 3113.25 | R3309-7 | P-50313 | Unsieved | 18.1 x 83.2 | GSC 140657 |
| 6 | 1 | *Maculatisporites undulatus* | Hopedale E-33 | 1960.10 | R3309-4C | P-50303 | +30 μm fraction | 22.8 x 93.6 | GSC 140658 |
| 6 | 2 | *Nodosisporites* sp. | North Leif I-05 | 3115.00 | R3309-12 | P-50318 | Unsieved | 14.8 x 81.8 | GSC 140659 |
| 6 | 3 | *Pilosisporites trichopapillosus* | Hopedale E-33 | 1960.10 | R3309-4C | P-50303 | +30 μm fraction | 17.0 x 93.0 | GSC 140660 |
| 6 | 4 | *Pilosisporites trichopapillosus* | Hopedale E-33 | 1964.50 | R3309-1C | P-50300 | +30 μm fraction | 18.4 x 94.0 | GSC 140661 |
| 6 | 5 | *Pilosisporites trichopapillosus* | Hopedale E-33 | 1963.30 | R3309-2C | P-50301 | +30 μm fraction | 15.0 x 93.0 | GSC 140662 |
| 6 | 6 | *Pilosisporites trichopapillosus* | Hopedale E-33 | 1963.30 | R3309-2C | P-50301 | +30 μm fraction | 15.0 x 93.0 | GSC 140662 |
| 6 | 7 | *Osmundacidites* sp. | Hopedale E-33 | 1960.10 | R3309-4C | P-50303 | +30 μm fraction | 8.8 x 82.0 | GSC 140663 |
| 6 | 8 | *Plicatella jansonii* | Hopedale E-33 | 1964.50 | R3309-1C | P-50300 | +30 μm fraction | 10.4 x 90.9 | GSC 140664 |
| 6 | 9 | *Ruffordiaspora australiensis* | Hopedale E-33 | 1960.10 | R3309-4C | P-50303 | +30 μm fraction | 17.3 x 90.6 | GSC 140665 |
| 6 | 10 | *Ruffordiaspora* sp. | North Bjarni F-06 | 2452.40 | R3309-51 | P-50312 | Unsieved | 17.7 x 91.6 | GSC 140666 |
| 6 | 11 | *Ruffordiaspora* sp. | Hopedale E-33 | 1963.30 | R3309-2C | P-50301 | +30 μm fraction | 15.0 x 91.0 | GSC 140667 |
| 6 | 12 | *Ruffordiaspora* sp. | Hopedale E-33 | 1963.30 | R3309-2C | P-50301 | +30 μm fraction | 15.0 x 91.0 | GSC 140667 |

**Table B-1.** (cont.)

| Plate | Figure | Taxon | Well | Depth (m) | External lab processing no. | GSC-A P-number | Fraction | Co-ordinates | GSC type no. |
|---|---|---|---|---|---|---|---|---|---|
| 6 | 13 | *Saxetia* sp. | Hopedale E-33 | 1960.10 | R3309-4C | P-50303 | Unsieved | 6.8 x 84.3 | GSC 140668 |
| 6 | 14 | *Sculptisporis aulosenensis* | Herjolf M-92 | 2632.76 | R3309-23 | P-50295 | Unsieved | 12.4 x 93.0 | GSC 140669 |
| 6 | 15 | *Verrucosisporites*? sp. | Tyrk P-100 | 1186.50 | R3309-32 | P-50361 | Unsieved | 13.0 x 83.2 | GSC 140670 |
| 7 | 1 | *Aquilapollenites* sp. | Karlsefni A-13 | 3328.25 | R3309-17 | P-50309 | Unsieved | 18.0 x 96.0 | GSC 140671 |
| 7 | 2 | *Azonia* sp. | Karlsefni A-13 | 3328.25 | R3309-17 | P-50309 | Unsieved | 19.8 x 96.1 | GSC 140672 |
| 7 | 3 | *Betulaepollenites* sp. | Snorri J-90 | 2504.10 | P3309-52 | P-50355 | Unsieved | 15.0 x 82.3 | GSC 140673 |
| 7 | 4 | *Callialasporites trilobatus* | Hopedale E-33 | 1961.65 | R3309-3C | P-50302 | +30 μm fraction | 15.5 x 92.1 | GSC 141065 |
| 7 | 5 | *Callialasporites turbatus* | Hopedale E-33 | 1960.10 | R3309-4C | P-50303 | +30 μm fraction | 27.5 x 81.0 | GSC 141066 |
| 7 | 6 | *Caryapollenites* sp. | Snorri J-90 | 2499.60 | R3309-54 | P-50357 | -30 μm fraction | 19.6 x 90.7 | GSC 141067 |
| 7 | 7 | *Eucommiidites troedssonii* | North Leif I-05 | 3111.05 | R3309-9 | P-50315 | Unsieved | 17.0 x 83.7 | GSC 141068 |
| 7 | 8 | *Gothanipollis* sp. | Bjarni O-82 | 2291.10 | P5330-1B | P-50271 | Unsieved | 9.4 x 97.2 | GSC 141069 |
| 7 | 9 | *Momipites tenuipolis* | Bjarni O-82 | 2291.10 | P5330-1B | P-50271 | Unsieved | 4.4 x 90.4 | GSC 141070 |
| 7 | 10 | *Momiipites ventifluminus* | Bjarni O-82 | 2291.10 | P5330-1B | P-50271 | Unsieved | 20.4 x 95.6 | GSC 141071 |
| 7 | 11 | Normapolles group? | Skolp E-07 | 1451.20 | P5331-15F | P-50350 | -30 μm fraction | 21.5 x 92.0 | GSC 141072 |
| 7 | 12 | *Ostryoipollenites* sp. | Bjarni O-82 | 2291.10 | P5330-1BA | P-50271 | Unsieved | 20.5 x 93.2 | GSC 141073 |
| 7 | 13 | *Ostryoipollenites* sp. | Snorri J-90 | 2504.10 | R3309-52 | P-50355 | Unsieved | 8.0 x 81.8 | GSC 141074 |
| 7 | 14 | *Parvisaccites amplus* | North Leif I-05 | 3110.00 | R3309-10 | P-50316 | +30 μm fraction | 20.3 x 91.0 | GSC 141075 |
| 7 | 15 | *Podocarpidites* sp. | Hopedale E-33 | 1964.50 | R3309-1C | P-50300 | +30 μm fraction | 14.0 x 91.4 | GSC 141076 |
| 7 | 16 | *Rugubivesiculites convolutus* | Tyrk P-100 | 1187.70 | R3309-33 | P-50360 | Unsieved | 20.0 x 91.0 | GSC 141077 |
| 7 | 17 | *Rugubivesiculites rugosus* | Tyrk P-100 | 1185.10 | P1185-10 | P-50362 | Unsieved | 14.6 x 91.4 | GSC 141078 |
| 7 | 18 | *Rugubivesiculites rugosus* | North Leif I-05 | 3110.00 | P1185-10 | P-50316 | +30 μm fraction | 16.0 x 91.0 | GSC 141079 |
| 7 | 19 | *Rugubivesiculites rugosus* | North Leif I-05 | 3110.00 | P1185-10 | P-50316 | +30 μm fraction | 13.6 x 90.7 | GSC 141080 |
| 7 | 20 | *Rugubivesiculites rugosus* | North Leif I-05 | 3112.55 | R3309-8 | P-50314 | +30 μm fraction | 18.2 x 91.0 | GSC 141081 |
| 8 | 1 | *Schizosporis*? sp. (an alga) | Snorri J-90 | 2501.85 | R3309-53 | P-50356 | +30 μm fraction | 9.1 x 93.3 | GSC 141082 |
| 8 | 2 | *Trudopollis* sp. | Snorri J-90 | 2501.85 | R3309-53 | P-50356 | Unsieved | 9.0 x 91.1 | GSC 141083 |
| 8 | 3 | *Trudopollis* sp. | Snorri J-90 | 2501.85 | R3309-53 | P-50356 | Unsieved | 19.0 x 95.0 | GSC 141084 |

# Plate 1

**Dinocysts from the conventional cores.**

Figure 1. *Alterbidinium* sp., Karlsefni A-13, 3326.9 m

Figure 2. *Apectodinium parvum*, Ogmund E-72, 1546 m

Figure 3. *Apectodinium parvum*, Snorri J-90, 2501.85 m

Figure 4. *Apectodinium quinquelatum*, Snorri J-90, 2501.85 m

Figure 5. *Areoligera gippingensis*, Snorri J-90, 2501.85 m

Figure 6. *Areoligera* cf. *gippingensis*, Snorri J-90, 2501.85 m

Figure 7. *Areoligera* cf. *gippingensis*, Snorri J-90, 2501.85 m

Figure 8. *Aptea* sp. A., Roberval K-92, 3016.75 m

Figure 9. *Aptea* sp. A., Roberval K-92, 3016.75 m

Figures 10, 11. *Aptea* sp. A., Roberval K-92, 3016.75 m

Figure 12. *Cerodinium diebelii*, Hopedale E-33, 1957 m

Figure 13. *Cerodinium speciosum*, Karlsefni A-13, 3332.87 m

Figure 14. *Chichaouadinium vestitum*, Herjolf M-92, 2639.58 m

Figure 15. *Cordosphaeridium* sp., Roberval K-92, 3015.4 m

Figure 16. *Cribroperidinium* sp., Hopedale E-33, 1957 m

Figure 17. *Cyclonephelium* sp., Gilbert F-53, 3254.1 m

Figure 18. *Disphaerogena* sp., Gilbert F-53, 3258 m

Figure 19. *Distatodinium* sp., Skolp E-07, 1279.35 m

Figure 20. *Tenua* sp., Roberval K-92, 3016.75 m

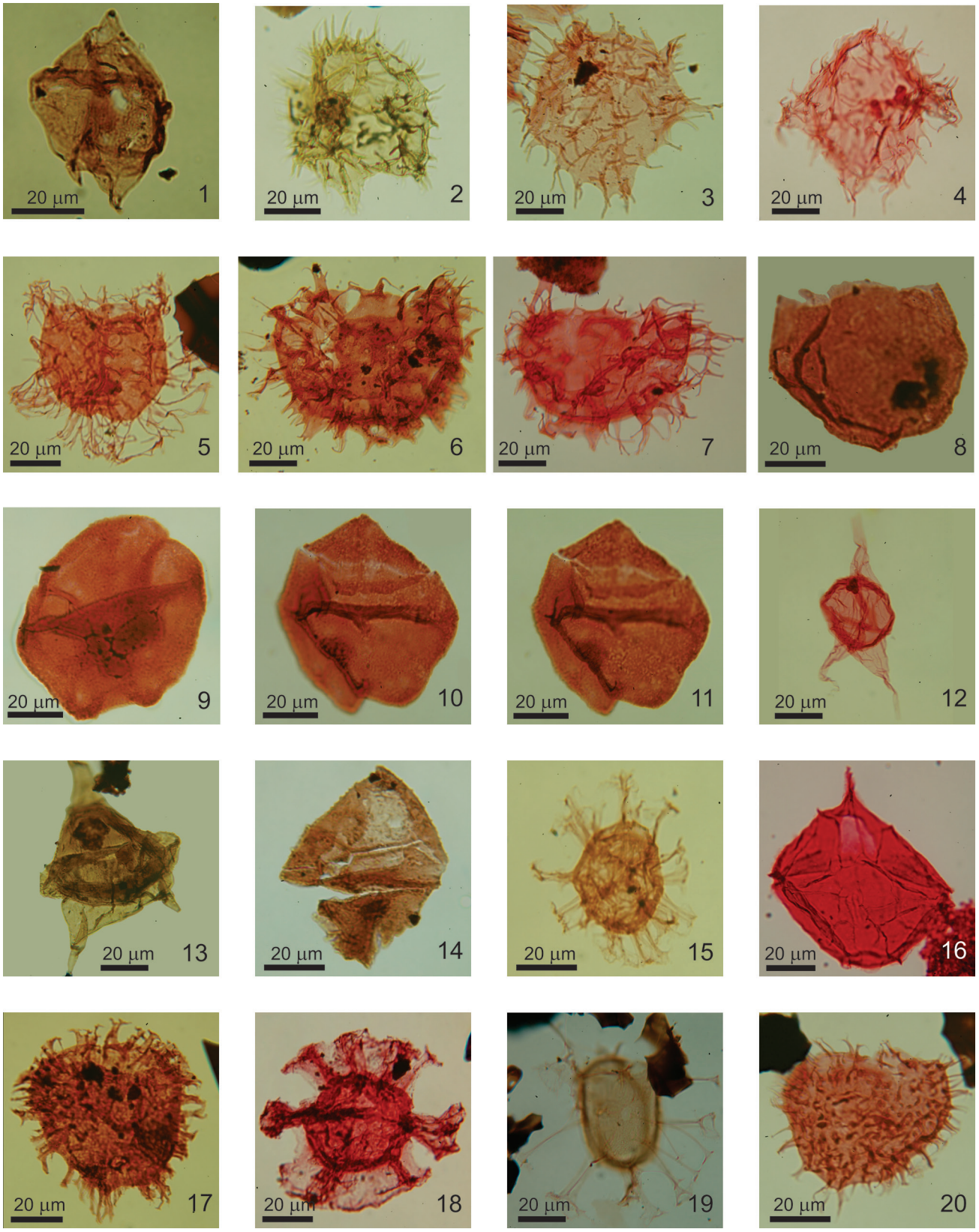
20 µm
1
20 µm
2
20 µm
3
20 µm
4
20 µm
5
20 µm
6
20 µm
7
20 µm
8
20 µm
9
20 µm
10
20 µm
11
20 µm
12
20 µm
13
20 µm
14
20 µm
15
20 µm
16
20 µm
17
20 µm
18
20 µm
19
20 µm
20

# Plate 2

**Dinocysts from the conventional cores.**

Figure 1. *Cleistosphaeridium*? sp., Gilbert F-53, 3254.1 m

Figure 2. *Eatonicysta* sp., Gilbert F-53, 3254.1 m

Figure 3. *Elytrocysta* sp., Gilbert F-53, 3251.25 m

Figure 4. *Exochosphaeridium arnace*, Gilbert F-53, 3254.1 m

Figure 5. *Fibrocysta vectensis*, Gilbert F-53, 3254.1 m

Figure 6. *Gillinia hymenophora*, Skolp E-07, 1451.2 m

Figure 7. *Gillinia hymenophora*, Skolp E-07, 1454.32 m

Figure 8. *Glaphyrocysta divaricata*, Snorri J-90, 2504.1 m

Figure 9. *Gonyaulacysta* sp., Gilbert F-53, 3251.25 m

Figure 10. *Heterosphaeridium bellii*, Roberval K-92, 3016.75 m

Figure 11. *Hystrichokolpoma* sp., Gilbert F-53, 3257.31 m

Figure 12. *Hystrichosphaeridium quadratum*, Gilbert F-53, 3257.31 m

Figure 13. *Hystrichosphaerina schindewolfii*, optical section, North Bjarni F-06, 2452.4 m

Figure 14. *Hystrichosphaeridium quadratum*, Skolp E-07, 1451.2 m

Figure 15. *Hystrichosphaeridium tubiferum*, Gilbert F-53, 3254.1 m

Figure 16. *Hystrichosphaeridium* sp., Gilbert F-53, 3254.1 m

Figure 17. *Hystrichosphaerina schindewolfii*, upper surface, North Bjarni F-06, 2452.4 m

Figure 18. *Impagidinium* sp., Roberval K-92, 3015.4 m

Figure 19. *Isabelidinium cooksoniae*, Gilbert F-53, 3251.25 m

Figure 20. *Isabelidinium cooksoniae*, Hopedale E-33, 1957 m

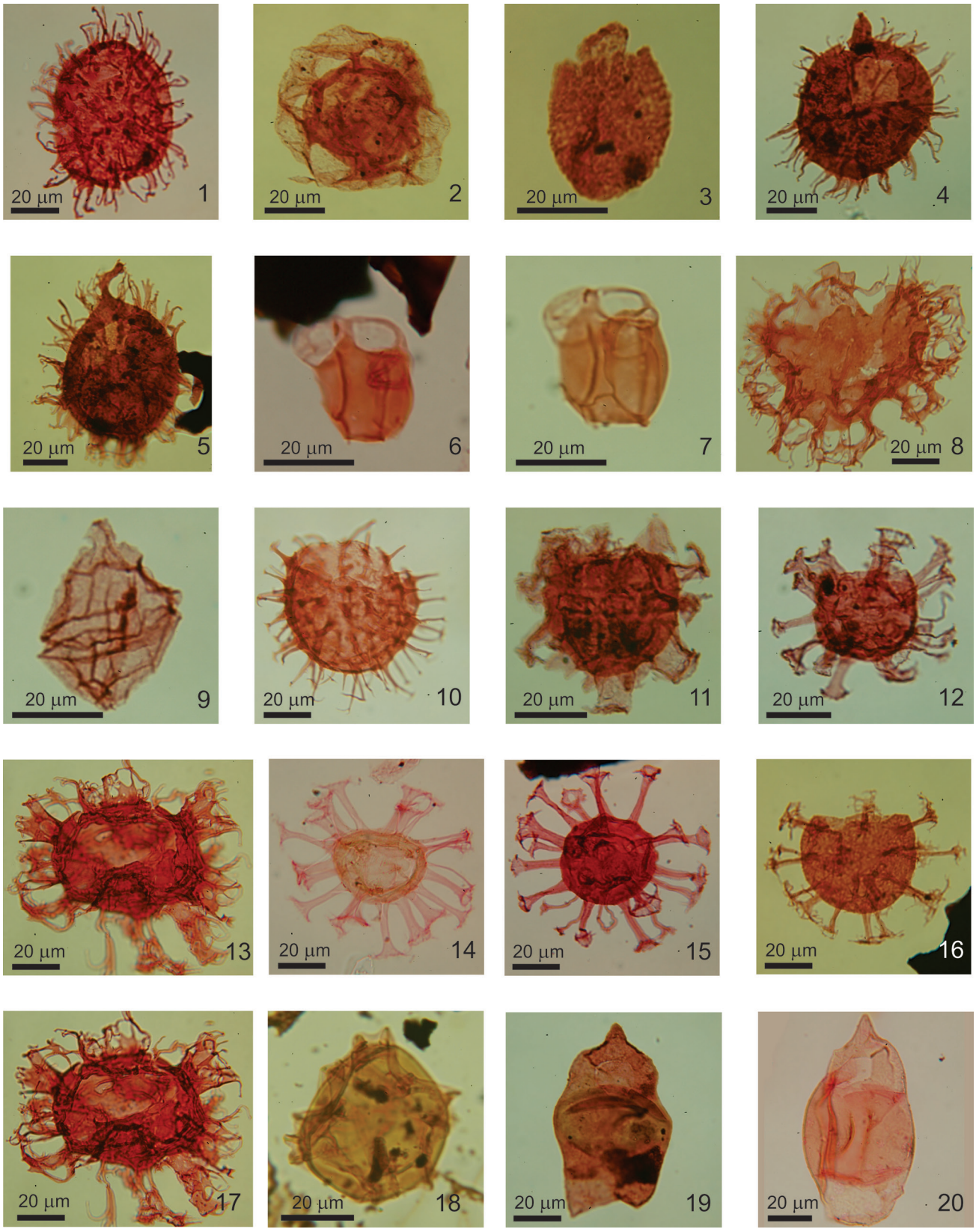
20 µm 1
20 µm 2
20 µm 3
20 µm 4
20 µm 5
20 µm 6
20 µm 7
20 µm 8
20 µm 9
20 µm 10
20 µm 11
20 µm 12
20 µm 13
20 µm 14
20 µm 15
20 µm 16
20 µm 17
20 µm 18
20 µm 19
20 µm 20

# Plate 3

**Dinocysts from the conventional cores.**

Figure 1. *Lagenorhytis* sp., North Bjarni F-06, 2452.40 m

Figure 2. *Manumiella* sp., Roberval K-92, 3016.75 m

Figure 3. *Microdinium sp*. A sensu Ioannides 1986, Gilbert F-53, 3251.25 m

Figure 4. *Microdinium* sp. A sensu Ioannides 1986, Roberval K-92, 3015.4 m

Figure 5. *Microdinium* sp., Skolp E-07, 1281.5 m

Figure 6. *Microdinium* sp., Skolp E-07, 1452.5 m

Figure 7. *Nyktericysta nebulosa*, Ogmund E-72, 2234.0 m

Figure 8. *Nyktericysta*? sp., Ogmund E-72, 2234.0 m

Figure 9. *Odontochitina costata*, Roberval K-92, 3016.75 m

Figure 10. *Odontochitina diducta*, Gilbert F-53, 3251.25 m

Figure 11. *Odontochitina* sp., Skolp E-07, 1450 m

Figure 12. *Phelodinium kozlowskii*, Gilbert F-53, 3254.1 m

Figure 13. *Pterodinium* sp. (dorsal view of dorsal surface), Skolp E-07, 1450 m

Figure 14. *Pterodinium* sp. (optical section), Skolp E-07, 1450 m

Figure 15. *Pterodinium* sp. (dorsal view of ventral surface), Skolp E-07, 1450 m

Figure 16. *Spinidinium echinoideum*, Gilbert F-53, 3254.1 m

Figure 17. *Spinidinium echinoideum*, Gilbert F-53, 3251.25 m

Figure 18. *Spiniferites ramosus*, Roberval K-92, 3016.75 m

Figure 19. *Spiniferites scabrosus*, Roberval K-92, 3016.75 m

Figure 20. *Spongodinium*?, Gilbert F-53, 3408.4 m

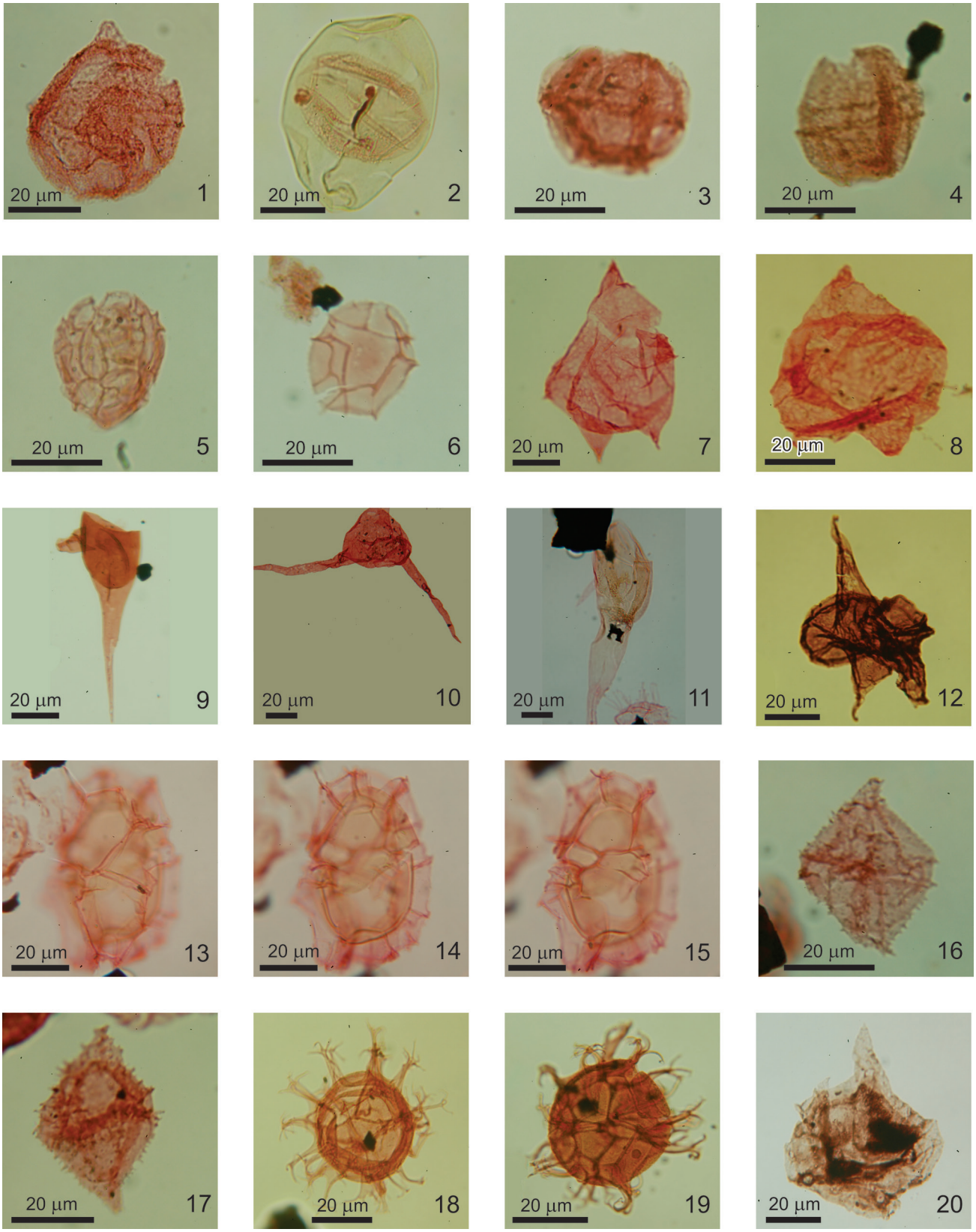
20 µm 1
20 µm 2
20 µm 3
20 µm 4
20 µm 5
20 µm 6
20 µm 7
20 µm 8
20 µm 9
20 µm 10
20 µm 11
20 µm 12
20 µm 13
20 µm 14
20 µm 15
20 µm 16
20 µm 17
20 µm 18
20 µm 19
20 µm 20

# Plate 4

**Dinocysts and one acritarch from the conventional cores.**

Figure 1. *Stiphrosphaeridium dictyophorum*, Snorri J-90, 2501.85 m

Figure 2. *Subtilisphaera* sp., Gilbert F-53, 3254.1 m

Figure 3. *Subtilisphaera* sp., Gilbert F-53, 3254.1 m

Figure 4. *Subtilisphaera*? sp., Gilbert F-53, 3408.4 m

Figure 5. *Systematophora complicata*, North Bjarni F-06, 2452.4 m

Figure 6. *Systematophora complicata*, North Bjarni F-06, 2452.4 m

Figure 7. *Trithyrodinium suspectum*, Gilbert F-53, 3254.1 m

Figure 8. *Alterbidinium* sp., Gilbert F-53, 3257.31 m

Figure 9. *Alterbidinium* sp., Gilbert F-53, 3257.31 m

Figure 10. *Fromea chytra* (an acritarch), Skolp E-07, 1281.5 m

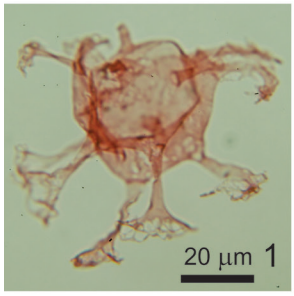
20 µm
1

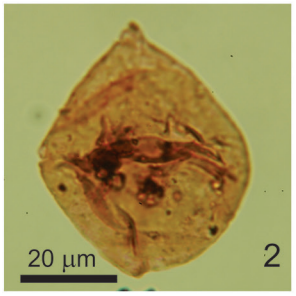
20 µm
2


20 µm
3

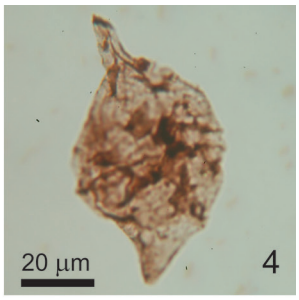
20 µm
4

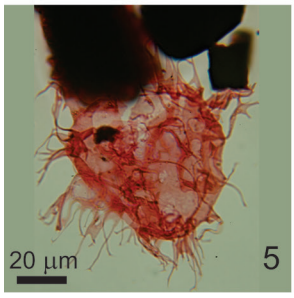
20 µm
5

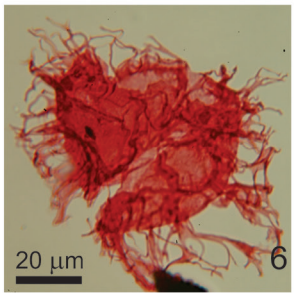
20 µm
6

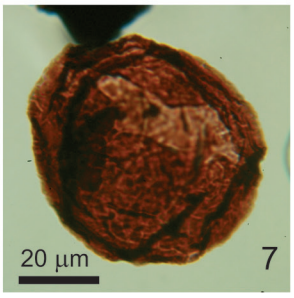
20 µm
7

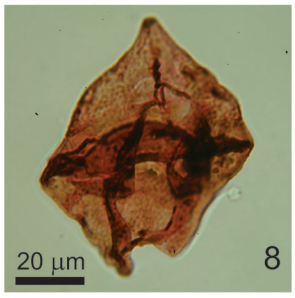
20 µm
8

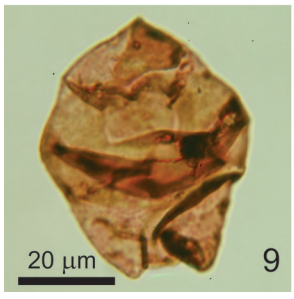
20 µm
9

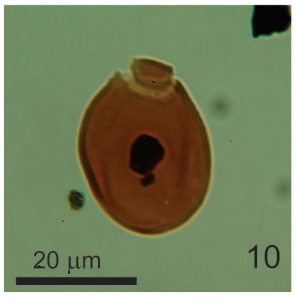
20 µm
10

# Plate 5

**Spores from the conventional cores.**

Figure 1. *Aequitriradites spinulosus*, Herjolf M-92, 3563.8 m

Figure 2. *Aequitriradites verrucosus*, Hopedale E-33, 1960.1 m

Figure 3. *Aequitriradites* cf. *verrucosus*, Herjolf M-92, 3563.8 m

Figure 4. *Aequitriradites* cf. *verrucosus*, Hopedale E-33, 1958.6 m

Figure 5. *Appendicisporites bilateralis*, North Leif I-05, 3110 m

Figure 6. *Fisciniasporites potomacensis*, Ogmund E-72, 2234 m

Figure 7. *Cicatricosisporites subrotundus*, Tyrk P-100, 1185.1 m

Figure 8. *Cicatricosisporites hallei*, Tyrk P-100, 1187.7 m

Figure 9. *Cicatricosisporites hallei*, Tyrk P-100, 1187.7 m

Figure 10. *Cicatricosisporites* sp., North Leif I-05, 3113.66 m

Figure 11. *Contignisporites cooksoniae*, Hopedale E-33, 1960.1 m

Figure 12. *Costatoperforosporites fistulosus*, Tyrk P-100, 1185.1 m

Figure 13. *Appendicisporites* sp., Tyrk P-100, 1187.7 m

Figure 14. *Distaltriangularis mutabilis*, Skolp E-07, 1289 m

Figure 15. *Distaltriangulisporites perplexus*, North Leif I-05, 3110 m

Figure 16. *Distaltriangulisporites* sp., Roberval K-92, 3015.4 m

Figure 17. *Distaltriangulisporites* sp., North Leif I-05, 3115 m

Figure 18. *Concavissimisporites* sp., North Leif I-05, 3115 m

Figure 19. *Ischyosporites* sp., Hopedale E-33, 1958.6 m

Figure 20. *Ischyosporites foveolatus*, North Leif I-05, 3113.25 m

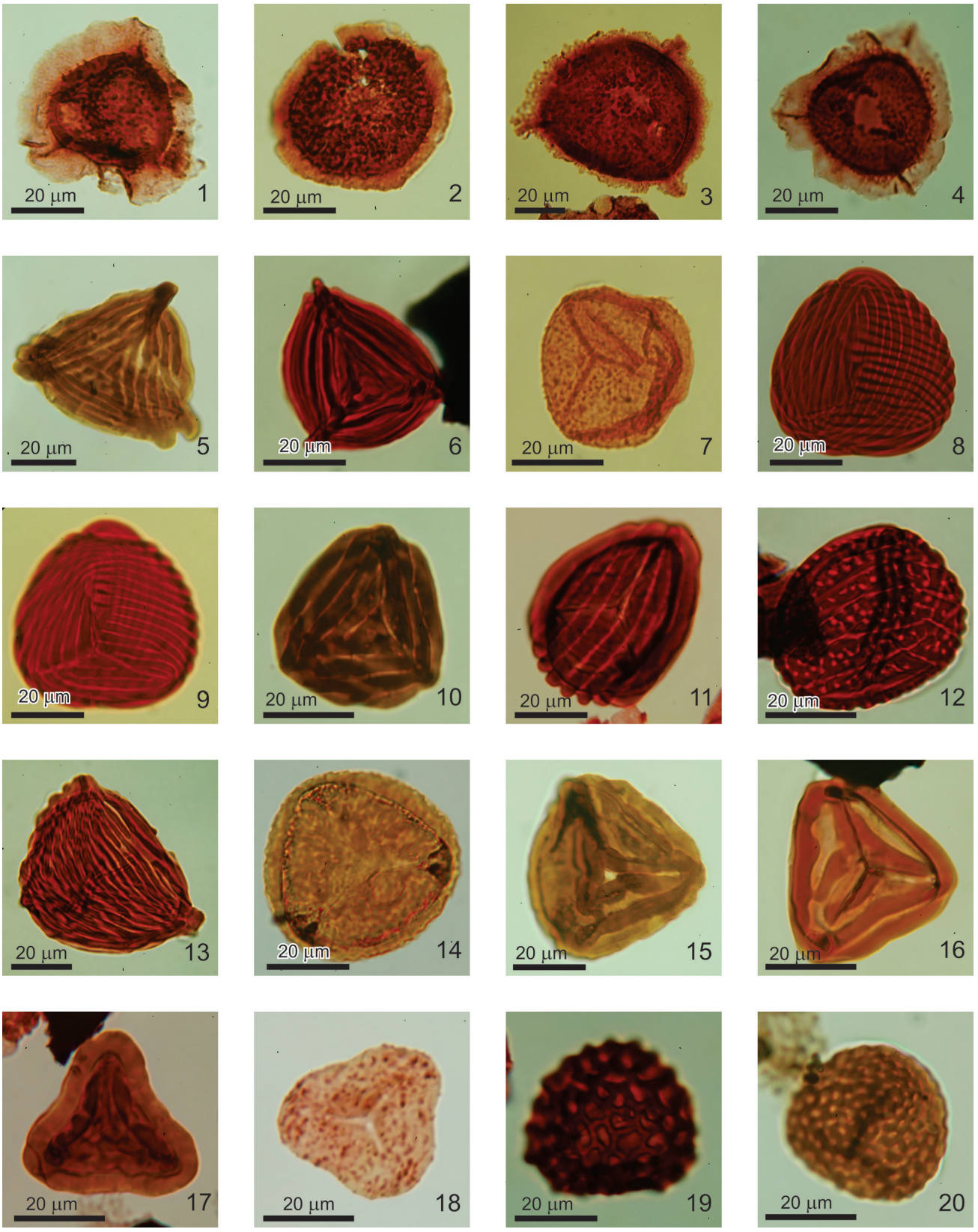
20 µm
1
20 µm
2
20 µm
3
20 µm
4
20 µm
5
20 µm
6
20 µm
7
20 µm
8
20 µm
9
20 µm
10
20 µm
11
20 µm
12
20 µm
13
20 µm
14
20 µm
15
20 µm
16
20 µm
17
20 µm
18
20 µm
19
20 µm
20

# Plate 6

**Spores from the conventional cores.**

Figure 1. *Maculatisporites undulatus*, Hopedale E-33, 1960.1 m

Figure 2. *Nodosisporites* sp., North Leif I-05, 3115 m

Figure 3. *Pilosisporites trichopapillosus*, Hopedale E-33, 1960.1 m

Figure 4. *Pilosisporites trichopapillosus*, Hopedale E-33, 1964.5 m

Figure 5. *Pilosisporites trichopapillosus*, Hopedale E-33, 1963.3 m

Figure 6. *Pilosisporites trichopapillosus*, Hopedale E-33, 1963.3 m

Figure 7. *Osmundacidites* sp., Hopedale E-33, 1960.1 m

Figure 8. *Plicatella jansonii*, Hopedale E-33, 1964.5 m

Figure 9. *Ruffordiaspora australiensis*, Hopedale E-33, 1960.1 m

Figure 10. *Ruffordiaspora* sp., North Bjarni F-06, 2452.4 m

Figure 11. *Ruffordiaspora australiensis*, Hopedale E-33, 1963.3 m

Figure 12. *Ruffordiaspora australiensis*, Hopedale E-33, 1963.3 m

Figure 13. *Saxetia* sp., Hopedale E-33, 1960.1 m

Figure 14. *Sculptisporis aulosenensis*, Herjolf M-92, 2632.76 m

Figure 15. *Verrucosisporites*? sp., Tyrk P-100, 1186.5 m

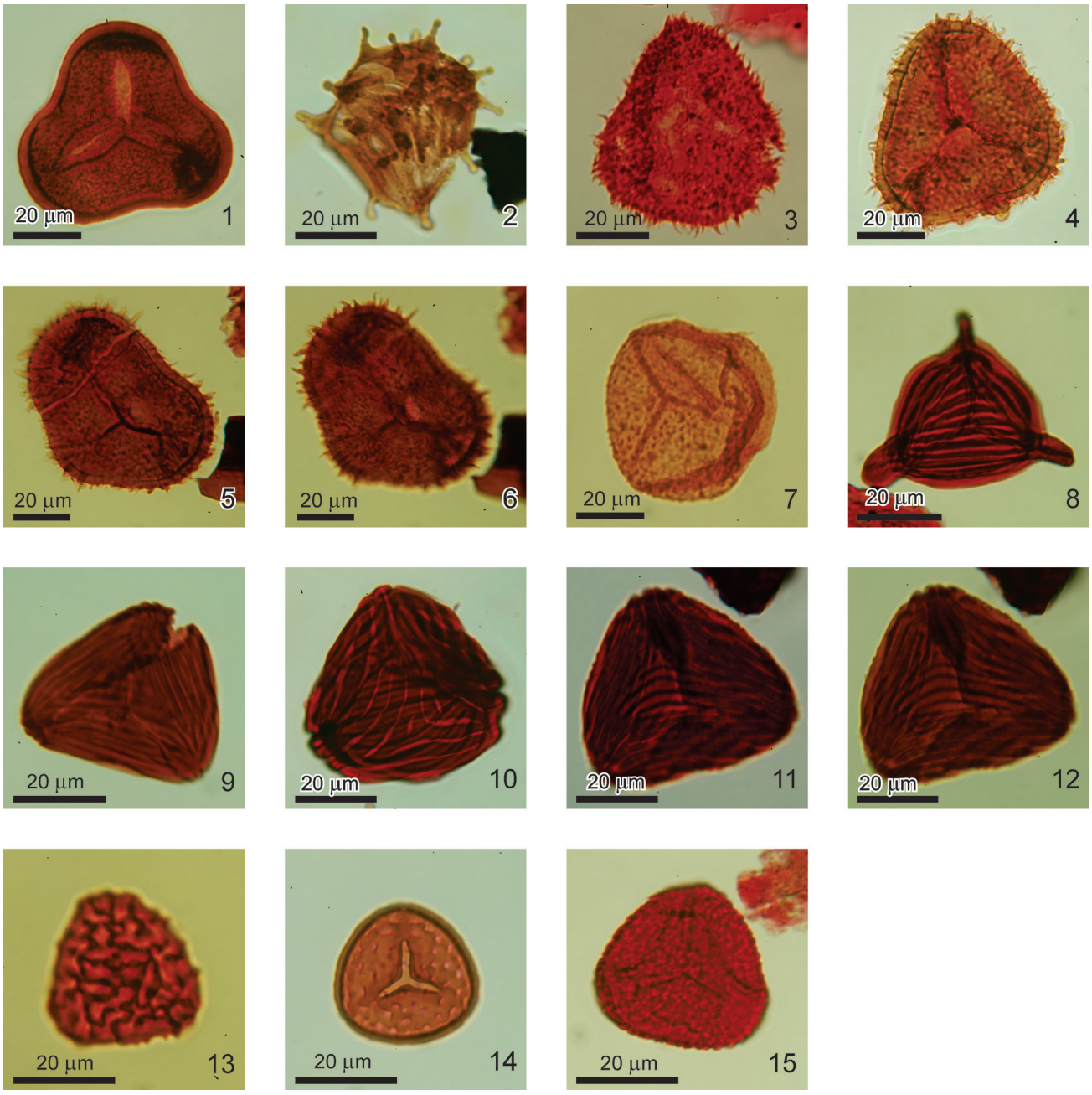
20 µm
1
20 µm
2
20 µm
3
20 µm
4
20 µm
5
20 µm
6
20 µm
7
20 µm
8
20 µm
9
20 µm
10
20 µm
11
20 µm
12
20 µm
13
20 µm
14
20 µm
15

# Plate 7

**Pollen from conventional cores.**

Figure 1. *Aquilapollenites* sp., Karlsefni A-13, 3328.25 m

Figure 2. *Azonia* sp., Karlsefni A-13, 3328.25 m

Figure 3. *Betulaepollenites* sp., Snorri J-90, 2504.1 m

Figure 4. *Callialasporites trilobatus*, Hopedale E-33, 1961.65 m

Figure 5. *Callialasporites turbatus*, Hopedale E-33, 1960.1 m

Figure 6. *Caryapollenites imparalis*, Snorri J-90, 2499.60 m

Figure 7. *Eucommiidites troedssonii*, North Leif I-05, 3111.05 m

Figure 8. *Gothanipollis* sp., Bjarni O-82, 2291.1 m

Figure 9. *Momipites tenuipolis*, Bjarni O-82, 2291.1 m

Figure 10. *Momipites ventifluminus*, Bjarni O-82, 2291.1 m

Figure 11. *Normapolles* group, Skolp E-07, 1451.2 m

Figure 12. *Ostryoipollenites* sp., Bjarni O-82, 2291.1 m

Figure 13. *Ostryoipollenites* sp., Snorri J-90, 2504.1 m

Figure 14. *Parvisaccites amplus*, North Leif I-05, 3110 m

Figure 15. *Podocarpidites* sp., Hopedale E-33, 1964.5 m

Figure 16. *Rugubivesiculites convolutus*, Tyrk P-100, 1187.7 m

Figure 17. *Rugubivesiculites rugosus*, Tyrk P-100, 1185.1 m

Figure 18. *Rugubivesiculites rugosus*, North Leif I-05, 3110 m

Figure 19. *Rugubivesiculites rugosus*, North Leif I-05, 3110 m

Figure 20. *Rugubivesiculites rugosus*, North Leif I-05, 3112.55 m

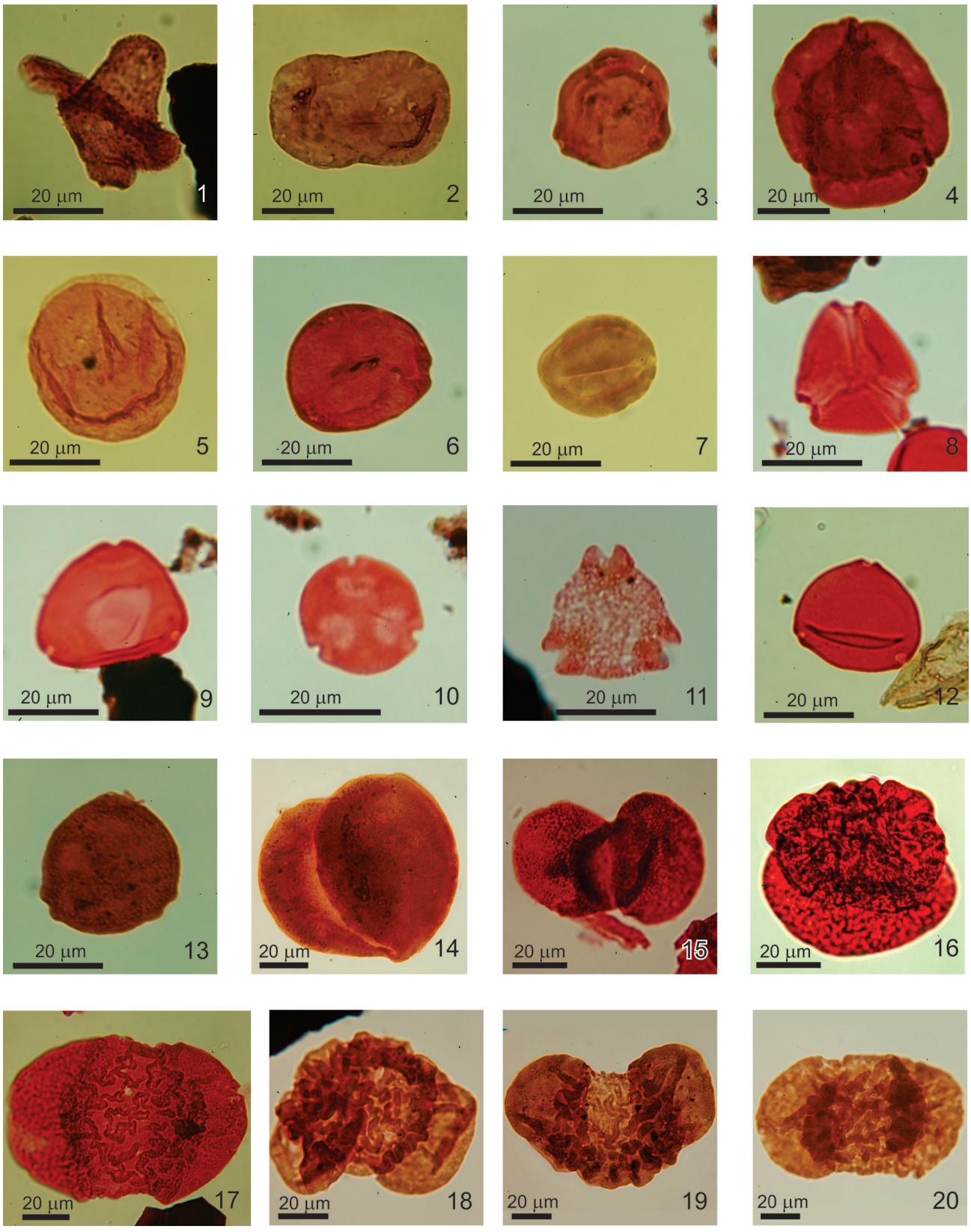
20 µm
1
20 µm
2
20 µm
3
20 µm
4
20 µm
5
20 µm
6
20 µm
7
20 µm
8
20 µm
9
20 µm
10
20 µm
11
20 µm
12
20 µm
13
20 µm
14
20 µm
15
20 µm
16
20 µm
17
20 µm
18
20 µm
19
20 µm
20

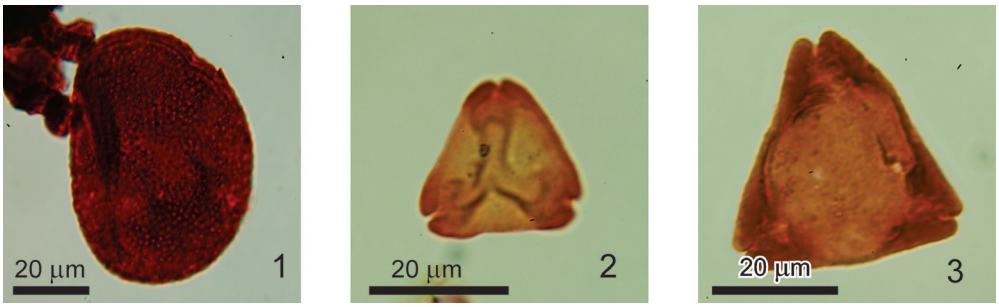


# Plate 8

**An alga and two pollen from conventional cores.**

Figure 1. *Schizosporis*? (an alga), Snorri J-90, 2501.85 m

Figure 2. *Trudopollis* sp., Snorri J-90, 2501.85 m

Figure 3. *Trudopollis* sp., Snorri J-90, 2501.85 m